Exploring the role of tumor necrosis factor-stimulated gene 6 in experimental ischaemic stroke.

A thesis submitted to The University of Manchester for the degree of Doctor of Philosophy in the Faculty of Life Sciences

2013

Hannah F Buggey

CONTENTS

Word count: 57,406

LIST OF FIGURES

LIST OF TABLES

ABBREVIATIONS

APP	Acute phase protein
APR	Acute phase response
BBB	Blood-brain barrier
BCA	Bicinchoninic acid
BDNF	Brain-derived neurotrophic factor
bFGF	Basic fibroblast growth factor
BSA	Bovine serum albumin
CBA	Cytometric bead array
CBF	Cerebral blood flow
CCA	Common carotid artery
cDNA	Complementary DNA
CEBP-α	CCAAT/enhancer-binding protein alpha
CRP	C reactive protein
CSPG	Chondroitin sulphate proteoglycan
DAB	Diaminobenzidine
DAMP	Danger associated molecular pattern
DEPC	Diethylpyrocarbonate
DMEM	Dulbecco's modified Eagle's medium
dNTP	Deoxyribonucleotide triphosphate
ECA	External carotid artery
ECM	Extra-cellular matrix
EF1-α	Elongation factor 1-alpha

ELISA	Enzyme-linked immunosorbent assay
ESAM	Endothelial cell-selective adhesion molecule
FABP4	Fatty acid binding protein 4
FCS	Foetal calf serum
FUDR	5'-fluro-2-deoxyuridine
GAG	Glycosaminoglycan
GAPDH	Glyceraldehyde 3-phosphate dehydrogenase
G-CSF	Granulocyte-colony stimulating factor
GF	Growth factor
GFP	Green fluorescent protein
GPCR	G protein-coupled receptor
H&E	Haematoxylin and eosin
HLA	Human leukocyte antigen
HMGB1	High-mobility group box 1
HPA	Hypothalamic-pituitary-adrenal
HPRT1	Hypoxanthine phosphoribosyltransferase 1
HRP	Horseradish peroxidase
HSP60	Heat shock protein 60
HT	Haemorrhagic transformation
IαI	Inter-alpha-inhibitor
ICA	Internal carotid artery
ICAM	Intercellular adhesion molecule
IDO	Indoleamine 2,3-dioxygenase

IFN	Interferon
IgG	Immunoglobulin G
IL	Interleukin
IL-1Ra	Interleukin-1 receptor antagonist
IL-1RAcP	Interleukin-1 receptor accessory protein
IMS	Industrial methylated spirits
JAM	Junctional adhesion molecule
LPS	Lipopolysaccharide
MCA	Middle cerebral artery
MCAo	Middle cerebral artery occlusion
MCP-1	Monocyte chemoattractant protein-1
MMP	Matrix metalloproteinase
MPO	Myeloperoxidase
MRI	Magnetic resonance imaging
MSC	Mesenchymal stem cell
NANOG	Nanog homeobox
NET	Neutrophil extracellular trap
NK	Natural killer
NO	Nitric oxide
NOD	Non-obese diabetic
OccA	Occipital artery
OCT4A	Octamer-binding transcription factor 4a
PBS	Phosphate buffered saline

PDGF	Platelet-derived growth factor
PDL	Poly-D-Lysine
PE	Phycoerythrin
PECAM	Platelet endothelial cell adhesion molecule
PFA	Paraformaldehyde
PGE2	Prostaglandin E2
PPAR2	Peroxisome proliferator-activated receptor 2
PTA	Pterygopalatine artery
PVR	Poliovirus receptor
qPCR	Quantitative polymerase chain reaction
r18.s	18.s ribosomal RNA
RD	Reagent diluent
RIPA	Radio-immunoprecipitation assay
RNA	Ribonucleic acid
ROS	Reactive oxygen species
RPL13a	60S ribosomal protein L13a
RUNX II	Runt-related transcription factor 2
SAA	Serum amyloid A
SDHA	Succinate dehydrogenase complex
TBI	Traumatic brain injury
TBP	TATA box binding protein
TGF	Transforming growth factor
TLR	Toll-like receptor

TNF-α	Tumor necrosis factor-alpha
tPA	Tissue plasminogen activator
TSG-6	Tumor necrosis factor-stimulated gene 6
VCAM	Vascular cell adhesion molecule
VEGF	Vascular endothelial growth factor
YWAHZ	14-3-3 protein zeta/delta

CONFERENCE PRESENTATIONS AND PUBLICATIONS

Many of the topics discussed in this thesis were reviewed in the following publication:

Systemic immune activation shapes stroke outcome.
Murray KN*, **Buggey HF***, Denes A, Allan SM.
Mol Cell Neurosci. 2013 Mar;53:14-25.

*These authors contributed equally.

In addition, results were presented at the following conferences:

Faculty of Life Sciences Research Symposium, Manchester, 2012, poster.
'The effect of TSG-6 on IL-1-induced brain damage and inflammation'.

Society for Neuroscience, New Orleans, 2012, poster.
'The effect of TSG-6 on IL-1-induced brain damage and inflammation'.

British Neuroscience Association, London, 2013, poster.
'Expression of TSG-6 in the brain in response to experimental ischaemic stroke'.

Neuroscience Research Institute, Manchester, 2013, poster.
'Expression of TSG-6 in the brain in response to experimental ischaemic stroke'.

UK Preclinical Stroke Symposium, Leicester, 2013, poster.
'Expression of TSG-6 in the brain in response to experimental ischaemic stroke'.

Faculty of Life Sciences PhD Conference, Manchester, 2013, oral presentation.
'Exploring the role of TSG-6 in experimental ischaemic stroke'.

ABSTRACT

The University of Manchester
Hannah F Buggey
Doctor of Philosophy
2013

Exploring the role of TSG-6 in experimental ischaemic stroke.

Ischaemic stroke occurs as a result of a blockage in one of the brain's arteries, leading to neuronal injury and death. Although stroke is a major cause of death and disability, there is no widely available treatment. Inflammation occurs in the brain and in the periphery following stroke, and both contribute to the ischaemic damage. Leukocytes such as neutrophils are key mediators of brain damage and inflammation, particularly in the presence of systemic inflammatory challenges such as interleukin-1 (IL-1). Tumor necrosis factor-stimulated gene 6 (TSG-6) is a potent inhibitor of neutrophil migration, and also modulates the immune response by dampening expression of cytokines and stabilising the extra-cellular matrix (ECM). Mesenchymal stem cells (MSCs) have shown immunomodulatory actions in many inflammatory conditions, and their benefit has often been attributed to the production of TSG-6. This work aimed to evaluate the potential of TSG-6 and TSG-6-expressing MSCs as therapies in cerebral ischaemia, and to investigate the expression profile of endogenous TSG-6 in response to stroke.

Mice were subjected to middle cerebral artery occlusion (MCAo) followed by reperfusion. We investigated whether IL-1-induced acute brain injury after stroke is reversed by TSG-6, and long-term recovery was evaluated in mice treated with TSG-6 or MSCs. Functional outcomes were assessed, and brains were sectioned and stained for analysis of lesion volume, haemorrhagic transformation, blood-brain barrier (BBB) disruption and neutrophil infiltration. The expression profile of TSG-6 was evaluated in mice allowed to recover for 4h, 24h, 3, 5 or 7 days. TSG-6 expression was determined by quantitative PCR and immunohistochemistry.

Treatment with TSG-6 reduced IL-1-induced neutrophil infiltration into the striatum, and led to decreased BBB disruption and haemorrhagic transformation at 24h. Treatment with TSG-6 in the absence of a systemic inflammatory challenge had no significant effect on lesion volume, BBB disruption or haemorrhagic transformation after 7 days reperfusion, however thalamic neutrophil infiltration was significantly reduced. Treatment with human MSCs had no significant effect on behavioural or histological outcomes, however a heightened inflammatory response in MSC-treated mice suggested rejection of the cells by the murine immune system. TSG-6 expression peaked in the ischaemic hemisphere at 5 days post-reperfusion, and was associated with astrocytes in the glial scar surrounding the infarcted tissue.

TSG-6 might be a promising therapy for the treatment of stroke in the presence of systemic inflammation. TSG-6-expressing MSCs might provide a broader therapeutic potential, and further work should optimise experimental conditions to prevent rejection of the cells. Expression of TSG-6 within the glial scar suggests a potential role in repair and recovery following ischaemic stroke. Modulating the peripheral immune response remains an attractive and accessible therapeutic target for the treatment of cerebral ischaemia.

DECLARATION

I declare that no portion of the work referred to in this thesis has been submitted in support of an application for another degree or qualification of this or any other university or institute of learning.

Hannah F Buggey 17th November 2013

COPYRIGHT STATEMENT

ACKNOWLEDGEMENTS

This rollercoaster three years has finally come to an end, and I'd like to thank everyone who has helped me through it. Firstly, I must say a huge thank you to my supervisors Stuart and Adam for your endless support, patience and enthusiasm, and for all the life chats and Hungarian words of wisdom shared in the pub. I will always remember to read more papers, be positive about my results and to never, ever sit at the corner of a table. I'd also like to thank my advisor Kathryn Else for always being so positive, having great input to discussions and for always making me feel like I was on the right track!

I would have been utterly useless without the support and help of the brilliant members of the lab – thanks to all of you for not making me feel stupid when asking those stupid questions! Thanks in particular must go to Sylvie, who has been an amazing mentor and an even better friend – your no-nonsense attitude and blunt sense of humour will be missed! Special thanks also go to Graham and Sarah G for endless help and support.

A lot of this work has stemmed from collaborations, so I would like to say a huge thank you to Tony Day, Doug and Jennifer for all their help with TSG-6, and to Cay Kielty, Teresa Massam-Wu and Steve Ball for helping me get an insight into the wonderful world of MSCs. Thanks must also go to the staff in the BSF, in particular Brian and Mike for always being happy to help.

And now for the people who have really made these three years memorable (or not, depending on how much we'd had to drink)! Katie Murray, my partner in crime…I'm not quite sure how I'm going to function without you by my side! Thanks for all the laughs, beers, gossip-filled lunches, dream-team netball matches, conference shenanigans and general leprechaun behaviour…potatoes! Fiona and Caroline – thanks for teaching me ALL the science, for convincing me that everything WILL be OK and for providing loads of laughs along the way, even after you'd left the lab. Mike – thanks for supplying my memory with ridiculous snippets of your antics over the years that still make me laugh out loud. Thanks also to Swapna, Emily, Bea, Holly, Tasha, Georgia and everyone else who have made this time of my life fun-filled and special.

Huge thanks must also go to the big bunch of dysfunctional people that I live with for always being willing to share a bottle of vino when I'd had a bad day, for always cracking out a bottle to celebrate when things were going right for once, and for providing a ridiculously fun place to live where I could forget about science! And Simon, thanks for keeping me calm when it got stressful, being patient when I was mardy, making me laugh ALL the time and for cooking all my meals! You are brilliant and these three years would have been a lot less fun without you!

I'd also like to thank my wonderful family for always acting interested and regularly asking whether I'd discovered anything yet! Thanks for always stressing the importance of taking a break and for providing brilliant fun-filled weekends with which to do so! I'm lucky to have such a fantastic family and I'm looking forward to seeing more of you now this is over.

Finally, thanks to the MRC for providing the all-important money!

CHAPTER 1:

INTRODUCTION

1.1 ISCHAEMIC STROKE

1.1.1 STROKE OVERVIEW

Stroke is the cause of 9% of all deaths in the UK and is the leading cause of disability, yet despite this there is still an urgent need for the development of effective therapies (Meairs et al., 2006). Cerebral ischaemia can be a result of subarachnoid haemorrhage, haemorrhagic stroke or ischaemic stroke, the latter of which will form the basis of this work. Cerebral ischaemia occurs as a result of a lack of blood flow to the brain. This deficit can be global or focal, and the resulting lack of oxygen and glucose compromises the metabolic demand of the brain tissue, resulting in cell death. There is a characteristic pattern of injury caused by cerebral ischaemia: the area where the blood flow is maximally reduced is known as the ischaemic core. Surrounding the core is the ischaemic penumbra, and cells here can potentially be rescued by neuroprotective strategies (Astrup et al., 1981). There is currently only one therapeutic intervention available for the treatment of ischaemic stroke: intravenous tissue plasminogen activator (tPA) (Grossman and Broderick, 2013). tPA facilitates thrombolysis by converting plasminogen into active plasmin, which can subsequently break down fibrin clots (Vassalli et al., 1991). However, tPA is severely limited in that it can only be safely used within 4.5 hours of the insult, due to an inherent risk of haemorrhagic transformation (HT: bleeding into the brain tissue) (Hacke et al., 2008; Saqqur et al., 2008).

1.1.2 MECHANISMS OF ISCHAEMIC CELL DEATH

There has been a vast amount of research into the mechanisms underlying the neurological damage caused by stroke. It has been determined that cell death occurs through a variety of mechanisms resulting in an 'ischaemic cascade' (Figure 1.1), which is one of the reasons for the difficulty in developing suitable therapies (Brouns and De Deyn, 2009).

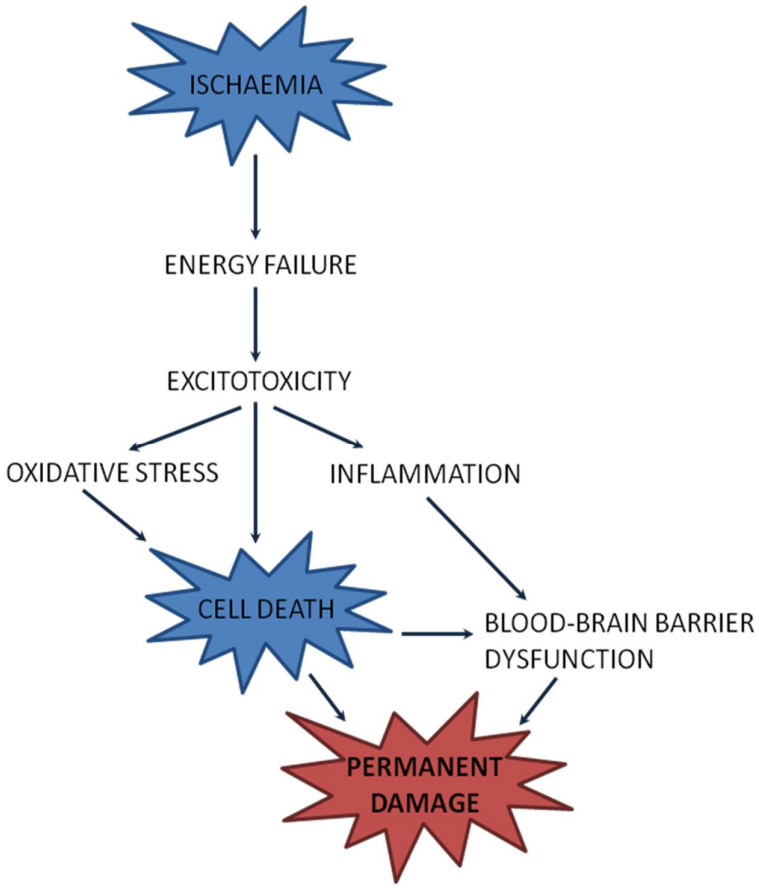

Figure 1.1: Mechanisms of ischaemic cell death. Neurotoxicity after stroke arises via a number of different mechanisms, which interact to exacerbate the initial ischaemic insult.

Following cerebral ischaemia, the initial "wave" of cell death is caused by a failure of energy supply to the brain tissue (Martin et al., 1994). Ionic balance is reliant on ATP-dependent pumps, therefore following a reduced glucose supply the functionality of the pumps is compromised. This leads to ionic imbalance, which can cause depolarization of neurones and the unregulated release of neurotransmitters from cells. The major excitatory neurotransmitter in the brain is glutamate, which exerts its effects via N-methyl-D-aspartate (NMDA) and α-amino-3-hydroxyl-5-methyl-4-isoxazole-propionate (AMPA) receptors (Monaghan et al., 1989). Upon binding to these receptors, glutamate stimulates the entry of Ca^{2+} and Na^{+} into cells, which have a number of detrimental downstream effects in cerebral ischaemia. This self-propagating cycle of depolarisation and ion entry is known as excitotoxicity, which amplifies ischaemic damage in a variety of ways. Excess intracellular Na^{+} draws fluid into cells by osmosis, causing cellular swelling and oedema, which can further limit blood supply to the damaged area. Oedema also affects the structural integrity of cells, which can be particularly detrimental to the endothelial cells of the blood-brain barrier (BBB) by increasing the barrier's permeability to circulating immune cells (Kahle et al., 2009). Ca^{2+} ions however can trigger numerous harmful processes. Firstly, these cations activate calpains and caspases, which initiate the activation and migration of pro-apoptotic proteins from the mitochondria to the cytosol, where they initiate cell death (Broughton et al., 2009). Ischaemia also initiates cell death via necrosis. This is the unregulated 'bursting' of cells, which can initiate a cascade of neurological damage in the surrounding cells due to more glutamate and toxins being released into the cellular environment (Martin et al., 1998). A further mechanism of ischaemic cell death is oxidative stress, which occurs as a result of increased free radical formation (Allen and Bayraktutan, 2009). Oxidative stress is the condition where cells are exposed to such high levels of reactive oxygen species (ROS) that they are unable to neutralise their effects with antioxidants. Types of ROS include superoxide anions (O_2-), hydroxyl radicals (-OH) and nitric oxide (NO). ROS contribute to cellular damage in a number of ways, including via disruption of cell membrane integrity and by increasing vascular permeability, leading to breakdown of the BBB and infiltration of circulating immune cells (Allen and Bayraktutan, 2009). Immune cell infiltration and central inflammation are further contributors to ischaemic damage, and these will be discussed in more detail later.

1.1.3 Experimental models of ischaemic stroke

Rodent models are frequently used in stroke research. Most models target the middle cerebral artery (MCA), as this is the most commonly occluded vessel during a clinical stroke (Derouesné et al., 1993). Occlusion of this vessel can precipitate damage in the motor and somatosensory cortices, the striatum and the internal capsule. The MCA occlusion (MCAo) model uses an intraluminal filament, which is advanced up through the internal carotid artery into the origin of the MCA, where it is left for an occlusion period before being withdrawn to allow reperfusion (Longa et al., 1989). Other models include ligation techniques, where the MCA is exposed and ligated directly, and thromboembolic approaches, which are sometimes favoured due to their close relationship to the human condition (Howells et al., 2010). In this work, the intraluminal filament MCAo model with reperfusion will be used. This model was chosen due to its ability to create a penumbral region, the opportunity to study the impact of occlusion and reperfusion, and due to the comparably high success rate and low mortality rate compared to other models.

1.2 The blood-brain barrier

The brain is protected from potentially harmful circulating mediators by a complex structural blockade known as the blood-brain barrier (BBB). As well as exerting a protective function, the components of the BBB are also essential for maintaining neuronal function and homeostasis by moderating neurotransmitter and ion concentrations (Abbott et al., 2010; Siegenthaler et al., 2013). The primary component of the BBB is brain endothelial cells. These cells possess tight junctions comprised of proteins including cadherins, claudins, occludins and junctional adhesion molecules (JAMs) which span the gap between adjacent cells and form a barrier against soluble plasma proteins and ions (Abbott et al., 2010). Tight junction assembly is modulated by intracellular scaffold proteins, which anchor junctional proteins to the cytoskeleton (Wolburg and Lippoldt, 2002). Maintenance of tight junction stability has been shown to depend on a close association with astrocytes (Abbott, 2002). Peripheral endothelial cells can also be induced to take on a BBB phenotype by transplantation of astrocytes (Janzer and Raff, 1987). Astrocyte end-feet, the basal lamina and pericytes all contribute to stability of the BBB, and these components along with neurones form the

"neurovascular unit" (Muldoon et al., 2013). A diagrammatic representation of the BBB in healthy tissue is shown in Figure 1.2:

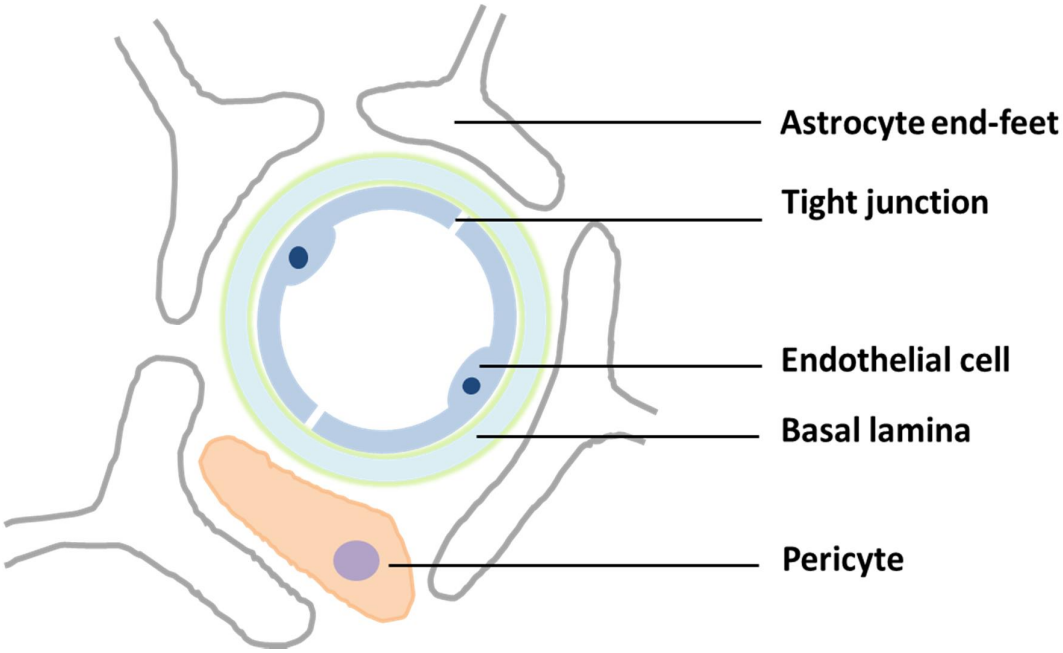

Figure 1.2: Structure of the blood-brain barrier. The key feature of the BBB is tight junctions between endothelial cells which form a barrier to transport between the blood and brain fluid. Astrocyte end-feet and pericytes add to structural stability and modulate the properties of the BBB.

1.3 INFLAMMATION AND STROKE

1.3.1 POST-STROKE NEUROINFLAMMATION

Neuroinflammation occurs rapidly after stroke, and persists for weeks afterwards. Dying neurones produce "danger signals" known as danger associated molecular patterns (DAMPs) including ATP, high-mobility group box 1 (HMGB1), uric acid, heparin sulphate and heat shock protein 60 (HSP60) (Chamorro et al., 2012). DAMPs activate purine receptors, toll-like receptors (TLRs) and other DAMP receptors on microglial and endothelial cells to initiate the neuroinflammatory cascade (Iadecola and Anrather, 2011). A summary of the cascade can be seen in Figure 1.3.

1.3.1.1 MICROGLIA

Microglia are the resident phagocytic immune cells of the brain, and they rapidly become activated and proliferate following ischaemia, peaking at 48-72h after stroke (Denes et al., 2007). Resting microglia are ramified and "survey" the brain environment by extending and retracting their processes, whereas upon activation they take an amoeboid phenotype and acquire a cell surface marker profile similar to circulating monocytes and macrophages (Nimmerjahn et al., 2005; Yenari et al., 2010). Conversion of microglia to an active phenotype involves stimulation of TLR4 receptors, resulting in the up-regulation and release of pro-inflammatory mediators such as interleukin-1 (IL-1), tumor necrosis factor-α (TNF-α) and matrix metalloproteinase-9 (MMP-9), and anti-inflammatory mediators such as IL-10 and transforming growth factor-β (TGF-β) (del Zoppo et al., 2012). Additionally, activated microglia release ROS and nitric oxide (NO), and can reverse glutamate transporters resulting in increased extracellular glutamate and excitotoxicity (Yenari et al., 2010). Microglia also express a range of cytokine and chemokine receptors, allowing communication with neurones, astrocytes and endothelial cells (Hanisch, 2002).

1.3.1.2 ASTROCYTES

As well as being a key component of the BBB, astrocytes are essential in maintaining brain homeostasis. However, they are also involved in the development of neuroinflammation. Following ischaemia, astrocytes produce NO to counteract the reduction in cerebral blood flow (CBF), although this also contributes to neuronal death (Chen and Swanson, 2003). Astrocytes also produce IL-1, TNF-α, IL-6 and IL-10 in

response to stroke, and have also been shown *in vitro* to produce MMP-9 (Chen and Swanson, 2003; Thornton et al., 2006). As well as through the production of pro-inflammatory mediators, astrocytes also contribute to neuroinflammation by proliferating and forming a glial scar around the ischaemic tissue: a process known as reactive astrogliosis (Fawcett and Asher, 1999). The glial scar is thought to be both detrimental and beneficial: on one hand it prevents neuroregeneration and produces pro-inflammatory mediators, yet on the other it creates a boundary protecting the brain from further damage (Jurynec et al., 2003).

1.3.1.3 ENDOTHELIAL CELLS

Neuroinflammation results in disruption to the integrity of the BBB. MMP-9 produced by astrocytes, microglia and invading neutrophils can directly break down endothelial tight junctions, and other products of ischaemia including ATP, ROS, NO and cytokines can also contribute to increased permeability (Abbott, 2002). IL-1 and TNF-α stimulate endothelial cells to express cell adhesion molecules (CAMs) and chemokines which facilitate neutrophil and other leukocyte transmigration into the brain parenchyma (Borregaard, 2010). Transmigrated neutrophils release ROS, MMP-9 and cytokines which further propagate the neuroinflammatory response (Jin et al., 2010). The infiltration of peripheral cells will be discussed in more detail later. Increased permeability of the BBB also facilitates oedema, as fluid leaks into the brain tissue causing it to swell. Oedema is responsible for a large proportion of deaths in stroke patients (Balami et al., 2011).

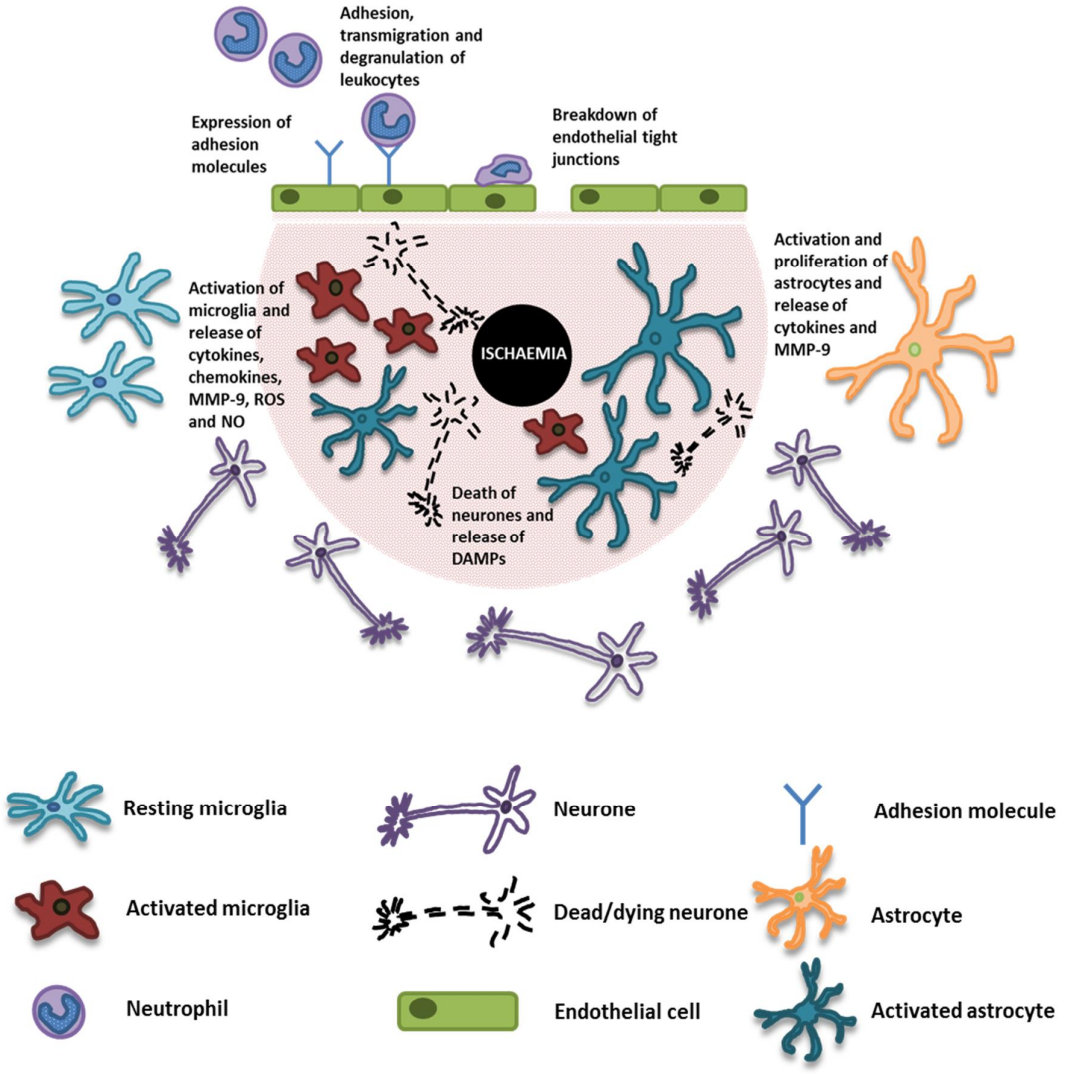

Figure 1.3: The neuroinflammatory cascade after cerebral ischaemia. The ischaemic insult results in neuronal death, causing release of DAMPs. DAMPS activate microglia which become phagocytic and release cytokines, chemokines, MMP-9, ROS and NO. Cytokines such as IL-1 and TNF-α activate astrocytes, which release further cytokines and MMP-9, and endothelial cells, which up-regulate expression of adhesion molecules. Leukocytes such as neutrophils adhere to the endothelium and transmigrate and release further cytokines and MMP-9 resulting in destruction of the BBB.

1.3.2 PRE-STROKE SYSTEMIC INFLAMMATION

The vast majority of stroke patients have an array of underlying risk factors or co-morbidities, including obesity, atherosclerosis, diabetes, infection and hypertension. In the general population, 60-80% of the risk of stroke is thought to be due to these factors (Emsley and Hopkins, 2008; Hankey, 2006). Clinically, these co-morbidities both increase the risk of having a cerebrovascular event and are correlated with a worse outcome, and there is extensive experimental data to back this up (reviewed in (McColl et al., 2009)). The common feature of these co-morbidities is that they are all associated with a raised peripheral inflammatory profile, either chronically or in acute bursts, such as in infection. This pre-existing inflammation can alter the aetiology of stroke, and it is important to consider the impact of a raised inflammatory profile when modelling stroke in pre-clinical experiments. Suggested mechanisms for the exacerbation of stroke by peripheral inflammation include heightened acute phase response (APR) initiation and recruitment of neutrophils (McColl et al., 2007), increased plasma C-reactive protein (CRP) levels (Emsley et al., 2003), increased BBB breakdown and oedema (Dénes et al., 2011) and increased plasma IL-6 and monocyte chemoattractant protein-1 (MCP-1) (Terao et al., 2008). In addition, peripheral inflammation can cause activation of brain cells including microglia, which could play a part in initiating a heightened inflammatory response and excessive ischaemic damage following stroke (Perry, 2004).

1.4 THE CELLULAR INFLAMMATORY RESPONSE

The inflammatory response is initiated by a diverse set of immune cells, which are derived from pluripotent self-renewing haematopoietic stem cells in the bone marrow. More than 10^9 mature blood cells are produced every day, and these bone marrow-derived cells undergo maturation in primary or secondary lymphoid organs of the body (Petvises and O'Neill, 2012). Over 60% of blood cells produced in the bone marrow are monocytes or granulocytes (Borregaard, 2010). During inflammation, immune cells are released into the blood, where they migrate to the site of damage or infection. Here they release soluble inflammatory mediators and express co-stimulatory and adhesion molecules. This cellular inflammatory response involves many subtypes of immune cells which work together to combat the insult. Myeloid cells initiate the early inflammatory response as part of the innate immune system. Lymphoid cells are

involved in adaptive immune responses, and the formation of an immune memory. Figure 1.4 details the development of the main immune cell lineages from stem cells:

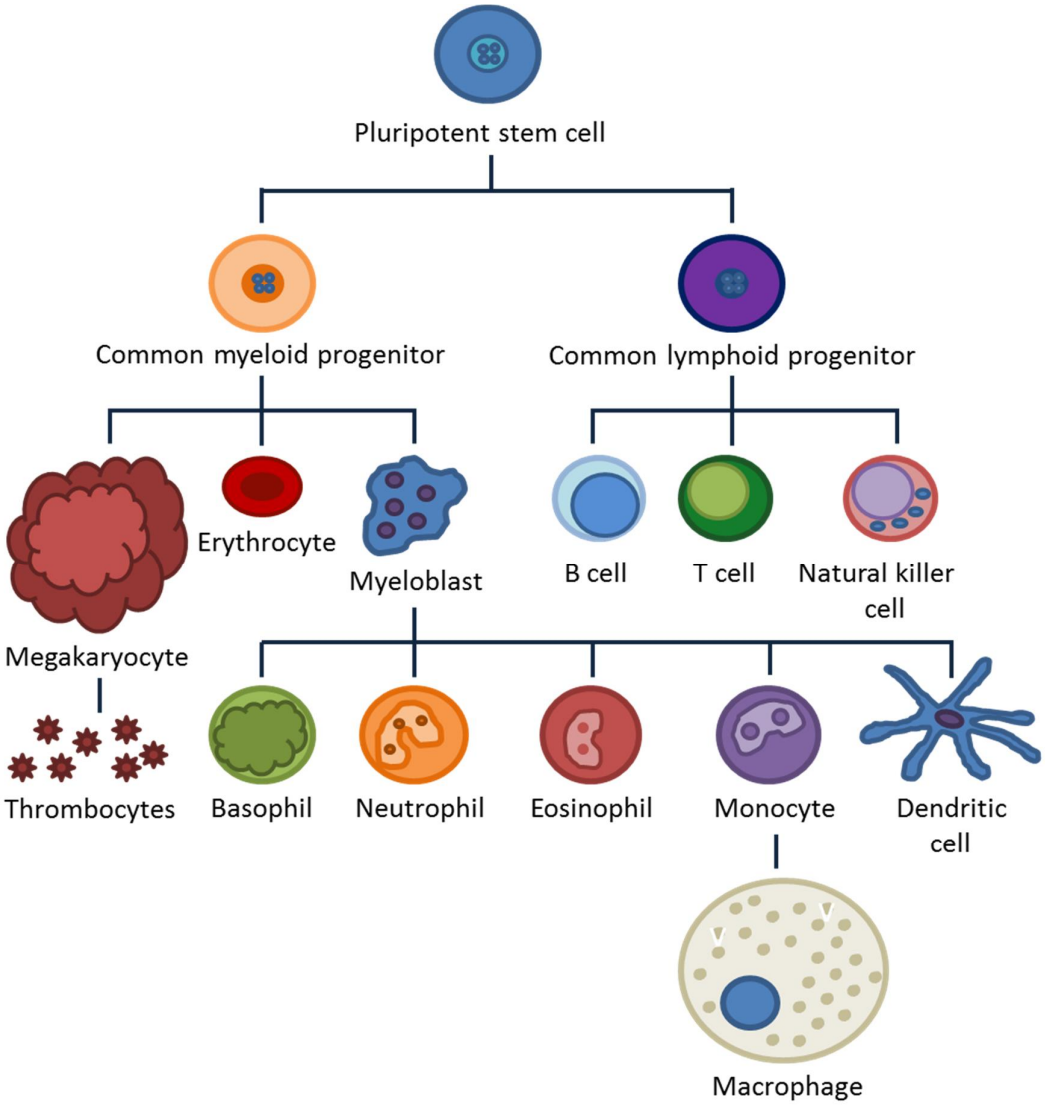

Figure 1.4: Haematopoiesis. All cells of the immune system are derived from pluripotent stem cells which reside in the bone marrow in adult mammals. Common myeloid and lymphoid progenitor cells differentiate to form mature immune cells, which enter the circulation to monitor and combat insults. The myeloid lineage gives rise to granulocytes, which include basophils, neutrophils and eosinophils. These cells contain granules in their cytoplasm, which contain factors that help to combat and resolve attacks when released during the immune response. Monocytes circulate in the blood and infiltrate tissue where they differentiate into macrophages. Dendritic cells present antigens to aid communication between the innate and adaptive immune systems. The lymphoid lineage of cells contribute to adaptive immune responses, whose primary function is the recognition and subsequent destruction of 'non-self' antigens and formation of the immunological memory.

It is possible to distinguish subpopulations of immune cells by the presence of cell surface markers. Each cell-type expresses a unique combination of markers in the plasma membrane, which can be taken advantage of by the use of antibodies during the process of flow cytometry. Flow cytometry analyses the combinations of cell surface markers expressed in a sample and uses it to deduce the immune cell populations present. Table 1.1 shows some of the cell surface markers used for analysis of samples:

	CD3	CD4	CD8	CD11b	CD19	CD45	CD115	Ly6G	MHCII
All T cells	+	-	-	-	-	+	-	-	-
T cells (helper)	+	+	-	-	-	+	-	-	-
T cells (cytotoxic)	+	-	+	-	-	+	-	-	-
B cells	-	-	-	-	+	+	-	-	+
Macrophages	-	-	-	+	-	+	+	-	+
Monocytes	-	-	-	+	-	+	+	-	-
Granulocytes	-	-	-	+	-	+	-	+	-

Table 2.1: Cell surface markers used for characterisation of immune cell subsets. Immune cell subtypes have differential expression of cell surface markers. This quality is assessed by flow cytometry with the use of fluorescently-conjugated antibodies against specific cell surface markers to identify the populations of leukocytes present in a sample.

Phagocytosis is the principal role of many of the inflammatory cells of the myeloid lineage, in particular mononuclear phagocytes and granulocytes. Circulating phagocytes include monocytes and neutrophils, and tissue-residing phagocytes include different types of macrophages and microglia, the latter being specific to the brain. Neutrophils appear to be the subset of immune cells that are recruited to the site of damage first, where they accumulate in large quantities (Kennedy and DeLeo, 2009). As well as through phagocytosis, neutrophils contribute to the inflammatory response by releasing a variety of inflammatory mediators. These molecules aid in the recruitment of further immune cells such as monocytes and the highly phagocytic macrophages, which are involved in the maintenance of chronic inflammation (Chaplin, 2010). The diverse cells of the immune system work in synergy with molecular mediators to combat and destroy invading pathogens and to restore homeostasis.

1.5 NEUTROPHILS

Neutrophils are polymorphonuclear myeloid leukocytes, and are generally the first cells to be recruited to the site of injury or infection (Kennedy and DeLeo, 2009). They are much more prevalent in humans than in mice: in humans they make up 50-70% of circulating leukocytes, whereas in mice they only account for 10-25% of white blood cells (Mestas and Hughes, 2004).

1.5.1 RETENTION AND RELEASE

Neutrophils are produced in the bone marrow and are released into the circulation in response to inflammatory stimuli. One of the main retention signals in the bone marrow is the CXCL-12/CXCR-4 axis (Martin et al., 2003). CXCL-12 (SDF-1α) is constitutively expressed at high levels in bone marrow stromal cells, whereas its receptor CXCR-4 is expressed on the surface of neutrophils (Furze and Rankin, 2008; Shirozu et al., 1995). Activation of CXCR-2 by its ligands CXCL-1 (KC), CXCL-2 (MIP-2) and CXCL-8 (interleukin-8 (IL-8)) antagonises signalling through CXCR-4, reducing retention signals and promoting the trafficking of neutrophils towards the vasculature (Eash et al., 2010). These three chemokines are all produced by bone marrow stromal cells in response to pro-inflammatory stimuli such as IL-1 and TNF-α, resulting in efflux of neutrophils into the vasculature (van Eeden and Terashima, 2000). Granulocyte-colony stimulating factor (G-CSF) is another potent stimulator of neutrophil release from the bone marrow into the circulation, thought to occur via down-regulation of the expression of CXCL-12 (Wengner et al., 2008). There is strong neural input into the bone-marrow, and there is evidence for some level of central regulation of neutrophil release into the circulation (Afan et al., 1997; Dénes et al., 2005; Shepherd et al., 2005). These humoral and neural signals must be tightly controlled to allow an appropriate neutrophil response to infection or injury.

1.5.2 GRANULES

Neutrophils contain granules full of proteins that can digest tissue and kill microbes (Borregaard, 2010). There are three heterogeneous types of granules, and their contents are determined by the time of formation (Le Cabec et al., 1996). Azurophilic (primary) granules contain myeloperoxidase (MPO), specific (secondary) granules contain lactoferrin, and gelatinse (tertiary) granules contain MMP-9 (Kolaczkowska and

Kubes, 2013). Granules are released by exocytosis, allowing migration of integrins to the cell surface to allow adhesion of neutrophils to the endothelium, or releasing pro-inflammatory mediators into the extracellular space (Borregaard, 2010).

1.5.3 TRANSMIGRATION OF NEUTROPHILS

When tissue-residing cells encounter a pathogen or injured tissue, they release mediators such as IL-1, TNF-α or IL-17 which result in changes to the surface of the endothelium (Ley et al., 2007). These endothelial changes are the foundation of neutrophil transmigration from the circulation into the tissue below. Endothelial cells are induced to express cell adhesion molecules P-selectin, E-selectin and integrins including intercellular adhesion molecule (ICAM) and vascular cell adhesion molecule (VCAM) on their luminal surface (Petri et al., 2008). These endothelial CAMs bind to P-selectin ligand 1, L-selectin, E-selectin ligand 1 and CD44 which are expressed on the surface of neutrophils, with different associations being prominent at the various stages of transmigration (Borregaard, 2010). These first interactions allow "tethering" to the endothelial surface and "rolling" – the first stages of neutrophil transmigration. The purpose of these stages is to localise neutrophils to the endothelial surface and to anchor them against the shear stress caused by blood flow. Neutrophil-endothelium bonds have to be carefully co-ordinated to allow smooth rolling: breaking the bond at the rear of the neutrophil must be balanced with a formation of a new bond at the front (Kolaczkowska and Kubes, 2013). "Firm adhesion" of neutrophils to the endothelial surface occurs when they encounter chemokines including CXCL-8 (IL-8) in humans, and CXCL-1 (KC), CXCL-2 and CXCL-5 in mice, which are expressed by endothelial cells in response to IL-1, TNF-α and IL-17 and are localised to the endothelium by binding to negatively charged heparin sulphates (Borregaard, 2010; Massena et al., 2010). These chemokines activate neutrophils by signalling through CXCR-2, which changes the conformation of integrins LFA-1 and MAC-1 on the neutrophil's surface, allowing stronger interaction with endothelial ICAMs (Phillipson et al., 2006). Following firm adhesion, neutrophils "crawl" along the endothelial surface to find a preferred point of paracellular migration, which is mediated by interactions between MAC-1 and ICAMs (Phillipson et al., 2006). Paracellular migration is a hugely complex process involving a large range of CAMs, including ICAMS, platelet endothelial cell adhesion molecule-1 (PECAM-1), JAMs, endothelial cell-selective

adhesion molecule (ESAM), poliovirus receptor (PVR), CD99, CD99L2 and VE-cadherin (Borregaard, 2010). Transcellular migration occurs in up to 20% of neutrophils, but much less is known about the mechanisms involved, although evidence suggests a key role for SNARE proteins (Carman et al., 2007). Once neutrophils have crossed the endothelial layer, they release proteases including elastase, MMP-8 and MMP-9 to break down the basement membrane and allow invasion into the underlying tissue (Borregaard, 2010). The process of transmigration is similar in peripheral tissues and the brain, however less is known about the exact mechanisms involved in migration across the BBB. A diagrammatic representation of the stages of neutrophil transmigration is shown in Figure 1.5:

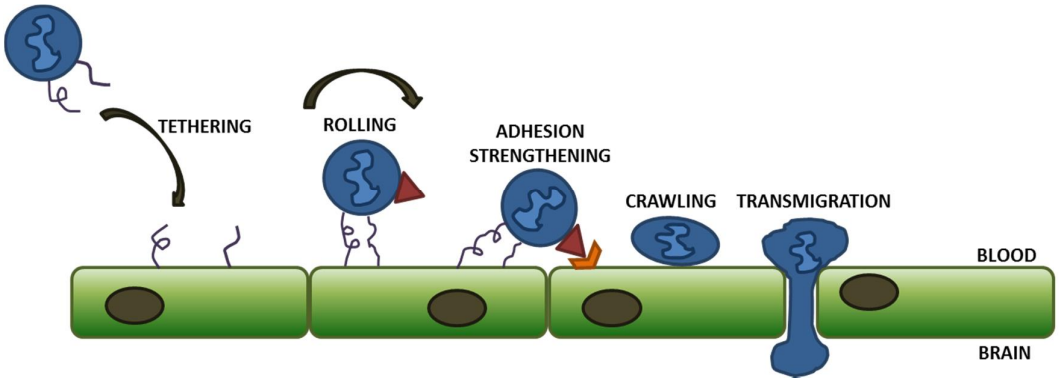

Figure 1.5: Neutrophil transmigration. During neuroinflammation, the integrity of the BBB is compromised. Endothelial cells start to express chemokines and cell adhesion molecules which contribute to the recruitment of immune cells to the endothelial surface. Cells tether, roll and crawl along the endothelium before transmigrating into the brain parenchyma.

The process of transmigration is known to be important in altering the phenotype of neutrophils. In peripheral vascular beds, transmigration induces increased production of reactive oxygen species by neutrophils and encourages degranulation (Nourshargh and Marelli-Berg, 2005). Neutrophils home to peripheral tissues under normal conditions as they “patrol” the environment. Neutrophils are not normally found within the brain parenchyma, however transmigration is triggered by IL-1, and transmigrated neutrophils acquire a neurotoxic phenotype. This neurotoxicity is mediated by release of proteases and decondensed DNA, known as neutrophil extracellular traps (NETS) (Allen et al., 2012). Neutrophils use NETS to destroy extracellular microorganisms: NETS immobilise pathogens allowing phagocytosis, but are also directly antimicrobial through histones and proteases attached to the DNA ”trap” (Papayannopoulos and Zychlinsky, 2009). However this protective function becomes detrimental in the brain, where NET-derived proteases contribute to neurotoxicity after an insult such as stroke.

1.6 POST-STROKE LEUKOCYTE RECRUITMENT

Following the induction of neuroinflammation, peripheral immune cells are recruited to the brain where they contribute to and prolong the inflammatory response. This thesis will focus on the role of neutrophils, however other cell subtypes will be discussed briefly below.

1.6.1 NEUTROPHIL RECRUITMENT

Neutrophils are the first cells to be recruited to the ischaemic brain, invading from 30 min after stroke. Infiltration peaks at 3 days but can continue for 2 weeks (Jin et al., 2010). Clinically, neutrophil recruitment into the ischaemic area is correlated with the extent of the damage and is associated with poor outcome (Akopov et al., 1996; Buck et al., 2008; Price et al., 2004). Neutrophils might contribute to exacerbation of ischaemic damage in a variety of ways, including production of ROS, production of pro-inflammatory cytokines and chemokines, release of proteolytic enzymes including MMP-9 and up-regulation of endothelial CAMs (Jin et al., 2010). Experimentally, numerous studies have shown protection in terms of lesion volume, functional outcomes, oedema and mortality by blocking CAMs and subsequently neutrophil transmigration. Examples of successful pre-clinical trials include blockade of ICAM-1 (Kitagawa et al., 1998; Zhang et al., 1995), Mac-1 (CD11b/18) (Chopp et al., 1994; Soriano et al., 1999; Zhang et al., 2003) and P-selectin (Ishikawa et al., 2004). However equally there have been studies in which blockade of neutrophils has had no effect on stroke outcome (Hayward et al., 1996; Takeshima et al., 1992). Neutrophil recruitment has been implicated as being particularly important in the pathogenesis of stroke when there is a raised systemic inflammatory profile. In a mouse model of peripheral inflammation, treatment with systemic IL-1β caused an exacerbated lesion and worse damage to the BBB, and it was shown that neutrophils and neutrophil-derived MMP-9 are required for this exacerbation (McColl et al., 2007, 2008). In the clinic, stroke patients who have had an infection in the previous weeks show elevated white blood cell counts and platelet-leukocyte interactions, and it is possible that this neutrophil-rich raised immune profile could contribute to the ischaemic cascade (Emsley et al., 2003; Zeller et al., 2005). Furthermore it was shown that patients with elevated circulating neutrophils were more likely to have neurological deterioration and poor functional outcomes (Kumar et al., 2012). One argument against neutrophils

participating in the development of ischaemic damage is that they infiltrate after the full progression of the lesion (Easton, 2013). However in the IL-1 exacerbation model it was clearly shown that neutrophils infiltrate the brain before the full evolution of ischaemic damage (McColl et al., 2007).

Another way in which neutrophils can contribute to ischaemic damage is through the "no-reflow" phenomenon. This occurs when endothelial cells in microvessels become activated and express CAMs, allowing adhesion of circulating neutrophils. The small diameter of the vessel means that flow past adherent neutrophils is disrupted (del Zoppo et al., 1991). Blocking neutrophil-endothelium interactions with an anti-CD18 antibody to prevent integrin-ICAM-1 binding protects against the blockage of microvessels (Mori et al., 1992). To exacerbate the blockage further, fibrin is produced allowing adherence of activated platelets and further aggregation (del Zoppo, 2008). This platelet-mediated blockage can be reduced by blocking platelet-fibrin interactions, although of course there is a need to be cautious when interfering with platelets so as to avoid haemorrhagic transformation (Abumiya et al., 2000).

Overall there is strong evidence for a detrimental role for neutrophils in the development of ischaemic injury. The broad aim of this thesis will be to use pharmacological interventions to reduce the impact of neutrophil-mediated damage.

1.6.2 Monocyte and macrophage responses in stroke

Monocytes are myeloid cells which transform into macrophages when they invade tissue. Due to the similarity in cell surface marker proteins between microglia, monocytes and macrophages it is difficult to distinguish the origin of such cells without the use of markers for blood-borne cells, such as green fluorescent protein (GFP) bone marrow chimeric mice. Such studies have revealed a more delayed invasion of blood-derived monocytes than neutrophils, with infiltration peaking at 4 days after stroke (Schilling et al., 2005). It has also been shown that resident microglia seem to play an earlier and more central role in phagocytosis than blood-derived macrophages (Schilling et al., 2003; Schilling et al., 2005). This delayed invasion of monocytes suggests that they are not pivotal in the evolution of ischaemic damage, however they might play a role in the propogation of neuroinflammation or in reparative processes. In human stroke patients, monocyte levels were shown to increase in the blood but had reduced expression of antigen-presenting molecules and TNF-α, which was correlated to an increased risk of post-stroke infection (Urra et al., 2009). A potential role for resident macrophages of the brain, e.g. perivascular macrophages, is currently under investigation, and might reveal a function in the initiation and propagation of neuroinflammation (Chiba and Umegaki, 2013).

1.6.3 T CELLS IN STROKE

T lymphocytes are bone marrow-derived and are a key cell type of the adaptive immune system. There are a multitude of subtypes of mature T cells: broadly they are divided into CD3+CD4+ T helper cells, which are not directly cytotoxic but help to organise an immune response, and CD3+CD8+ cytotoxic T cells which directly kill pathogens (Seder and Ahmed, 2003). T cells have not been investigated as extensively in stroke as myeloid cells, however there are numerous reports of T cell deficient mice having smaller lesion volumes and improved functional outcomes compared to controls (Hurn et al., 2007; Kleinschnitz et al., 2010; Shichita et al., 2009; Yilmaz et al., 2006b). T cells and the adaptive immune system become activated in stroke when brain antigens are released by dying cells or are presented by microglia, infiltrating macrophages or dendritic cells (Hanisch and Kettenmann, 2007). Further work aimed to elucidate the contributions of T helper and cytotoxic T cells, and it was found that both subtypes contribute to the development of ischaemic injury (Liesz et al., 2011; Yilmaz et al., 2006a). However, γδT cells and natural killer (NK) T cells have been shown to not contribute to ischaemic brain damage, and the role of regulatory T cells in stroke is the topic of much debate (Brait et al., 2012; Kleinschnitz et al., 2010). T cells accumulate in the brain from 24h after stroke, and numbers peak at 72h (Brait et al., 2010; Schroeter et al., 1994). The mechanisms of T cell-mediated brain damage are not known, although it is possible that they have actions similar to other leukocytes, through the release of cytokines, chemokines and ROS (Brait et al., 2012). Although it seems that some subtypes of T cell do have a role in stroke pathogenesis, therapies targeting the adaptive immune system should be used with caution, due to the presence of stroke-induced immunosuppression seen in many patients leaving them susceptible to infection.

1.6.4 B CELLS IN STROKE

There is limited detail in the literature surrounding the role of B cells in stroke. However, one group has recently shown that B cell deficient mice do worse after MCAo, and that B cells are beneficial to stroke due to their production of IL-10 (Bodhankar et al., 2013).

1.7 Main molecular elements of the inflammatory response

The recruitment of immune cells and the overall control of the inflammatory response are regulated by inflammatory mediators. When immune cells encounter pathogenic products, such mediators are synthesised and secreted, following which they destroy pathogens and recruit further immune cells to the site of damage (Wood, 2006). There is a diverse range of different mediators involved in the inflammatory response, the main groups of which will be discussed in further detail below.

1.7.1 Cytokines

Cytokines are proteinaceous inter-cellular signalling compounds, which are secreted from immune cells and act locally to activate plasma membrane receptors on target cells (Luheshi et al., 2009). A defining feature of inflammatory cytokines is that they are normally expressed at extremely low levels, and are rapidly up-regulated in response to tissue damage or infection, where they work as a "cytokine cocktail" to mediate a vast array of different physiological effects. As cytokines work by binding to specific cell-surface receptors, their effects vary depending on the type and combinations of receptors expressed by the target cell. Cytokines are separated into various families, the main ones being ILs, interferons (IFN), TNF, growth factors (GF) and chemokines (Wood, 2006). Interleukins are a diverse group of cytokines, including members IL-1 to IL-37, some of which are pro-inflammatory and others which have anti-inflammatory effects. IL-1 is perhaps the most heavily-researched of the interleukins, and will be explained in more detail below.

1.7.1.1 Interleukin-1

IL-1 is a pro-inflammatory cytokine implicated in a number of disease states. The IL-1 family includes three distinct proteins; the agonists IL-1α and IL-1β, as well as the naturally-occurring antagonist IL-1Ra (Allan et al., 2005). All three cytokines are produced via cleavage from precursor proteins by proteases including calpains and caspases (Carruth et al., 1991; Thornberry et al., 1992). IL-1 mediates its effects by binding to the type I receptor (IL-1R1), which is a member of the TLR superfamily (O'Neill and Dinarello, 2000). Binding of IL-1 and recruitment of the IL-1 receptor accessory protein (IL-1RAcP) to form a complex with IL-1R1 leads to the expression of pro-inflammatory proteins via the transcription factor NF-κB (Korherr et al., 1997). IL-1

is able to initiate a pro-inflammatory cascade and is used frequently in models of inflammation. It has been shown that systemic delivery of IL-1 exacerbates ischaemic damage, and this model will be used in this work (McColl et al., 2007).

1.7.2 CHEMOKINES

Chemokines are small proteins of around 8-17kDa, with their hallmark feature being their chemotactic properties (Lazennec and Richmond, 2010). Chemokines create concentration gradients, which facilitate the recruitment and guided migration of immune cells such as neutrophils and monocytes to the site of damage via binding to G protein-coupled receptors (GPCR) (Le et al., 2004). Although most chemokines are pro-inflammatory, some also have important roles in development and homeostasis. The chemokine nomenclature system separates the molecules into four subgroups: C, CC, CXC and CX_3C (Zlotnik and Yoshie, 2000). This classification is based on the conformation of two conserved cysteine residues in the N-terminal of the protein depending on whether they have other amino acids between them in the sequence. Members of the CXC family are involved in several inflammatory processes, such as neutrophil recruitment, and the CC family promotes the trafficking of monocytes (Mirabelli-Badenier et al., 2011). Chemokines are also thought to be important mediators of neuro-immune communication (reviewed in (Rostène et al., 2011)).

1.8 The Acute Phase Response

The innate immune response is part of the body's early defence against invading pathogens or tissue damage. This early defence system launches a systemic reaction, known as the acute phase response (APR), which aims to clear the pathogen, restore homeostasis and promote healing (Cray et al., 2009). The APR results in a number of symptoms such as fever, leukocyte trafficking, increased vascular permeability and augmentation of host defences (Baumann and Gauldie, 1994). These symptoms are thought to be initiated in part by pro-inflammatory cytokines such as IL-1, which promote neural and neuroendocrine responses to heighten innate immunity and initiate the metabolic changes necessary to restore homeostasis (Borghetti et al., 2009). Cytokines also induce the production of a number of plasma proteins in the liver, which assist in the immune response. These proteins are called acute phase proteins (APP), and have a vast range of effects, including moderating inflammatory processes, acting as transport molecules and aiding tissue healing (Tilg et al., 1997). Examples of APPs include CRP (mostly in humans), serum amyloid A (SAA) (in humans and mice), plasminogen and IL-1Ra (Baumann and Gauldie, 1994). Elucidating the exact processes carried out by each of the APPs is a complex task, but could ultimately provide a viable therapeutic target for manipulation of the immune response.

1.9 STROKE-INDUCED PERIPHERAL INFLAMMATION

Previously it was thought that stroke is purely a condition of the brain, whereas in fact an ischaemic attack launches a full body response. Clinically, stroke patients present with elevated levels of plasma CRP, leukocytes and IL-6, regardless of whether or not pre-stroke infection was present (Emsley et al., 2003). Additionally, a positive correlation was found between peak plasma IL-6 levels and the size of brain infarct at 3 months, as well as a correlation with stroke severity and functional outcomes (Smith et al., 2004).

Experimental stroke results in increased plasma concentrations of cytokines including IL-6, IFN-γ and MCP-1 and a raised inflammatory profile in the spleen and lymph nodes (Offner et al., 2006). Investigating the peripheral response in more detail revealed that it peaks at 4h after stroke – far earlier than the central inflammatory response which peaks at 24h (Chapman et al., 2009). In this study CXCL-1 (KC) was found to increase dramatically after stroke in the blood, lung and liver, with a much later induction in the brain, suggesting a role for this chemokine in setting up gradients and organising mobilisation of neutrophils and recruitment to the brain.

Peripheral inflammatory responses could be vital for the initiation of a central response, and so offer important and accessible therapeutic targets for the treatment of stroke.

1.10 POST-STROKE IMMUNOSUPPRESSION

Post-stroke infection is a huge problem, with it being estimated that 30% of stroke patients develop some sort of infection, most commonly pneumonia or urinary tract infections (Westendorp et al., 2011). Pneumonia was shown to increase mortality in stroke patients at 30 days and 1 year after the insult (Finlayson et al., 2011). It is believed that the prevalence of infection after stroke is due to an immunosuppression induced by central activation of humoral and neural pathways including the hypothalamic-pituitary-adrenal (HPA) axis, the vagus nerve and the sympathetic nervous system (Chamorro et al., 2012). These pathways cause an overall dampening of the immune response, with decreased production of pro-inflammatory cytokines such as TNF-α, increased expression of anti-inflammatory IL-10, splenic atrophy and lymphopenia, which can leave the body susceptible to infection (Offner et al., 2009). Prophylactic antibiotic therapy is currently under trial, and a large meta-analysis concluded that it reduced the incidence of post-stroke infection by around 30%, although there was no effect on mortality (Westendorp et al., 2012). However a large clinical trial of ceftriaxone is on-going, with results expected in 2014 (Nederkoorn et al., 2011). There is also potential that treatment with antibiotics could offer neuroprotective benefits. Ceftriaxone and minocycline have both been shown experimentally to improve outcome after stroke, so there is potential that treatment with antibiotics could both reduce infection-induced complications and reduce neurological damage (Lee et al., 2009a; Rothstein et al., 2005).

1.11 TSG-6

1.11.1 TSG-6 OVERVIEW

This thesis will focus on experiments testing the therapeutic potential of an endogenous protein, tumor necrosis factor-stimulated gene 6 (TSG-6), in experimental stroke. TSG-6 is a 35kDa secreted glycoprotein comprised of Link and CUB modules, and was first described after analysis of cDNAs produced after stimulation of fibroblasts with TNF-α (Lee et al., 1990; Lee et al., 1992). Analyses of the structural components of TSG-6 have shown that most of its functions and interactions depend on the Link module, therefore in much of this work recombinant Link_TSG6 has been used. The Link module of TSG-6 comprises amino acids 37-128 (Milner et al., 2006).

1.11.2 TSG-6 BINDING PARTNERS

TSG-6 does not have a known receptor *per se*, however it mediates its effects through interactions with many binding partners. TSG-6 interacts with a range of glycosaminoglycans (GAGs) including hyaluronan, heparin, heparan sulphate, dermatan sulphate and chondroitin-4-sulphate, all of which apart from hyaluronan and heparin are attached to a core protein (Milner et al., 2006). These GAGs have widespread functions arising from interactions with matrix proteins, proteases, lipases, lipoproteins, growth factors, cytokines, chemokines, collectins and antimicrobial peptides (Park et al., 2000). TSG-6 binding through its Link module to hyaluronan results in cross-linking and formation of a rigid matrix, which is thought to impact on signalling through CD44 and subsequent leukocyte migration (Lesley et al., 2004). The function of TSG-6-heparin interactions is unknown, although heparin can affect the ability of TSG-6 to carry out another of its functions relating to inter-alpha-inhibitor (IαI). TSG-6 can potentiate the serine protease inhibitory activity (resulting in inhibition of plasmin) of IαI from 5% to 40%, and this effect is increased further in the presence of heparin (Mahoney et al., 2005). It is thought that this anti-plasmin activity plays a role in remodelling of the extra-cellular matrix (ECM), as plasmin normally activates MMPs allowing degradation of the ECM (Verma and Hansch, 2007). In addition to binding to GAGs, the Link module of TSG-6 can interact with proteins including thrombospondin-1 (involved in wound repair), pentraxin-3 (an acute phase protein), RANKL (involved in osteogenesis and dendritic cell maturation) and bone morphogenic proteins (Kuznetsova et al., 2005; Leali et al., 2012; Mahoney et al., 2008).

1.11.3 TSG-6 EXPRESSION

TSG-6 is not generally expressed constitutively, although it is stored under normal conditions in human neutrophil granules, and is expressed in human skin and in mouse bone marrow (although this might be due to the presence of neutrophils) (Mahoney et al., 2008; Maina et al., 2009; Tan et al., 2011). TSG-6 expression is up-regulated in inflammatory conditions in response to stimuli including IL-1, TNF-α, lipopolysaccharide (LPS), prostaglandin E2 (PGE2), IL-6, TGF-β and INF-γ (reviewed in (Milner and Day, 2003)). TSG-6 has been identified in a vast range of cell types, including fibroblasts, synoviocytes, neutrophils, dendritic cells, macrophages, mast cells, epithelila cells, endothelial cells, smooth muscle cells, chondrocytes and mesenchymal stem cells (MSCs) (Choi et al., 2011; Fessler et al., 2002; Lee et al., 2001; Lee et al., 1992; Lilly et al., 2005; Maina et al., 2009; Malcolm et al., 2003; Nagyeri et al., 2011; Wisniewski et al., 1993). Anti-inflammatory stimuli IL-4 and IL-10 can also down-regulate expression of TSG-6 (Maina et al., 2009). TSG-6 has not been extensively studied in the brain, although cerebral expression has been identified in samples from human stroke patients, although this was thought to be mainly from invading leukocytes (Al'Qteishat et al., 2006).

1.11.4 TSG-6 IN INFLAMMATION

TSG-6 was chosen for this thesis to study in the context of stroke due to its anti-inflammatory properties. A role for TSG-6 in inflammation was first proposed due to its expression in inflammatory situations. The bulk of the research investigating TSG-6 in inflammation has focussed on arthritis: TSG-6 was found to be absent in the synovial fluid of normal subjects, but was highly prevalent in the joint fluid and blood (at lower levels) of patients with arthritis (Wisniewski et al., 1993). Additionally, plasma concentrations of TSG-6 were found to correlate with the severity of disease progression in a mouse model of arthritis (Nagyeri et al., 2011). TSG-6 is also implicated in fertility and ovulation: inflammation-like processes. TSG-6 knockout mice (TSG-$6^{-/-}$) are infertile, and TSG-6 expression has been reported in the ovary during ovulation (Fülöp et al., 1997; Fülöp et al., 2003; Yoshioka et al., 2000). The expression of TSG-6 in response to inflammatory stimuli, and its presence in inflammatory scenarios point to a role in the modulation of inflammation. Further work in animal models of inflammation has helped to elucidate this further, and will be discussed in more detail below.

Intraperitoneal treatment with recombinant TSG-6 led to amelioration of symptoms in an animal model of collagen-induced arthritis, including footpad swelling, overall disease incidence, arthritis index and histological assessments of arthritis severity (Mindrescu et al., 2000). In a different model of arthritis (proteoglycan-induced arthritis), intravenous administration of TSG-6 had no effect on incidence or time of onset of disease. However TSG-6 treatment resulted in long term improvements in joint oedema, with no effect on the systemic inflammatory profile being detected (Bárdos et al., 2001). In another study, transgenic mice with cartilage-specific expression of TSG-6 displayed less joint damage than wild-type mice after antigen-induced arthritis, and showed a better recovery with cartilage showing almost no sign of damage (Glant et al., 2002). Interestingly in this study there was no direct anti-inflammatory action of TSG-6 in terms of changes in cytokine expression or leukocyte infiltration, however TSG-6 exerted its beneficial effect by inhibiting MMPs and thereby preserving joint integrity. TSG-$6^{-/-}$ knockout mice also showed a more severe response to proteoglycan-induced arthritis than their wild-type counterparts, with heightened cartilage destruction, deformities of the joint and bone erosion.

Furthermore, the knockout mice had increased levels of circulating IL-6 and SAA, suggesting a raised systemic inflammatory profile (Szántó et al., 2004). In this study the effect of TSG-6 on neutrophils was highlighted: TSG-6 knockout mice had increased neutrophil infiltration into the arthritic joint, which was reversible with addition of recombinant TSG-6. An inhibitory effect on neutrophil migration was also observed in a model of corneal damage: rats treated with TSG-6 displayed decreased extent of injury, lower expression of cytokines, decreased MMP-9 expression and reduced infiltration of neutrophils (Oh et al., 2010). This study also demonstrated a reduction in circulating neutrophils for 3 days after injury. TSG-6 also improved lesion size and expression of pro-inflammatory cytokines in a mouse model of retinal injury, although neutrophil migration was not studied in this publication (Tuo et al., 2012). TSG-6 reduced the extent of neutrophil invasion in the air-pouch model in response to IL-1 or zymosan (Getting et al., 2002; Wisniewski et al., 1996). Crucially for this thesis, the work by Getting et al. concluded that the inhibitory effect of TSG-6 on neutrophil migration can be replicated with treatment solely with the Link module of the protein. In addition to reduced neutrophil infiltration, mice treated with TSG-6 had decreased expression of KC, TNF-α and PGE2, suggesting a broadly anti-inflammatory action of TSG-6 (Getting et al., 2002). Link_TSG6 was also demonstrated as a potent inhibitor of neutrophil migration and KC expression in a model of IL-1-induced peritonitis (Cao et al., 2004). In the non-obese diabetic (NOD) mouse model of diabetes, TSG-6 delayed the onset of spontaneous autoimmune diabetes, and inhibited the activation of T cells and antigen-presenting cells, adding to the profile of anti-inflammatory effects that TSG-6 is able to exert (Kota et al., 2013).

Until recently, the protective effects of TSG-6 had only been demonstrated in peripheral inflammatory challenges. However, it was recently shown that intravenous TSG-6 resulted in improved outcome after traumatic brain injury, with mice treated with TSG-6 displaying reduced neutrophil infiltration, decreased lesion volume, reduced expression of MMP-9, improved BBB integrity and long-term improvements in memory and functional outcomes (Watanabe et al., 2013). In addition, TSG-6 delivered into the lateral ventricle was recently shown to improve neurological score, functional improvement and cortical expression of pro-inflammatory cytokines and neutrophil elastase after cardiac arrest-induced global ischaemia (Lin et al., 2013).

Many of these published studies have demonstrated a beneficial therapeutic effect of TSG-6 due to its inhibitory effect on neutrophil migration, and it is this property that will be investigated in this thesis. In addition, many researchers have demonstrated therapeutic potency of mesenchymal stem cells (MSCs) in a range of inflammatory diseases, and have attributed their protective effect to production of TSG-6. The relationship between MSCs and TSG-6 will be discussed in more detail later.

1.11.5 TSG-6 MECHANISMS OF ACTION

As eluded to in the above sections, TSG-6 has a wide range of properties and a variety of mechanisms of action have been proposed in each of the studies described. TSG-6's potentiation of IαI-induced inhibition of plasmin has been proposed as a potential mechanism involved in attenuating neutrophil migration, however it was shown that this property is maintained in the absence of TSG-6-IαI interactions. Furthermore this study also concluded that binding with hyaluronan is not required for the anti-neutrophil effect (Getting et al., 2002). TSG-6 is known to activate CD44 (found on macrophages), and through this can down-regulate TLR2 signalling, resulting in decreased expression of NFκB-induced cytokines and chemokines including IL-6, CXCL8 and CCL2. This was proposed as a mechanism of TSG-6-induced inhibition of neutrophil migration (Choi et al., 2011). However, TSG-6 is able to inhibit trans-endothelial neutrophil migration in *in vitro* assays in the absence of macrophages, therefore it is likely that the mechanisms of action of TSG-6 are more diverse than this (Cao et al., 2004). The role of TSG-6 in ECM stability and remodelling might have an indirect effect on neutrophil migration: inhibition of MMPs and interaction with pentraxin-3 both support the integrity of the ECM, which is incompatible with neutrophil transmigration (Mahoney et al., 2005; Maina et al., 2009).

Full understanding of the mechanisms of action of TSG-6 is still lacking, with further research on-going to try and elucidate it further. Despite the lack of clear knowledge of how TSG-6 mediates its inhibition on neutrophil migration, this property will still be exploited and explored in this work.

1.12 MESENCHYMAL STEM CELLS

As mentioned above, there have been many reports of MSCs being used therapeutically in a range of inflammatory diseases, with their potency often being attributed to their production of TSG-6. In this thesis, MSCs will be explored as a potential systemic immunomodulatory tool in experimental stroke.

1.12.1 MSC ORIGIN AND CHARACTERISATION

Stem cells are unspecialised, and are able to differentiate into a range of different cell types whilst retaining the ability to self-renew, creating a constant source of new cells. MSCs are found in a multitude of tissues within the body, but are most commonly obtained from bone marrow, adipose tissue or umbilical cord, and can be easily expanded *in vitro* (Wei et al., 2013). Whilst the majority of stem cell research has focussed on pluripotent embryonic stem cells, there has been a surge in interest in MSCs, partly due to the lack of ethical or teratoma concerns. The differentiation potential of MSCs is generally more limited than that of embryonic stem cells, although they readily differentiate into the mesodermic chondrogenic, osteogenic and adipogenic lineages, and can be manipulated to differentiate into ectodermic and endodermic lineages such as neurones, myocytes and hepatocytes (Chamberlain et al., 2007; Wakitani et al., 1995; Woodbury et al., 2000).

In 2006, the Mesenchymal and Tissue Stem Cell Committee of the International Society for Cellular Therapy published a set of guidelines for the characterisation of MSCs, due to concerns that research was not always being carried out with truly multipotent MSCs (Dominici et al., 2006). There are three main criteria which must be characterised before any experiments are carried out using MSCs. Firstly, MSCs must adhere to tissue culture plastic. Secondly, MSCs must have a specific cell surface marker profile: positive for CD73, CD90 and CD105 and negative for CD14, CD34 and CD45. Thirdly, MSCs must demonstrate their potential for tri-lineage differentiation into adipocytes, chondroblasts and osteoblasts. It was proposed that these robust standards would help to further research and discovery into the therapeutic potentials of MSCs (Dominici et al., 2006).

1.12.2 PARACRINE ACTIONS OF MSCS

Early research into MSCs focussed on manipulating their regenerative potential to engraft and replace tissue damaged and lost by disease (Pittenger et al., 1999). However, more recently the focus has shifted to trying to harness the paracrine and immunomodulatory potential of MSCs, and to manipulate their potent and varied anti-inflammatory secretome. MSCs have diverse effects on both the innate and adaptive immune systems, and therefore have been investigated as a potential therapy in a wide range of inflammatory diseases (English, 2013). Emerging evidence suggests that MSCs are able to sense cues in the environment and react as effector cells to modulate inflammation.

In *in vitro* assays, MSCs have been shown to be able to migrate in response to cues including complement proteins, growth factors, cytokines and chemokines (English, 2013). However, the same migratory potential of MSCs has not always been evident *in vivo*, and in many cases a beneficial effect seems to have been exerted from a distance, for example after entrapment in the lung (Lee et al., 2009b; Roddy et al., 2011). However, migration of MSCs was seen *in vivo* in models of kidney ischaemia and skin wounds, suggesting differential roles in different types of injury (Liu et al., 2012a; Sasaki et al., 2008). The potency of MSCs in the absence of migration or engraftment has also been demonstrated through experiments using conditioned media from cultured MSCs. Proteomic analysis of MSC conditioned media has revealed a vast range of factors involved in immune modulation, cell survival, cell differentiation and angiogenesis (Kupcova Skalnikova, 2013). In a model of diabetic cardiac autonomic neuropathy, conditioned media from MSCs was shown to exert the same level of beneficial effect as transplanted MSCs (Wang et al., 2013). Conditioned media also protected against photo-aging from UVA and UVB radiation in mice (Liu et al., 2013). Hepatocytes cultured after acute lung injury were shown to undergo less apoptosis in the presence of conditioned MSC media than control media, preceded by a rise in expression of IL-6 (Xagorari et al., 2013). The paracrine action of MSCs was highlighted in one study investigating renal injury: MSCs were delivered intravenously, intraperitoneally or into the renal subcapsular space. A tiny minority of MSCs migrated to the kidneys after intravenous administration, but none migrated from the other two routes. Despite this, renal morphology and function were protected from all three

delivery routes, and the protective effects were mimicked by application of conditioned media (Cheng et al., 2013). Other examples of models in which conditioned MSC media has shown beneficial effects include liver injury, glaucoma and ovariectomy-induced bone loss (An et al., 2013; Du et al., 2013; Manuguerra-Gagné et al., 2013). These studies and many more highlight that migration is not necessarily required for MSCs to exert beneficial therapeutic effects, and that paracrine actions can be successful even when originating distal to the site of injury.

1.12.3 Immunomodulatory effects of MSCs

The beneficial actions of MSCs have often been attributed to their ability to modulate immune responses. These immunomodulatory effects are induced by production of soluble factors or through modulation of immune cell actions.

1.12.3.1 MSC secreted factors

The full secretome of MSCs is as yet unknown, however they produce a number of key factors which are thought to play a role in modulating immune responses. PGE2 is constitutively expressed by MSCs, but is up-regulated in response to IFN-γ, TNF-α and TLR3 ligands (English et al., 2007; Waterman et al., 2010). Interestingly, the study by Waterman et al. concluded that TLR4-mediated stimulation of MSCs results in a pro-inflammatory phenotype, rather than an immunosuppressive one. MSC-derived PGE2 can suppress T cell activation *in vitro* and *in vivo* (Najar et al., 2010). Furthermore, MSC-derived PGE2 can reprogram macrophages to increase their production of anti-inflammatory IL-10 and IL-1Ra, and decrease expression of pro-inflammatory TNF-α, CXCL-2 and IL-6 (Németh et al., 2009; Ylöstalo et al., 2012). PGE2 also plays a role in inhibiting the maturation of dendritic cells (Spaggiari et al., 2009).

Another important immunomodulatory factor secreted by MSCs is NO. NO expression is stimulated by IFN-γ in combination with TNF-α or IL-1, and MSC-derived NO inhibits proliferation of T cells and induces their apoptosis (Ren et al., 2008). This study also showed that MSCs produce chemokines including CXCL-9 and CXCL-10 that bring T cells into close proximity to the MSC to maximise the effect of NO.

A further potent immunosuppressive molecule secreted by MSCs is indoleamine 2,3-dioxygenase (IDO) – an enzyme involved in breaking down tryptophan into metabolites important for the regulation of T cell proliferation (Mellor and Munn, 1999). IDO

expression is induced in MSCs after stimulation with IFN-γ or ligands for TLR3 and TLR4 (English et al., 2007; Opitz et al., 2009). MSC-derived IDO exerts a range of immunosuppressive effects, including inducing macrophage polarisation to an anti-inflammatory M2 phenotype (François et al., 2012), promotion of a Th1-Th2 T cell phenotypic switch (Ge et al., 2010), inhibition of T cell differentiation (Tatara et al., 2011) and reduction of T cell and NK cell proliferation (English et al., 2007; Spaggiari et al., 2006).

1.12.3.2 MSC SECRETION OF TSG-6

In addition to PGE2, NO and IDO, MSCs also secrete TSG-6. This was originally discovered when intravenously administered MSCs became trapped in the lung, distal to the site of inflammation, yet still had a potent beneficial effect on the model of myocardial infarction (Lee et al., 2009b). Knockdown of MSC-derived TSG-6 with siRNA reduced the beneficial effect. The therapeutic efficacy of MSCs has since been attributed to TSG-6 in a wide range of models including corneal injury (Oh et al., 2010), lung injury (Danchuk et al., 2011), diabetes (Kota et al., 2013), global ischaemia (Lin et al., 2013), traumatic brain injury (TBI) (Watanabe et al., 2013), peritoneal injury (Choi et al., 2011; Wang et al., 2012) and multiple sclerosis (Fisher-Shoval et al., 2012). The main mechanism by which MSC-derived TSG-6 has been suggested to exert its effect is by reducing the early inflammatory response through inhibiting neutrophil migration and down-regulating pro-inflammatory cytokine expression (English, 2013). Further investigations found that culturing MSCs in 3D spheroids increases their expression of TSG-6, therefore this might be a useful system to enhance the anti-inflammatory properties of MSCs (Bartosh et al., 2010).

1.12.3.3 MSC ACTIONS ON IMMUNE CELLS

MSCs can affect many different immune cells, either by contact or through secretion of the immunomodulatory factors described above. As already mentioned, MSCs have the capacity to switch macrophages from a pro-inflammatory M1 phenotype to an anti-inflammatory M2 phenotype, resulting in increased production of IL-10 and heightened phagocytic activity (François et al., 2012). MSCs have also been shown to be able to reduce microglial activation and to stimulate production of neuroprotective factors (Giunti et al., 2012; Ohtaki et al., 2008). As stated above, MSCs are able to modulate T cells by promoting a Th1-Th2 switch (Ge et al., 2010), inhibiting T cell

differentiation (Tatara et al., 2011) and reducing proliferation (English et al., 2007). In addition, MSCs promote induction of regulatory T cells, which has shown beneficial effects in allergic airway disease (Kavanagh and Mahon, 2011), type-1 diabetes (Madec et al., 2009) and inflammatory bowel disease (Zhang et al., 2009). Dendritic cells are also affected by MSCs, with maturation from monocytes and CD34+ precursors being blocked (Spaggiari and Moretta, 2013). Furthermore MSCs can inhibit maturation and migration of NK cells and inhibit their antigen-presenting capabilities (English et al., 2008; Spaggiari et al., 2006). The effect of MSCs on B cells remains unclear, with conflicting data available in the literature. Further work is needed to elucidate whether MSCs suppress or promote B cell responses during inflammation (Griffin et al., 2013).

The broad range of effects of MSCs on immune cells allows them to exert a potent and wide-reaching immunosuppressive effect, which is key to their potential as a therapy for inflammatory diseases.

1.12.4 MSCs AS A THERAPY FOR STROKE

MSCs are under investigation as a potential therapy for a vast range of diseases, and stroke is no exception. There are diverse mechanisms through which MSCs are proposed to provide benefit to the ischaemic brain. Firstly, as stroke induces a substantial immune response, both centrally and peripherally, the immunomodulatory properties described above are of much interest. It is anticipated that the secretion of anti-inflammatory molecules, the down-regulation of immune cells and the inhibition of leukocyte trafficking will dampen the on-going inflammatory challenge which contributes to brain damage after stroke (Eckert et al., 2013). It was shown that systemic delivery of umbilical cord-derived MSCs resulted in lower numbers of immune cells in the brain after experimental stroke and decreased expression of pro-inflammatory cytokines, along with a reduction in lesion volume (Vendrame et al., 2005). In addition, intracranial delivery of MSCs after stroke resulted in decreased microglial activation and reduced lesion volume (Mora-Lee et al., 2012). Secondly, MSCs have been shown to secrete a number of neurotrophic factors including brain-derived neurotrophic factor (BDNF), platelet-derived growth factor (PDGF), angiopoietin and TGF-β (Borlongan et al., 2004; Lin et al., 2011; Wilkins et al., 2009). Should MSCs enter the brain, it is thought that release of these factors will promote neuronal survival, enhance differentiation of neural progenitor cells and promote

remodelling (Eckert et al., 2013). MSCs are also thought to support angiogenesis through the release of pro-angiogenic factors such as vascular endothelial growth factor (VEGF) and basic fibroblast growth factor (bFGF) (Liu et al., 2006). In addition MSCs secrete TSG-6, which has been shown to promote angiogenesis through binding to fibroblast growth factor 2 (FGF2) (Leali et al., 2012). Many angiogenic factors also have anti-inflammatory and neurotrophic roles, for example stem cell-derived VEGF is able to stimulate neural progenitor cells, promote angiogenesis and reduce inflammation after stroke (Horie et al., 2011). MSCs have been shown to differentiate into neuronal cells *in vitro*, and have differentiated into cells expressing neuronal markers *in vivo* (Woodbury et al., 2000; Zhao et al., 2002). However, it is thought that MSCs are unlikely to differentiate into functional neurones, and it was shown that MSC-derived "neurones" do not express the voltage-gated ion channels essential for the generation of action potentials (Hofstetter et al., 2002). This further supports the evidence that MSCs exert their beneficial effects through secretion of paracrine factors, rather than through engraftment and differentiation. However, MSCs might still promote an increase in cell numbers without actually differentiating themselves by stimulating neural progenitor cells and secreting growth factors (Eckert et al., 2013). The potency of MSC-derived paracrine factors was also demonstrated through ventricular delivery of MSC conditioned media after MCAo, which resulted in improvements in motor function and lesion volume (Cho et al., 2012). Despite the growing evidence that MSCs do not engraft, the vast majority of pre-clinical trials have injected MSCs directly into the brain. However, more and more reports of success with intravenous administration are emerging. For example, many groups have shown that intravenous MSCs result in improved motor function, decreased lesion volume and increased neuro- and angiogenesis, sometimes in the absence of migration to the brain (Gutiérrez-Fernández et al., 2013; Honma et al., 2006; Iihoshi et al., 2004). There has been one attempt to increase the translational value of MSC research by studying the effect of intravenous MSCs in a non-human primate model of stroke. No significant effect was observed, although there was a trend for increased functional improvement in the MSC-treated monkeys, and no adverse effects were recorded (Sasaki et al., 2011). There seems to be some discrepancy surrounding migration to the brain: some groups have reported beneficial effects without any evidence of MSCs entering the brain parenchyma (Gutiérrez-Fernández et al., 2013). On the other hand, analysis of

MSC migration using radiolabelled cells revealed that a small proportion of cells do enter the damaged brain tissue after MCAo, whereas others get trapped in the lungs before excretion via the kidneys (Detante et al., 2009). A number of publications have reported beneficial effects of MSCs accompanied by some level of migration into the ischaemic tissue, although the number of migrated cells is consistently low (Chen et al., 2003; Chen et al., 2001b).

Overall, there is extensive evidence that MSCs could be a potent therapeutic option for the treatment of ischaemic stroke. Their diverse mechanisms of action, ranging from immunomodulatory through to neurotrophic, mean that they have a good chance of exerting a broad beneficial effect. Whilst most work has focussed on cerebral delivery of MSCs, there is much scope to further elucidate the effects of systemic delivery, particularly with the view of manipulating the immunosuppressive effects of MSCs. In light of the overwhelming evidence of the contribution of systemic inflammation to stroke pathogenesis, this peripheral immunomodulatory action of MSCs might be a strong candidate for effective therapeutic efficacy.

1.13 SUMMARY AND AIMS

Systemic inflammation plays a key role in the pathogenesis of ischaemic stroke. Co-morbidities and infection lead to a heightened immune profile, and stroke-induced peripheral inflammation and recruitment of leukocytes can contribute to the development of ischaemic brain damage. The broad aim of this thesis is to investigate the potential of systemic immunomodulatory therapies in experimental stroke – firstly by exploring the actions of TSG-6, and secondly by examining the systemic paracrine actions of TSG-6-expressing MSCs.

1.14 OBJECTIVES

1. To investigate the effect of TSG-6 on IL-1-induced brain damage and inflammation.

2. To explore the temporal and spatial expression pattern of TSG-6 in the brain after experimental ischaemic stroke.

3. To examine the effects of TSG-6 on post-acute histological, immunological and behavioural outcomes after experimental stroke.

4. To investigate the expression of TSG-6 by MSCs grown in 2D and 3D cultures and in response to IL-1.

5. To explore the potential of systemic MSC transplants as immunomodulatory therapies for ischaemic stroke.

CHAPTER 2:

MATERIALS AND METHODS

2.1 ANIMALS

All procedures were carried out in accordance with the UK Animals (Scientific Procedures) Act, 1986. Experiments were performed on male C57BL/6J/OLA mice (Harlan-Olac, UK) weighing 28-35g. Mice were housed in cages of 5 at 21°C ± 2°C in a 12h light-dark cycle with access to food and water ad libitum.

2.2 TRANSIENT FOCAL CEREBRAL ISCHAEMIA

An adapted method of the intraluminal filament middle cerebral artery occlusion (MCAo) model was used to induce transient focal cerebral ischaemia for 20, 30 or 45 min (Longa et al., 1989).

Anaesthesia was induced (4%) and maintained (2-2.5%) with isoflurane (Aesica Queenborough Ltd, UK) in 30% O_2 and 70% N_2O. Anaesthesia was maintained with a face mask, and the depth of anaesthesia was monitored before and throughout procedures by the rate of respiration and the toe pinch reflex. Body temperature was maintained at 37°C using a rectal probe and feedback-controlled homeothermic blanket (Harvard Apparatus, UK).

Transcranial laser Doppler flowmetry was used to indirectly monitor the red blood cell perfusion of tissue. The area between the left eye and ear was shaved and sterilised with Videne antiseptic solution (Adams, UK) and a small incision was made. A small hole was made in the muscle extending down to the skull, approximately mid-way between the eye and the ear, over the area supplied by the MCA. The Doppler probe (Moor Instruments, UK) was inserted into the hole and secured to the skull with Vetbond™ Tissue Adhesive (3M, UK). Cerebral blood flow was monitored for the duration of the procedure, with a drop in signal used to verify occlusion of the MCA.

In studies involving administration of substances, drugs were delivered either:

A. intraperitoneally using a 0.5ml insulin syringe. The time of injection was after fixation of the Doppler probe but before the main surgery was started, which corresponded to 30-40 min before onset of ischaemia.

or

B. subcutaneously using a 1ml syringe with a 21-gauge needle (MSC studies) or 25-gauge needle (TSG-6 dose-response study). The time of injection was either 30 min prior to onset of occlusion or 10 min post-reperfusion.

Vehicle was 0.5% low-endotoxin bovine serum albumin (BSA, Sigma, UK) in sterile phosphate buffered saline (PBS) for all studies except those involving MSCs, in which the vehicle was PBS or matrigel (diluted 3:1 matrigel:medium, BD Biosciences, UK).

The mouse was placed in a supine position and the neck area shaved and cleaned with Videne. A midline neck incision was made and the skin was opened to reveal the salivary glands. Glands were dissected from connective tissue, retracted cranially and secured with gauze soaked in saline solution to expose the underlying surgical area. Under a microscope (StemiSV11, Zeiss, Germany), connective tissue and muscle were dissected to reveal the left common carotid artery (CCA) and vagus nerve. The vagus nerve was dissected away from the CCA, and further dissection cranially to the CCA revealed the bifurcation of the external carotid artery (ECA) and internal carotid artery (ICA). The ECA was further dissected to expose the superior thyroid artery, and dissection of the ICA revealed the occipital artery. These two small vessels were electro-coagulated using a bipolar coagulation unit (Eschmann, UK), and cut. A 6-0 silk ligature (Fine Science Tools, USA) was tied tightly around the distal end of the ECA, and a second was tied loosely next to the bifurcation for securing the filament once inserted. A long ligature was placed around the ICA, to allow tension to be placed on the vessel to prevent bleeding. The portion of the ECA distal to the tight ligature was electro-coagulated, and a microvascular aneurysm clip (Fine Science Tools, USA) was placed on the CCA. The thread around the ICA was pulled tight, and an incision was made in the ECA between the two ligatures. The electro-coagulated region of the ECA was cut, and the vessel repositioned until parallel with the CCA. A 6-0 silicon rubber-

coated monofilament (210µm diameter, coating length >=5mm) (Doccol Corporation, USA) was inserted into the ECA and secured with the loose ligature. The thread around the ICA was loosened, and the filament was advanced into the ICA until resistance was felt and a drop on the Doppler monitoring system was seen, indicating occlusion of the MCA (Figure 2.1). The filament was secured, the surgical site was filled with saline and isoflurane was reduced to 1.5% for the duration of the occlusion.

Following occlusion, reperfusion was achieved by withdrawal of the filament out of the vessel. The loose ligature was secured tightly around the vessel to prevent bleeding, and the aneurysm clip and long ligature were removed. The wound was cleaned and the salivary glands were repositioned, before the incision was closed with 6-0 sutures (Ethicon, UK). The wound was cleaned again with Videne and a local anaesthetic cream containing lidocaine and prilocaine (EMLA) (AstraZeneca, UK) was applied.

The Doppler probe was removed and the wound closed with Vetbond™. Videne and EMLA were applied to the surgical area.

Sterile Hartmann's solution (0.5ml; compound sodium lactate solution, Baxters Healthcare Ltd, UK) and 0.05mg/kg buprenorphine (Vetergesic, Alstoe Ltd, UK) were administered subcutaneously, the isoflurane and N_2O were switched off and the oxygen was increased to 500ml/min for initial recovery. Animals were transferred to a clean cage on a heated mat and monitored closely for at least 4h before return to normal housing. Reperfusion occurred for 4h, 24h or 3, 5, 7 or 14 days.

Sham surgery was carried out as above except the filament was withdrawn as soon as resistance was felt. Sham animals were exposed to anaesthetic for the same period of time as stroke animals.

Animals were excluded from the study if the time taken to insert the filament exceeded 60 min (as previous work from the lab showed an increase in variability with long surgeries), if subarachnoid haemorrhage was present, if no stroke damage was visible or if the animal died before the pre-determined end-point.

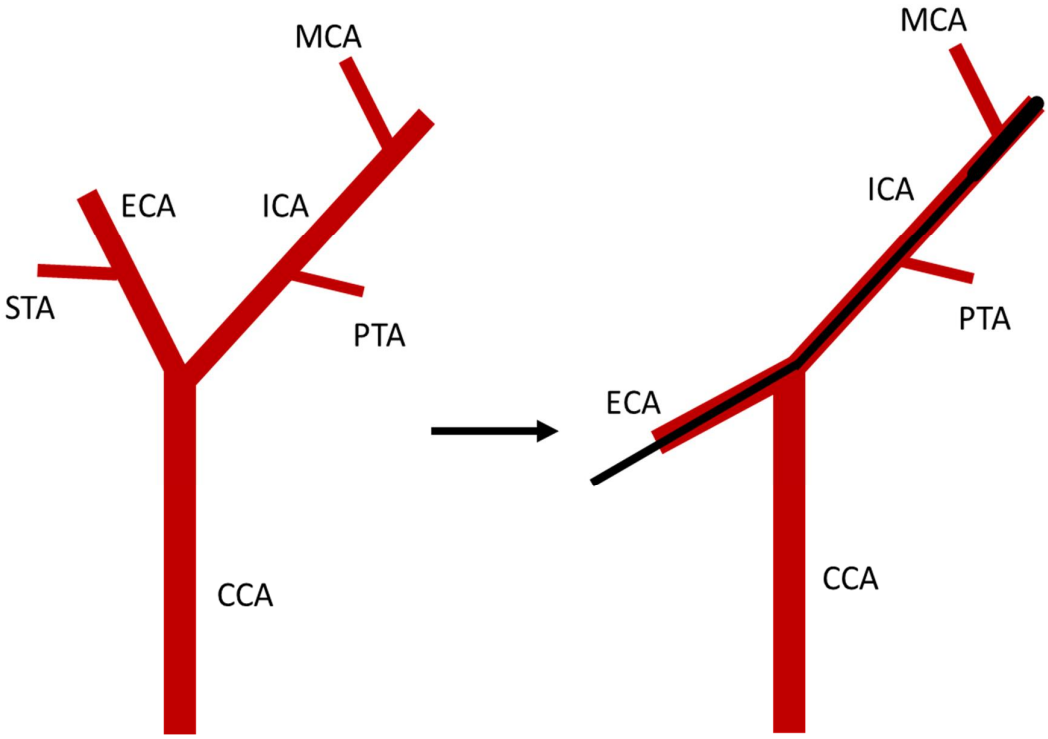

Figure 2.1: Vascular organisation of the mouse as seen during left middle cerebral artery occlusion. After the vasculature is dissected and exposed, the superior thyroid artery (STA) and occipital artery (OccA) are coagulated and cut. The filament is then inserted into the internal carotid artery (ICA) via the external carotid artery (ECA) until it blocks the origin of the middle cerebral artery (MCA). CCA, common carotid artery; PTA, pterygopalatine artery.

2.3 BLOOD SAMPLING

Tail vein blood was sampled before surgery, after surgery completion (corresponding to 10min reperfusion) and after 4h, 24h, 3 days and 7 days reperfusion (depending on the study). The vein was punctured using a 23-gauge needle and slight pressure was applied to extract blood. Blood was collected into tubes containing 5µl of 3.8% tri-sodium citrate made up in distilled water. For each labelling group required for flow cytometry analysis 5µl of blood was taken, and 15µl was taken for cytometric bead array (CBA) analysis. After blood sampling, pressure was applied to the wound until bleeding ceased.

2.4 BEHAVIOURAL TESTS

A variety of tests were performed across different studies to assess the functional deficit and neurological symptoms of stroke.

2.4.1 SIMPLE NEUROLOGICAL SCORE

Simple neurological score was used to give a basic estimation of the ischaemic damage. Mice were scored according to the following criteria after 2h reperfusion:

0 - No observable deficit

1 - Torso flexion to the right when picked up by tail

2 - Spontaneous circling to the right

3 - Leaning or falling to the right

4 - No spontaneous movement.

2.4.2 BEHAVIOURAL CHARACTERISATION AND COMPLEX NEUROLOGICAL SCORE

Behavioural characterisation:

A more detailed neurological scoring system was used for experiments with long term recovery, using a modified version of the procedure described by (Hunter et al., 2000). Mice were transferred into a clean empty cage and were scored on the following criteria:

Body position: 0, completely flat; 4, up-right position.

Spontaneous activity: 0, none; 3, repeated vigorous movement.

Transfer arousal: 0, coma; 5, extremely excited.

Gait: 0, absolute incapacity; 3, normal.

Touch escape: 0, none: 3, extremely vigorous.

Positional passivity: 0, no struggle when held with hand; 4, maximal struggle.

Maximum score = 22

Complex neurological score:

Additionally, mice were picked up by their tail and scored according to the following criteria:

0 - No deficit

1 - Failure to extend right forepaw fully

2 - Decreased grip of right forelimb

3 - Torso flexion to the right

4 - Spontaneous circling to the right

5 - No response to stimulation.

Mice were assessed at 24h, 3 days, 7 days and 14 days following stroke, depending on the study.

2.4.3 Open field test

The open field test was performed to assess spontaneous locomotor activity in mice at 24h, 7 days and 14 days post-stroke. Mice were allowed to acclimatize in the procedure room for 20 min before the onset of experiments. Mice were placed in the centre of a clean 50cmx50cm square arena with 35cm high opaque black sides. Each mouse was filmed for 5 min using a camera and ANY-maze video tracking software (Stoelting Co., USA). Parameters including average speed, total time active/inactive, number of line crosses, number of grooming episodes and number of rearing episodes were collated by the software.

2.5 TRANSCARDIAL PERFUSION

After the reperfusion period, animals were deeply anaesthetised (4% isoflurane in 30% O_2 and 70% N_2O) and placed on a down-draft table. A midline incision was made along the length of the chest and abdomen, and the muscle, diaphragm and ribs were dissected to expose the heart. Cardiac blood was sampled by inserting a 23-gauge needle into the right ventricle and withdrawing blood, which was mixed with 100µl 3.8% tri-sodium citrate to prevent coagulation. A 25-INT butterfly needle was inserted into the left ventricle and clamped, and a hole was cut into the right atrium. 20ml ice-cold 0.9% saline or diethylpyrocarbonate- (DEPC) treated saline solution was perfused at a rate of 10ml/min using a syringe pump (Harvard Apparatus, UK). For flow cytometry, the spleen and bone marrow from the left tibia and femur were removed and put in 2ml FACS buffer (0.1% BSA and 0.05% sodium azide in PBS). The spleen was mashed and the bone marrow was flushed and homogenised by withdrawal and ejection through a 25-gauge needle and 1ml syringe. For other studies, the spleen, liver and lung were removed and snap-frozen on dry-ice. For expression studies, the brain was removed at this point, separated into two hemispheres and snap-frozen on dry ice.

For studies not involving quantitative polymerase chain reaction (PCR), following perfusion with saline and organ removal, 20ml ice-cold paraformaldehyde (PFA) was perfused. 4% PFA was made up in distilled water with 25% 0.4M PB, and was filtered and set to a pH of 7.4. After PFA perfusion, animals were decapitated and the brains removed. Brains were post-fixed by submergence in 20% sucrose-PFA at 4°C for 24h, followed by cryoprotecting in 20% sucrose-PBS at 4°C for at least 4h before processing.

2.6 HISTOLOGICAL ANALYSIS

Histological techniques were used to assess the volume of ischaemic damage and to identify the presence of haemorrhagic transformation (HT).

2.6.1 BRAIN SECTIONING

A sledge microtome (8000 Microtome, Bright, UK) and freezing unit (Bright solid state freezer, Bright, UK) were used to slice brains. Brains were mounted onto the platform using distilled water and were frozen in place using crushed dry ice. The blade was fitted and fixed at 15°. Eleven series of 20 or 30µm thick coronal sections were taken and placed in cryoprotectant solution (500ml distilled water, 6.6g $Na_2HPO_4*2H_2O$, 0.79g $NaH_2PO_4*H_2O$, 300ml anhydrous ethylene glycol, 200ml glycerol) before freezing at -20°C.

2.6.2 CRESYL VIOLET STAINING

Cresyl violet was used to assess the ischaemic damage present in brain sections. This dye stains the nuclei and rough endoplasmic reticulum of cells, and therefore stains both neurones and glia. In ischaemic tissue, damaged cells shrink, resulting in pale areas in the stained tissue, contrasting with purple areas of undamaged tissue.

Sections were mounted onto glass slides using a paintbrush, and were left to dry. Sections were defatted by being placed in increasing and decreasing concentrations of industrial methylated spirits (IMS): 2 min in 95% IMS, 3 min in 99% IMS, 3 min in 99% IMS, 10 min in xylene, 2 min in 99% IMS, 2 min in 99% IMS, 2 min in 95% IMS. Sections were washed for 2 min in gently running distilled water, before being placed in 1% cresyl violet for 2.5 min. Slides were rinsed in running distilled water until the run-off was clear, and then left in 95% IMS for 40 min-1h to allow the contrast to develop. Sections were then dehydrated in two solutions of 99% IMS for 3 min each, before being placed in two solutions of xylene for 5 min each. Coverslips were mounted onto slides using DePex mounting medium (VWR, UK).

2.6.3 HEAMATOXYLIN AND EOSIN STAINING

Haematoxylin and eosin (H&E) staining was used to identify the presence of HT and for confirmation of lesion volume. Haematoxylin stains the nuclei of cells blue, whereas eosin stains eosinophilic structures in the cell various shades of red. For the identification of HT, red blood cells were recognised by intense red staining. Sections were mounted onto glass slides using a paintbrush, and were left to dry before being stained by the following protocol; slides were placed in decreasing concentrations of ethanol (100%, 90%, 70% for 2 min each). Sections were then rinsed in running distilled water before being placed in haematoxylin for 5 min, then were washed again until the run-off was clear. Sections were placed in acid alcohol (0.5% HCl in 70% ethanol) for a few seconds, then were washed again and left in Scott's tap water (3.5g sodium bicarbonate, 20g magnesium sulphate in 1 litre distilled water – blueing solution) for 30s. Slides were washed and placed in eosin for 30s, then were washed again. Sections were placed in increasing concentrations of ethanol (70%, 90%, 100% for 2 min each) before being left in xylene for 30 min. Slides were coverslipped using DePex mounting medium.

2.6.4 ANALYSIS OF LESION VOLUME

Cresyl violet-stained slides were placed on a light box next to a ruler for scaling and a digital photo was taken. Image J software (available at www.rsbweb.nih.gov/ij/) was used for analysis of ischaemic lesion volume using an adaption of a method developed by Dr Barry McColl (McColl, 2004). Eight coronal sections were selected at specific neuroanatomical locations in respect to bregma. With reference to the stereotaxic mouse brain atlas (Paxinos, 2004), brain sections at 2.22, 1.54, 0.98, 0.14, -0.58, -1.22, -1.82 and -2.54mm from bregma were selected. Ischaemic tissue was traced around, corrected for oedema and quantified using Image J. The total infarct volume was calculated by plotting these values against the distance between coronal sections using GraphPad Prism software (version 5.0), with the area under the curve representing the ischaemic volume. Blinding was in place for lesion volume analysis.

2.6.5 Analysis of presence of HT

HT was identified by gross inspection of slides under a light microscope. Areas of HT were drawn onto brain maps of the eight coronal levels described in 2.5.4. Brain maps were scanned in and digitalised, and opened with Image J. Areas of HT were traced and the total area over 8 sections was deduced. Blinding was in place for HT analysis.

2.7 Flow cytometry

Flow cytometry was used to identify the populations of immune cells found in the blood before and after surgery, and after 4 and 24h reperfusion. The populations of immune cells in the bone marrow and spleen after 24h were also analysed. Flow cytometry takes advantage of the variety of cell surface markers expressed by different cell populations. For example, T cells can broadly be identified by the presence of cell surface marker CD3. This population can be further subdivided into T helper cells (positive for CD3 and CD4) and cytotoxic T cells (CD3 and CD8). Flow cytometry utilises fluorescent labelling of cell surface markers to quantify the populations of cells present at each time point.

2.7.1 Flow cytometry labelling of blood

Blood was labelled for flow cytometry using the following protocol. 0.25µl FC block (Anti–mouse CD16/CD32, eBioscience, UK) was added to each sample (5µl blood + 5µl tri-sodium citrate), and tubes were vortexed and refrigerated for 15 min. Antibody cocktails were made up as follows: 5µl polybeads (1.7x107 beads/ml) (Polysciences Europe GmbH, Germany) were added to 95µl FACS buffer, and antibodies were added in the concentrations shown in Table 2.1. Following incubation with FC block, 10µl antibody cocktail was added to samples, which were vortexed and incubated at 4°C for 30 min. 300µl BD FACS lysing solution (BD Biosciences, UK) (diluted 1:10 from stock in dH_2O) was added to each tube, which were vortexed and refrigerated until samples were read (within 24h) on a BD LSR II Flow Cytometer (BD Biosciences, UK).

2.7.2 Flow cytometry labelling of bone marrow and spleen

Spleens and bone marrow were homogenised in FACS buffer as described in section 2.4. Samples were centrifuged at 400xg for 8 min, supernatants were discarded and pellets were disrupted. 1ml ACK buffer (8.29g NH_4Cl, 1g $KHCO_3$ and 0.0367g Na_2-EDTA in 1 litre distilled water, pH 7.4) was applied to samples for 1 min to lyse red blood

cells. 10ml PBS was added to samples to restore osmolarity and tubes were centrifuged at 400xg for 8 min. Supernatants were discarded and pellets were disrupted. 2ml FACS buffer was added to each sample, followed by filtering through 80µm mesh. 200µl sample was added into wells of a 96-well round-bottomed plate, including wells for single labelling. 250µl PFA was added to the remainder of samples to fix for cell counting. Plates were centrifuged at 400xg for 3 min, supernatants were discarded and pellets were disrupted. FC block (eBioscience, UK) was diluted 1:200 in FACS buffer and 30µl was added to wells for 30 min on an orbital shaker. 200µl FACS buffer was added to each well, and plates were centrifuged at 400xg for 3 min. Supernatants were discarded and pellets were disrupted. Antibody cocktails (as in Table 2.1) (eBioscience, UK; R&D Systems, UK; BD Biosciences, UK) were made up in FACS buffer and 30µl was added to each well, including wells for single labelling. Plates were wrapped in aluminium foil and were incubated at 4°C on an orbital shaker for 30 min. Wells were topped up with 200µl FACS buffer and were centrifuged at 400xg for 3 min. Supernatants were discarded and pellets were disrupted. 200µl FACS-FIX (1% PFA in FACS buffer) was added to each well. Plates were wrapped in foil and refrigerated until being read (within 48 h).

FACSDiva Software (BD Biosciences, USA) was used for gating and analysis of flow cytometry data. For bone marrow and spleen samples, cell populations were calculated as a percentage of viable cells. For blood samples, beads included in the sample preparation allowed for the calculation of cells per microliter of blood. Examples of plots used in the analysis of flow cytometry data are shown in Figures 2.2 and 2.3:

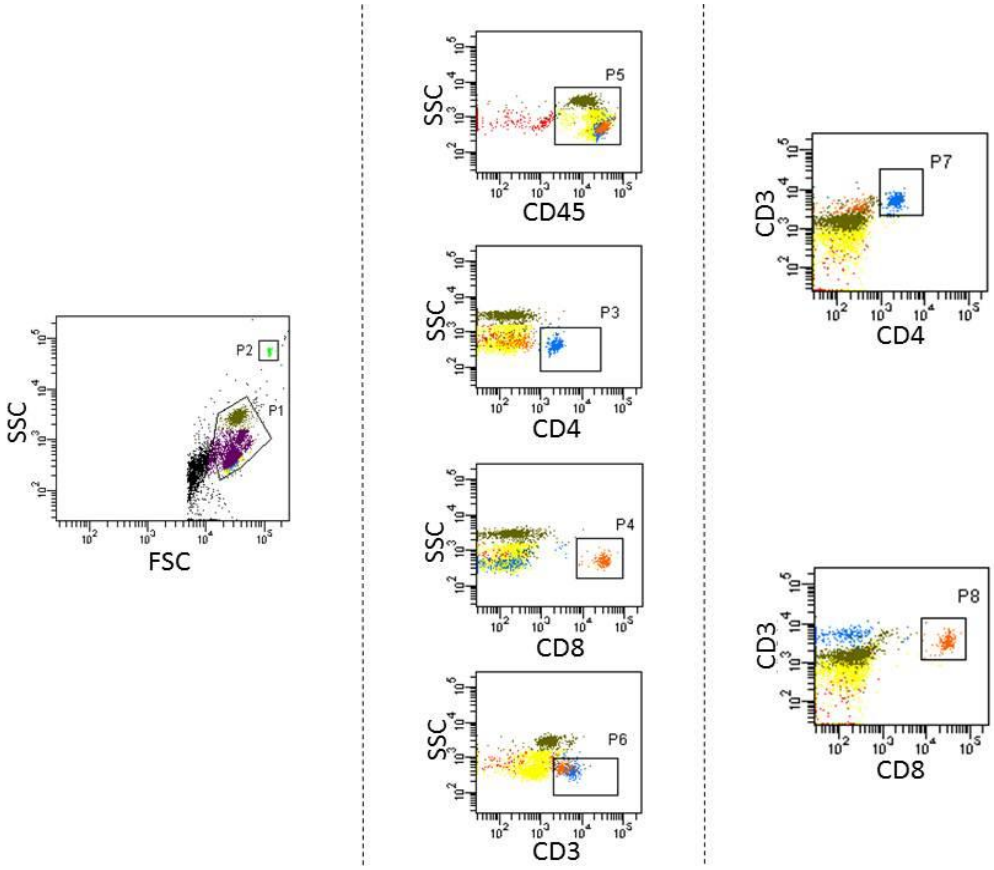

Figure 2.2: Gating strategy for identification of T cell subpopulations in blood. In the first panel, analysis of side scatter (SSC) and forward scatter (FSC) allows for the identification of major cell populations and exclusion of cell debris, gated with P1. P2 indicates beads, which assist in calculating cells/µl blood. In the second stage (panel 2), single colours are plotted against SSC to reveal gross populations. P5 shows CD45+ cells: a general marker for leukocytes. These populations are separated out further in the third stage (panel 3). All CD3+ cells (T cell) are separated into CD3+CD4+ populations (P7) (T helper cells) and CD3+CD8+ populations (P8) (cytotoxic T cells).

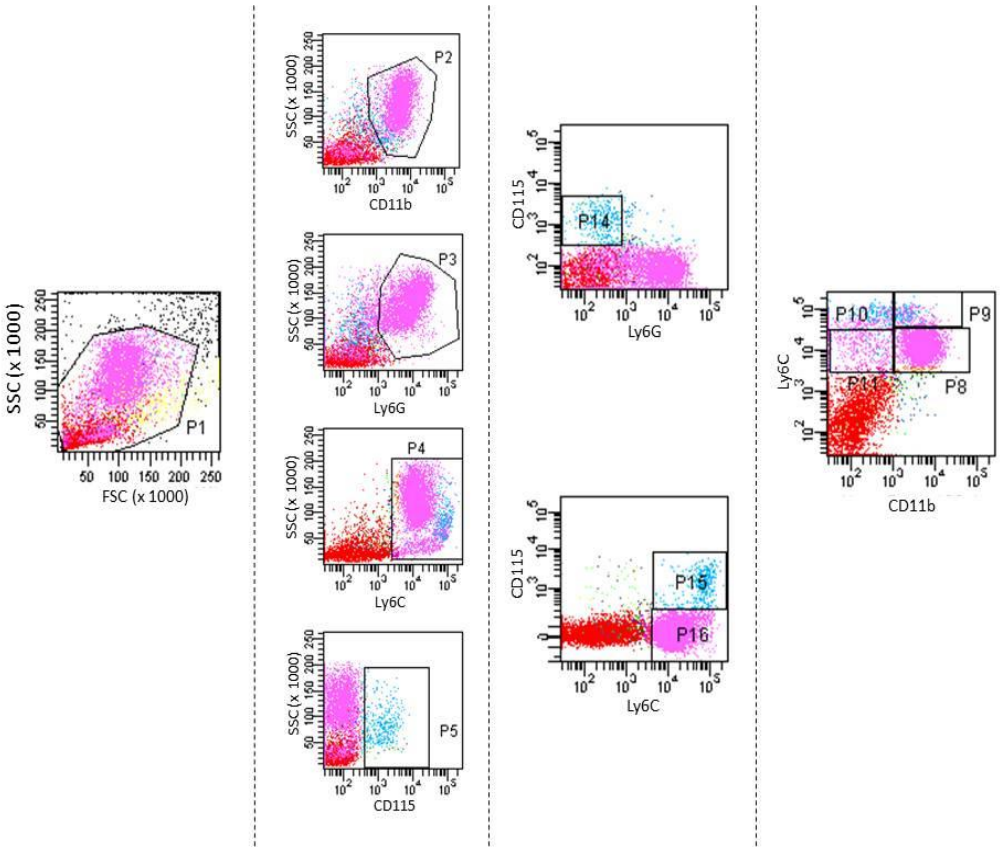

Figure 2.3: Gating strategy for identification of monocytes and granulocytes in bone marrow and spleen. In the first panel, analysis of side scatter (SSC) and forward scatter (FSC) allows for the identification of major cell populations and exclusion of cell debris, gated with P1. The gating in the second panel shows single-colour populations against SSC. These populations can be further divided by plotting two markers against each other (panel 3). P14 gates Ly6G-CD115+ cells, which correspond to either monocytes or macrophages. P15 gates Ly6C+CD115+ cells which are likely to be monocytes, however these populations (shown in blue) can be split further, as shown in panel 4. Gates here distinguish cells expressing 'high' or 'very high' levels of Ly6C. Monocytes express very high levels of Ly6C, distinguished by gates P9 and P10. These two gates separate CD11b+ and CD11b- monocytes. P8 highlights CD11b+Ly6C^{high} cells which correspond mainly to granulocytes and other mature or immature myeloid cells. P11 gates CD11- myeloid cells.

ANTIBODY	FLUOROCHROME	CONCENTRATION
BLOOD		
COCKTAIL A: T cells		
CD45[1]	PerCP Cy 5.5	1:200
CD3[1]	APC	1:100
CD4[1]	FITC	1:100
CD8[1]	PE	1:100
COCKTAIL B: B cells/myeloid cells		
CD19[1]	FITC	1:50
CD11b[1]	PE	1:200
Ly6C[1]	PerCP Cy 5.5	1:200
MHCII[1]	APC	1:200
BONE MARROW AND SPLEEN		
COCKTAIL A: T cells		
CD3[1]	APC	1:200
CD4[1]	FITC	1:200
CD8[1]	PE	1:400
COCKTAIL B: Monocytes/macrophages/granulocytes		
CD11b[1]	FITC	1:200
Ly6G[1]	PE (1A8 Clone)	1:400
Ly6C[1]	PerCP Cy 5.5	1:400
CD115[1]	APC	1:200
COCKTAIL C: Granulocyte/monocyte subsets		
CD11b[1]	FITC	1:200
CXCR2[2]	APC	1:100
CCR5[3]	PE	1:100
COCKTAIL D: B cells/Dendritic cells		
CD19[1]	FITC	1:100
CD11c[1]	PE	1:200
MHCII[1]	APC	1:400

Table 2.1: Antibody cocktails used in flow cytometry analysis of samples. Cell surface markers were labelled with fluorescently-conjugated antibodies to allow identification of immune cell populations. Antibodies were from eBioscience, UK[1], R&D Systems, UK[2] or BD Biosciences, UK[3] .

2.8 IMMUNOHISTOCHEMISTRY

2.8.1 FLUORESCENT IMMUNOHISTOCHEMISTRY

Fluorescent immunohistochemistry was used to identify and to assess localisation of proteins within brain sections. The protocol took place on free-floating sections after sectioning, with mounting onto slides taking place after the staining was complete.

Brain sections were transferred into a 24-well plate and were washed in PBS twice for 10 min each on an orbital shaker. Non-specific binding was blocked by incubating sections in 250µl 2% normal donkey serum (Jackson Laboratories, USA) made up in primary diluent (0.3% Triton, 20µM sodium azide in PBS) for 1h. 250µl primary antibodies (see Table 2.2) made up in primary diluent was added to each well, and samples were incubated at 4°C on an orbital shaker overnight. The following day, samples were washed three times in PBS for 10 min on an orbital shaker. 250µl fluorescently-conjugated secondary antibodies (see Table 2.2) made up in primary diluent were added to wells, which were incubated at room temperature in the dark on an orbital shaker for 3h. Sections were washed three times in PBS and mounted onto glass slides (coated with 0.5% gelatine (BDH Laboratory Supplies, UK) and 0.05% chromium potassium sulphate (BDH Laboratory Supplies, UK)) using a paintbrush. Slides were coverslipped using Prolong Gold Anti-fade Reagent with DAPI (Invitrogen, UK). Images were captured on an upright microscope (BX51, Olympus, UK) and Coolsnap ES camera (Photometrics, UK) using MetaVue Software (Molecular Devices, UK). Filter sets for DAPI, FITC and Texas Red were in place to allow visualisation of individual channels.

PRIMARY ANTIBODY	CONCENTRATION	SECONDARY ANTIBODY
Rabbit anti-mouse TSG-6 (Produced in-house in the laboratory of Professor Anthony Day, University of Manchester. Produced as described in (Carrette et al., 2001))	1:500	Donkey anti-rabbit IgG Alexa Fluor 594 (Vector Laboratories, USA)
Rat anti-mouse CD45 (Serotec, UK)	1:250	Donkey anti-rat IgG Alexa Fluor 488 (Vector Laboratories)
Rabbit anti-mouse SJC-4 (Produced and kindly donated by the laboratory of Dr Daniel Anthony, Oxford University)	1:10,000	Donkey anti-rabbit IgG Alexa Fluor 594 (Vector Laboratories, USA)
Chicken anti-mouse glial fibrillary acidic protein GFAP (Serotec, UK)	1:1000	Goat anti-chicken IgG Alexa Fluor 488 (Vector Laboratories)

Table 2.2: Antibodies used for immunohistochemistry. TSG-6 identified TSG-6 protein, CD45 identified leukocytes, SJC-4 identified neutrophils and GFAP identified astrocytes. All secondary antibodies were used at a concentration of 1:500.

2.8.2 DAB IMMUNOHISTOCHEMISTRY FOR ANALYSIS OF BLOOD-BRAIN BARRIER BREAKDOWN

Brain sections were stained for immunoglobulin G (IgG), with extravasation into the brain parenchyma indicating loss of integrity of the BBB.

Sections were washed in PBS and were incubated with 1% hydrogen peroxide (H_2O_2, Sigma, UK) in water for 30 min to block endogenous peroxidase activity. Sections were washed in PBS, and non-specific binding was blocked by incubating for 1-2h with 5% normal horse serum (Vector Laboratories, UK) diluted in primary diluent (0.3% Triton X-100 (Sigma, UK), 20µM sodium azide in PBS). Sections were washed in PBS and were incubated at 4°C overnight with horse anti-mouse biotinylated IgG (1:500 in primary diluent, Vector Laboratories, UK). Sections were washed in PBS and Vectastain ABC kit (Vector Laboratories, UK) was added (1:500 in PBS) for 1h. Sections were washed in PBS and were developed with 50mg/ml diaminobenzidine (DAB, Vector Laboratories, UK) made up in water until a good level of contrast was seen (3-5 min), followed by two 30 min washes in PBS. Sections were mounted onto slides and dried overnight, followed by dehydration by dipping sections in increasing concentrations of ethanol (70%, 90%, and 100% for 3 min each) followed by xylene for 5 min. Coverslips were mounted onto slides with DePex mounting solution.

The area of BBB breakdown was calculated using the same method for lesion volume (described in section 2.6.4).

2.9 ENZYME-LINKED IMMUNOSORBENT ASSAY (ELISA)

Commercial ELISA kits were purchased from R&D Systems (UK), and the manufacturer's protocol was followed. The whole procedure was conducted at room temperature. Briefly, Nunc-immuno plates were coated overnight with capture antibody diluted in PBS. Plates were washed in wash buffer (0.05% tween (v/v) in PBS) and blocked in reagent diluent (RD, 1% BSA in PBS) for 1h. Plates were washed, and standards and samples were added for 2h. After washing, detection antibody (diluted in RD) was added to each well for 2h, followed by another wash. Streptavidin horseradish peroxidase (HRP) was diluted 1:200 in RD and was added to wells for 20 min with plates being kept in the dark. Plates were washed, and substrate reagents A and B (BD Biosciences, UK) were combined and added to wells for 20 min in the dark. The reaction was stopped by adding 1M H_2SO_4, and plates were read at 490nm and 570nm, with correction of optical densities taking place. Data were analysed using GraphPad Prism software, version 5.0.

2.10 CYTOMETRIC BEAD ARRAY

Plasma samples were analysed using cytometric bead array (CBA) for detection of cytokines and chemokines. CBA Mouse Soluble Protein Flex Sets (BD Biosciences, UK) were used for the analysis of CD62, G-CSF, IL-1α, IL-1β, IL-6, IL-10, IL-12, IL-17, KC, MCP-1, RANTES and TNF-α. The protocol was conducted according to the manufacturer's instructions but in smaller volumes. Briefly, a ten-point standard curve was constructed, and capture beads were diluted and pooled in capture bead diluent. Plasma samples were diluted 1:2 in assay diluent, and 10µl of sample or standard was loaded into wells of a 96-well plate. The plate was shaken on an orbital shaker for 5 min, then was incubated at room temperature for 1h. Phycoerythrin (PE) detection reagents for each cytokine/chemokine were mixed in detection reagent diluent, and 10µl was added to each well. The plates were shaken for 5 min on an orbital shaker, followed by incubation at room temperature for 1h. Plates were washed with wash buffer, and were centrifuged at 1000xg for 4 min. The supernatant was discarded, and samples were re-suspended in 70µl wash buffer. Samples were read on a MACSQuant Analyzer (Miltenyi Biotech, UK) and were analysed using FCAP Array v3.0 software (BD Biosciences, UK).

2.11 PRIMARY MIXED GLIAL CULTURE

C57/BL6 mouse pups (aged 1 to 3 days) were decapitated and cortical tissue was collected. Brains were rolled on filter paper to remove blood and meninges, and were re-suspended in glial medium (Dulbecco's modified Eagle's medium (DMEM) (Sigma, UK), 10% foetal calf serum (FCS) (PAA Laboratories, UK), 100µg/ml penicillin (Sigma, UK), 100U/ml streptomycin (Sigma, UK)). The suspension was centrifuged at 250xg for 10 min, the supernatant was discarded and cells were re-suspended and seeded in 24 well plates (1 brain per plate) and maintained at 37°C in a humidified atmosphere with 5% CO_2. Media was initially changed on day 5 followed by every 3 days thereafter. Experiments began when cells were confluent (around day 12).

2.12 PRIMARY CORTICAL NEURONAL CULTURE

24-well plates were coated overnight in 2% Poly-D-Lysine (PDL) (Sigma, UK) in sterile water. PDL was aspirated before cells were seeded. E15-E16 embryos were removed from pregnant C57/BL6 mice euthanized by cervical dislocation. Cortical tissue was dissected and was incubated in a shaking incubator (50rpm) at 37°C for 30 min in dissociation medium (DMEM, 100µg/ml penicillin, 100U/ml streptomycin, 2mM glutamine (Invitrogen, UK), 1x trypsin (Invitrogen, UK) 375U/ml DNase (Invitrogen, UK)). Medium was aspirated and brains were covered in ice-cold FCS for 2 min to neutralise trypsin. FCS was aspirated and brains were washed 3x in wash medium (DMEM, 10% FCS, 100µg/ml penicillin, 100U/ml streptomycin). After the final wash, brains were dissociated and re-suspended in 10ml seeding medium (Neurobasal media (Invitrogen, UK), 5% (v/v) plasma-derived serum (First Link Ltd, UK), 100µg/ml penicillin, 100U/ml streptomycin, 2mM glutamine, 2% (v/v) B27 **with** antioxidants (Invitrogen, UK)) and were filtered through sterile nylon 80µm mesh to remove meninges. 3µM 5'-fluro-2-deoxyuridine (FUDR) (Sigma, UK) was added to inhibit glial proliferation, and cells were seeded in 24-well plates at 600,000 cells/ml. Cells were maintained at 37°C in a humidified atmosphere with 5% CO_2. After 4 or 5 days in culture, a full media change was performed (Change medium: Neurobasal media, 5% plasma-derived serum, 100µg/ml penicillin, 100U/ml streptomycin, 2mM glutamine, 2% B27 **without** antioxidants (Invitrogen, UK)). At day 7, a half media change was

performed using change medium, and on day 11 a half change was performed using serum-free change medium. Cultures were treated on day 12.

2.13 bEND5 CELL CULTURE

bEND5 mouse brain endothelial cells are a cell line which closely resemble primary brain endothelial cells in culture. Cells were purchased from the Health Protection Agency Culture Collections (Salisbury, U.K.) and were cultured in T75 flasks (DMEM, 10% FCS, 1% non-essential amino acids (Sigma, UK), 100µg/ml penicillin, 100U/ml streptomycin, 2mM glutamine) at 37°C in a humidified atmosphere with 5% CO_2. Cells were used up to passage 30, and were plated in 24-well plates at 300,000 cells/ml 24h before treatment.

2.14 HUMAN MESENCHYMAL STEM CELL CULTURE

Normal human MSCs were sourced from the bone marrow of two male donors (donors M183402 and M33, Lonza, UK. Lot numbers 0000183402 and 6F4085). Cells were cultured in MesenPRO RS basal growth medium (Invitrogen, UK, supplemented with 2% growth supplement (Invitrogen, UK), 1% penicillin-streptomycin and 1% glutamine) in T75 flasks coated with 0.1% gelatine (Sigma, UK) until 75% confluent. MSCs were maintained at 37°C in a humidified atmosphere with 5% CO_2, and were used at passage 5 for all experiments.

For treatment, cells were plated in 6-well plates at 60,000 cells/well for 2D cultures, and at 60,000 cells/well in 96-well low-cell binding plates for 3D cultures. Cells were left for 5 days to reach confluency and to allow spontaneous spheroid formation.

2.15 CHARACTERISATION OF MSCS

Before MSCs were used experimentally, their multipotency and cell-surface marker profile were characterised.

2.15.1 FLOW CYTOMETRY

MSCs were detached with accutase (Invitrogen, UK) and were counted. Cells were re-suspended to 100,000 cells/ml in MesenPRO RS media (supplemented with 2% growth supplement (Invitrogen, UK), 1% penicillin-streptomycin and 1% glutamine) and incubated at 37°C for 30 min to allow cell surface markers to recover. Cell suspensions were centrifuged at 250xg for 4 min, and the pellet was re-suspended in 1ml ice-cold PBS^{-CaCl2}/0.5% BSA (repeated a total of 3 times). Cells were seeded in 96-well plates at 75,000 cells/well and were centrifuged at 250xg for 3 min. Pellets were re-suspended in 100µl ice-cold PBS^{-CaCl2}/0.5% BSA, and 1µl primary antibody was added to each well. Plates were incubated on ice for 1h. The antibodies used are shown in Table 2.3. Plates were washed 3x by centrifugation at 250xg for 3 min and adding 100µl ice-cold PBS^{-CaCl2}/0.5% BSA to each well. 0.5µl secondary antibody or 1µl fluorescently conjugated primary antibody was added to each well, and plates were incubated on ice for 45 min. Plates were centrifuged at 250xg for 3 min and cells were re-suspended in 200µl ice-cold PBS^{-CaCl2}/0.5% BSA (repeated a total of 3 times). The pellet was re-suspended in a final volume of 400µl ice-cold PBS^{-CaCl2}/0.5% BSA and was analysed immediately on a Cyan ADP Analyzer (Beckman Coulter, UK).

Antibody	Source	Positive/negative MSC marker	Conjugated?	Secondary
CD29	BD Biosciences, UK	+	Yes – PE	None required
CD44	BD Biosciences, UK	+	Yes – PE	None required
CD73	BD Biosciences, UK	+	No	Donkey anti-mouse IgG 488
CD90	BD Biosciences, UK	+	No	Donkey anti-mouse IgG 488
CD105	R & D Systems, UK	+	Yes - PE	None required
CD166	BD Biosciences, UK	+	No	Donkey anti-mouse IgG 488
Stro-1	R & D Systems, UK	+	No	Goat anti-mouse IgM 488
CD14	BD Biosciences, UK	-	No	Donkey anti-mouse IgG 488
CD34	Chemicon International, UK	-	No	Donkey anti-mouse IgG 488
CD45	BD Biosciences, UK	-	No	Donkey anti-mouse IgG 488

Table 2.3: Antibodies used for flow cytometry labelling of MSCs. All secondary antibodies were from Invitrogen, UK.

2.15.2 DIFFERENTIATION ASSAY

The multipotency of MSCs was confirmed by stimulating cells to follow adipogenic, ostegenic and chondrogenic lineages using a Human Mesenchymal Stem Cell Functional Identification Kit (R&D Systems, UK). The protocol was performed according to the manufacturer's instructions, and is summarised as follows. Non-specific binding was blocked with 2% fish skin gelatine (Sigma, UK) in PBS, and all antibodies were diluted in 3% BSA in PBS. Non-differentiated control cells were maintained in MesenPRO RS basal medium or in the manufacturer's recommended basal medium.

Adipogenic Differentiation:

Cells were seeded in MesenPRO RS basal medium at 37,000 cells/well on coverslips in 24-well plates (coated with 0.05% gelatine in PBS) for immunofluorescence, and at 150,000 cells/well in 6-well plates for qPCR. Once 100% confluent, medium was replaced with adipogenic differentiation medium (α-MEM (Invitrogen, UK) containing adipogenic differentiation supplement (hydrocortisone, isobutylmethylanthine and indomethacin, R&D kit), 10% FCS, 100U/ml penicillin, 100µg/ml streptomycin and 2mM L-glutamine). Medium was replaced every 3-4 days for 21 days, then cells were fixed in 4% PFA and were stained for lipid droplets with BIODIPY (1:500) and FABP4 (1:500) (R&D kit).

Osteogenic Differentiation:

Cells were seeded in MesenPRO RS basal medium at 7400 cells/well on coverslips in 24-well plates (coated with 0.05% gelatine in PBS) for immunofluorescence, and at 40,000 cells/well in 6-well plates for RNA extraction. After 24h, cells were at 50-70% confluency, and medium was replaced with osteogeneic differentiation medium (α-MEM (Invitrogen, UK) containing osteogenic differentiation supplement (dexamethasone, ascorbate-phosphate and β-glycerophosphate, R&D kit), 10% FCS, 100U/ml penicillin, 100µg/ml streptomycin and 2mM L-glutamine). Medium was replaced every 3-4 days for 28 days, and then cells were fixed in 4% PFA and were stained for osteocalcin (1:100) and phalloidin (1:500) (R&D kit).

Chondrogenic Differentiation:

Cells were seeded in MesenPRO RS basal medium at 50,0000 cells/well in a 96-well low cell binding plate. After 5 days, cells spontaneously formed 3D spheroids, and medium was replaced with chondrogenic differentiation medium (D-MEM/F-12 (Invitrogen, UK) containing chondrogenic differentiation supplement (dexamethasone, ascorbate-phosphate, proline, pyruvate and TGFβ3, R&D kit), 1% ITS supplement (100X concentrated solution containing insulin, transferrin, selenious acid, bovine serum albumin and linoleic acid, R&D kit), 100U/ml penicillin, 100µg/ml streptomycin and 2mM L-glutamine). Media was replaced every 3-4 days for 28 days, and then spheroids were fixed in 4% PFA and were stained for aggrecan (1:100) (R&D kit).

2.16 TREATMENT OF CULTURES

Media was changed prior to treatment. Cell cultures were treated with vehicle (0.5% low endotoxin BSA in sterile PBS), 10µg/ml IL-1Ra (Kineret, Biovitrum, Sweden), 10ng/ml IL-1β (R&D systems, UK), full-length TSG-6 (1-500ng/ml, produced in-house and kindly donated by Professor Tony Day, University of Manchester), Link_TSG6 (amino acids 37-128, 0.36-181ng/ml, produced in-house and kindly donated by Professor Tony Day, University of Manchester) or combinations thereof. When IL-1Ra was used, it was applied 10 min prior to other treatments. The treatment period was 24h for glial, neuronal and bEND5 cultures, and 3h for MSCs.

2.17 RIBONUCLEIC ACID (RNA) EXTRACTION AND ANALYSIS

2.17.1 RNA EXTRACTION FROM MSCS

RNA was purified from MSCs using a ReliaPrep RNA Cell Miniprep System kit (Promega, UK) following the manufacturer's 'quick protocol'. Briefly, 250µl lysis buffer (BL + TG buffers) was added to each well of a 6-well plate for 2D cultures, or to each tube of 3 pooled and sonicated spheroids for 3D cultures. Cells were dispersed by vortexing, and 85µl 100% isopropanol was added to each sample. Cells were vortexed and transferred into a Minicolumn in a collection tube, and were centrifuged at 12,000xg for 30s. Liquid was discarded, and 500µl RNA wash solution was added to each Minicolumn followed by centrifugation at 12,000xg for 30s. DNase I Incubation Mix was prepared (for each sample: 24µl Yellow Core Buffer, 3µl 0.09M $MnCl_2$, 3µl DNase I) and 30µl was added to each Minicolumn. Tubes were incubated for 15 min at 20-25°C, then 200µl Column Wash Solution was added and samples were centrifuged at 12,000xg for 15s. 500ul RNA Wash Solution was added to each column, followed by centrifugation at 12,000xg for 30s. Minicolumns were placed into a new collection tube, and 300µl RNA Wash Solution was added, followed by centrifugation at 12,000xg for 2 min. Minicolumns were transferred to elution tubes, and 15µl nuclease-free water was added to each column, followed by centrifugation at 12,000xg for 1 min.

RNA concentration was quantified using a Nanodrop 2000 spectrophotometer (Thermo Scientific, UK), and samples were stored at -80°C until further analysis.

2.17.2 RNA EXTRACTION FROM TISSUE

Trizol reagent (1ml; Invitrogen, UK) was added to each sample, and tissue was homogenised using a mechanical homogeniser. Chloroform (200µl; Sigma, UK) was added to each sample, followed by vigorous shaking and centrifugation at 13,000rpm for 15 min at 4°C. The clear aqueous phase was transferred to a new tube, and 500µl 100% isopropanol was added. Samples were vortexed, incubated at room temperature for 10 min then centrifuged at 13,000rpm for 10 min at 4°C. The supernatant was discarded, and the pellet was washed in 1ml 70% ethanol made up in sterile water. Samples were centrifuged at 8,000 rpm for 5 min at 4°C, the supernatant was removed and pellets were air dried for 5 min. RNA was re-suspended in 20-50µl RNase-free

water (Invitrogen, UK), and RNA concentration was quantified using a Nanodrop 2000 spectrophotometer. Samples were stored at -80°C until further analysis.

2.18 Reverse transcription polymerase chain reaction

Complementary DNA (cDNA) was synthesised from a consistent amount of RNA for each tissue (spleen, liver, lung, brain: 2.5µg; bone marrow, 80ng). RNA, 1µl oligo-(dT) 12-18 (Invitrogen, UK), 1µl 10mM deoxyribonucleotide triphosphates (dNTPs) (Invitrogen, UK) and RNase-free water in a total volume of 12µl were heated to 65°C for 5 min, followed by cooling on ice. 4µl 5X first strand buffer, 2µl 0.1M dtt and 1µl RNase out (all Invitrogen, UK) were added to each sample, followed by heating to 37°C for 2 min. 1µl (200U) of M-MLV reverse transcriptase (Invitrogen, UK) was added, and samples were incubated at 37°C for 50 min, followed by 70°C for 15 min and pausing at 4°C.

2.19 Quantitative polymerase chain reaction (qPCR)

2.19.1 qPCR: Tissue

A 384-well system was used, with each well containing 1µl cDNA, 1µl primers, 5µl SYBR green (Invitrogen, UK) and 3µl water. Primers were Quantitect Primers Assays from Qiagen (UK), or were designed using BLAST software and manufactured by Eurofins (UK). Designed primer sequences were as follows: mouse TSG-6 forward: 5'-ATTTGAAGGTGGTCGTCTCG-3', mouse TSG-6 reverse: 5'-GTTTCACAATGGGGTATCCG-3'. A fast real-time PCR system (7900 HT, Applied Biosystems, UK) was used. The expression of housekeeping genes for glyceraldehyde 3-phosphate dehydrogenase (GAPDH), succinate dehydrogenase complex (SDHA), β-Actin, 14-3-3 protein zeta/delta (YWAHZ), hypoxanthine phosphoribosyltransferase 1 (HPRT1) and 18.s ribosomal RNA (r18.s) was analysed, and the most stable gene across test conditions was chosen for normalisation for each tissue. The expression level for each condition was defined as the fold-change in expression compared to naïve mice, and was deduced using the comparative Ct (2-[delta][delta]Ct) method.

2.19.2 qPCR: MSCs

The same system was used as for tissue, except designed primers (for the MSC differentiation assay) were used at 0.1µl per well, and Quantitect Primers Assays (IL-6/IL-8 for 2D versus 3D IL-1 stimulation experiments) (Qiagen, UK) were used at 1µl per well. Human TSG-6 primer sequences were as follows: forward: 5'-AACCCACACGCAAAGGAG-3'; reverse: 5'-TCATTTGGGAAGCCTGGA-3'. The expression of housekeeping genes for GAPDH, 60S ribosomal protein L13a (RPL13a), elongation factor 1-alpha (EF1-α) and TATA box binding protein (TBP) were analysed and were used for normalisation. Primers for the MSC differentiation assay were purchased from MWG Bitech, UK, and sequences are shown in Table 2.4:

Gene	Forward Sequence (5'-3')	Reverse Sequence (5'-3')
GAPDH	AAGGGCATCCTGGGCTAC	GTGGAGGAGTGGGTGTCG
EF1-α	CAACCCCGACACAGTAGCAT	AAGGCATGTTAGCACTTGGC
RPL13a	GTGGTGGTCGTACGCTGTG	GCAAAGCCAGGTACTTCAACTT
TBP	TCGTGCCCGAAACGCCGAAT	CAGTGCCGTGGTTCGTGGCT
OCT4A	GCCCGAAACCCACACTGC	ACACTCGGACCACATCCTTC
NANOG	GAAATACCTCAGCCTCCAGCA	CCAGGTCTTCACCTGTTTGT
Collagen II	GGCTCCCAGAACATCACC	ATGAGCAGGGCCTTCTTG
Collagen IX	AGGAATAGGGCGGCTTTC	AAGATGGCCAGTGGAGGA
RUNX II	CTTCCTGCCATCACCGATGT	GCCAGAGGCAGAAGTCAGAG
Osteopontin	TCCAAAGTCAGCCGTGAA	TGGGGTCTACAACCAGCA
Alkaline Phosphatase	CTTGGGCAGGCAGAGAGT	GCCTCTGGGTCTGGAGAA
PPAR2	CTGCGAAAGCCTTTTGGT	TTGCCAAGTCGCTGTCAT
FABP4	AAACTGGTGGTGGAATGCGT	GGTCAACGTCCCTTGGCTTA
CEBP	CAAGTGCCGCGACAAGGC	GCTTGCGCAGGCGTCATTC

Table 2.4. Primer sequences for qPCR for differentiation assay of human MSCs.

The expression level for each condition was defined as the fold-change in expression compared to untreated cells, and was deduced using the comparative Ct (2-[delta][delta]Ct) method.

2.20 LINK_TSG6

Unless otherwise specified, all experiments using TSG-6 treatment utilise Link_TSG6. The Link module of TSG-6 comprises amino acids 37-128, and is produced via an *E. Coli* expression system, as described in (Day et al., 1996). Link_TSG6 and full length TSG-6 protein were kindly provided by Prof. Anthony Day (University of Manchester).

2.21 STATISTICS AND STUDY DESIGN

All statistics were completed using GraphPad Prism software (version 5.0). Data were tested for normal distribution, and appropriate parametric or non-parametric tests followed by post-hoc analyses were carried out (ANOVA + Bonferroni's multiple comparison test or Kruskall-Wallis followed by Dunn's multiple comparison test). Data were considered significant at $p<0.05$.

All studies and analyses were carried out in a blinded and randomised manner. Blinding of treatment groups was carried out by an impartial colleague, with blinding remaining in place throughout all analyses. Blinding involved replacing the name of the treatment with a letter (e.g. A, B etc.). Randomisation was conducted with an online tool available at www.randomizer.org. Group sizes were determined with assistance of sample size calculators at www.statstodo.com.

CHAPTER 3:

THE EFFECT OF TSG-6 ON IL-1-INDUCED BRAIN DAMAGE AND INFLAMMATION

3.1 INTRODUCTION

The pro-inflammatory cytokine IL-1 is one of the key components of the inflammatory response. It is up-regulated in response to neurological challenges such as stroke, and is associated with many of the clinical conditions that predispose to stroke and worsen outcome, such as obesity, atherosclerosis and pneumonia (Allan et al., 2005; Barbarroja et al., 2010; Calbo et al., 2010; Frostegård et al., 1999; Galea et al., 1996). IL-1 has been shown to be an important mediator of brain injury, and it has been demonstrated experimentally that mice challenged with peripheral IL-1β have a worse outcome after stroke (McColl et al., 2007). Neutrophils are key mediators of IL-1-induced brain damage, and inhibiting the granulocyte response protects against IL-1-induced exacerbation of ischaemic injury (McColl et al., 2007). Exacerbation of ischaemic injury by systemic IL-1 can be seen as a model of underlying peripheral inflammation, such as that seen in the common co-morbidities observed in stroke patients.

TSG-6 is a glycoprotein that has a low or non-existent expression level under normal conditions, but is rapidly up-regulated in response to inflammatory stimuli such as LPS, TNF-α and prostaglandins (Milner and Day, 2003). TSG-6 possesses a number of anti-inflammatory properties, including down-regulation of matrix metalloproteinases (MMPs) and inhibition of neutrophil migration (Getting et al., 2002; Mahoney et al., 2005). There are few reports of TSG-6 actions in the brain, though it has been shown to have potent anti-inflammatory effects in numerous peripheral conditions including arthritis, myocardial infarction and ocular injury (Lee et al., 2009b; Nagyeri et al., 2011; Oh et al., 2010).

Inflammation is a key component of stroke pathophysiology, and is a popular target for the investigation of potential therapeutic interventions. As neutrophils have been shown to be an important mediator of IL-1-induced brain injury in stroke, the aim of this chapter was to investigate whether TSG-6 can protect against exacerbation of brain damage through its inhibitory effects on neutrophils.

IL-1 is a potent inducer of inflammatory molecules in brain cells *in vitro*, and this is blocked by administration of IL-1Ra. TSG-6 was tested in cultures of glia, neurones and

brain endothelial cells to deduce whether it could dampen IL-1-induced pro-inflammatory responses.

3.2 AIMS

1. To characterise dose-dependent actions of peripheral IL-1 on ischaemic brain injury.
2. To test the effect of LINK_TSG6 on IL-1-induced brain damage and inflammation in MCAo.
3. To test the effect of TSG-6 on IL-1-induced inflammatory responses in brain cells *in vitro*.

3.3 METHODS

Male C57BL/6J mice were subjected to 20min MCAo followed by 24h reperfusion (see section 2.2). Mortality for this study was 4%, however during optimisation 30min MCAo and use of human IL-1β led to 40% mortality. 30min prior to the onset of occlusion, mice were injected intraperitoneally with either vehicle (0.5% low-endotoxin BSA in sterile PBS), or one of two doses of murine IL-1β (0.5ng/ml or 5ng/ml in a volume of 100µl/25g mouse, corresponding to 2 or 20ng/kg). Tail vein blood was taken before surgery, and at 0, 4 and 24h reperfusion. After 24h reperfusion, mice were trans-cardially perfused with 0.9% saline, and the spleen and bone marrow from the left tibia and femur were removed and homogenised in FACS buffer. The brain was fixed in PFA, and lesion volume was deduced after sectioning by staining with cresyl violet. Flow cytometric analysis of blood, spleen and bone marrow determined populations of granulocytes, monocytes, T cells and B cells.

Based on the results of the above study, 5ng/ml IL-1β was chosen for the investigation into TSG-6. Male C57BL/6J mice were subjected to 20min MCAo followed by 24h reperfusion. Mortality for this study was 4%. 30min prior to the onset of occlusion, mice were injected intraperitoneally with vehicle, 5ng/ml IL-1β, 5µg recombinant human Link_TSG6 (the module of TSG-6 protein shown to be responsible for the inhibitory effect on neutrophils) or 5ng/ml IL-1β + 5µg Link_TSG6 in combination. Tail vein blood was taken before surgery, and at 0, 4 and 24h reperfusion. Simple neurological score was assessed after 2h reperfusion. After 24h, mice were trans-

cardially perfused with saline and PFA, and brains were sectioned and stained with cresyl violet for assessment of lesion volume. Sections were stained with haematoxylin and eosin for quantification of haemorrhagic transformation, with anti-neutrophil serum (SJC-4) for analysis of neutrophil numbers, and for IgG for assessment of blood-brain barrier disruption. Blood samples were analysed by CBA according to the protocol described in section 2.10.

The effect of TSG-6 on IL-1-induced responses was tested in primary glial and neuronal cultures, and in a mouse brain endothelial cell line (bEND5). Cultures were prepared as described in sections 2.11-2.13. Cells were seeded in 24-well plates and once confluent fresh media was applied. Wells were treated with vehicle (0.5% low-endotoxin BSA in PBS), 10ng/ml murine IL-1β, 10μg/ml IL-1RA, IL-1β + IL-1RA, 1, 5, 50 or 500ng/ml full length recombinant human TSG-6, 0.36, 1.8, 18.1 or 181ng/ml human Link_TSG6 (equimolar concentrations to the full length doses), or combinations of IL-1 + full length or Link_TSG6. Treatments of IL-1RA and TSG-6 were applied 10min prior to addition of IL-1β. Treatments were for 24h, after which media was collected. Levels of KC and IL-6 were measured by ELISA.

Statistical analysis was performed using GraphPad Prism (version 5.0), with parametric or non-parametric tests (ANOVA or Kruskal-Wallis) being chosen depending on the distribution of the specific data-set. Linear regression was used to assess correlations. Significance was set at $P<0.05$.

3.4 RESULTS

3.4.1 CHARACTERISATION OF IL-1-MEDIATED EXACERBATION OF ISCHAEMIC BRAIN INJURY

To confirm previous data on IL-1-induced brain injury (McColl et al., 2007) and to investigate if peripheral IL-1 has dose-dependent actions on the exacerbation of ischaemic brain injury, it was necessary to perform a dose-response study to deduce the optimum dose of IL-1 to produce significant exacerbation of the lesion volume without causing considerable mortality. This dose would be taken forward into further studies investigating the effect of TSG-6. C57BL/6J mice were subjected to 20min transient MCAo surgery followed by 24h reperfusion. 30min prior to occlusion onset, mice were injected intraperitoneally with vehicle (0.5% BSA in PBS), 0.5ng/ml IL-1 or 5ng/ml IL-1.

3.4.1.1 LESION VOLUME

Lesion volume was visualised on brain sections by cresyl violet staining. There was no significant difference between mice treated with vehicle or 0.5ng/ml mIL-1 (Figure 3.1). Mice treated with the higher dose of 5ng/ml mIL-1 had significantly larger lesion volumes than vehicle-treated animals, with an exacerbation of 106% ($p<0.01$). Vehicle-treated mice had lesions mostly confined to the striatum, whereas most mice treated with the high dose of IL-1 had lesions extending into the cortex. Coefficients of variation for vehicle, 0.5ng/ml mIL-1 and 5ng/ml mIL-1 were 40%, 35% and 30% respectively.

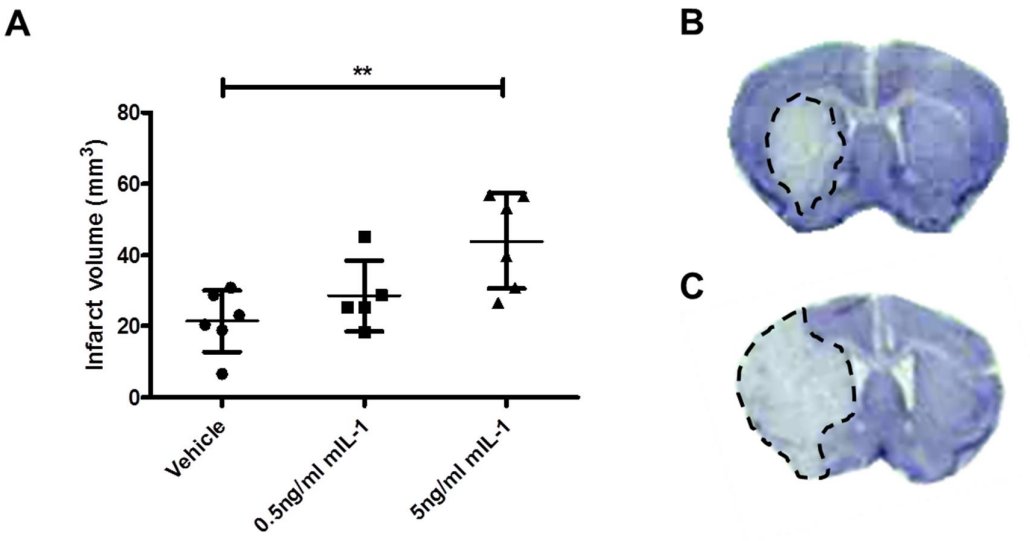

Figure 3.1: Analysis of lesion volume in vehicle- and IL-1-treated mice. Lesion volume was visualised by cresyl violet, with pale staining representing infarcted tissue. **A:** Mice treated with 5ng/ml mIL-1 had significantly larger lesion volumes than vehicle-treated mice. **B:** Typical section from the brain of a mouse treated with vehicle. **C:** Typical brain section from a mouse treated with 5ng/ml mIL-1. Data presented as mean ± SD. **P<0.01 (ANOVA, Bonferroni's multiple comparison test). n=5 (mIL-1) or 6 (vehicle).

3.4.1.2 LEUKOCYTE RESPONSES IN THE BLOOD TO IL-1

Tail vein blood was taken from mice before surgery onset, and at 0, 4 and 24h reperfusion. Immune cell populations were analysed by flow cytometry. There were no differences between treatment groups in any population investigated (Figure 3.2). Although non-significant, some populations showed trends for time-related changes. Monocytes and granulocytes appeared to peak in the blood at 4h post-reperfusion. Granulocyte numbers in the blood began to rise immediately after surgery, and were still elevated at 24h. Monocytes numbers had a more transient peak at 4h, and were restored to baseline by 24h. B cell numbers remained relatively constant over the duration of the surgery, but were severely depleted from the blood by 4h reperfusion. There wasn't such a distinct temporal change in T cells, however a small decline was seen over 24h.

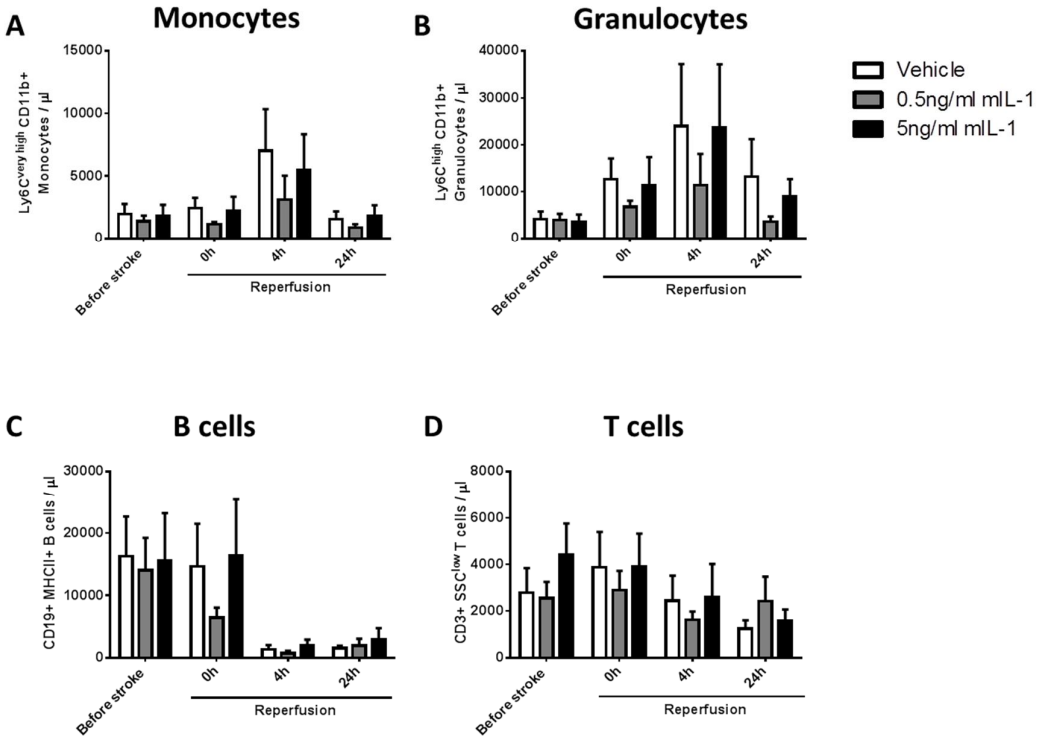

Figure 3.2: Immune cell populations in the blood following MCAo. Immune cell populations were analysed by flow cytometry. There were no significant differences between treatment groups or time-points (Two-way ANOVA). A: Ly6C$^{very\ high}$ CD11b+ monocytes. B: Ly6C^{high} CD11b+ granulocytes. C: CD19+ MHCII+ B cells. D: CD3+ SSC^{low} T cells. Data presented as mean ±SD. N=5 or 6.

The same immune cell populations were also analysed in bone marrow (Figure 3.3) and spleen (Figure 3.4) at 24h reperfusion. No significant differences were seen between treatment groups in any population. The most marked trend was a 1.7-fold increase in splenic B cells in IL-1-treated mice compared to control mice (P=0.0524). There was also an average 1.2-fold increase in bone marrow B cells in IL-1-treated mice compared to vehicle-treated mice.

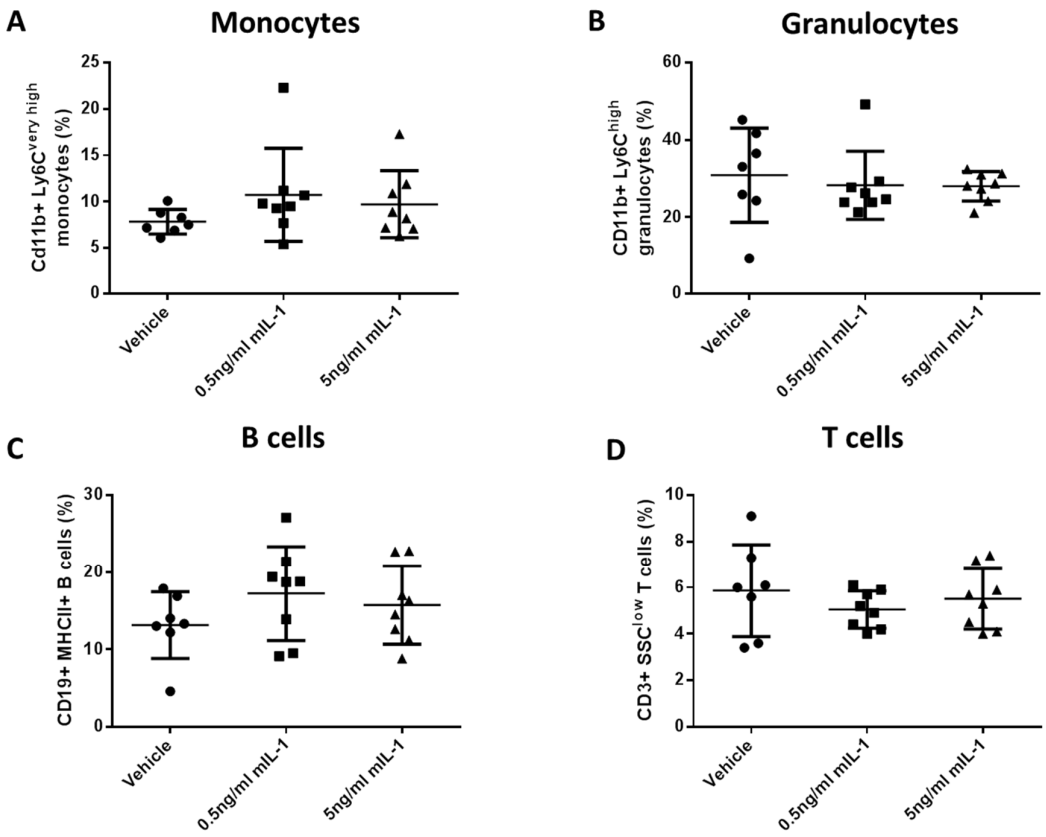

Figure 3.3: Immune cell populations in the bone marrow following MCAo. Immune cell populations were analysed by flow cytometry. There were no significant differences between treatment groups in any population. (ANOVA, Bonferroni's multiple comparison test). A: Ly6C$^{very\ high}$ CD11b+ monocytes. B: Ly6C^{high} CD11b+ granulocytes. C: CD19+ MHCII+ B cells. D: CD3+ SSC^{low} T cells. Data presented as mean ±SD. N= 7 or 8.

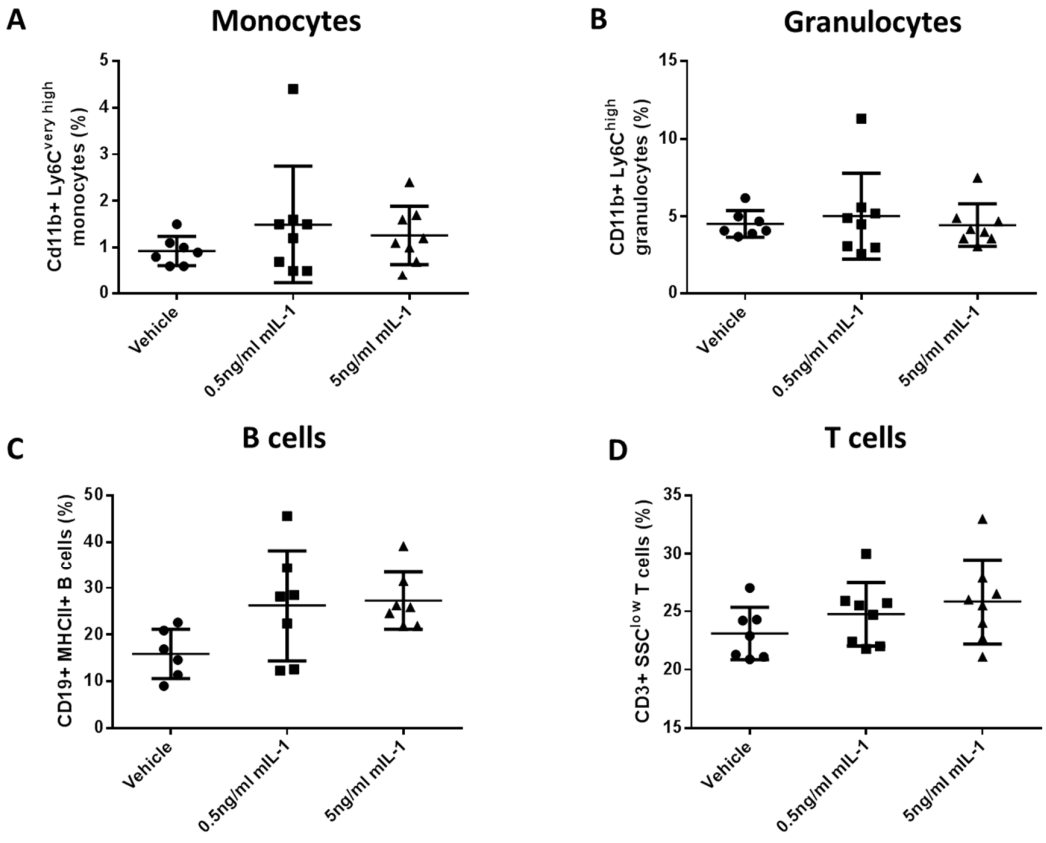

Figure 3.4: Immune cell populations in the spleen following MCAo. Immune cell populations were analysed by flow cytometry. There were no significant differences between treatment groups in any population. (ANOVA, Bonferroni's multiple comparison test). A: Ly6C$^{very\ high}$ CD11b+ monocytes. B: Ly6C^{high} CD11b+ granulocytes. C: CD19+ MHCII+ B cells. D: CD3+ SSC^{low} T cells. Data presented as mean ±SD. N= 7 or 8.

3.4.2 THE EFFECT OF LINK_TSG6 ON IL-1-INDUCED BRAIN DAMAGE

A study was designed to test the hypothesis that LINK_TSG6 could reduce IL-1-mediated exacerbation of ischaemic brain damage through its inhibitory effect on neutrophils. Mice were subjected to 20min transient MCAo followed by 24h reperfusion. 30min prior to occlusion onset mice were injected intraperitoneally with vehicle (0.5% BSA in PBS), 5ng/ml mIL-1, 5µg Link_TSG6 or 5ng/ml mIL-1 + 5µg Link_TSG6.

3.4.2.1 LESION VOLUME AND NEUROLOGICAL DEFICIT

Lesion volume was assessed at 24h reperfusion by cresyl violet. There was no significant difference between treatment groups, although there was a trend for exacerbation of lesion volume in the IL-1-treated group (Figure 3.5). The mean exacerbation was 78%, however 3 animals in this group showed no increase in stroke damage. There was a trend for a reduction in lesion volume in the IL-1 + Link_TSG6 group compared to the IL-1-treated group (mean lesion volumes were 28.3 and 37.1mm^3 respectively). There was substantial variation in all treatment groups apart from vehicle (coefficient of variation ~48%).

Neurological deficit was assessed after 2h recovery using a grading score of increasing severity of deficit (Bederson et al., 1986). There was no significant difference between treatment groups, however twice as many animals were observed circling (level 2 on the scale) in the IL-1-treated group compared to all other groups (shown in Figure 3.5-B).

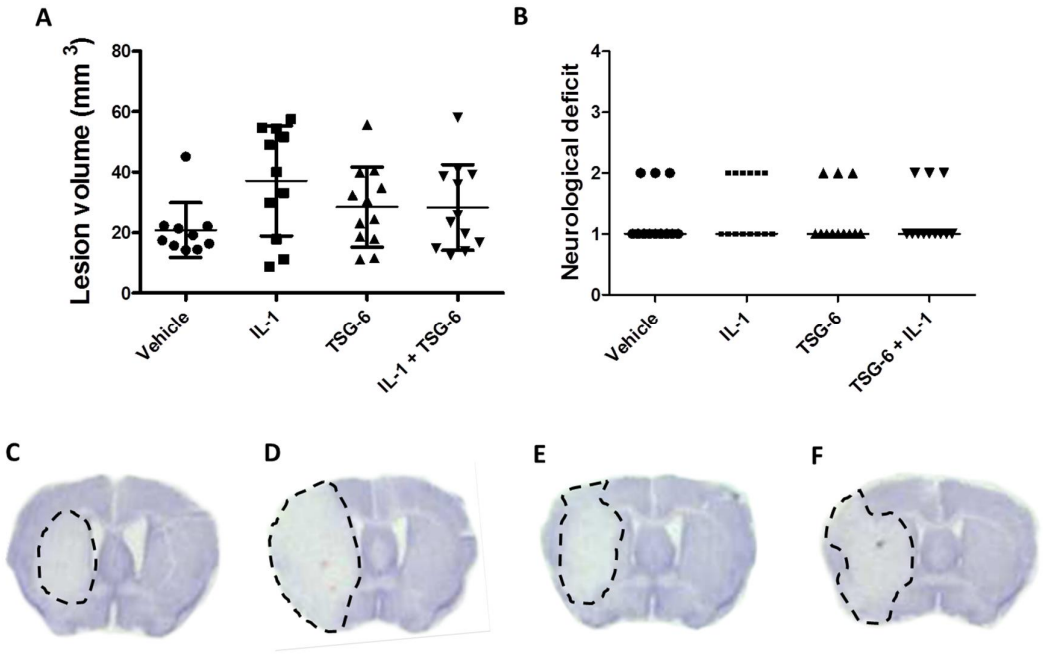

Figure 3.5: A: Analysis of lesion volume in vehicle-, Link_TSG6- and IL-1-treated mice. Lesion volume was visualised by cresyl violet at 24h after 20min MCAo. There was no significant difference between treatment groups, although there was a trend for exacerbation with IL-1 treatment. Data presented as mean ± SD. (ANOVA, Bonferroni's multiple comparison test). **B: Analysis of neurological deficit 2h after 20min MCAO.** There was no significant difference between treatment groups, although twice as many mice were circling in the IL-1-treated group than in all the other groups. 0, no observable deficit; 1, torso flexion to right; 2, spontaneous circling to right; 3, leaning/falling to right; 4, no spontaneous movement. Data presented as median. (ANOVA, Bonferroni's multiple comparison test). **Representative cresyl violet sections from brains of mice treated with vehicle (C), IL-1 (D), Link_TSG6 (E) and IL-1 + Link_TSG6 (F).** The pale area is indicative of cell death. Vehicle-treated mice largely had lesions restricted to the striatum, whereas mice in the other groups had lesions extending into the cortex. N = 11 or 12.

Correlation analysis was conducted to assess the effect of body weight on infarct volume (shown in Figure 3.6). There was a significant positive correlation between the two variables (P>0.01), with an R squared value of 0.2, meaning that body weight contributed to 20% of the variation seen in lesion volume.

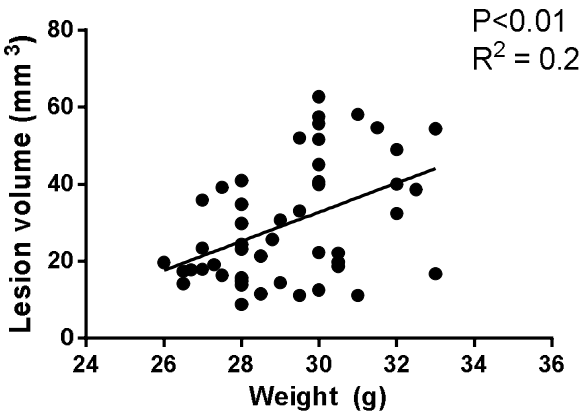

Figure 3.6: Correlation between body weight and lesion volume. There was a significant correlation between the weight of mice and the lesion volume produced from MCAo. (Linear regression). P<0.01, R squared = 0.2.

The correlation between body temperature at onset of occlusion and lesion volume was also investigated (Figure 3.7). There was a significant correlation between temperature and lesion volume (P<0.01), with an R squared value of 0.15 meaning that body temperature contributed to 15% of the variation.

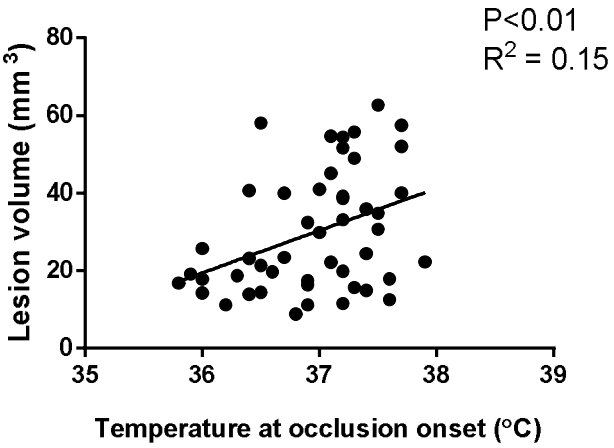

Figure 3.7: Correlation between body temperature and lesion volume. There was a significant correlation between the temperature of mice at the onset of occlusion and the lesion volume produced from MCAo. (Linear regression). P<0.01, R squared = 0.15.

3.4.2.2 NEUTROPHIL RECRUITMENT

Neutrophils have been shown to be a key mediator of IL-1-induced brain injury, and TSG-6 has previously been shown to inhibit neutrophil migration. Neutrophils were visualised in the core of the infarct by staining brain sections with SJC-4. There was a significant increase in the number of neutrophils in the striatum of IL-1-treated mice ($P<0.05$) (see Figure 3.8). There was no significant effect seen on the number of neutrophils in the cortex, although twice as many IL-1-treated mice had cortical neutrophils than mice given IL-1 + Link_TSG6. There was large within-group variability, with coefficients of variation ranging from 120-286%.

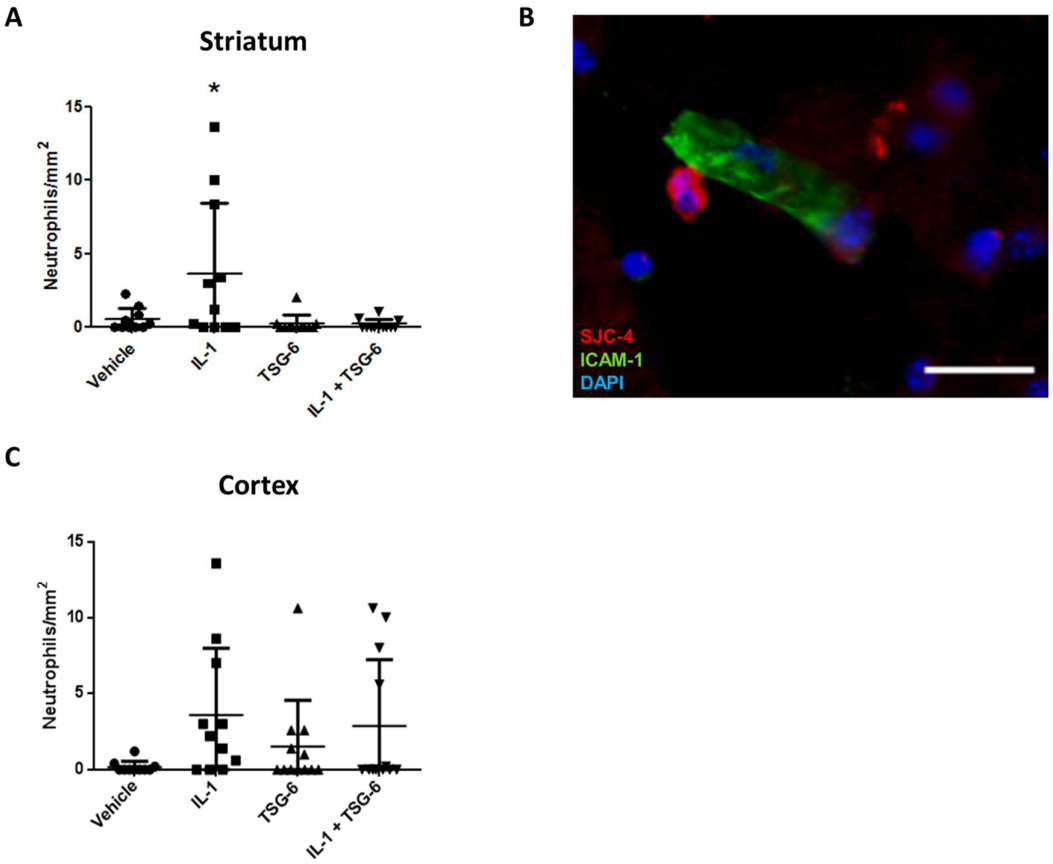

Figure 3.8: Neutrophils in the brain at 24h after MCAo. A: Striatum. IL-1 treatment resulted in recruitment of neutrophils into the striatal ischaemic core. Co-administration of IL-1 + Link_TSG6 inhibited neutrophil migration. B: Neutrophils were identified by immunohistological staining of neutrophils (SJC-4, red) and activated vessels (ICAM-1, green). Blue = DAPI. Scale bar = 10µm. C: Cortex. There was no significant effect on the number of neutrophils seen in the cortex. *$P<0.05$ vs all other groups (Kruskal-Wallis). Data presented as mean ± SD. N = 11 or 12.

3.4.2.3 HAEMORRHAGIC TRANSFORMATION

Haemorrhagic transformation occurs when blood leaks out of blood vessels and into the brain parenchyma. HT was visualised across 8 brain sections by staining with haematoxylin and eosin. Haemorrhages were identified by the intense red staining of red blood cells (example shown in Figure 3.9 part B). IL-1-treated mice had more bleeds than any of the other groups, and had a 5.7-fold increase in the area of haemorrhagic transformation when compared with mice treated with IL-1 + TSG-6, which just failed to reach significance (P=0.0504). Coefficients of variation ranged from 112-290%.

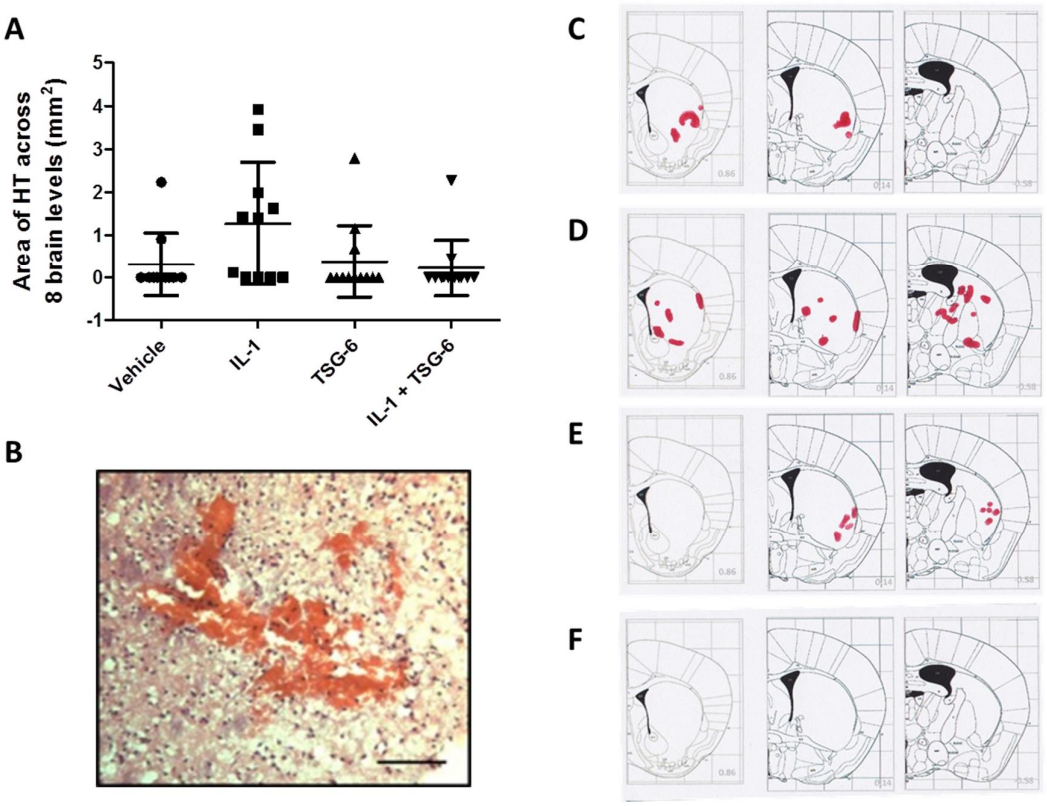

Figure 3.9: Haemorrhagic transformation at 24h. A: There was a trend for an increase in haemorrhagic transformation in IL-1-treated mice, with Link_TSG6 appearing to reduce the incidence of HT. B: Red blood cell (RBC) clusters were visualised by haematoxylin and eosin staining. Scale bar = 50µm. C-F: Brain maps indicating the typical location and quantity of bleeds in the brains of mice treated with C: vehicle, D: IL-1, E: Link_TSG6, F: IL-1 + Link_TSG6. Data presented as mean ± SD. (ANOVA, Bonferroni's multiple comparison test). N = 11 or 12.

3.4.2.4 BLOOD-BRAIN BARRIER DISRUPTION

Blood-brain barrier integrity was visualised by staining with IgG: extravasation of IgG into the brain parenchyma indicated a compromised blood-brain barrier. IL-1-treated mice had a 5.8-fold increase in the area of disrupted blood-brain barrier compared to vehicle- and IL-1 + TSG-6-treated mice, which again fell just short of significance (P=0.056) (shown in Figure 3.10). Only 1 out of 12 mice treated with IL-1 + LINK_TSG6 had any IgG staining, compared to 50% of IL-1-treated mice. There was large within-group variability, with coefficients of variation ranging from 112-346%.

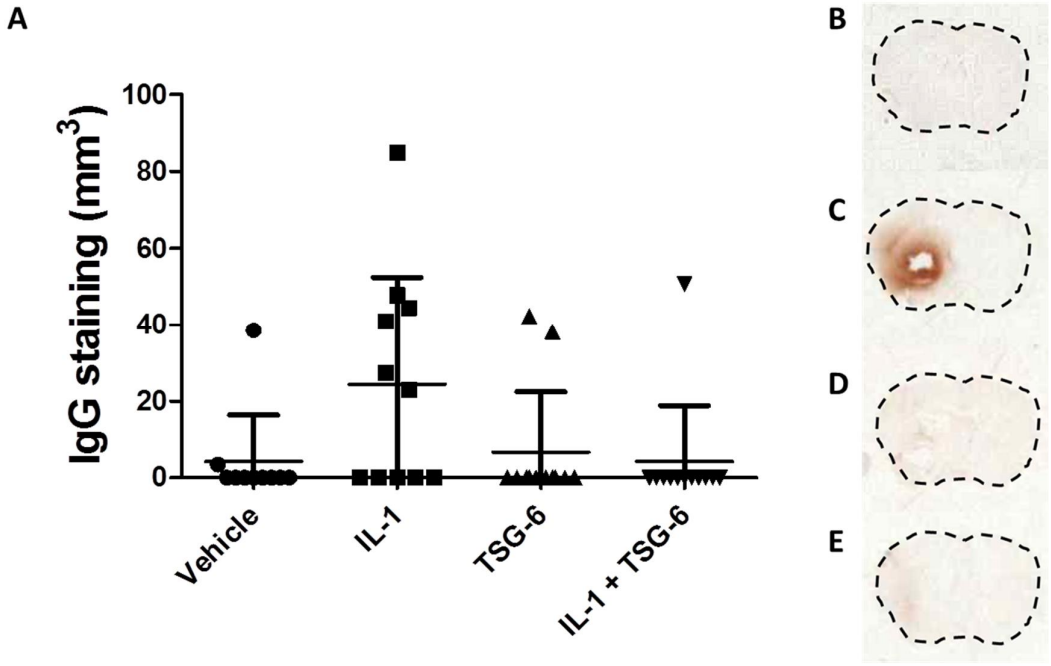

Figure 3.10: Blood-brain barrier disruption at 24h. BBB disruption was visualised by staining for IgG. A: There was a non-significant trend for an increase in blood-brain barrier disruption in IL-1 treated mice compared to mice treated with IL-1 + LINK_TSG6. Examples of typical patterns of IgG staining in the brains of mice treated with vehicle (B), IL-1 (C), LINK_TSG6 (D) and IL-1 + LINK_TSG6 (E). Data presented as mean ± SD. (Kruskal-Wallis, Dunn's multiple comparison test). N = 11 or 12.

3.4.2.5 POST-MCAO PLASMA CYTOKINE LEVELS

Three IL-1-treated mice failed to show effects of IL-1 exacerbation in lesion volume, neutrophil recruitment, haemorrhagic transformation and blood-brain barrier disruption. Plasma samples taken at 15min reperfusion were tested in a cytometric bead array to assess cytokine levels in the IL-1- and IL-1 + TSG-6-treated mice. The three IL-1-treated 'non-responders' had significantly lower (~5.5-fold) plasma concentrations of IL-6 than the other IL-1-treated mice and the mice treated with IL-1 + LINK_TSG6 ($P<0.05$) (shown in Figure 3.11). The non-responders also displayed a non-significant reduction in plasma IL-1α (2-fold), IL-10 (2-fold), KC (2.2-fold) and monocyte chemoattractant protein-1 (MCP-1, 2-fold) compared to the responders or to mice treated with IL-1 + TSG-6.

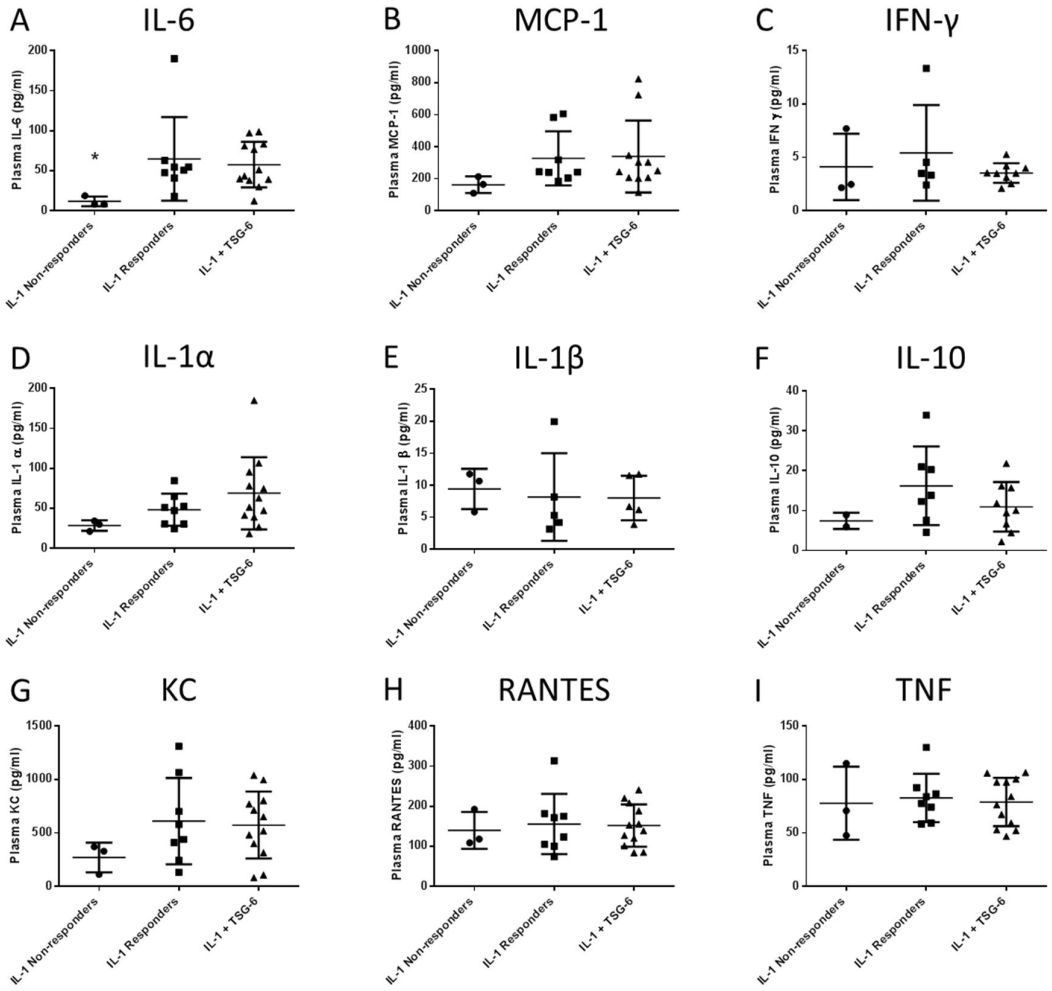

Figure 3.11: Plasma cytokines at 15min reperfusion in IL-1- and IL-1 + TSG-6-treated mice. Three IL-1-treated mice failed to show effects of IL-1 exacerbation (non-responders). Cytometric bead array was used to assess the cytokine profile in the plasma of IL-1- and IL-1 + LINK_TSG6-treated animals. Non-responders had significantly lower plasma concentrations of IL-6 (A) than IL-1-treated mice that showed effects of exacerbation (responders) and mice treated with IL-1 + TSG-6. There was no significant difference in plasma concentrations of MCP-1 (B), IFN-γ (C), IL-1α (D), IL-1β (E), IL-10 (F), KC (G), RANTES (H) or TNF-α (I). Data presented as mean ±SD. *P<0.05 compared to IL-1 Responders and IL-1 + LINK_TSG6 (Kruskall-Wallis, Dunn's multiple comparison test). N = 3 (IL-1 non-responders), 5-8 (IL-1 responders) or 5-12 (IL-1 + TSG-6).

3.4.3 THE EFFECT OF TSG-6 ON BRAIN CELLS *IN VITRO*

A study was conducted to assess whether TSG-6 had any effect on the main inflammatory responses of brain cells *in vitro*, both by itself and in the presence of IL-1. Primary mouse neurones and mixed glial cultures, and bEND5 cells (a mouse brain endothelial cell line) were treated with combinations of IL-1, IL-1Ra, full length TSG-6 and Link_TSG6 for 24h. Media concentrations of IL-6 and KC were measured by ELISA.

In all cell types, there was no induction of IL-6 (Figure 3.12) or KC (Figure 3.13) after treatment with vehicle, IL-1Ra or with any concentration of full length TSG-6 or Link_TSG6 alone. Treatment with IL-1 led to a significant increase in IL-6 levels in mixed glia and in bEND5 cells ($P<0.01$), and there was a trend for induction of IL-6 in neurones and of KC in all three cell types. This induction was reversed by co-administration of IL-1Ra with IL-1.

No 'dampening' effect of TSG-6 on IL-1-mediated responses was seen. When IL-1 was co-administered with various concentrations of full length TSG-6 or Link_TSG6, the resulting media concentration of IL-6 or KC was comparable to that induced by IL-1 alone (Figures 3.12 and 3.13).

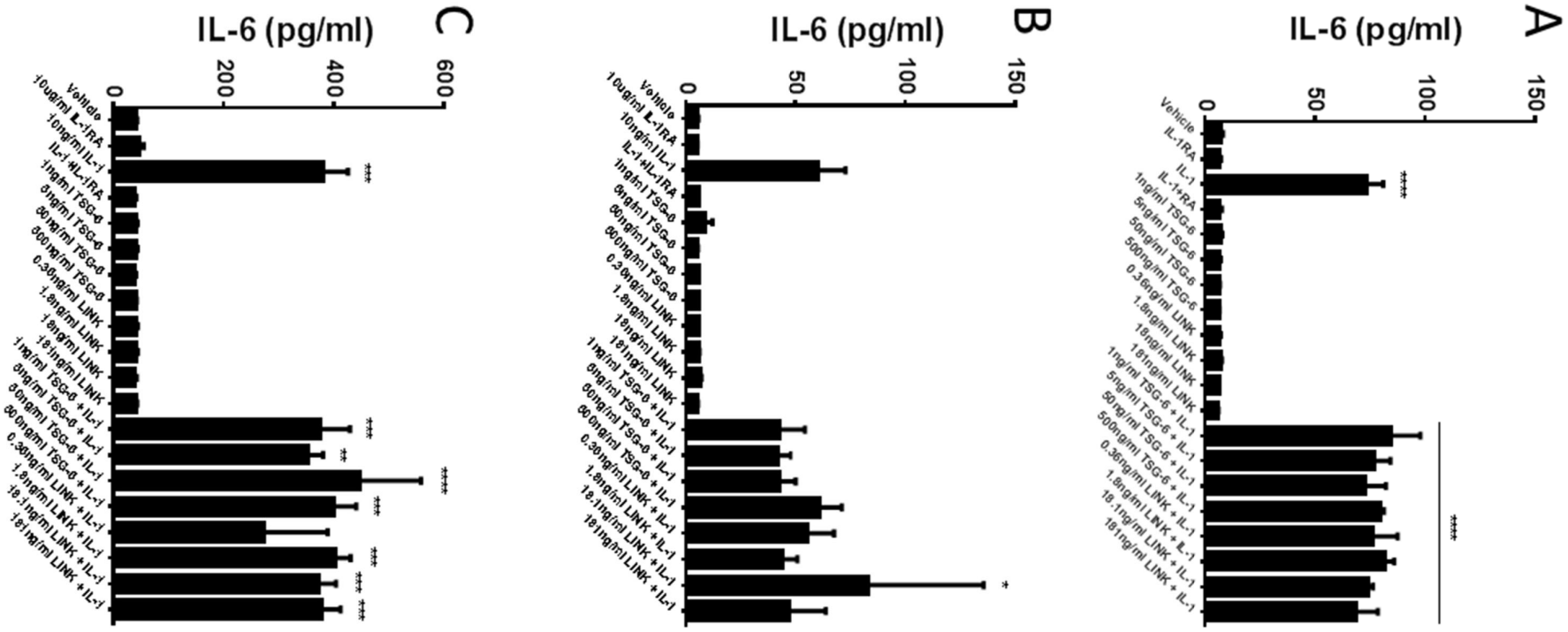

Figure 3.12: Media concentrations of IL-6 after 24h treatment with IL-1, IL-1Ra and TSG-6. IL-1 induced an increase in media levels of IL-6, but this was not reversed by co -administration with full length TSG -6 or Link_TSG6. IL -1Ra inhibited the effect of IL -1. TSG-6 had no effect on IL -6 when administered alone. A: Primary mixed glial cells. B : Primary neuronal cells. C: bEND5 cells. Data presented as mean ±SD. *P<0.05, **P<0.01, ***P<0.001, ***P<0.0001 vs vehicle (ANOVA, Bonferroni's multiple comparison test). N=3.

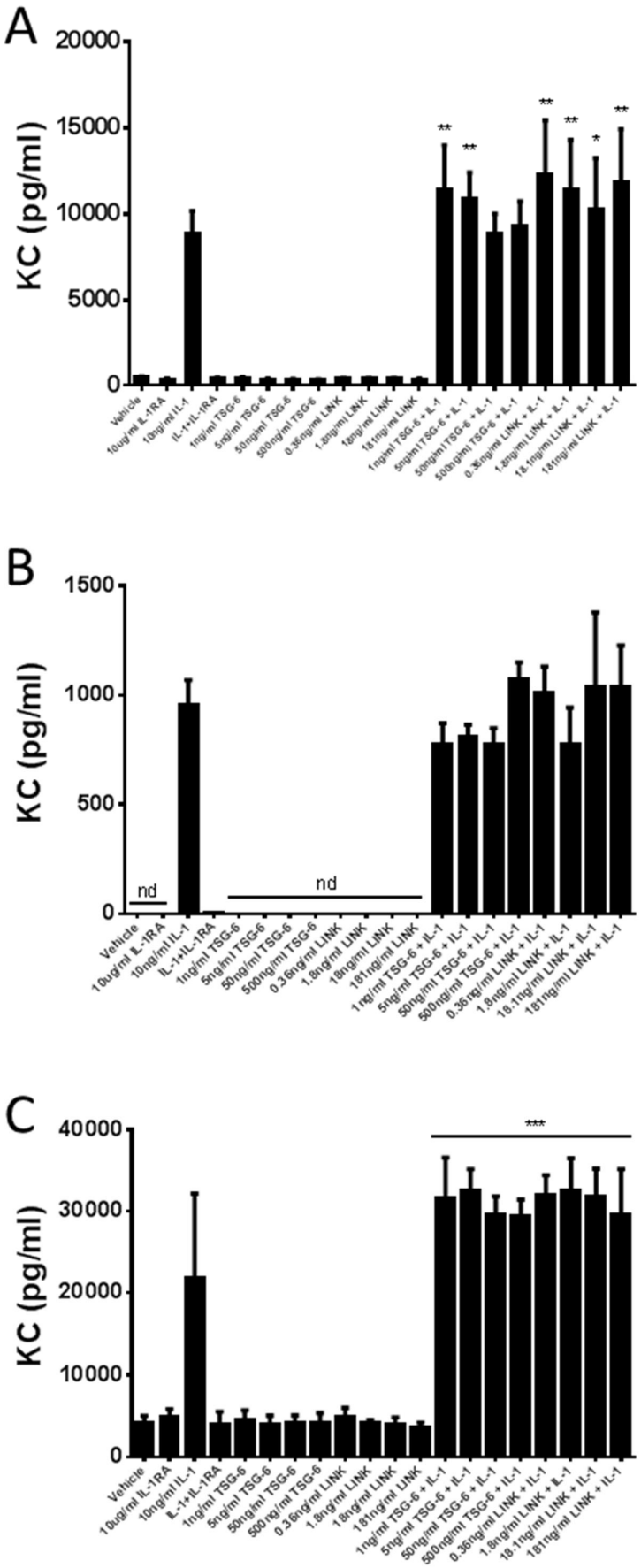

Figure 3.13: Media concentrations of KC after 24h treatment with IL-1, IL-1Ra and TSG-6. IL-1 induced a non-significant increase in media levels of KC, but this was not reversed by co-administration with full length TSG-6 or Link_TSG6. IL-1Ra inhibited the effect of IL-1. TSG-6 had no effect on KC when administered alone. A: Pri mary mixed glial cells. B: Primary neuronal cells. C: bEND5 cells. Data presented as mean ±SD. *P<0.05, **P<0.01, ***P<0.001 vs vehicle (ANOVA, Bonferroni's multiple comparison test). nd = non-detectable. N=3.

3.5 DISCUSSION

This chapter of work has been based on the finding that peripheral IL-1 exacerbates stroke in a neutrophil-dependent manner (McColl et al., 2007). This IL-1 exacerbation model of MCAo was originally characterised using human IL-1β with a 30min occlusion period. Early attempts to replicate this work were marred by high mortality rates, so the decision was made to use murine IL-1β and conduct a dose-response study using a shorter occlusion period of 20min. It was not possible to precisely infer a dose from the published work, as this reported a dosage based on batch-specific activity of the human IL-1 (100,000 international units (IU)/μg). The study with human IL-1β reported an exacerbation in lesion volume of >150% (McColl et al., 2007), whereas the high dose of murine IL-1β used in this chapter's dose response study produced an exacerbation of 106%. Both works analysed outcomes after 24h reperfusion.

The primary issue with the results gained from the TSG-6 study in this chapter is that there was no significant exacerbation with IL-1. In this study, an exacerbation of only 78% was seen. The majority of mice in the IL-1-treated group displayed cortical damage, however three mice did not respond to the IL-1 challenge and had small striatal lesions with no visible blood-brain barrier disruption, neutrophil infiltration or haemorrhagic transformation. This meant that the IL-1 exacerbation model did not fully reproduce, and thus made it difficult to see any protective effect of TSG-6.

Further investigation into these three non-responders provided a few potential reasons as to why they may have failed to show exacerbation. CBA analysis of plasma taken 15min after reperfusion (corresponding to 60-70min post-injection of IL-1) revealed a significant difference in IL-6 between the non-responders of the IL-1-treated group and the responders and IL-1 + TSG-6-treated mice. Plasma IL-6 has been suggested as a clinical biomarker for stroke risk, due to its role in promotion of coagulation and plaque disruption (Cesari et al., 2003; Kerr et al., 2001). IL-6 also induces production of C reactive protein (CRP), the main clinical biomarker of stroke risk and outcome (Kaptoge et al., 2010). Experimentally, CRP has been shown to exacerbate stroke outcome (Gill et al., 2004). It is possible that part of the exacerbation effect of IL-1 comes from induction of IL-6 and subsequently CRP, and the failure of the three non-responders to induce such a response could have contributed

to their smaller lesion volumes. However, CRP is not the main acute phase protein in mice as it is in humans. In mice serum amyloid A (SAA) is the main driver of cytokine production, although IL-6 is still able to induce SAA in mice so this is still a viable pathway of exacerbation (Uhlar and Whitehead, 1999). There was also a non-significant 2-fold reduction in MCP-1 in the non-responders. Plasma MCP-1 is increased in stroke patients (Arakelyan et al., 2005), and the recruitment of monocytes to the brain and their subsequent transformation into macrophages and production of inflammatory mediators is another source of exacerbation that could have been lacking in the three non-responders (Chiba and Umegaki, 2013). Similarly, the non-responders had a trend for lower levels of plasma KC than the other IL-1-treated mice, which could have resulted in a key failure in the mobilisation of neutrophils and their proven subsequent role in exacerbation. A possible reason for this reduced initiation of an inflammatory response, and subsequent lack of IL-1-mediated exacerbation of the ischaemic damage could be incorrect technique during the intraperitoneal injection. Although due care was taken, the injection could potentially have penetrated the bladder or cecum, resulting in excretion of the IL-1. Although these data indicate a lower responsiveness of the non-responders to IL-1, this is not sufficient to exclude these mice from the experiment as no such criteria were set pre-hoc. However, if these mice were removed from analysis, significant exacerbation with IL-1 and significant protection with Link_TSG6 is seen on lesion volume, neutrophil recruitment, BBB breakdown and haemorrhagic transformation.

Further review of the surgical records associated with this study revealed another potential source of the variation seen with the IL-1-treated group. The surgeries for this study were conducted over 5 weeks to allow time for perfusions and sectioning at 24h time-points. This resulted in a range of ages of mouse being used, from 12-16 weeks old. The three non-responders' surgeries were all conducted in the first week of the study, at an age of 12 weeks old. The 13-16 week old mice had a 255% increase in lesion volume compared to the three 12-week old non-responders. Doppler flowmetry confirmed a reduction in cerebral blood flow in the non-responders. Although it is highly unlikely that a week could make a difference, age has been shown to affect lesion volume in experimental stroke, particularly in the presence of peripheral inflammation (Dhungana et al., 2013; Rosen et al., 2005).

Despite the problem of not having a robust exacerbation model, TSG-6-treated mice displayed a significant reduction in the number of neutrophils in the striatum, corresponding to the ischaemic core. This confirms that the Link_TSG6 was functionally active *in vivo,* at least to some degree, although there was no difference seen in cortical neutrophils. The fact that a reduction in striatal neutrophils was seen without any effect on lesion volume suggests that infiltration might not necessarily be required for exacerbation to occur. It is possible that neutrophils are not actually responsible for exacerbation themselves, however they simply accumulate after the ischaemic damage is complete in a scavenger role. Temporal studies have shown that neutrophil infiltration often occurs after the full development of the infarct, suggesting that infiltration is not responsible for the expansion of the damage (Zhang et al., 1994). However, in this IL-1 exacerbation model it was shown that neutrophil accumulation does occur prior to the completion of ischaemic damage (McColl et al., 2007). It could be the case that neutrophils are able to exert some deleterious effect from the blood without entering the brain parenchyma, perhaps by release of reactive oxygen species, cytokines or proteases. However, a spatial specificity of the neurotoxic effect of neutrophils has been previously demonstrated. It was shown that neutropenia is able to attenuate ischaemic damage in the cortex but not in the striatum, even when a reduction in neutrophils is seen here (Beray-Berthat et al., 2003). Although in this chapter no reduction was seen in cortical damage or cortical neutrophils, it does help to explain why the reduction in striatal neutrophils had no effect on lesion volume. The striatum is vulnerable to a more severe ischemia than the cortex, due to a lack of collateral arteries and a more pronounced reduction in blood flow (Tamura et al., 1981). It is possible that this striatal lesion is unsalvageable, even when neutrophil infiltration is reduced. Taking all this into account, it is probable that had Link_TSG6 successfully reduced cortical neutrophil infiltration, a protective effect on lesion volume might have been seen.

TSG-6, both the full length protein and the Link module, has been shown to potently inhibit neutrophil migration in a range of models. Examples include reduced neutrophils seen in the synovium in models of arthritis (Szántó et al., 2004), in the air-pouch model (Getting et al., 2002; Wisniewski et al., 1996), in corneal injury (Oh et al., 2010) and in IL-1β-induced peritonitis (Cao et al., 2004). In the corneal injury model,

protection was seen with as little as 2ng TSG-6 (5µg was used in the work in this chapter). In addition to these *in vivo* models, TSG-6 can also inhibit neutrophil migration *in vitro* (Cao et al., 2004). There is just one report of TSG-6 reducing neutrophil migration into the brain in a neurological model (Watanabe et al., 2013), and it could be that differences in central and peripheral vascular beds can affect the ability of TSG-6 to function in this way. Indeed, this paper investigates traumatic brain injury, which has a very different aetiology to ischaemic stroke. Furthermore, the fact that stroke can result in disruption to the BBB means that neutrophil extravasation into the brain parenchyma might become uncontrolled, and so whichever mechanism TSG-6 works by in the periphery might be redundant in a BBB-compromised brain.

Despite the lack of a clear-cut effect seen in the TSG-6 study, the trends for protection seen in BBB disruption and haemorrhagic transformation made us hopeful that a true protective role for Link_TSG6 was being masked by the lack of a robust exacerbation model. The evidence that TSG-6 can down-regulate MMPs made it seem likely that a protective effect on the integrity of the BBB could be real (Mahoney et al., 2005). The decision was therefore made to repeat the study to try and elucidate the findings. However, the repeat resulted in no such trends, and the variation within groups was too great to distinguish any effect. The fact that all groups had such large variability suggests a potential contamination in the vehicle used. The bottle of PBS used was thought to be sterile and used solely for tissue culture, however it is possible that it could have become contaminated in some way.

Aside from contamination there are numerous factors which can contribute to variation in the MCAo model. Surgical experience and duration of the surgery can have huge implications on the outcome. The reason for longer surgeries resulting in larger infarcts is probably a combination of increased surgical trauma, and longer duration of anaesthesia leading to a drop in blood pressure, creating hypoperfusion before the occlusion has started. Isoflurane has been shown to inhibit vasoconstriction, suggesting that it could contribute to hypotension if administered for extended periods (Shimogai et al., 2010). Additionally, isoflurane can exacerbate haemorrhagic transformation (Hu et al., 2011). On the other hand, reports have shown that isoflurane is neuroprotective, although this is a long-term effect seen beyond the 24h time-point used in this work, and is a controversial argument (Sakai et al., 2007).

Surgeries that took more than 60min from anaesthetising the mouse to insertion of the filament were excluded, however reducing this cut-off further might help to reduce variability. Variation can also arise from temperature changes: increasing brain temperature by 1.2°C has been shown to triple infarct volume (Warner et al., 1993). This highlights the importance of using a homeothermically controlled heat blanket to maintain body temperature throughout the procedure. Although a blanket was used, temperatures still varied somewhat which might explain the in-group variability. Correlation analysis of temperature at onset of occlusion and lesion volume revealed that temperature contributed to 15% of the variation seen. A further source of variation could be the size of animals used. Although a relatively narrow weight range (25-30g) was used, it has been shown that greater reproducibility in infarct size can be achieved by using animals within a very narrow weight range (29 ± 0.9g) (McColl et al., 2004). This is however not always the most logistically practical solution and so a reasonable weight range must be expected, especially when considering the 3 Rs. In this chapter there was a significant correlation between body weight and infarct volume, with the R squared value indicating that body weight was responsible for ~20% of the variation. Therefore future work should aim to use as narrow a weight range as possible. In the protocol used in this work, the pterygopalatine artery (PPA) is not occluded. It has been shown that not occluding this vessel produces greater variability than when blood flow through the PPA is blocked (Chen et al., 2008). It has however also been argued that not occluding the PPA results in less surgical trauma and damage to the vagus nerve, thereby reducing variability (McColl et al., 2004). However, collateral blood supply from this vessel, along with inconsistencies in the structure of the circle of Willis could be key contributors to the variability seen in the MCAo model. Indeed, there does seem to be batch-to-batch/study-to-study differences in variability which cannot solely be due to methodology.

In this chapter, the leukocyte responses in the blood to IL-1 were investigated. No treatment-dependent effects were observed, although some time-dependent trends were reported. The inflammatory cell profile in the blood described in this work is in line with previously described data (Denes et al., 2010). Isoflurane and experimental stroke are able to induce profound changes in leukocyte populations, including release of granulocytes from the bone marrow into the circulation, and a recruitment of B cells

and T cells to the bone marrow. It is possible that the potent effect that isoflurane can have on leukocyte trafficking may have masked any differential effect of IL-1.

TSG-6 has been shown to reduce pro-inflammatory cytokines and chemokines (including IL-6 and KC) in a model of corneal injury (Oh et al., 2010). In addition, TSG-6 null mice have higher plasma concentrations of IL-6 (Szántó et al., 2004). It was hypothesised that TSG-6 might be able to regulate the production of pro-inflammatory mediators by brain cells, however no effect was seen on IL-1-mediated production of KC or IL-6 by primary glial, primary neuronal or bEND5 cells. The bEND5 cell line was chosen initially as it is far easier to culture and maintain than primary endothelial cells. It has been thoroughly characterised in the literature, and has been shown to have comparable levels of endothelial-specific cell adhesion molecules to primary cells (Steiner et al., 2011). However, the cell line is not a perfect replica of primary endothelial cells, and some differences have been noted, such as reduced expression of tight junction protein occludin (Lyck et al., 2009). It is possible that primary endothelial cells might have responded differently, but as there was no apparent effect in any cell type the study was not pursued any further. If this work were continued, an investigation into co-cultures and earlier time-points could also yield interesting results.

3.6 SUMMARY

This chapter aimed to elucidate a role for TSG-6 in reducing IL-1-mediated exacerbation of brain damage and inflammation. This exacerbation is known to be dependent on neutrophils, however in this model Link_TSG6 was unable to fully protect against neutrophil infiltration into the brain, although some reduction was seen. Perhaps as a result of this, no significant effects were seen on brain damage or inflammation, although there were some promising trends for an effect on BBB breakdown and haemorrhagic transformation. The lack of a robust model of IL-1 exacerbation caused difficulty in interpreting the results in this chapter, and further work and optimisation could be beneficial in clarifying any protective effect of TSG-6.

CHAPTER 4:

THE EXPRESSION PROFILE OF TSG-6 IN RESPONSE TO EXPERIMENTAL ISCHAEMIC STROKE

4.1 INTRODUCTION

TSG-6 is a glycoprotein with a number of anti-inflammatory properties including inhibition of neutrophil migration and down-regulation of MMPs, rendering it an interesting molecule in the context of stroke (Getting et al., 2002; Mahoney et al., 2005). In general, constitutive expression of TSG-6 is low or non-existent in most cells, although neutrophils express TSG-6 constitutively and store the protein in their granules (Maina et al., 2009). Expression of TSG-6 can be induced by a number of inflammatory stimuli including LPS, TNF-α, IL-1 and prostaglandins (Milner and Day, 2003), and a wide range of cell and tissue types have the capability to express TSG-6 under inflammatory conditions. Expression of TSG-6 has been described in fibroblasts, monocytes, synoviocytes, chondrocytes, dendritic cells, macrophages, various epithelial and endothelial cells, smooth muscle cells and MSCs (Lee et al., 2009b; Lee et al., 2001; Lilly et al., 2005; Maier et al., 1996; Maina et al., 2009; Tan et al., 2011; Wisniewski et al., 1993; Ye et al., 1997).

TSG-6 has not been extensively studied in the brain, and the single report of CNS expression attributes it to invading leukocytes, rather than expression by brain cells themselves (Al'Qteishat et al., 2006). Therefore the aim of this chapter was to reveal the temporal and spatial expression pattern of TSG-6 in the brain following experimental stroke.

4.2 AIMS

1. To elucidate the temporal pattern of expression of TSG-6 mRNA transcripts in the brain after MCAo and sham surgery.
2. To show the spatial pattern of TSG-6 protein expression in brain sections at various time-points after MCAo.
3. To investigate the cellular expression profile of TSG-6 in the brain after MCAo.

4.3 METHODS

Male C57BL/6 mice were subjected to 30 or 45min MCAo or sham surgery (as described in section 2.2). Mortality for these studies was 5%. Following 4h, 24h, 3, 5 or 7 days reperfusion mice were transcardially perfused with DEPC-treated 0.9% saline and peripheral organs were removed. For qPCR, brains were removed, split into two hemispheres and snap-frozen. For immunohistochemistry, mice were perfused with 4% PFA and brains were removed, fixed in PFA, cryoprotected in 20% sucrose and sectioned.

Brain hemispheres were homogenised in Trizol for extraction of RNA. cDNA was produced by reverse transcription PCR, and TSG-6 expression was analysed by qPCR (primer sequences were mouse TSG-6 forward: 5'-ATTTGAAGGTGGTCGTCTCG-3', mouse TSG-6 reverse: 5'-GTTTCACAATGGGGTATCCG-3'). Expression of housekeeping genes GAPDH, SDHA, YWAHZ and r18.s were tested and used for normalisation. See sections 2.17-2.19 for details.

qPCR data were analysed using the comparative Ct (2-[delta][delta]Ct) method. Fold changes were plotted using GraphPad Prism (version 5.0), and ANOVA or Kruskall-Wallis tests were performed depending on the distribution of the data. Significance was set at $P<0.05$.

TSG-6 protein was identified by fluorescent immunohistochemistry. Brain sections were blocked with 2% normal donkey serum and were incubated overnight with primary antibodies (TSG-6 + GFAP or CD45). Sections were washed in PBS and incubated with fluorescently-conjugated secondary antibodies for 3h (donkey anti-rabbit 594 + donkey anti-chicken 488 or donkey anti-rat 488). Sections were mounted and coverslipped using Prolong Gold Anti-fade Reagent with DAPI, and were analysed on an upright microscope (Olympus BX51) and Coolsnap ES camera using MetaVue Software.

4.4 RESULTS

4.4.1 SHORT-TERM EXPRESSION OF TSG-6 MRNA AFTER CEREBRAL ISCHAEMIA

There was no difference in TSG-6 expression between naïve mice and 4h or 24h MCAo time-points in either hemisphere after 45min MCAo (Figure 4.1). At 3 days there was a 2.8-fold increase in TSG-6 in the ipsilateral hemisphere, and a 3.9-fold increase in the contralateral hemisphere (compared to naïve mice, 4h and 24h time-points) ($P<0.05$). Four different housekeeping genes were tested, and GAPDH was chosen for normalisation as it was the most stable reference gene across the different time-points.

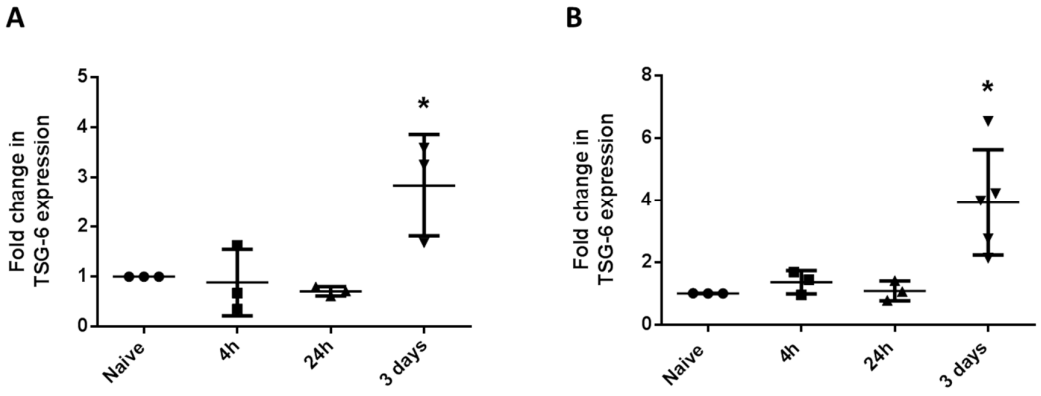

Figure 4.1: TSG-6 expression in the brain after 45min MCAo. There was no change in expression of TSG-6 in either hemisphere after 4h or 24h reperfusion. After 3 days reperfusion, there was a significant increase in expression of TSG-6 in the ipsilateral (A) and contralateral (B) hemispheres. Data presented as mean ± SD. *$P<0.05$ compared to naïve, 4h and 24h (ANOVA, Bonferroni's multiple comparison test). Expression levels normalised to GAPDH. N = 3 or 5.

4.4.2 LONG-TERM EXPRESSION OF TSG-6 MRNA AFTER CEREBRAL ISCHAEMIA

Due to high mortality (~50%) experienced with an attempted repeat of the 45min occlusion time, mice were subjected to 30min MCAo followed by 3, 5 or 7 days reperfusion. There was a significant increase in expression of TSG-6 in both hemispheres after 5 days reperfusion, as shown in Figure 4.2 (ipsilateral: 1.4-fold, contralateral: 1.7-fold). There was no significant change in expression at 3 or 7 days post-reperfusion. Four different housekeeping genes were tested, and r18.s was chosen as the most stable reference gene across the different time-points. GAPDH showed significant changes in expression across the different time-points so was unsuitable for use as a reference gene in this case.

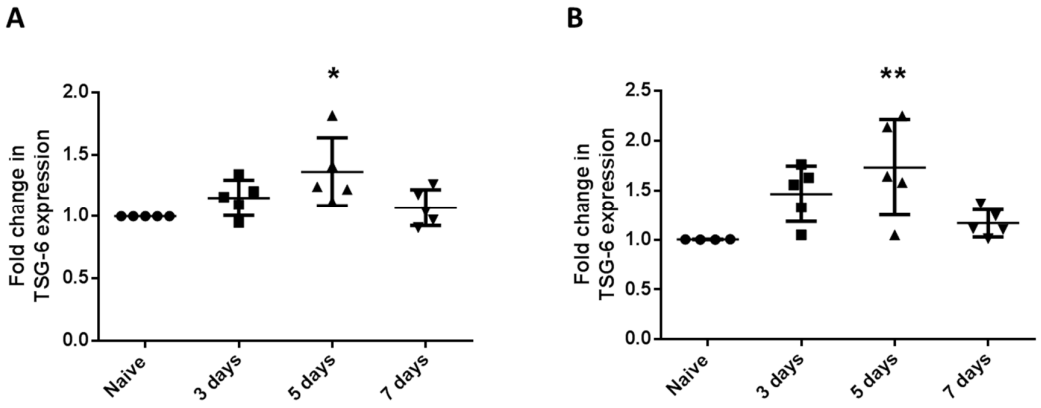

Figure 4.2: TSG-6 expression in the brain after 30min MCAo. There was no significant change in expression of TSG-6 in either hemisphere after 3 or 7 days reperfusion. After 5 days reperfusion, there was a significant increase in expression of TSG-6 in the ipsilateral (A) and contralateral (B) hemispheres. Data presented as mean ± SD. *P<0.05, **P<0.01 compared to naïve (Kruskall-Wallis, Dunn's multiple comparison test). Expression levels normalised to r18.s. N = 4 or 5.

4.4.3 Short-term expression of TSG-6 mRNA after Sham surgery

There was a slight non-significant decrease in TSG-6 expression in the ipsilateral hemisphere at 4h and 24h after sham surgery (0.3- and 0.4-fold respectively), with the mean returning to naïve levels at 24h (Figure 4.3). In the contralateral hemisphere, there was no change in expression at 4h or 24h after surgery, however there was a non-significant mean 2.1-fold increase in TSG-6 expression at 3 days after surgery. The variation was large in this group, with two mice showing a 3-fold increase in expression and two mice showing no change (coefficient of variation 53%). Four different housekeeping genes were tested, and GAPDH was chosen as the most stable reference gene across the different time-points.

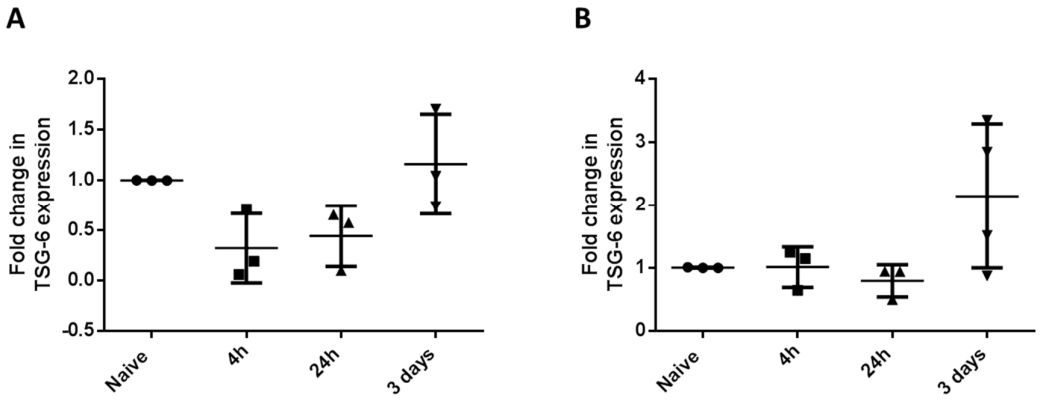

Figure 4.3: TSG-6 expression in the brain after sham MCAo. There was no significant change in expression of TSG-6 in the ipsilsteral hemisphere (A) or contralateral hemisphere (B) at any time-point following sham MCAo, although there was a trend for increased expression in the contralateral hemisphere after 3 days reperfusion. Data presented as mean ± SD. (ANOVA, Bonferroni's multiple comparison test). Expression levels normalised to GAPDH. N = 3 or 4.

4.4.4 Long-term expression of TSG-6 mRNA after Sham surgery

TSG-6 expression was also quantified after sham surgery. There was no significant induction of TSG-6 in the ipsilateral hemisphere after sham surgery at any time-point (Figure 4.4). In the contralateral hemisphere, there was a small increase (1.6-fold) in TSG-6 expression at 7 days compared to the expression at 5 days ($P<0.05$). Contralateral expression remained comparable to naïve mice at 3 and 5 days post-surgery. Four different housekeeping genes were tested, and r18.s was chosen as the most stable reference gene across the different time-points.

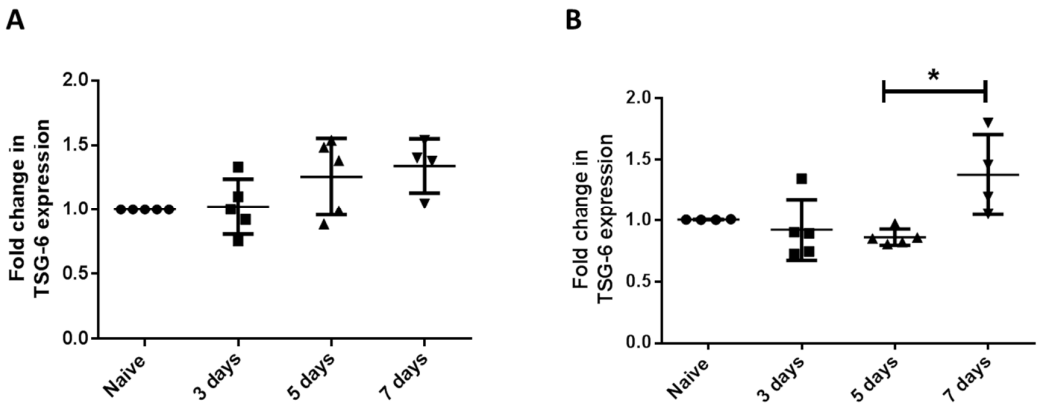

Figure 4.4: TSG-6 expression in the brain after sham MCAo. There was no significant change in expression of TSG-6 in the ipsilsteral hemisphere (A) at any time-point after sham MCAo. In the contralateral hemisphere (B) there was a small induction in expression at 7 days. Data presented as mean ± SD. *P<0.05 (Kruskall-Wallis, Dunn's multiple comparison test). Expression levels normalised to r18.s. N = 4 or 5.

4.4.5 Long-term expression of TSG-6 protein in the brain after cerebral ischaemia

Mice were subjected to 30min MCAo followed by 3, 5 or 7 days reperfusion. Brains were sectioned and dual-stained for TSG-6 and GFAP (an astrocyte marker). After 3 days reperfusion, there was no co-localisation of TSG-6 and GFAP: astrocytes were present within the infarct core, whereas TSG-6 was more prevalent outside of the infarcted area, forming a border around the damaged tissue (typical sections shown in Figure 4.5). After 5 and 7 days reperfusion, TSG-6 formed a ring around the infarcted tissue, which was associated with astrocytes forming the glial scar. TSG-6 staining was also visible in the contralateral primary motor cortex at all time-points, and in the ipsilateral motor cortex at 5 days. This patch of staining also seemed to be associated with GFAP.

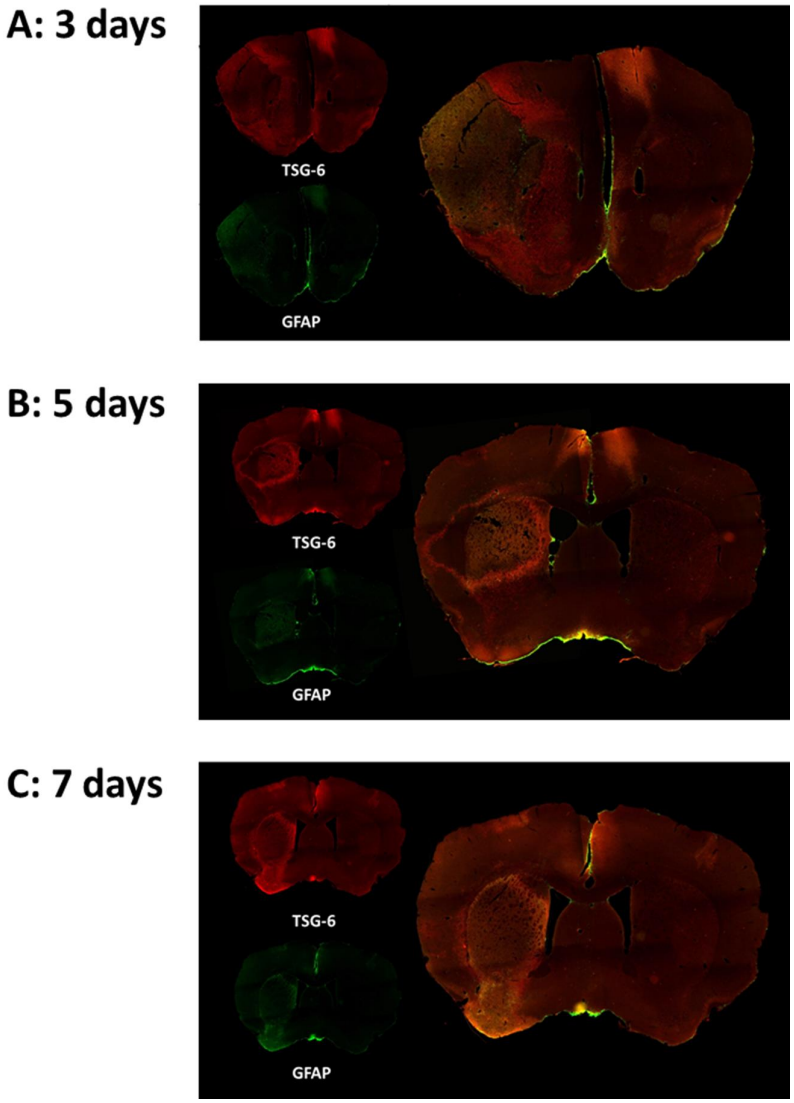

Figure 4.5: Representative sections showing expression of TSG-6 and GFAP in the brain after 30min MCAo. After 3 days MCAo (A), there was no co-localisation of TSG-6 and GFAP, with astrocytes residing in the infarct core and TSG-6 being more prevalent outside of the ischaemic area. After 5 (B) and 7 (C) days reperfusion, TSG-6 was associated with the glial scar, and formed an astrocyte-associated ring around the outside of the infarct. Red: TSG-6, Green: GFAP.

4.4.6 Expression of TSG-6 within the glial scar

Immunofluorescence staining of brain sections revealed an association of TSG-6 with astrocytes in the glial scar at 5 and 7 days post-reperfusion. The staining pattern resembled a ring surrounding the infarct, as seen in Figure 4.6. No such staining was seen in the contralateral hemisphere.

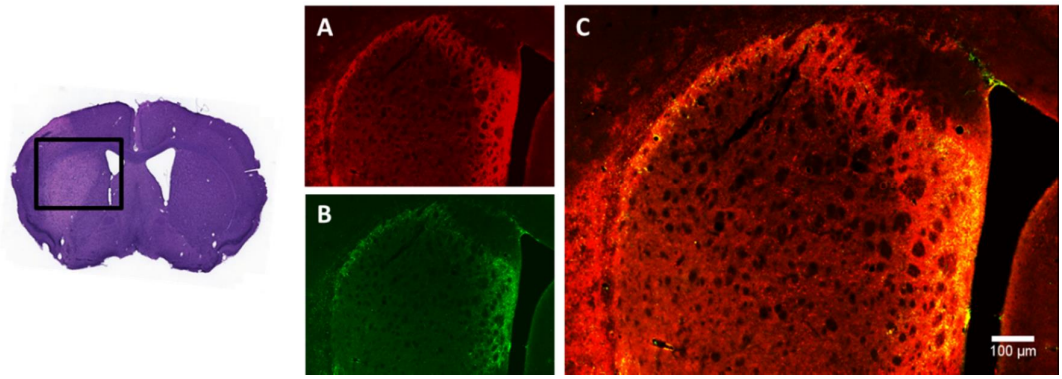

Figure 4.6: A typical brain section at 5 days post-MCAo displaying the characteristic pattern of staining surrounding the infarct. Immunofluorescence staining revealed a typical pattern of staining in which TSG-6 (A, red) and astrocytes (GFAP, B, green) formed a ring surrounding the infarcted tissue (C, combined). Scale bar = 100µm.

Whereas the majority of the TSG-6 staining appeared to be non-astrocytic (this could be neutrophil-derived or a component of the ECM), some co-localised staining was present, suggesting expression of TSG-6 by astrocytes in the glial scar (shown in Figure 4.7).

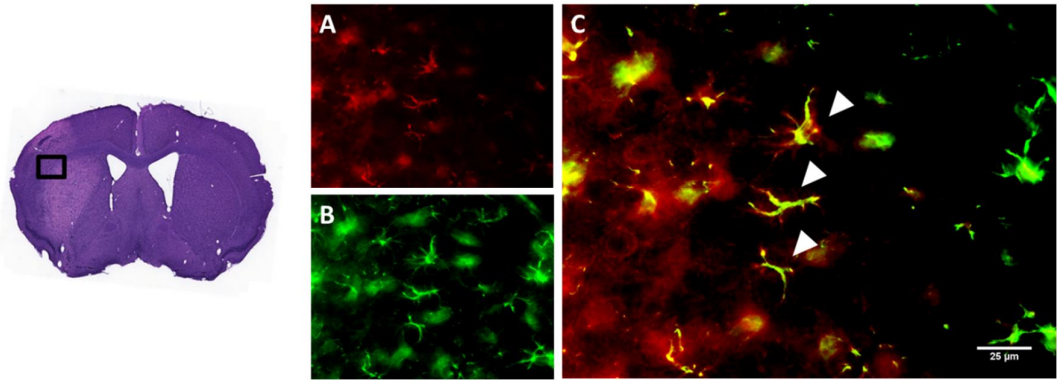

Figure 4.7: A typical brain section at 5 days post-MCAo showing co-localisation of GFAP and TSG-6 within the glial scar. Immunofluorescence staining revealed a typical pattern of staining in which TSG-6 (A, red) and GFAP (B, green) formed a ring surrounding the infarcted tissue. Although the majority of TSG-6 staining was extracellular, some astrocytes appeared to express TSG-6 (C, combined. White arrows indicate co-localised staining). Scale bar = 25µm.

This glial association of TSG-6 was astrocyte specific: no co-localisation was seen with microglia. Activated microglia/macrophages were seen in the core of the infarct, with TSG-6 remaining around the perimeter (Figure 4.8). An antibody against CD45 was used, which also stains leukocytes, but TSG-6 did not co-localise with leukocytes (round, CD45 highly-expressing cells) or activated microglia (ramified or amoeboid CD45+ cells).

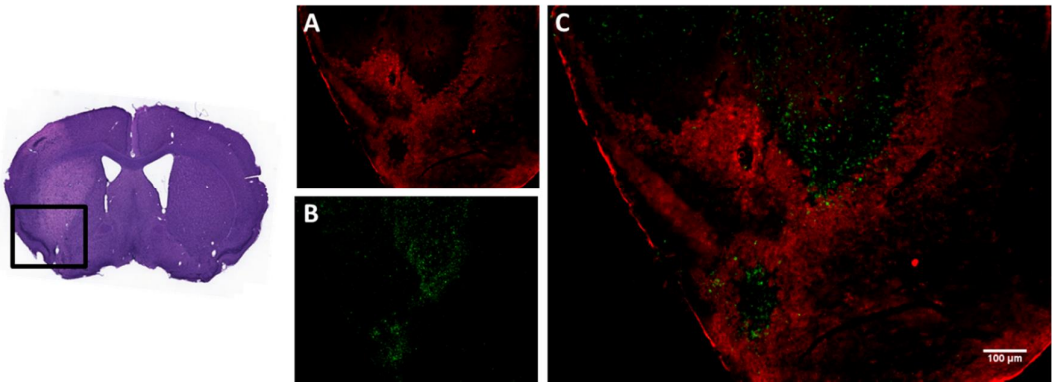

Figure 4.8: A typical brain section at 5 days post-MCAo showing no co-localisation of microglia (CD45) and TSG-6. Immunofluorescence staining revealed a typical pattern of TSG-6 staining (A, red), in which it formed a ring-like structure surrounding the infarct. Microglia (B, green, CD45) were more prominent within the infarcted tissue, and no co-localisation was observed (C, combined). Scale bar = 100µm.

4.5 DISCUSSION

This chapter of work was conducted with the aim of determining the temporal and spatial pattern of TSG-6 expression in the brain after MCAo. TSG-6 expression can be induced by inflammatory stimuli in a wide range of cell types, but has not been extensively described in the brain.

In this chapter, TSG-6 expression was found to be significantly induced at 3 days after 45min MCAo, and to a lesser magnitude at 5 days after 30min MCAo, when analysed by qPCR. In the hands of the investigator, 45min MCAo produces a much more severe infarct than 30min, with greater cortical damage. This most likely results in a greater inflammatory profile in the brain, with increased infiltration of leukocytes and expression of pro-inflammatory mediators. One of the main inducers of TSG-6 expression is TNF-α, and this cytokine has been shown to increase 35-fold in the ipsilateral hemisphere 3 days after MCAo (Winters et al., 2013). It is therefore logical that this longer occlusion period would result in a more profound induction of TSG-6 than 30min MCAo. Indeed, if we directly compare the 3 day reperfusion time-points, 45min MCAo resulted in a 2.8-fold increase in TSG-6 whereas 30min MCAo only induced a 1.15-fold increase. It therefore appears from this work that the extent of TSG-6 expression is dependent on the severity of the insult.

After 30min MCAo, mRNA transcripts indicated a peak in TSG-6 expression at 5 days which returned to baseline after 7 days. Immunohistochemistry however revealed a ring-like formation of TSG-6 staining, which was present at both 5 and 7 days after MCAo. mRNA levels are often taken as an indicator of protein expression. Multiple studies have investigated the correlation between RNA and protein expression, and whilst they have found an overall positive correlation, the strength of the association does vary from gene to gene (Gry et al., 2009; Guo et al., 2008). Naturally, differences in the sensitivity of the two techniques can lead to differences in results. Discrepancies in RNA and protein levels can also arise from differences in their rate of production: a typical mammalian cell will only produce two copies of a certain mRNA per hour, whereas in the same time-frame dozens of copies of the corresponding protein can be produced (Vogel and Marcotte, 2012). In addition, the two have vastly different stabilities: mammalian mRNA has an average half-life of 2.6-7 hours whereas protein

has an average half-life of 46 hours (Schwanhäusser et al., 2011; Sharova et al., 2009; Yen et al., 2008). Taking this into account, it is understandable that mRNA levels returned to baseline by 7 days, but protein persisted.

In this chapter, it was shown that TSG-6 is associated with astrocytes in the glial scar from 5 days after MCAo. Traditionally, the glial scar was thought to be detrimental to recovery after stroke, as it forms a barrier to neurotrophic factors and neurite outgrowth (Silver and Miller, 2004). Furthermore, activated astrocytes can produce pro-inflammatory mediators including IL-1 and TNF-α (Lau and Yu, 2001). As both of these cytokines can stimulate production of TSG-6, it is possible that TSG-6 is expressed within the glial scar due to the presence of these inflammatory mediators. However, more recent research has highlighted a role of the glial scar in repair and recovery, as it is thought to protect bordering tissue from becoming ischaemic, restore glutamate homeostasis to prevent excitotoxicity, remodel the BBB, scavenge free-radicals and promote neurogenesis (Copin et al., 1992; Håberg et al., 2001; Song et al., 2002; Willis et al., 2004). The known properties of TSG-6 in modelling of the ECM lend itself to a role in repair processes, and it is possible that its presence within the glial scar contributes to recovery of the ischaemic area. Astrocytes can express chondroitin sulphate proteoglycans (CSPGs) in response to stimuli such as TGF-β (Smith and Strunz, 2005). TSG-6 binds potently to these ECM components, and their expression by astrocytes could be instrumental in localising TSG-6 to the scar (Milner et al., 2006). It has been shown that TSG-6 can potentiate the inhibition of plasmin by 80%, especially at acidic pH levels of ~pH6 such as those seen during acidosis after ischaemia (Mahoney et al., 2005; Rehncrona, 1985). Plasmin can degrade ECM components including laminin, fibronectin and vitronectin (Saksela and Rifkin, 1988), and can activate MMPs such as MMP-1, MMP-3 and MMP-9 (Murphy et al., 1992). If TSG-6 maintains this inhibitory effect on plasmin in the brain, it could contribute to stabilisation of the ECM and limitation of inflammation, as well as preservation of the tight-junctions of the BBB. Having said that, the CSPGs that are essential for the inhibitory effect of TSG-6 on plasmin are also thought to be detrimental to regeneration. In spinal cord injury, degrading these ECM components was shown to enhance the regeneration of axons through the glial scar (Bradbury et al., 2002). Furthermore, *in vitro* experiments have shown an alarming ability of ECM containing

aggrecan (a CSPG) to repel axonal growth cones (Hynds and Snow, 1999). However, it might not be the case that CSPGs are inhibitory to regeneration all of the time: developing thalamocortical axons preferentially project via regions of the brain which are rich in CSPGs (Bicknese et al., 1994). All this aside, the time-points analysed in this chapter are too early for neurogenesis, so the presence of CSPGs and subsequently TSG-6 within the glial scar at 5 or 7 days post-stroke are unlikely to be detrimental for regeneration, and it is possible that the beneficial effects of TSG-6 could outweigh the negative impact of CSPGs.

Another way in which TSG-6 might contribute to repair and recovery after stroke is through promotion of angiogenesis. TSG-6 is able to promote angiogenesis by binding to fibroblast growth factor 2 (FGF2) (Leali et al., 2012). FGF2-stimulated angiogenesis is normally inhibited by an interaction between FGF2 and pentraxin-3, however TSG-6 can antagonise this interaction to promote angiogenesis (Leali et al., 2012). The location of TSG-6 within the glial scar would be logical for this role, as it is in close proximity to the most severely ischaemic and damaged part of the lesion.

As mentioned here and in the previous chapter, one of the most researched properties of TSG-6 is its ability to inhibit neutrophil migration. Neutrophils are among the first responders to stroke, and accumulate in the brain within the first hour post-insult. Although neutrophil numbers peak in the brain after three days, recruitment continues for two weeks after stroke (Jin et al., 2010). Therefore the sustained presence of TSG-6 in the glial scar could help to limit this prolonged infiltration of neutrophils, thereby reducing secondary damage and excessive inflammation.

Figure 4.5 showed an area of TSG-6 and GFAP expression in the contralateral primary motor cortex at all time-points. Stroke commonly results in motor deficits, and it is well reported that following ischaemia the contralateral cortex is able to compensate for the loss of function in the ipsilateral hemisphere (Johansen-Berg, 2003). It is possible that the staining seen here is a result of this remodelling. Indeed, it has been shown that astrocytes are critical in this synaptic reorganisation and functional remodelling in the contralateral cortex after stroke (Takatsuru et al., 2013). It could be the case that the GFAP staining is present as a result of this compensation and remodelling, and TSG-6 could be produced by astrocytes as seen in the glial scar.

However, the time-points investigated in this chapter are probably too early for such mechanisms to be seen. The interconnected nature of the two hemispheres means that collateral changes are possible after focal brain injury, so it is possible that the staining seen here is a result of this. Furthermore, following ischaemia the CSF becomes rich in inflammatory mediators including TNF-α, so contralateral expression of TSG-6 could be as a result of induction via the CSF (Zaremba et al., 2001).

For each qPCR experiment conducted in this chapter, multiple housekeeping genes were examined. In the short-term experiments after 45min MCAo, GAPDH was chosen as the most stable gene for normalisation, whereas in the longer term experiments after 30min MCAo r18.s was more stably expressed. It is vital that the chosen reference gene is stable across the experimental conditions tested, otherwise a supposed difference in expression of the target gene can actually just reflect a change in expression of the housekeeping gene. The fact that different reference genes were chosen for the two experiments means that the results cannot be directly compared. Equally, there were significant differences in reference gene expression between sham and MCAo groups, meaning that these groups could not be directly compared and had to be analysed separately. The differences seen between experiments might be due to the severity of the stroke: it appeared that a more severe stroke affected genes such as r18.s and SDHA, whereas the milder stroke altered GAPDH. It has been reported that SDHA, HPRT and YWAHZ are the best reference genes for permanent MCAo experiments (Gubern et al., 2009), however in this chapter these genes were shown to be unsuitable. Variability is often reported in the quest for a perfect housekeeping gene, and experimental conditions affect different genes in diverse ways. Therefore it is paramount to identify the most suitable reference gene for the specific experiment, in order to produce the most reliable data.

4.6 SUMMARY

The aim of this chapter was to elucidate the temporal and spatial pattern of TSG-6 expression in the brain after stroke. It was shown that TSG-6 is associated with astrocytes in the glial scar at 5-7 days after stroke. It is possible that from here, TSG-6 assists in remodelling of the ECM, preservation of the BBB, promotion of angiogenesis and inhibition of neutrophil migration, all contributing to a beneficial function in the repair and recovery phase of stroke.

CHAPTER 5:

THE EFFECT OF TSG-6 ON POST-ACUTE OUTCOMES AFTER EXPERIMENTAL STROKE

5.1 INTRODUCTION

Ischaemic stroke is a complex disease with many mediators and mechanisms of cell death (Allan et al., 2005). Following the initial insult, the integrity of the BBB is disrupted, and this, along with the expression of pro-inflammatory cytokines and chemokines, allows recruitment of neutrophils into the cerebrovasculature and sometimes into the ischaemic lesion itself. Neutrophils are thought to contribute to the expansion of the ischaemic lesion, and many studies have demonstrated protection by blocking neutrophil infiltration into the brain (Jin et al., 2010). Potential methods by which neutrophils mediate cell death include production of reactive oxygen species, pro-inflammatory mediators, MMPs and up-regulation of adhesion molecules (Jin et al., 2010).

TSG-6 is a glycoprotein which is up-regulated in response to inflammatory stimuli including IL-1 and TNF-α (Milner and Day, 2003). It has a number of anti-inflammatory properties, including inhibition of neutrophil migration and down-regulation of plasmin, which results in reduced activity of MMPs (Cao et al., 2004; Mahoney et al., 2005). The therapeutic potential of TSG-6 has been demonstrated in conditions including arthritis, myocardial infarction and ocular injury, and has recently been shown for the first time in a neurological condition, traumatic brain injury (Lee et al., 2009b; Nagyeri et al., 2011; Oh et al., 2010; Watanabe et al., 2013).

The previous chapter described expression of TSG-6 within the glial scar from 5 days after experimental stroke, suggesting a potential role in repair and recovery. The aim of the current chapter was to assess the therapeutic potential of Link_TSG6 in the post-acute phase after MCAo.

5.2 AIMS

1. To assess lesion volume, BBB integrity and neutrophil infiltration at 7 days after cerebral ischaemia in mice treated with vehicle, low dose Link_TSG6 or high dose Link_TSG6.
2. To assess behavioural outcomes at 24h, 3 days and 7 days after cerebral ischaemia in mice treated with vehicle, low dose Link_TSG6 or high dose Link_TSG6.

5.3 METHODS

Male C57BL/6 mice were subjected to 30min MCAo followed by 7 days reperfusion. Mortality for this study was 5%, however attempts to use a 45min occlusion resulted in 58% mortality. At 0h reperfusion, mice were given a subcutaneous injection of vehicle (0.5% BSA in PBS), low dose Link_TSG6 (10µg) or high dose Link_TSG6 (30µg) (the Link module of TSG-6 is responsible for its inhibitory effects on neutrophil migration). At 24h, a second injection was given of vehicle, low dose Link_TSG6 (5µg) or high dose Link_TSG6 (15µg). After 24h, 3 days and 7 days neurological score and behavioural characteristics (described in full in section 2.4.2) were tested. The open field test (described in section 2.4.3) was performed in control mice before MCAo, and at 24h and 7 day time-points after MCAo.

After 7 days reperfusion, mice were trans-cardially perfused with 0.9% saline and 4% PFA, and brains were sectioned for histological analysis. Lesion volume and haemorrhagic transformation were assessed by staining with H&E, and BBB disruption was quantified by staining for IgG. Sections were stained with an anti-neutrophil serum, SJC-4 to identify neutrophils.

Open field test data were analysed using ANY-maze animal tracking software. All data were plotted and analysed using GraphPad Prism, with parametric or non-parametric tests (ANOVA or Kruskall-Wallis) being chosen depending on the distribution of the specific data-set. Significance was set at $P<0.05$.

5.4 RESULTS

5.4.1 LESION VOLUME

Lesion volume was visualised by staining with H&E, with the infarcted area being identified by pallor and shrunken cell bodies. There was no significant difference between treatment groups, although there was a trend for reduction in lesion volume with Link_TSG6 (Figure 5.1). The trend suggested a dose-dependent effect of Link_TSG6: mice treated with the low dose of Link_TSG6 had a 15% reduction in lesion volume compared to vehicle-treated mice, whereas mice treated with the high dose of Link_TSG6 had a 29% reduction in lesion volume. Across all treatment groups, lesions were limited to a narrow anterior-posterior range, with very little damage being visible in the front-most or back-most regions of the brain. All mice displayed striatal lesions, and there were cortical lesions in 55%, 42% and 50% of mice treated with vehicle, low dose Link_TSG6 and high dose Link_TSG6 respectively. This led to considerable in-group variation, with the coefficient of variation being 61% for vehicle, 55% for low dose Link_TSG6 and 72% for high dose Link_TSG6. The coefficient of variation during characterisation of the model with no interventions was 54%.

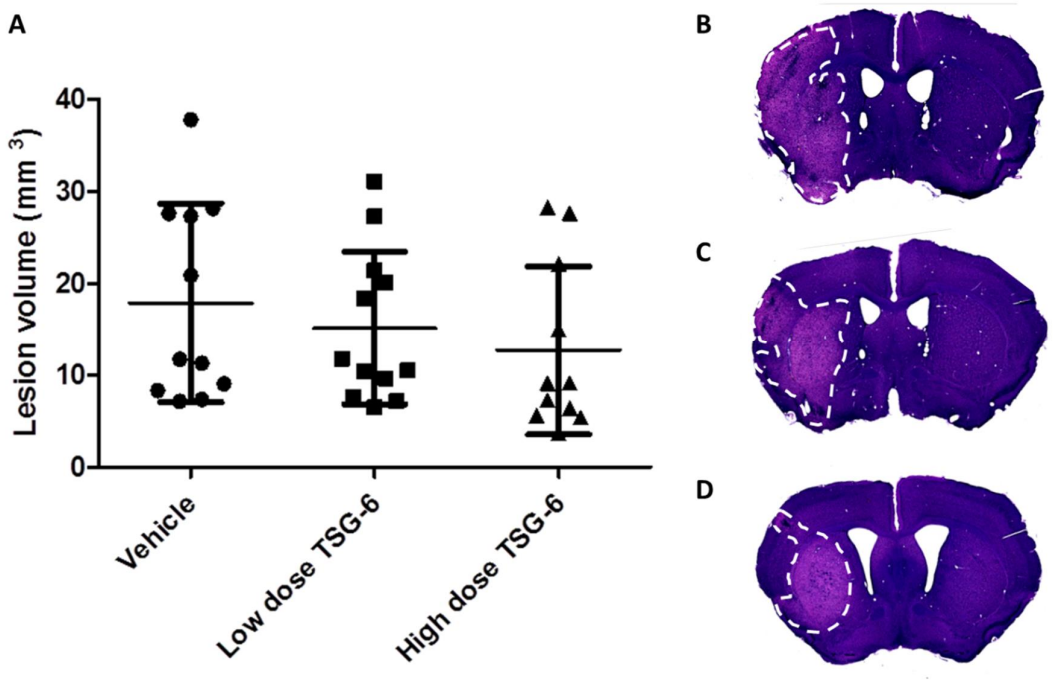

Figure 5.1: Analysis of lesion volume in mice treated with vehicle, low dose TSG-6 or high dose TSG-6. A: Lesion volume was identified by staining sections with haematoxylin and eosin. There was a non-significant trend for a dose-dependent reduction in lesion volume with TSG-6. Typical brain sections are shown from mice treated with (B) vehicle, (C) low dose TSG-6 and (D) high dose TSG-6. Data presented as mean ±SD. (ANOVA, Bonferroni's multiple comparison test). N = 11 or 12.

5.4.2 NEUTROPHIL RECRUITMENT

Brain sections were stained for neutrophils with SJC-4, and neutrophils were counted in the striatum, cortex, thalamus and hippocampus. Figure 5.2 shows the results for each brain region. Overall there were very few striatal neutrophils present, but there was a trend for more neutrophils in the vehicle-treated mice than the two groups treated with TSG-6. There was a similar trend in the cortex, with more mice in the vehicle-treated group having cortical neutrophils present than mice treated with TSG-6. Cerebral ischaemia induced an increase in thalamic neutrophils which was significantly reversed (65-fold) by TSG-6 ($P<0.05$). One mouse treated with vehicle had a substantial presence of neutrophils in the hippocampus, but aside from that there were very few neutrophils present in this region.

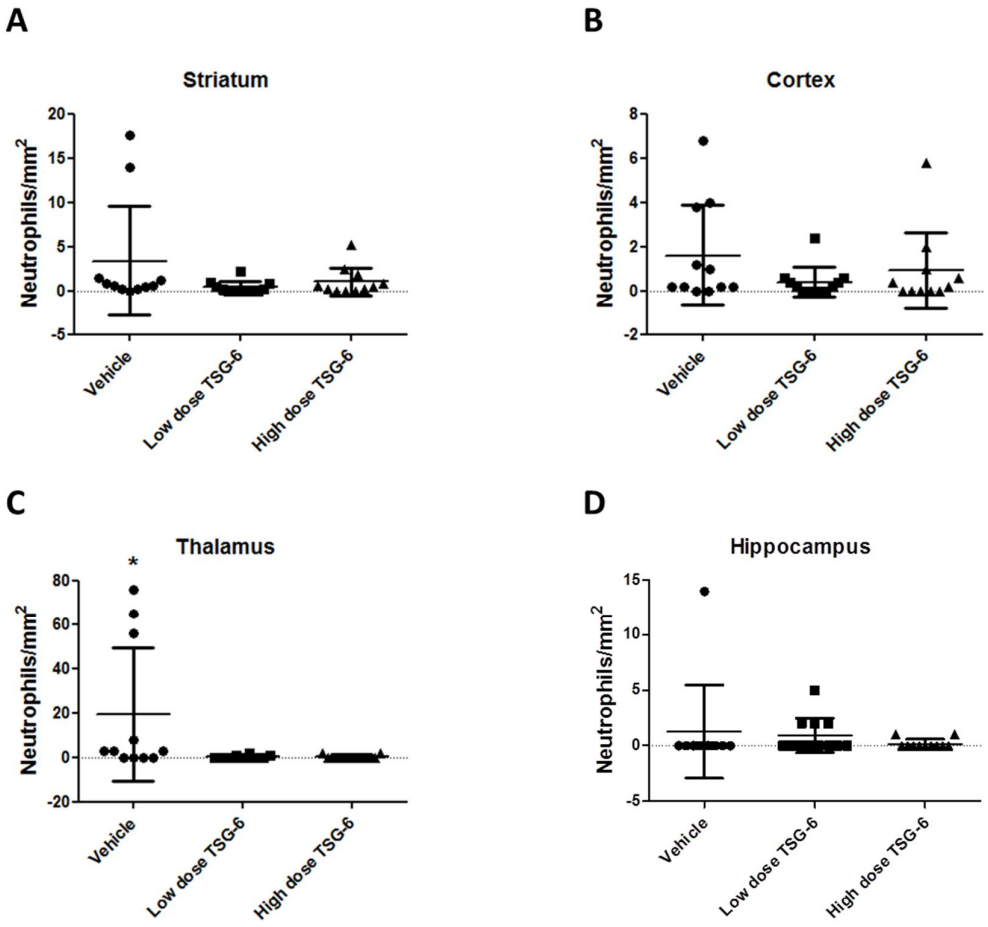

Figure 5.2: Neutrophils in the brain 7 days after 30min MCAo. Neutrophils were identified by immunohistological staining of neutrophils (SJC-4) and activated vessels (ICAM-1). **A: Striatum.** There was a non-significant trend for a reduction in striatal neutrophils with Link_TSG6 treatment. **B: Cortex.** There was no significant difference, although more vehicle-treated mice had cortical neutrophils than mice treated with TSG-6. **C. Thalamus.** Vehicle treated mice had a 65-fold increase in thalamic neutrophils than mice treated with TSG-6**. D. Hippocampus.** There was no significant difference between treatment groups. *P<0.05 compared to low dose Link_TSG6 and high dose Link_TSG6. (Kruskal-Wallis, Dunn's multiple comparison test). Data presented as mean ± SD. N = 11 or 12.

5.4.3 HAEMORRHAGIC TRANSFORMATION

Haemorrhagic transformation was identified by staining brain sections with H&E. Haemorrhages were identified by intense red staining of red blood cells. Bleeds were drawn onto brain maps which were analysed using ImageJ software. Overall there was very little HT in any of the treatment groups (Figure 5.3). There was one vehicle-treated mouse with much more HT than any of the other mice, but in general each mouse only had a few small bleeds in the posterior cortex and thalamus. Mice treated with high dose TSG-6 had a 69% increase in HT compared to mice treated with the low dose, although the overall amount of bleeding was still very low. Coefficients of variation ranged from 109% to 174%.

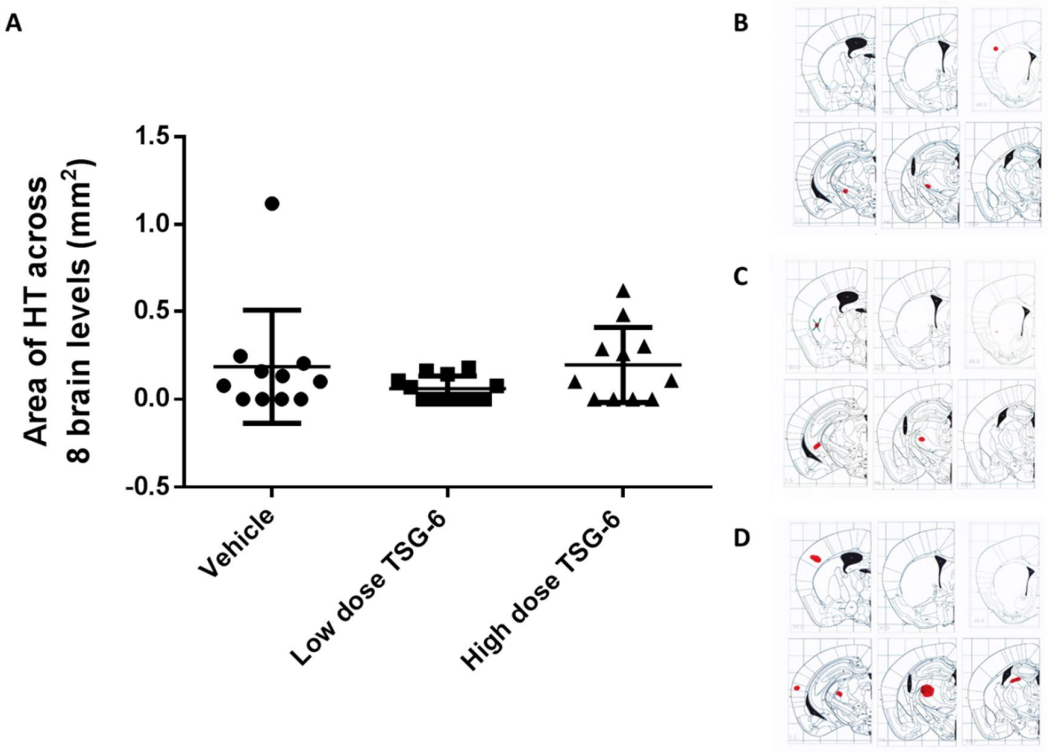

Figure 5.3: Haemorrhagic transformation at 7 days after 30min MCAo. A: There was no significant difference between treatment groups in the amount of HT seen. B-D: Brain maps indicating the typical location and quantity of bleeds in the brains of mice treated with B: vehicle, C: low dose Link_TSG6 and D: High dose Link_TSG6. No bleeds were visible in the two most anterior brain sections analysed, which are not shown. Data presented as mean ± SD. (Kruskall-Wallis, Dunn's multiple comparison test). N = 11 or 12.

5.4.4 BLOOD-BRAIN BARRIER DISRUPTION

BBB disruption was visualised by staining brain sections for IgG. Normally this protein is retained in the circulation, but when the BBB is compromised it can infiltrate into the brain parenchyma. There was no significant difference in the extent of IgG staining seen between treatment groups (Figure 5.4). There was a trend for a dose-dependent mean reduction in BBB breakdown with TSG-6 (13% reduction with low dose, 20% reduction with high dose). High dose TSG-6 seemed to result in a larger variation in BBB disruption than the low dose (46% vs 14% coefficient of variation). However, 36% of mice treated with high dose TSG-6 had BBB disruption limited to the striatum, whereas all mice in the other treatment groups had disruption extending into the cortex.

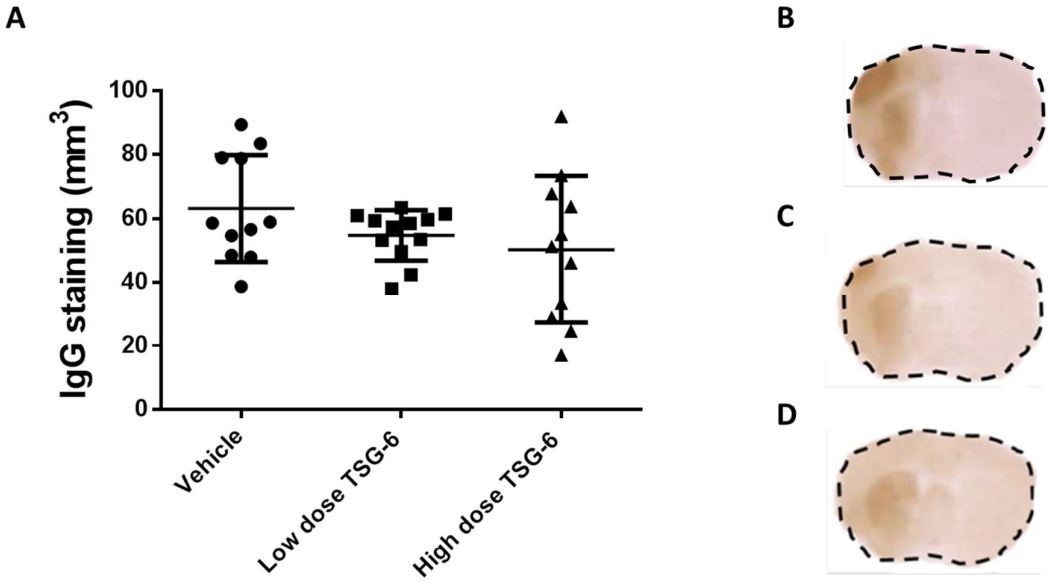

Figure 5.4: BBB breakdown at 7 days after 30min MCAo. A: There was no significant difference between treatment groups in the amount of BBB disruption seen. There was a slight trend for a decrease in breakdown after treatment with TSG-6. B-D: Typical brain sections indicating the extent of BBB disruption in the brains of mice treated with B: Vehicle, C: Low dose Link_TSG6 and D: High dose Link_TSG6. Data presented as mean ± SD. (Kruskall-Wallis, Dunn's multiple comparison test). N = 11 or 12.

5.4.5 NEUROLOGICAL SCORE

Complex neurological score (described in detail in section 2.4.2) was used to assess the neurological deficit after 24h, 3 days and 7 days reperfusion. At 24h, there was no difference in neurological score between the treatment groups (Figure 5.5). After 3 days reperfusion, mice treated with low dose TSG-6 had a significantly improved neurological score compared to vehicle-treated mice ($P<0.05$). Mice treated with high dose TSG-6 had an intermediate mean score of 2.9 at this time-point. By 7 days reperfusion, there was no significant difference between treatment groups. Mice treated with low dose TSG-6 maintained the best neurological score (mean 2.7), whereas mice treated with vehicle or high dose TSG-6 both had a mean score of 3.0.

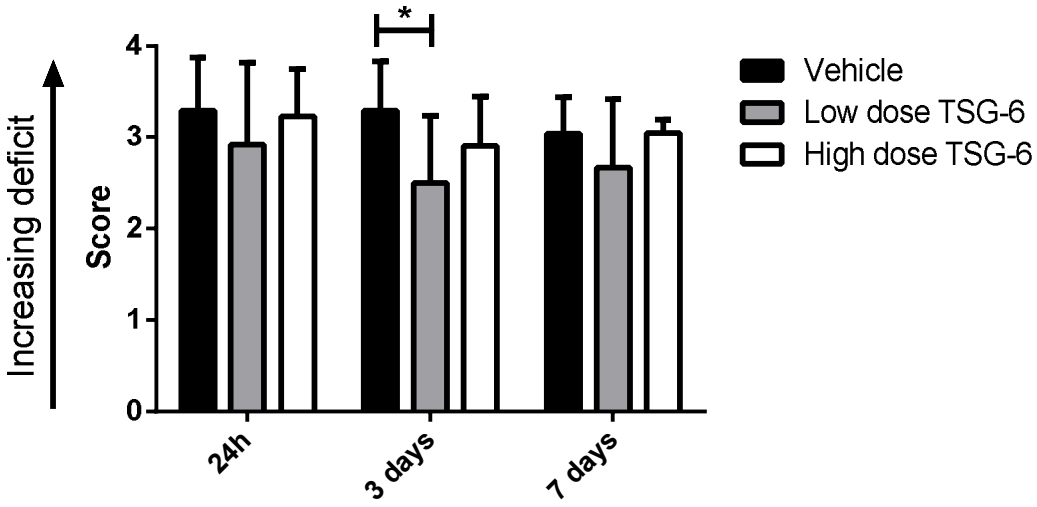

Figure 5.5: Neurological score at 24h, 3 days and 7 days after 30min MCAo. At 24h, there was no significant difference between treatment groups. After 3 days reperfusion, mice treated with low dose Link_TSG6 had significantly improved neurological scores compared to vehicle-treated mice. By 7 days reperfusion there was no difference in neurological score between treatment groups. Data presented as mean ± SD. (Two-way ANOVA). N=11 (vehicle and high dose TSG-6) or 12 (low dose TSG-6).

5.4.6 BEHAVIOURAL CHARACTERISATION

After 24h, 3 days and 7 days reperfusion, mice were assessed on the behavioural characteristics described in section 2.4.2. There were no significant differences between treatment groups at any time-point in any of the parameters tested (Figure 5.6). There was a slight trend for a small improvement in body position, spontaneous activity, transfer arousal, gait and touch escape in mice treated with TSG-6, more so with low dose than high dose. The trend was most apparent at the 3 day time-point, for example for transfer arousal mice treated with vehicle, low dose TSG-6 and high dose TSG-6 had mean scores of 2.1, 2.8 and 2.6 respectively. Within treatment groups, scores remained relatively constant over the different time-points, or showed a small improvement at 7 days.

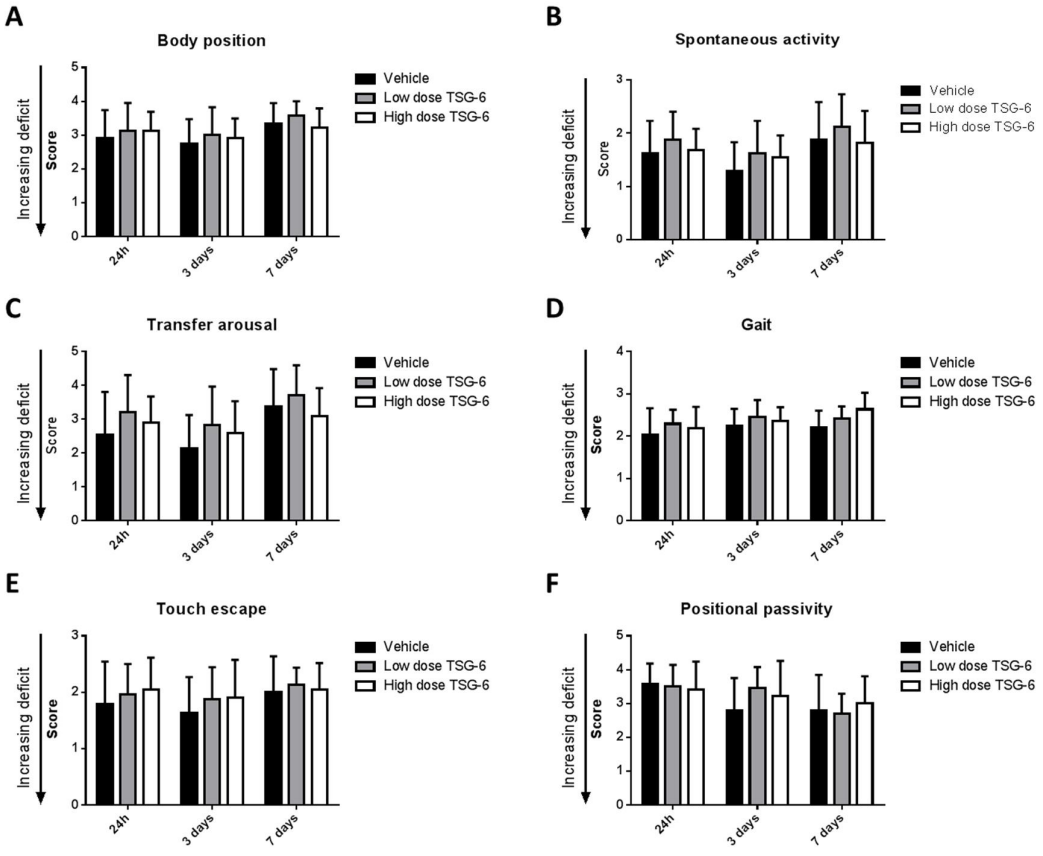

Figure 5.6: Behavioural characterisation scores at 24h, 3 days and 7 days after 30min MCAo. There was no significant difference between treatment groups at any time-point. There was a slight trend for improvements in behavioural characteristics in mice treated with low dose TSG-6, particularly after 3 days. Data presented as mean ± SD. (Two-way ANOVA). N=11 (vehicle and high dose TSG-6) or 12 (low dose TSG-6).

5.4.7 OPEN FIELD TEST

The open field test (described in section 2.4.3) was used to assess spontaneous locomotor function in mice after 24h and 7 days reperfusion. Control mice were tested before MCAo. ANY-maze video tracking software analysed a large range of parameters and rears were counted manually, but there was no significant difference seen between treatment groups in any parameter tested. For distance travelled and average speed (Figures 5.7A and B), mice treated with high dose TSG-6 showed a significant 1.7-fold decline after 24h, and all treatment groups showed a significant ~2-fold decline after 7 days ($P<0.05$). None of the treatment groups had significantly fewer line crossings than control at 24h, but by 7 days all groups had significantly declined, with mice treated with vehicle, low dose TSG-6 and high dose TSG-6 showing reductions of 40%, 47% and 56% respectively ($P<0.05$) (Figure 5.7C). All treatment groups showed a significant ~65% reduction in the number of rears at 24h and 7 days compared to control mice (Figure 5.7D).

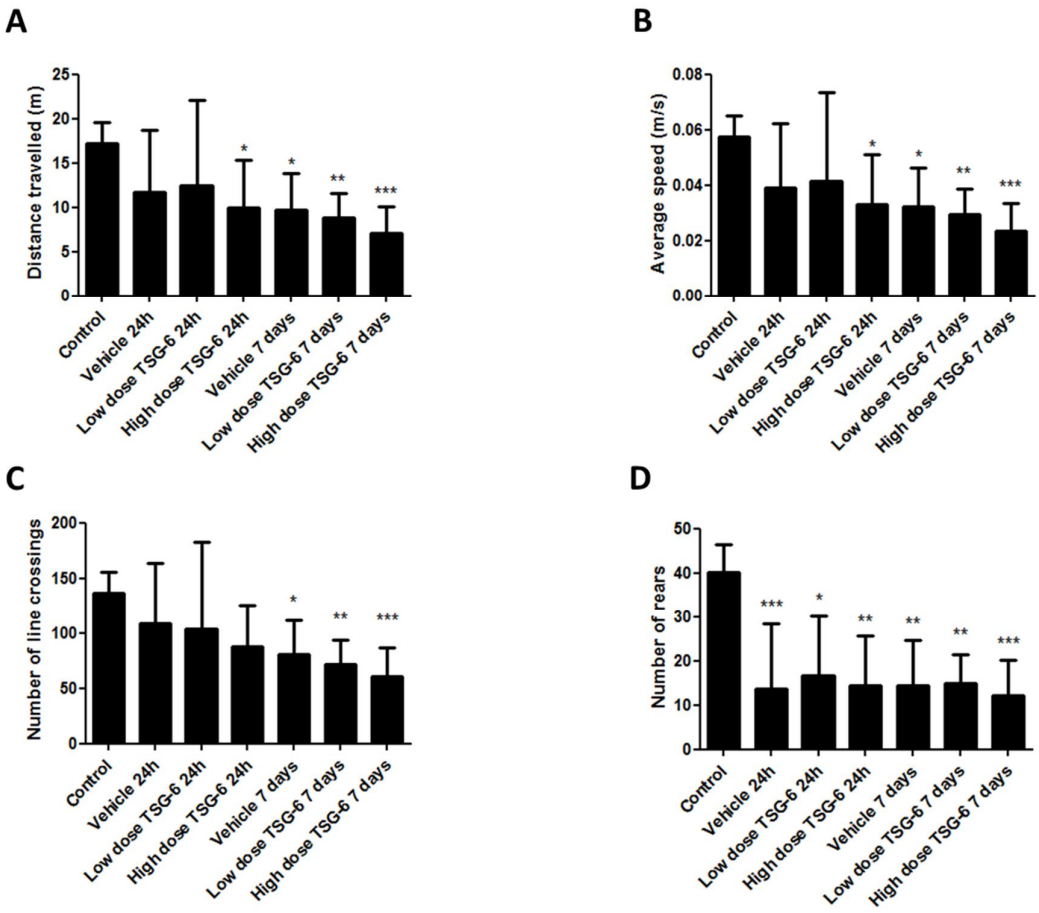

Figure 5.7: Open field test scores at 24h and 7 days after 30min MCAo. There was no significant difference between treatment groups in any parameter at any time-point. For distance travelled (A) and average speed (B), high dose Link_TSG6 significantly declined at 24h, and all treatment groups significantly declined after 7 days. There was no change in the number of line crossings (C) at 24h, but by 7 days all groups had significantly declined. There was a significant reduction in the number of rears (D) in all treatment groups at 24h and 7 days. *P<0.05, **P<0.01, ***P<0.001 compared to control. Data presented as mean ± SD. (Kruskall-Wallis, Dunn's multiple comparison test). N=11 (vehicle and high dose TSG-6) or 12 (control and low dose TSG-6).

5.5 DISCUSSION

The aim of this chapter was to assess the effects of Link_TSG6 on histological and behavioural outcomes in the 7 days following MCAo. There were trends seen for protection of lesion volume and BBB disruption with Link_TSG6, but no significant improvement was observed. Link_TSG6 significantly reduced neutrophil recruitment in the thalamus, and there was a trend for reduced infiltration in the striatum, cortex and hippocampus. Low dose Link_TSG6 led to a significant improvement in neurological score at 3 days after MCAo, but no other beneficial effects were observed on behavioural outcomes.

TSG-6 has shown therapeutic effects in numerous conditions with an inflammatory component, including arthritis, myocardial infarction and chemical ocular injury (Lee et al., 2009b; Oh et al., 2010; Szántó et al., 2004). At the time of this study being conducted, there had been no reports of TSG-6 showing efficacy in any neurological conditions, however a recent publication has described the therapeutic potential of TSG-6 in traumatic brain injury (TBI) (Watanabe et al., 2013). TBI is similar to stroke in that brain damage is mediated by inflammation, excitotoxicity and free radical formation, however the exact aetiologies of the two conditions differ somewhat.

One possible reason for the differences in the effect seen from TSG-6 between the published studies and the data in this chapter is the route of administration. In the majority of the published works, TSG-6 was delivered intravenously, whereas in this chapter subcutaneous administration was used. Intravenous administration was attempted in this study, however the vasoconstrictive effects of isoflurane made injection whilst the mice were anaesthetised extremely difficult, and attempts to restrain mice for injection early after recovery resulted in deaths due to barrel rolling inside the restrainer. Subcutaneous administration was chosen over intraperitoneal injection due to the variation seen from this route in chapter 3. Subcutaneous injection is often used clinically for administration of proteins including insulin and growth hormones (Porter and Charman, 2000). This route results in a slower rate of absorption than intravenous administration, due to proteins having to be processed through the lymphatic system. Whilst subcutaneous administration generally

eventually leads to a good plasma bioavailability of protein, it might not have been the ideal choice for TSG-6 due to the prevalence of glycosaminoglycans (GAGs) in the interstitial space (Porter and Charman, 2000). TSG-6 interacts potently with a range of GAGs (Milner et al., 2006), so the presence of these proteins in the subcutaneous space might have limited the absorbance of TSG-6 into the blood. Unfortunately it was not possible to measure the plasma concentration of TSG-6 in this work, due to the lack of availability of a suitable ELISA kit. Despite this, the fact that treatment with TSG-6 virtually abolished thalamic neutrophils suggests that the protein was bioavailable and functionally active to some degree. However, future work would benefit from optimisation of the intravenous injection technique to allow administration via this route, in order to be comparable with published studies.

In this work, a time-point of 7 days was chosen for analysis of histological outcomes. Neutrophils peak in the brain at three days after MCAo, and although infiltration does continue for two weeks after stroke, numbers are lower due to reduced recruitment and phagocytosis by macrophages (Jin et al., 2010). Had neutrophil numbers been examined at an earlier time-point, it is possible that a more marked effect in the striatum and cortex might have been seen with TSG-6 treatment. However, the 7 day time-point was chosen in order to assess functional outcomes, and it is impractical and not in keeping with the 3 Rs to use groups of mice at different time-points for only one outcome each. Having said that, the behavioural data did not show any marked effect of TSG-6, and the open field test in particular showed that all mice were still declining at 7 days, irrespective of treatment group. It would therefore be beneficial to extend the recovery period further in order to assess behavioural outcomes and to see whether TSG-6 has any effect on functional recovery. In the investigation into TBI, behavioural outcomes were assessed between 28-70 days after injury, and treatment with TSG-6 resulted in improved memory and neurogenesis (Watanabe et al., 2013). In this case, it would be necessary to have multiple cohorts of animals, with some tested for long-term functional improvements and others sacrificed early for histological assessments. The inclusion of a more sophisticated array of behavioural tests would help to determine any effect of TSG-6 on functional outcome. Tests could include the catwalk test for detailed gait analysis, the novel object test for memory and the forced swim test for depression.

The investigation into TSG-6 in TBI is the most similar published data compared to the work in this chapter. There are a number of key differences between the two studies which could explain the differences in results seen. Table 5.1 summarises the key features of the work by Watanabe et al. and the study conducted in this chapter:

	Watanabe et al. 2013	Chapter 5
Model	Traumatic brain injury	MCAo
TSG-6	Full length protein	Link_TSG6
Administration	Intravenous	Subcutaneous
Dose	2 x 50µg (6h + 24h)	30µg + 15µg OR 10µg + 5µg (0h + 24h)
Outcomes	Lesion volume (14 days) BBB breakdown (3 days) Neutrophil migration (24h) Mood + memory (4-10 weeks)	Lesion volume (7 days) BBB breakdown (7 days) Neutrophil migration (7 days) HT (7 days) Behaviour (24h, 3 + 7 days)

Table 5.1: Key features of the published work by Watanabe et al. 2013 and the study conducted in this chapter. Differences in study design might explain the differences in the results obtained from the two studies.

Despite the lack of a robust effect, there was a trend for a dose-dependent improvement with Link_TSG6 on lesion volume and BBB integrity. A useful addition to the study would be to assess lesion volume by magnetic resonance imaging (MRI) in the acute phase (24-48h post-reperfusion) to determine whether TSG-6 has any effect on the evolution of the infarct. IgG is a useful way of determining BBB breakdown as it only requires one serial set of brain sections, meaning that fewer animals can be used. However by the 7 day time-point the staining is more diffuse than at more acute time-points, meaning that the border of staining is more difficult to accurately define. More accurate quantitative methods for analysing BBB disruption would require a separate cohort of animals, so are not in keeping with the 3 Rs. Such methods could include analysis of Evan's blue extravasation followed by quantification of homogenates by spectrophotometry, or qPCR and protein analysis to determine expression levels of tight junction proteins such as claudin and occludin. However, the fact that a

correlation was seen between the trends in lesion volume and BBB disruption suggests that the analysis was relatively accurate. In a model of TBI, TSG-6 led to significant improvements in lesion volume after 2 weeks, and in BBB disruption after 3 days (Watanabe et al., 2013). As mentioned before, the progression of injury in TBI is different to stroke, however this study suggests that a more potent effect of TSG-6 might have been seen if outcomes were assessed at the peak of their progression. Overall the trends in lesion volume and BBB suggest that Link_TSG6 is having a protective effect, however the variability of the model makes it difficult to reach significance.

Despite the trend for protection seen in BBB disruption, there was hardly any difference seen between treatment groups in the extent of HT. Overall the area of bleeding was low, suggesting that by 7 days macrophages had cleared red blood cells. However, any bleeds that were present were mainly located in the thalamus, which is where neutrophils were most prevalent in vehicle-treated mice but were absent in mice treated with TSG-6. The thalamus was largely protected from ischaemic damage, however IgG staining was seen here in 50% of vehicle-treated mice, 8% of mice treated with low dose Link_TSG6 and 25% of mice treated with high dose Link_TSG6. It has been shown that the thalamus is susceptible to BBB disruption following MCAo, even when the lesion does not extend to that area (Li et al., 2011). The trend in thalamic BBB disruption suggests that Link_TSG6 might be able to protect against this remote damage, thereby preventing infiltration of neutrophils into this area of the brain.

5.6 SUMMARY

In this chapter of work it was shown that Link_TSG6 is able to protect against thalamic infiltration of neutrophils, and there was a trend for a reduction in lesion volume and BBB disruption. This study could be optimised by administering the drug intravenously to allow better bioavailability and to mirror published work. A further improvement to the study would be more careful selection of time-points, with earlier assessment of histological outcomes and an extended recovery period to get a clearer idea of any effect on functional outcomes. However, the doses of Link_TSG6 used didn't display any toxic effects and the trends suggest that TSG-6 might still be an attractive therapeutic option for the treatment of ischaemic stroke.

CHAPTER 6:

THE EFFECT OF TSG-6-EXPRESSING MESENCHYMAL STEM CELLS ON POST-ACUTE OUTCOMES AFTER EXPERIMENTAL STROKE

6.1 INTRODUCTION

Mesenchymal stem cells (MSCs) have been heavily researched as a potential therapeutic tool for a wide range of diseases. In a number of disease models, the beneficial effects of MSCs have persisted in the absence of engraftment, and have been shown to be due to expression of TSG-6. Examples where this is the case include diabetes (Kota et al., 2013), corneal injury and transplant (Oh et al., 2012; Roddy et al., 2011), myocardial infarction (Lee et al., 2009b), peritoneal injury (Wang et al., 2012) and acute lung injury (Danchuk et al., 2011). Whilst many of these reports have shown potent effects by using MSCs cultured in a 2D monolayer, it has been demonstrated that growing the cells in a 3D spheroid can enhance their anti-inflammatory properties and increase expression of TSG-6 (Bartosh et al., 2010). Past publications have cultured 3D spheroids then dissociated the cells before intravenous infusion. In this chapter, the paracrine potential of 3D MSC cultures was tested by subcutaneous transplantation of intact 3D spheroids.

There are many reports of intracerebral or intravenous delivery of MSCs providing benefit in animal models of stroke (Chen et al., 2001a; Chen et al., 2001b; Honma et al., 2006; Li et al., 2002; Moisan et al., 2012). The 'holy grail' of stem cell research in stroke has been to promote engraftment of cells and contribution to neurogenesis. However, there is growing evidence surrounding the paracrine anti-inflammatory properties of MSCs: not just their expression of TSG-6, but also production of IL-1Ra (Ortiz et al., 2007) and induction of macrophages to produce IL-10 (Németh et al., 2009). Peripheral inflammation is known to be a key contributor to stroke pathophysiology, and it is possible that using MSCs to reduce the peripheral inflammatory burden will be a potent and accessible therapeutic option.

6.2 AIMS

1. To characterise the morphology, cell surface marker profile and differentiation potential of cultured MSCs.
2. To measure the expression of TSG-6, IL-6 and IL-8 by MSCs in 3D and 2D cultures, under basal conditions and in the presence of IL-1.
3. To assess the effect of subcutaneous transplantation of 3D MSC spheroids on histological, immunological and behavioural outcomes after experimental stroke.

6.3 METHODS

Human MSCs from two patients were cultured in 2D monolayers as described in section 2.14, and were used at P5 for all experiments. Cell surface markers were analysed by flow cytometry, described in full in section 2.15.1. MSCs from patient male 33 (lot number 6F4085) were used for a differentiation assay inducing cells to become adipogenic, osteogenic and chondrogenic, which was conducted according to manufacturer's instructions (described in full in section 2.15.2).

MSCs were cultured in 2D monolayers or in 3D spheroids (see section 2.14). Cells were treated for 3h with MesenPRO, vehicle (0.5% BSA in PBS), 10µg/ml IL-1Ra, 10ng/ml IL-1β or IL-1β+IL-1Ra. Following treatment, RNA was extracted and cDNA was produced, as described in sections 2.17-2.18. qPCR was performed to analyse expression of TSG-6, IL-6 and IL-8 (section 2.19).

For the first pilot *in vivo* experiment, 3D MSC spheroids were cultured with 60,000 cells per spheroid (Ball et al., 2013). MCAo with an occlusion time of 45 min was performed (as in section 2.2). Mortality for this study was 10%. Mice were injected subcutaneously at the back of the neck with PBS or with 10 spheroids in PBS 30 min prior to occlusion onset. Neurological and behavioural testing was carried out after 24h, 3 days and 7 days reperfusion. After 7 days mice were trans-cardially perfused and brains were fixed and sectioned. Brain sections were stained with H&E for lesion volume analysis, with SJC-4 for neutrophil quantification, and for IgG for analysis of BBB disruption. Blood samples were analysed by flow cytometry for quantification of

leukocyte populations, and CBA analysis of plasma samples allowed analysis of circulating cytokines.

The second pilot *in vivo* experiment was performed as above except for the following changes. 3D MSC spheroids were cultured as normal, or in the presence of a small molecule PDGF receptor antagonist (Merck, UK) (Ball et al., 2013). This inhibitor was of interest due to published data indicating its ability to increase the multipotency of MSCs, including conferring angiogenic potential (Ball et al., 2013; Ball et al., 2012). MCAo was performed with an occlusion time of 30 min. Mortality for this study was 5.5%. Mice were injected subcutaneously after 10 min reperfusion with either matrigel (diluted 3:1 matrigel:MesenPRO), 10 MSC spheroids or 10 PDGF-inhibited MSC spheroids. Neurological and behavioural testing (including the open field test) was carried out after 24h, 7 days and 14 days. Reperfusion was for 14 days, after which mice were trans-cardially perfused and brains were fixed and sectioned. Brain sections were stained for IgG and SJC-4. Plasma cytokine concentrations were analysed by CBA.

Graphpad Prism was used for statistical analysis of data, and unpaired T-test, ANOVA or Two-way ANOVA tests were performed depending on the data-set. Significance was set at $P<0.05$.

6.4 RESULTS

6.4.1 MSC CHARACTERISATION: MORPHOLOGY AND EXPRESSION OF SURFACE MARKERS

MSCs from two patients were characterised for their morphology and cell surface marker expression profile. Both cultures adhered to plastic and showed the characteristic spindle-shaped morphology, shown in Figure 6.1:

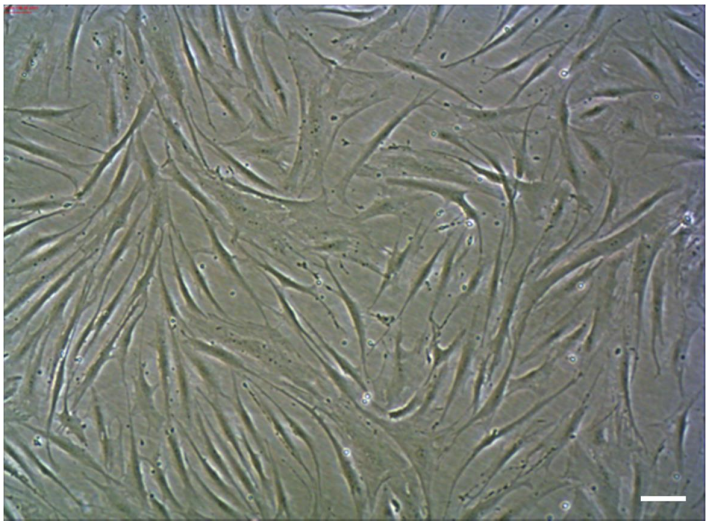

Figure 6.1: Characteristic morphology of MSCs at P5. MSCs in 2D culture adhere to plastic and show a typical spindle-shaped morphology. Cells shown are from the line used for *in vivo* experiments, a male 33-year old patient, lot number 6F4085. Scale bar = 100µm.

Flow cytometry was used to analyse the surface marker expression profile of the two cultures. Cells from both cultures expressed MSC markers CD29 (integrin β1 chain), CD44 (hyaluronan receptor), CD105 (endoglin), CD73, CD90 (Thy-1), CD166 (activated leukocyte cell adhesion molecule) and Stro-1 (Figure 6.2). MSCs were negative for expression of CD14, CD34 and CD45.

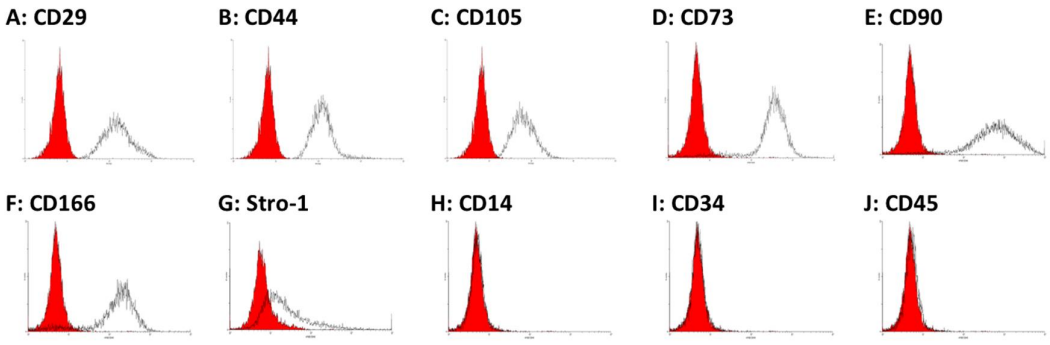

Figure 6.2: Cell surface marker expression profile of MSCs. Flow cytometry was used to assess the cell surface marker profile of two MSC cell lines. Both cultures were positive for expression of CD29 (A), CD44 (B), CD105 (C), CD73 (D), CD90 (E), CD166 (F) and Stro-1 (G). MSC cultures did not express CD14 (H), CD34 (I) or CD45 (J). Red peaks indicate the isotype control antibody. The example plots shown are from the line used for *in vivo* experiments, a male 33-year old patient, lot number 6F4085.

6.4.2 MSC CHARACTERISATION: DIFFERENTIATION POTENTIAL

Primary MSC cultures were tested for multipotency by differentiation down three separate lineages, according to published criteria (Dominici et al., 2006). Cells were incubated with differentiation supplements for 21 or 28 days, and their expression profiles were analysed by immunohistochemistry and qPCR.

6.4.2.1 ADIPOGENIC POTENTIAL

Treatment of MSCs with a supplement containing hydrocortisone, isobutylmethylanthine and indomethacin resulted in differentiation into adipocytes. Cells were stained for lipid droplets with BIODIPY and for fatty acid binding protein FABP4. There was no lipid droplet staining visible in cells cultured in MesenPRO or the manufacturer's control, and these cultures showed very low levels of FABP4 staining, although cells treated with the manufacturer's control expressed higher levels of FABP4 than those treated with MesenPRO (Figure 6.3). Cells treated with the differentiation supplement displayed strong FABP4 staining, and numerous lipid vacuoles were visible.

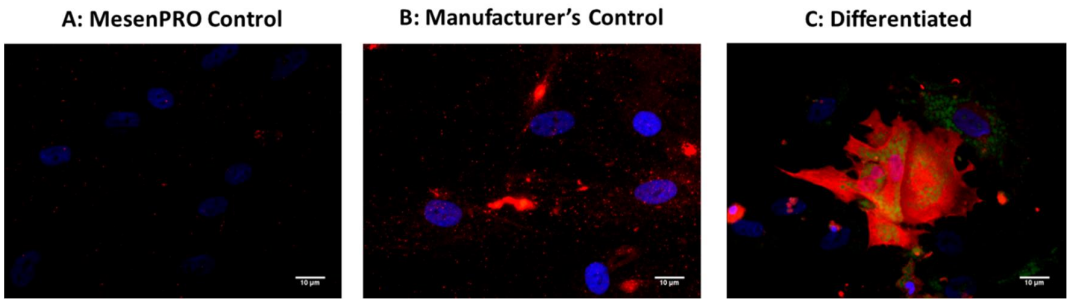

Figure 6.3: Adipogenic differentiation of MSCs. MSC cultures were cultured with MesenPRO (A), manufacturer's control (B) or adipogenic differentiation supplement containing hydrocortisone, isobutylmethylanthine and indomethacin (C). Cells were stained for FABP4 (red), lipid droplets (BIODIPY, green) and DAPI nuclear stain (blue). There was no lipid droplet staining and very little FABP4 staining visible in control cultures, whereas differentiated cells showed strong FABP4 immunoreactivity with numerous visible lipid droplets. Scale bar = 10µm.

RNA was extracted from cells and qPCR was used to determine the expression of adipogenic markers. Control cells expressed extremely low levels of adipogenic markers FABP4 (a fatty acid binding protein), CEBP and PPAR2 (factors involved in inducing adipogenesis) (Figure 6.4). Differentiated cells had 70,000- and 180,000-fold higher expression of FABP4 than cells cultured with MesenPRO or manufacturer's control respectively ($P<0.01$). CEBP was expressed 90 to 100-fold higher in differentiated cells than the control cells ($P<0.01$). Differentiated cells expressed 32- or 46-fold more PPAR2 than the control cells ($P<0.01$).

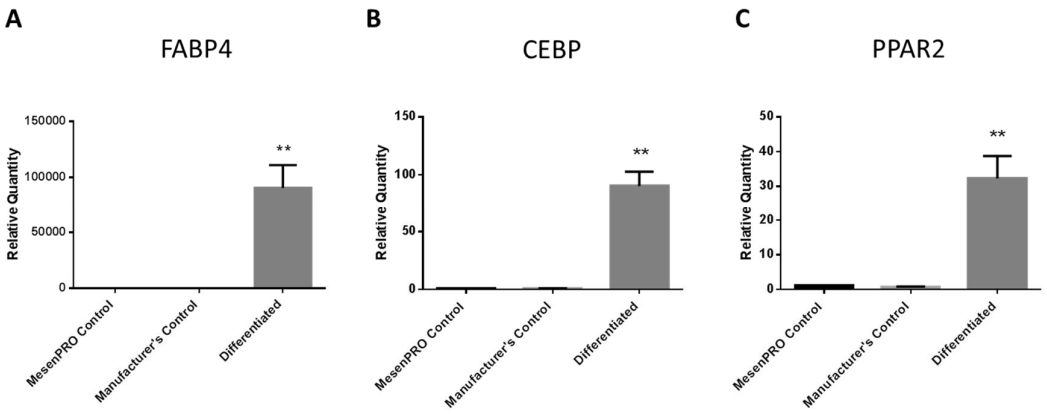

Figure 6.4: Adipogenic marker expression after differentiation. MSC cultures were treated with MesenPRO, manufacturer's control or adipogenic differentiation supplement containing hydrocortisone, isobutylmethylanthine and indomethacin. RNA was extracted and qPCR quantified expression of adipogenic markers FABP4 (A), CEBP (B) and PPAR2 (C). Differentiated cells expressed significantly more adipogenic markers than the non-differentiated control cells. (ANOVA, Bonferroni's multiple comparison test). **$P<0.01$ compared to MesenPRO control and manufacturer's control. Expression normalised to GAPDH. Data shown as mean±SD. N=3.

6.4.2.2 OSTEOGENIC POTENTIAL

Osteogenic differentiation of MSCs was stimulated by addition of a supplement containing dexamethasone, ascorbate-phosphate and β-glycerophosphate. Cells were stained for osteocalcin (a protein found in bone) and phalloidin to identify F-actin. No osteocalcin was visible in undifferentiated cells (Figure 6.5). Cells treated with the differentiation supplement displayed widespread osteocalcin staining. Control cells displayed organised actin bundles extending throughout the cytoplasm. Actin staining in differentiated cells showed more focal points of expression, rather than the long fibres seen in undifferentiated cells.

Figure 6.5: Osteogenic differentiation of MSCs. MSC cultures were treated with MesenPRO (A), manufacturer's control (B) or osteogenic differentiation supplement containing dexamethasone, ascorbate-phosphate and β-glycerophosphate (C). Cells were stained for F-actin with phalloidin (red), osteocalcin (green) and DAPI nuclear stain (blue). There was no osteocalcin staining visible in control cultures, whereas differentiated cells showed strong staining throughout the culture. Control cells had organised actin fibres extending through the cytoplasm, whereas differentiated cells had patchier mesh-like staining. Scale bar = 10µm.

Expression levels of osteogenic markers Runx2 (a transcription factor involved in osteoblast differentiation), osteopontin (a protein expressed in bone) and alkaline phosphatase (an enzyme highly expressed in bone) were measured by qPCR. There was no significant difference between differentiated and control cells in expression levels of any of the markers tested (Figure 6.6). Differentiated cells had 56% and 18% higher expression of Runx2 than the MesenPRO and manufacturer's controls respectively. Differentiated cells had 2.5-fold higher expression of osteopontin than cells treated with MesenPRO, however cultures treated with the manufacturer's control had 10.7-fold higher expression than the differentiated cells. Differentiated cells had a trend for a 33-fold and 22-fold increase in expression of alkaline phosphatase compared to cells treated with MesenPRO and the manufacturer's control respectively (P=0.067).

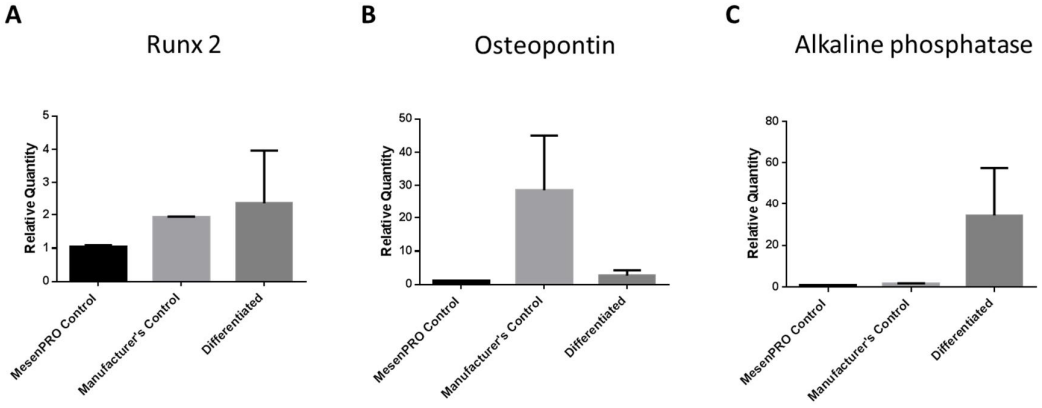

Figure 6.6: Osteogenic marker expression after differentiation. MSC cultures were treated with MesenPRO, manufacturer's control or osteogenic differentiation supplement containing dexamethasone, ascorbate-phosphate and β-glycerophosphate. RNA was extracted and qPCR quantified expression of osteogenic markers Runx2 (A), Osteopontin (B) and alkaline phosphatase (C). There was no significant difference seen between treatment groups, although there was a trend for higher expression of Runx2 and alkaline phosphatase in the differentiated cells compared to control cells. Cells treated with the manufacturer's control appeared to have a trend for increased osteopontin expression compared to the other groups. (ANOVA, Bonferroni's multiple comparison test). Expression normalised to GAPDH. Data shown as mean±SD. N=3.

6.4.2.3 CHONDROGENIC POTENTIAL

MSC pellets were stimulated to differentiate into chondrocytes by addition of a supplement containing dexamethasone, ascorbate-phosphate, proline, pyruvate and transforming growth factor-β3 (TGFβ3). Cell pellets were stained for aggregan, a cartilage-specific proteoglycan. There was a basal level of aggrecan expression in cells treated with MesenPRO or the manufacturer's control (Figure 6.7). Differentiated cells displayed much stronger aggrecan staining than the control cells, and differentiated cell pellets appeared to be more densely packed. This experiment was unfortunately accidentally discarded before pictures were taken, so the images in Figure 6.7 were kindly provided by Samantha Roberts (Kielty lab), and are consistent with the results produced routinely in this laboratory.

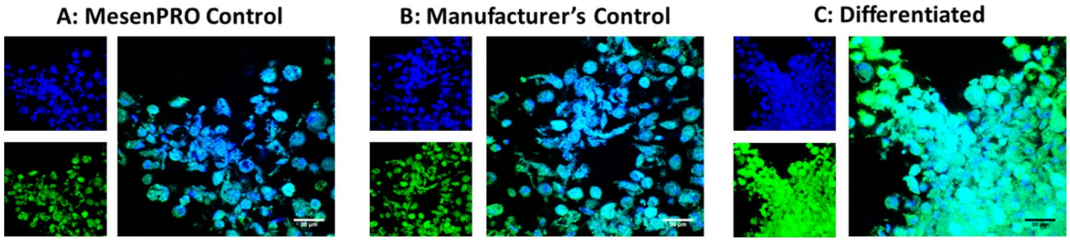

Figure 6.7: Chondrogenic differentiation of MSCs. MSC pellets were treated with MesenPRO (A), manufacturer's control (B) or chonrogenic differentiation supplement containing dexamethasone, ascorbate-phosphate, proline, pyruvate and TGFβ3 (C). Cells were stained for aggrecan (green) and DAPI nuclear stain (blue). There was a basal level of aggrecan staining in both control groups, but differentiated cells showed much stronger immunoreactivity, and more densely packed cell pellets. Pictures were captured on Nikon C1 confocal microscope. Scale bar = 30µm. Images courtesy of Samantha Roberts (Kielty laboratory).

Expression levels of two collagen subtypes found in cartilage were measured by qPCR. Collagen II was expressed 3.5-fold (P<0.01) and 18-fold (P<0.001) higher in differentiated cultures than in cells treated with MesenPRO or manufacturer's control respectively (Figure 6.8). Additionally, cells treated with the manufacturer's control had 5.2-fold lower expression of collagen II than cultures treated with MesenPRO (P<0.05). There was no significant difference in expression of collagen IX, although differentiated cells had 5-fold and 2.5-fold higher expression than cells treated with MesenPRO and manufacturer's control respectively.

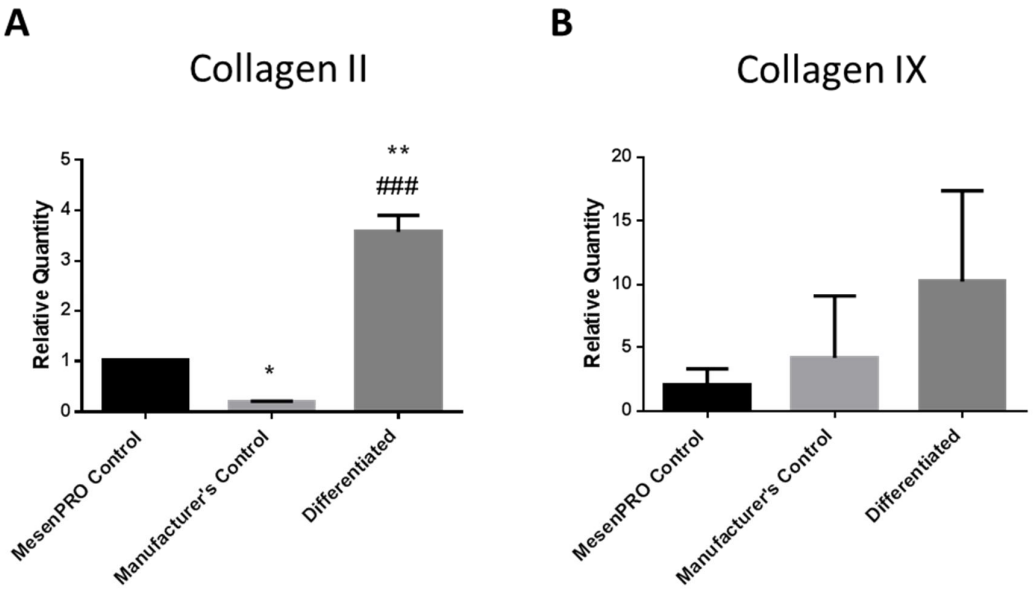

Figure 6.8: Chondrogenic marker expression after differentiation. MSC pellets were treated with MesenPRO, manufacturer's control or chondrogenic differentiation supplement containing dexamethasone, ascorbate-phosphate, proline, pyruvate and TGFβ3. RNA was extracted and qPCR quantified expression of chondrogenic markers collagen II (A) and collagen IX (B). Differentiated cells expressed significantly more collagen II than both control groups. Cells treated with the manufacturer's control had significantly lower collagen II expression than cultures treated with MesenPRO. There was a trend for increased collagen IX expression in differentiated cells compared to the control cultures. *P<0.05, **P<0.01 compared to MesenPRO control. ###P<0.001 compared to manufacturer's control. (ANOVA, Bonferroni's multiple comparison test). Expression normalised to GAPDH. Data shown as mean±SD. N=3.

6.4.3 The expression profile of 3D and 2D MSC cultures in response to IL-1

MSCs were grown in 2D monolayers or 3D spheroids and their expression profile in response to treatment with IL-1 for 3h was measured by qPCR. As well as TSG-6, expression levels of IL-6 and IL-8 were measured. This was to assess the impact of culture conditions on cytokines which could be potentially detrimental to stroke pathogenesis, alongside attempting to potentiate expression of TSG-6.

6.4.3.1 TSG-6 expression in 3D and 2D MSC cultures in response to IL-1

3D MSCs treated with MesenPRO had significantly higher basal expression of TSG-6 than 2D MSCs (all groups) ($P<0.01$) (Figure 6.9). Treatment of 3D or 2D cultures with IL-1Ra resulted in significantly decreased expression of TSG-6 compared to 3D cultures maintained in MesenPRO ($P<0.05$, $P<0.01$ respectively), but there was no difference between 2D cultures treated with MesenPRO or IL-1Ra. Treatment of 3D cultures with IL-1 induced a significant increase in TSG-6 expression compared to 3D MesenPRO control and to 2D cultures treated with IL-1 ($P<0.0001$). This induction was significantly reversed with co-administration of IL-1Ra ($P<0.0001$). Treatment of 2D cultures with IL-1 did not induce expression of TSG-6. 3D cultures treated with IL-1 + IL-1Ra had significantly higher expression of TSG-6 than 2D cells given the same treatment ($P<0.001$).

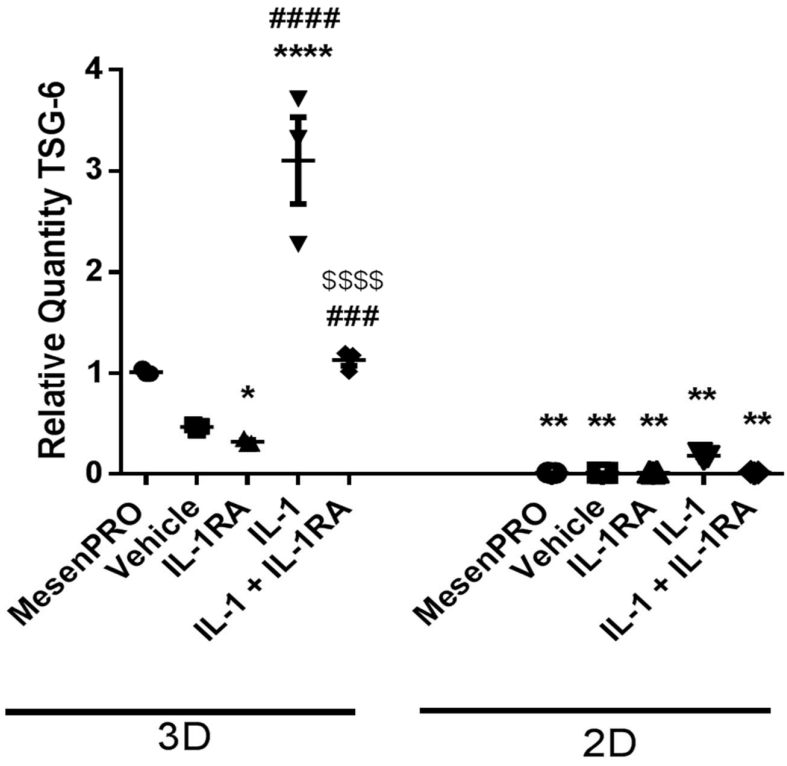

Figure 6.9: TSG-6 expression in 3D and 2D MSC cultures. Cultures were treated for 3h before RNA extraction and qPCR analysis took place. 3D cultures treated with MesenPRO had significantly higher expression of TSG-6 than all 2D culture treatment groups. Treatment of 3D cultures with IL-1Ra resulted in significantly reduced TSG-6 expression. IL-1 treatment induced TSG-6 expression in 3D cultures, but not in 2D cultures, and was reversible by co-administration of IL-1Ra. 3D cultures treated with IL-1 or IL-1 + IL-1Ra had significantly higher TSG-6 expression than the equivalent treatment in 2D cultures. *P<0.05, **P<0.01, ****P<0.0001 compared to 3D MesenPRO. ###P<0.001, ####P<0.0001 compared to equivalent treatment in 2D cultures. $$$$P<0.0001 compared to 3D IL-1. (TWO-WAY ANOVA, Bonferroni's multiple comparison test). Data shown as mean±SD. Expression normalised to GAPDH. N = 3.

6.4.3.2 IL-6 EXPRESSION IN 3D AND 2D MSC CULTURES IN RESPONSE TO IL-1

There was no difference in expression of IL-6 between 3D and 2D cultures treated with MesenPRO, vehicle, IL-1Ra or IL-1 + IL-1Ra (Figure 6.10). IL-1 treatment significantly induced IL-6 expression in 3D cultures, but not in 2D cultures ($P<0.0001$). This induction was reversed by co-treatment with IL-1Ra ($P<0.0001$).

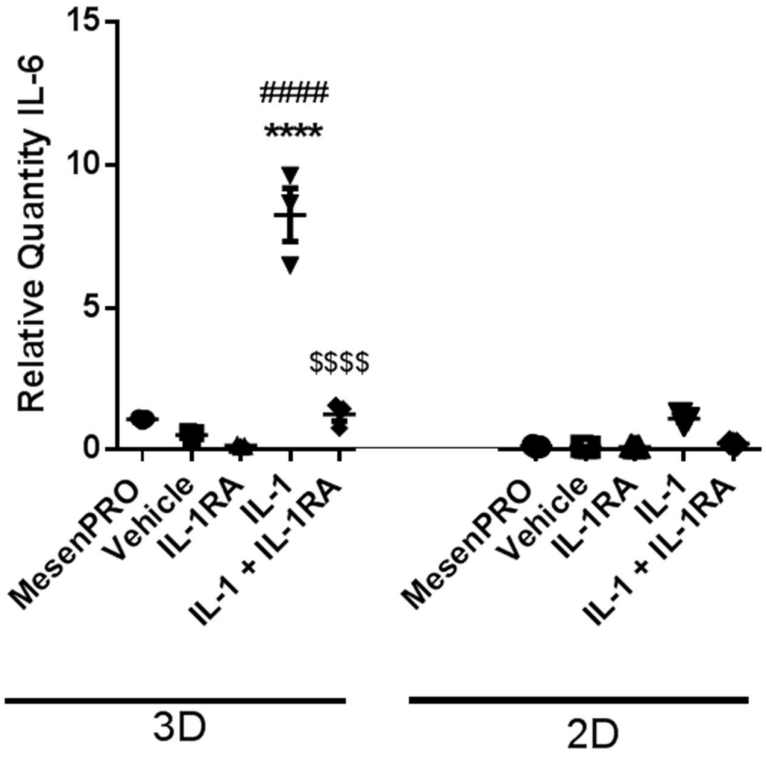

Figure 6.10: IL-6 expression in 3D and 2D MSC cultures. Cultures were treated for 3h before RNA extraction and qPCR analysis took place. There was no difference in IL-6 expression between 3D and 2D cultures treated with MesenPRO, vehicle, IL-1Ra or IL-1 + IL-1Ra. IL-1 treatment induced expression of IL-6 in 3D cultures but not in 2D cultures. IL-1Ra reversed this IL-1-induced induction of expression. ****$P<0.0001$ compared to 3D MesenPRO. ####$P<0.0001$ compared to IL-1 treatment in 2D cultures. $$$$$P<0.0001$ compared to 3D IL-1. (TWO-WAY ANOVA, Bonferroni's multiple comparison test). Data shown as mean±SD. Expression normalised to GAPDH. N = 3.

6.4.3.3 IL-8 EXPRESSION IN 3D AND 2D MSC CULTURES IN RESPONSE TO IL-1

3D control cultures treated with MesenPRO had significantly higher expression of IL-8 than 3D cultures treated with vehicle or IL-1Ra ($P<0.05$) and 2D cultures treated with MesenPRO, vehicle, IL-1Ra ($P<0.001$) and IL-1 + IL-1Ra ($P<0.01$) (Figure 6.11). IL-1 treatment induced a significant increase in 3D cultures ($P<0.0001$) and 2D cultures ($P<0.001$), which was reversed by co-administration with IL-1Ra in both cases. IL-1 treatment in 3D cultures resulted in significantly higher IL-8 expression than it did in 2D cultures ($P<0.0001$). IL-1 treatment in 2D cultures resulted in a level of IL-8 expression comparable to MesenPRO-treated control 3D cultures. 3D cultures treated with IL-1 + IL-1RA had significantly higher expression of IL-8 than the equivalent treatment in 2D cultures ($P<0.05$).

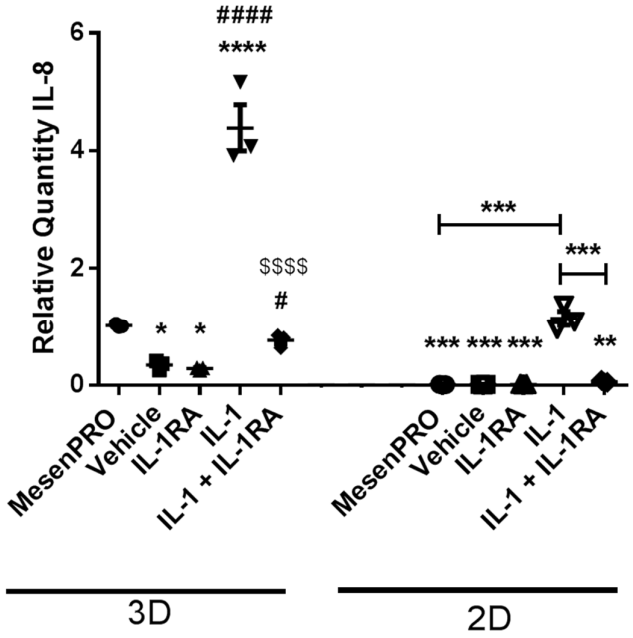

Figure 6.11: IL-8 expression in 3D and 2D MSC cultures. Cultures were treated for 3h before RNA extraction and qPCR analysis took place. 3D cultures treated with MesenPRO had higher IL-8 expression than 3D cultures treated with vehicle or IL-1Ra and 2D cultures treated with MesenPRO, vehicle, IL-1Ra and IL-1 + IL-1Ra. IL-1 treatment induced expression of IL-8 in both 3D and 2D cultures, which was reversed by co-administration of IL-1Ra. IL-1 or IL-1 + IL-1Ra treatment induced higher expression in 3D cultures than it did in 2D cultures. *P<0.05, **P<0.01, **P<0.001, ****P<0.0001 compared to 3D MesenPRO unless otherwise indicated. #P<0.05, ####P<0.0001 compared to equivalent treatment in 2D cultures. $$$$P<0.0001 compared to 3D IL-1. (TWO-WAY ANOVA, Bonferroni's multiple comparison test). Data shown as mean±SD. Expression normalised to GAPDH. N=3.

A pilot study was conducted to assess the effects of peripherally-administered 3D MSC spheroids on histological and behavioural outcomes in the 7 days post-stroke. 10 MSC spheroids (kindly cultured by Steve Ball) or PBS were administered subcutaneously, 30 min before the onset of occlusion (45 min). Reperfusion was for 7 days.

6.4.4.1 LESION VOLUME

Brain sections were stained with H&E and the lesion was defined by identification of shrunken cell bodies and pallor. There was no significant difference between the treatment groups (Figure 6.12). Mice treated with MSCs had a 20% larger average lesion size than the control mice. 3 out of 4 PBS-treated mice had small lesions mainly restricted to the striatum, whereas one had damage extending into the cortex. This variability resulted in a coefficient of variation of 92%. 60% of mice treated with MSCs had some degree of cortical damage, and the coefficient of variation in this group was 47%.

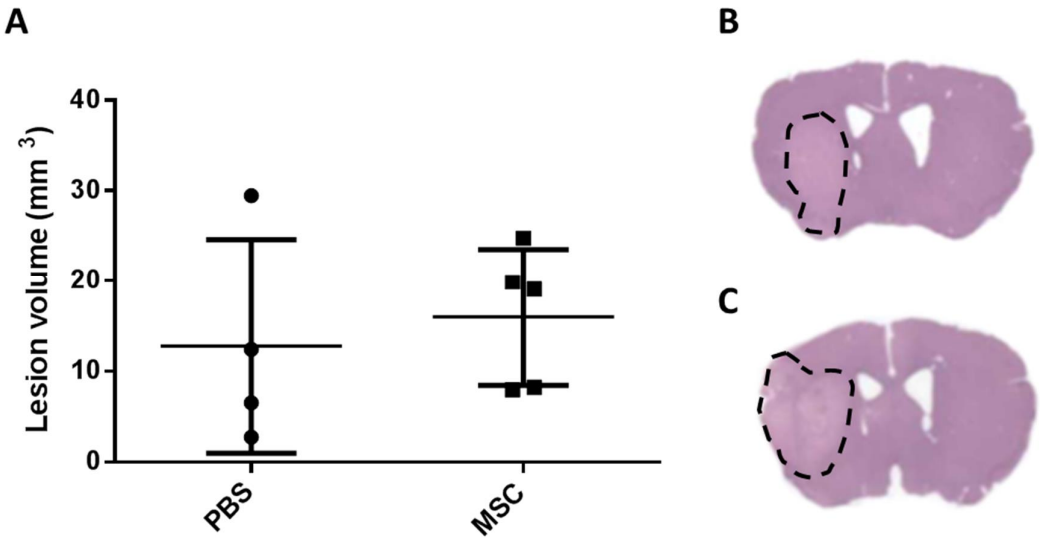

Figure 6.12: Lesion volumes of mice treated with PBS or 10 MSC spheroids followed by 45min MCAo and 7 days reperfusion. A: There was no significant difference in lesion volume between the two treatment groups, although mice treated with MSCs had a 20% larger mean lesion volume than control mice. Typical brain sections stained with H&E are shown from mice treated with PBS (B) and MSCs (C). (Unpaired t-test). Data presented as mean ±SD. N=4 or 5.

6.4.4.2 BLOOD-BRAIN BARRIER DISRUPTION

BBB disruption was quantified by staining for IgG extravasation into the brain parenchyma. There was no significant difference between treatment groups in the extent of BBB disruption seen, although there was a small 6.5% decrease in the MSC-treated group (Figure 6.13). All mice had substantial BBB breakdown throughout the hemisphere, and the coefficients of variation were 19% and 11% for mice treated with PBS and MSCs respectively.

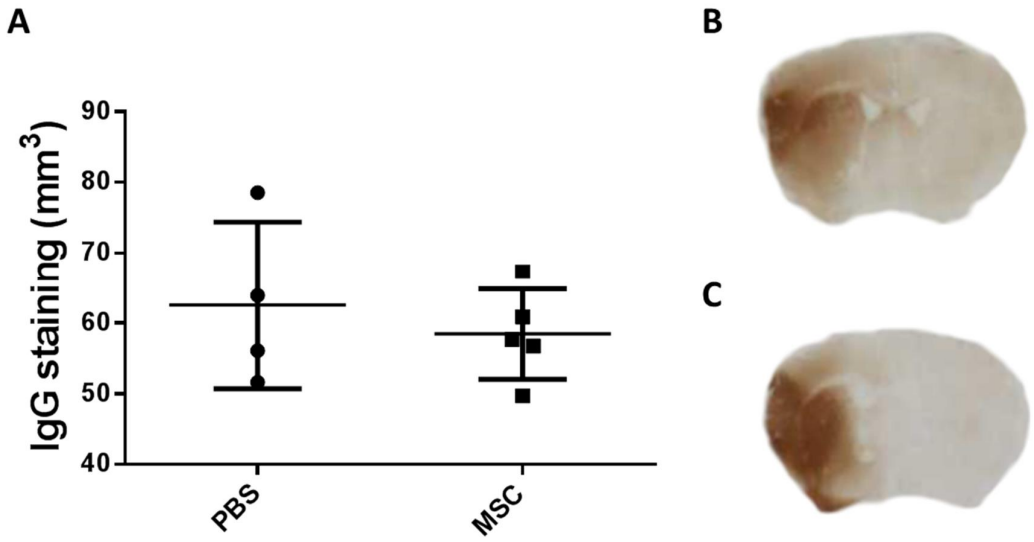

Figure 6.13: BBB disruption in mice treated with PBS or 10 MSC spheroids followed by 45min MCAo and 7 days reperfusion. A: There was no significant difference in BBB breakdown between the two treatment groups. Typical brain sections stained for IgG are shown from mice treated with PBS (B) and MSCs (C). (Unpaired T-test). Data presented as mean ±SD. N=4 or 5.

6.4.4.3 NEUTROPHIL INFILTRATION

Brain sections were stained for neutrophils with SJC-4. There were no neutrophils present in the brains of mice treated with PBS (Figure 6.14). However, 60% and 80% of MSC-treated mice had neutrophils present in the striatum and cortex respectively. One mouse treated with MSCs had very extensive neutrophil infiltration into the cortex: this was enough to lead to a significant difference between treatment groups ($P<0.05$).

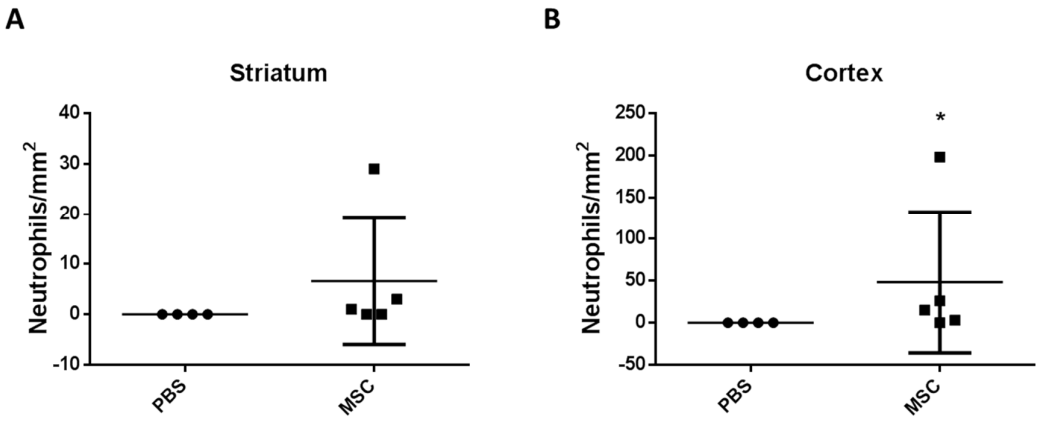

Figure 6.14: Neutrophil infiltration into the brain in mice treated with PBS or 10 MSC spheroids followed by 45min MCAo and 7 days reperfusion. A: Striatum. There was no significant difference between the treatment groups, although there were no neutrophils present in the brains of PBS-treated mice, and 60% of MSC-treated mice had some degree of neutrophil recruitment. B: Cortex. MSC-treated mice had significantly more cortical neutrophils than control mice. *$P<0.05$. (Unpaired t-test). Data presented as mean ±SD. N=4 or 5.

6.4.4.4 MOTOR-NEUROLOGICAL CHARACTERISATION

Mice were scored on their motor-neurological characteristics after 24h, 3 days and 7 days reperfusion. There was no significant difference between treatment groups, although at all time-points there was a slight trend for improved neurological score in mice treated with MSCs (Figure 6.15).

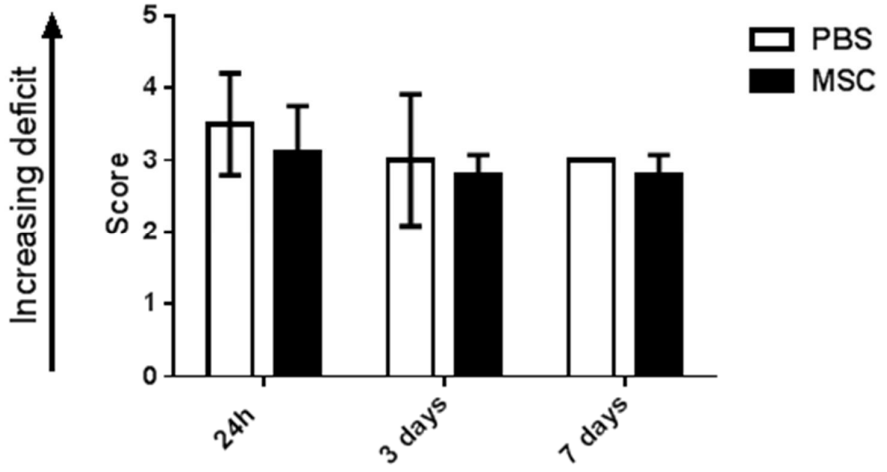

Figure 6.15: Motor-neurological characterisation of mice treated with PBS or 10 MSC spheroids followed by 45min MCAo. There was no difference in neurological score seen between treatment groups at any time-point. There was a trend for improved motor-neurological behaviour in MSC-treated mice at all time-points, particularly 24h. (Two-way ANOVA). Data presented as mean ±SD. N=4 (PBS) or 5 (MSC).

6.4.4.5 BEHAVIOURAL CHARACTERISATION

Behavioural characteristics of mice were assessed after 24h, 3 days and 7 days reperfusion. There was no significant difference between the two groups at any time-point, however MSC-treated mice showed a trend for improvements in body position, spontaneous activity, transfer arousal and gait (Figure 6.16). MSC-treated mice had an average 1.2-1.6 fold improvement in body position, a 1.3-1.4 improvement in spontaneous activity, a 1.2-1.3-fold improvement in transfer arousal and a 1.4-fold improvement in gait compared to control mice.

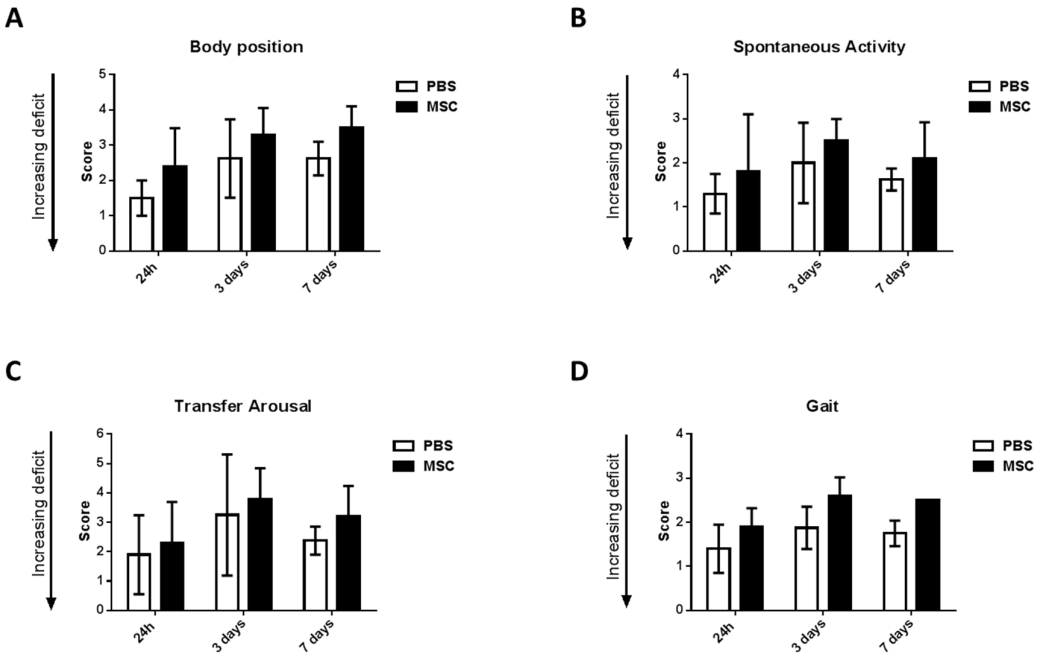

Figure 6.16: Behavioural characterisation of mice treated with PBS or 10 MSC spheroids followed by 45min MCAo. There was no significant difference in any behavioural score seen between treatment groups at any time-point. There was a trend for improved body position (A), spontaneous activity (B), transfer arousal (C) and gait (D) in MSC-treated mice at all time-points. (Two-way ANOVA). Data presented as mean ±SD. N=4 (PBS) or 5 (MSC).

6.4.4.6 LEUKOCYTE POPULATIONS IN THE BLOOD

Leukocyte populations in the blood before and after MCAo were measured by flow cytometry. There was no significant difference in the number of granulocytes, monocytes, B cells or T cells at any time-point (Figure 6.17). Granulocytes showed their characteristic pattern of peaking at 24h, before returning to baseline by 3 days. Monocytes also peaked at 24h then reduced in numbers over the next 6 days. Monocytes appeared to remain in the blood for longer in MSC-treated mice, with mice treated with MSCs having 26% more monocytes than control mice in the blood at 3 days and 7 days. B cells remained relatively constant over the whole 7 days. Both treatment groups had a reduction in T cells over the first 3 days, which was increasing by 7 days reperfusion. However after 7 days, control mice had 23% more T cells in the blood than mice treated with MSCs.

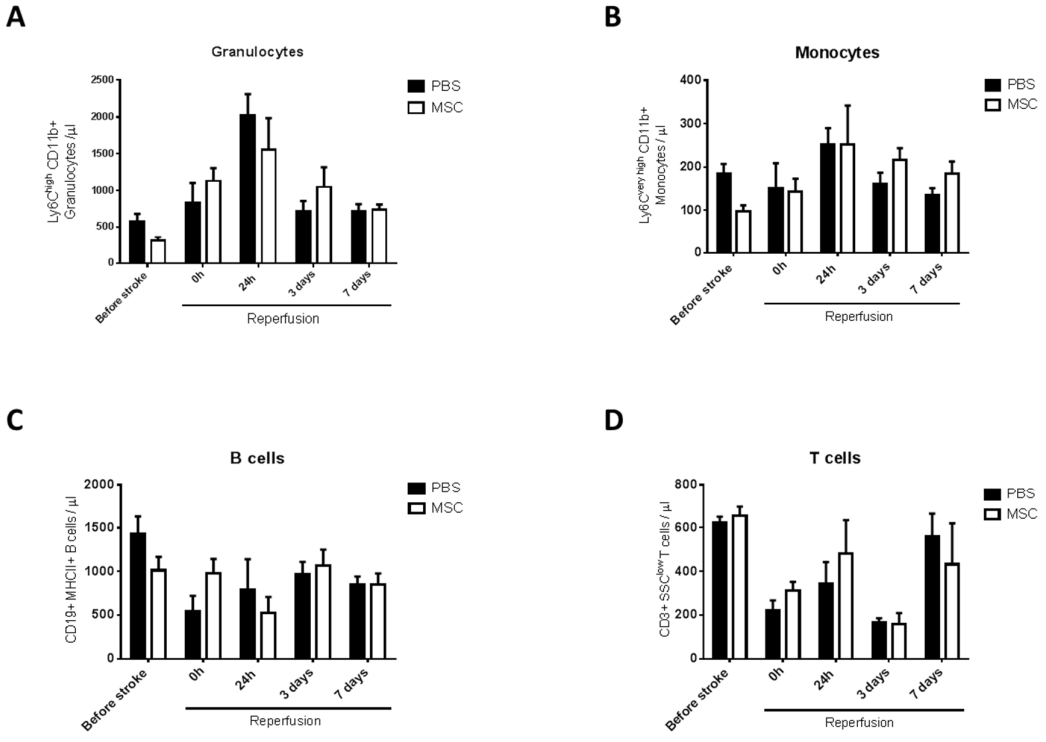

Figure 6.17: Leukocyte populations in the blood of mice treated with PBS or 10 MSC spheroids followed by 45min MCAo. There was no significant difference between treatment groups in any leukocyte population. A: Granulocytes (Ly6C^{high} CD11b+). B: Monocytes (Ly6C$^{very\ high}$ CD11b+). C: B cells (CD19+ MHCII+). D: T cells (CD3+ SSC^{low}). (Two-way ANOVA). Data presented as mean ±SD. N=4 (PBS) or 5 (MSC).

6.4.4.7 CYTOKINE PROFILE OF THE BLOOD

Blood samples were analysed by CBA to measure the concentration of circulating cytokines. There was no significant difference in KC, RANTES, G-CSF or IL-6 between the two treatment groups at any time-point (Figure 6.18). KC increased in the blood immediately following reperfusion, with MSC-treated mice having a 4.8-fold greater induction at this time-point. MSC-treated mice had 6-fold more circulating KC than control mice after 24h, and this cytokine was still detectable at 3 days in mice treated with MSCs, whereas control mice had none by this time-point. One PBS-treated mouse had elevated plasma RANTES before onset of surgery so was excluded from analysis. MSC-treated mice showed increase plasma RANTES from 0h reperfusion which declined over 3 days. G-CSF peaked in the blood at 24h, with MSC-treated mouse having 2-fold higher expression than control mice. IL-6 expression rose progressively over the 3 days following reperfusion, but levels were 2-fold higher in MSC-treated mice than in PBS-treated mice. Both groups had no IL-6 expression after 7 days reperfusion.

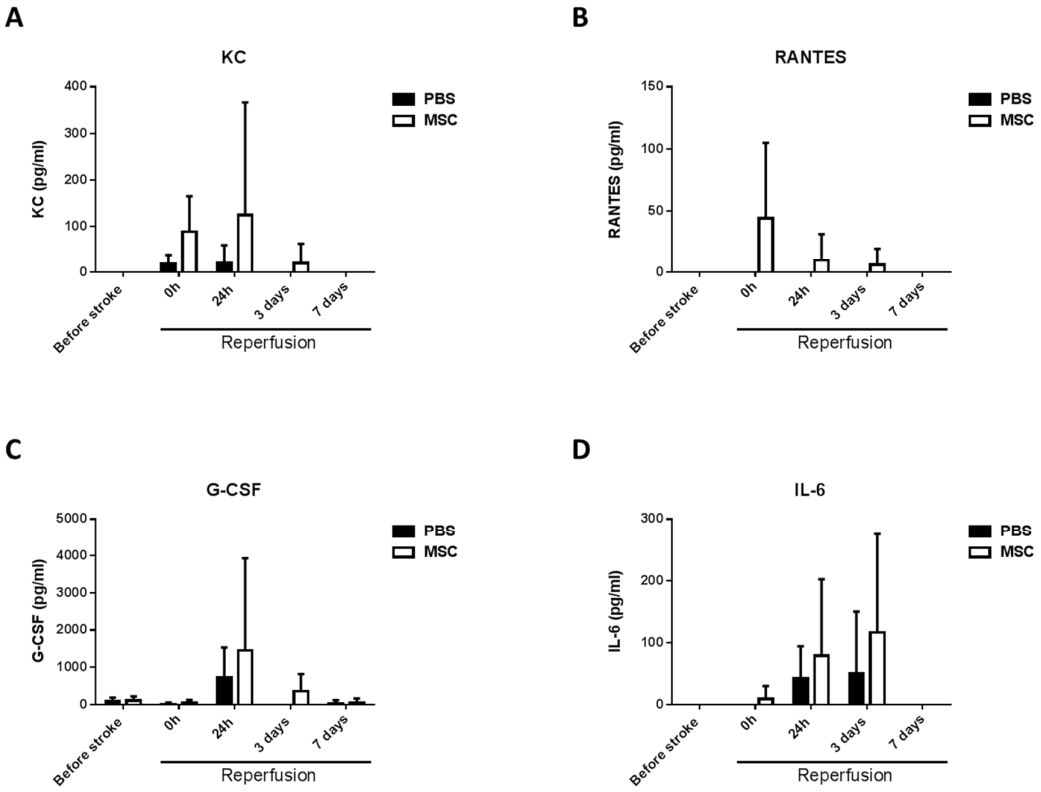

Figure 6.18: Cytokine expression in the blood of mice treated with PBS or 10 MSC spheroids followed by 45min MCAo. There was no significant difference between treatment groups in any cytokine measured. However, mice treated with MSCs appeared to have higher circulating levels of KC (A), RANTES (B), G-CSF (C) andIL-6 (D) than control mice treated with PBS. (Two-way ANOVA). Data presented as mean ±SD. N=4 (PBS) or 5 (MSC).

6.4.5 THE EFFECT OF PDGF-INHIBITED 3D MSCS ON POST-ACUTE OUTCOMES AFTER EXPERIMENTAL STROKE

A second pilot study was conducted to investigate the effects of MSC spheroids treated with a PDGF receptor inhibitor on post-acute outcomes after MCAo. Inhibiting the PDGF receptor increases the multipotency of MCSs, allowing more potential lineages than just adipogenic, osteogenic and chondrogenic (Ball et al., 2012). 10 treated or untreated MSC spheroids or matrigel control were administered 10 min after reperfusion (30 min MCAo). Reperfusion was for 14 days.

6.4.5.1 BLOOD-BRAIN BARRIER DISRUPTION

There was no significant difference in BBB breakdown seen between the three groups, although MSC-treated mice had a 2-fold higher average area of breakdown than the control mice treated with matrigel, and mice treated with the PDGF-inhibited MSCs had a 2.1-fold increase (Figure 6.19). There was a high degree of variability in the two MSC-treated groups, with some mice only having disruption to striatal or hippocampal areas, with others having BBB breakdown extending throughout the hemisphere. The coefficients of variation for mice treated with matrigel, MSCs and PDGF-inhibited MSCs were 36%, 52% and 58% respectively.

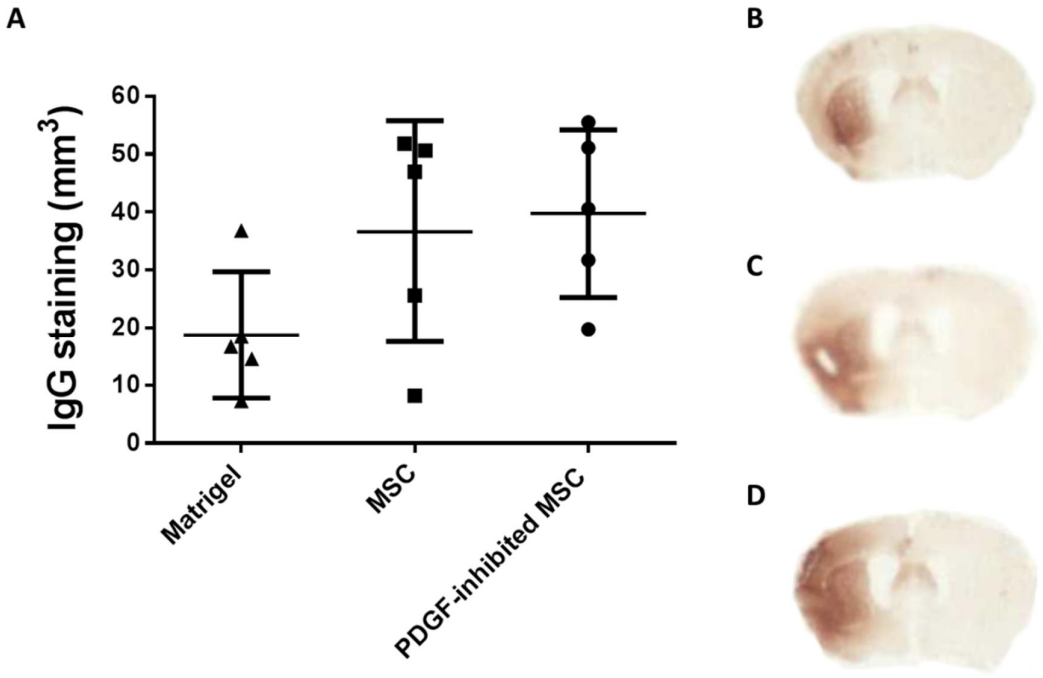

Figure 6.19: BBB disruption in mice treated with matrigel, 10 MSC spheroids or 10 PDGF-inhibited MSC spheroids after 30 min MCAo and 14 days reperfusion. A: There was no significant difference in BBB breakdown between the three treatment groups. There was a trend for increased disruption (~2-fold) in the two groups treated with MSCs. Typical brain sections stained for IgG are shown from mice treated with matrigel (B), MSC spheroids (C) and PDGF-inhibited MSC spheroids (D). (ANOVA, Bonferroni's multiple comparison test). Data presented as mean ±SD. N=5.

6.4.5.2 NEUTROPHIL INFILTRATION

Neutrophil infiltration into the striatum and cortex was quantified by staining brain sections with SJC-4. There was no significant difference between treatment groups in either brain area (Figure 6.20). Most mice had very few striatal neutrophils, although one control mouse and two mice treated with PDGF-inhibited MSCs had marked infiltration. In the cortex, there was a trend for increased neutrophil infiltration with both MSC treatments. Mice treated with normal or PDGF-inhibited MSCs had a 2.2- or 3.1-fold increase in average cortical neutrophils compared to control mice. However, 40% of each MSC-treated group had no or very little cortical neutrophil infiltration.

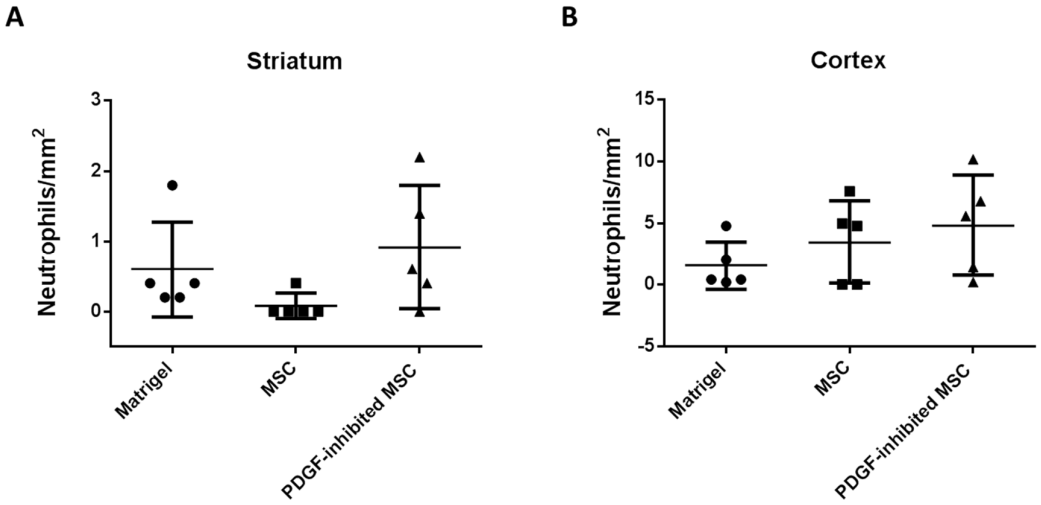

Figure 6.20: Neutrophil infiltration into the brain in mice treated with matrigel, 10 MSC spheroids or 10 PDGF-inhibited MSC spheroids after 30min MCAo and 14 days reperfusion. A: Striatum. There was no significant difference between the treatment groups. B: Cortex. There was a trend for increased cortical neutrophil infiltration in the mice treated with MSCs. (ANOVA, Bonferroni's multiple comparison test). Data presented as mean ±SD. N=5.

6.4.5.3 NEUROLOGICAL SCORE

Mice were assessed for their motor-neurological characteristics after 24h, 7 days and 14 days reperfusion. At 24h, MSC-treated mice showed a significantly larger (1.5-fold) neurological deficit than control mice (Figure 6.21). Mice treated with the PDGF-inhibited MSCs had a deficit intermediate to the other two groups. There was no significant difference between groups at later time-points, however matrigel-treated control mice appeared to decline over 14 days (mean scores at 24h and 14 days were 2.3 and 2.8 respectively), whereas MSC-treated mice appeared to improve (mean scores at 24h and 14 days were 3.5 and 2.6 respectively). Mice treated with PDGF-inhibited MSCs remained relatively constant over the two weeks. By day 14 there was very little difference seen between the treatment groups.

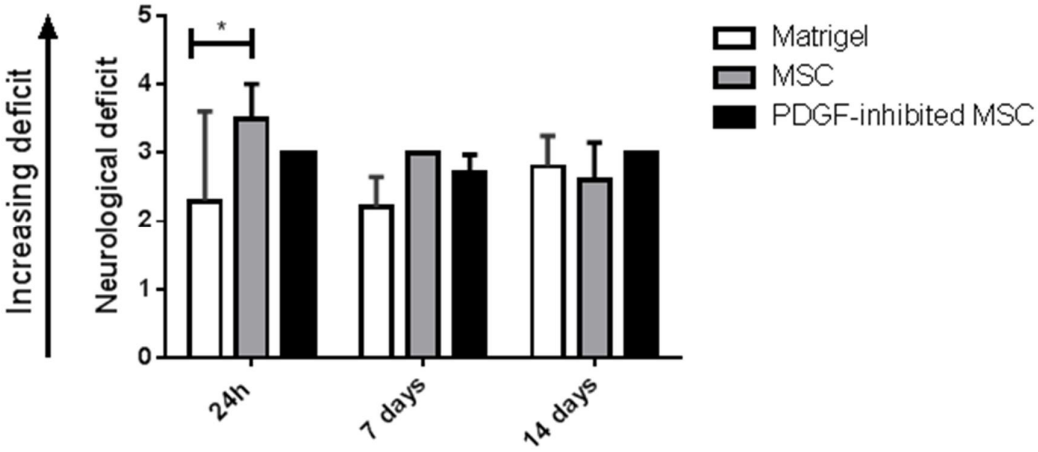

Figure 6.21: Motor-neurological characterisation of mice treated with matrigel, 10 MSC spheroids or 10 PDGF-inhibited MSC spheroids after 30min MCAo. At 24h, MSC-treated mice had a significantly worse neurological deficit than control mice. By 14 days there was no marked difference between the three treatment groups. MSC-treated mice improved over two weeks, whereas matrigel-treated mice declined. *P<0.05. (Two-way ANOVA). Data presented as mean ±SD. Where no error bars are present, all values are equal. N=5.

6.4.5.4 BEHAVIOURAL CHARACTERISATION

Behavioural characteristics were assessed after 24h, 7 days and 14 days reperfusion. There was a general trend across all characteristics for a worse deficit in the two MSC-treated groups compared to the control group (Figure 6.22). MSC-treated mice scored significantly lower than control mice for body position after 7 days ($P<0.05$), and mice treated with PDGF-inhibited MSCs scored significantly lower than control mice for transfer arousal at 24h ($P<0.01$). Across most characteristics, matrigel-treated mice scored fairly consistently across the three time-points, whereas MSC-treated mice appeared to improve. Mice treated with PDGF-inhibited MSC spheroids seemed to slightly improve at 7 days then decline again at 14 days, although these trends were not significant.

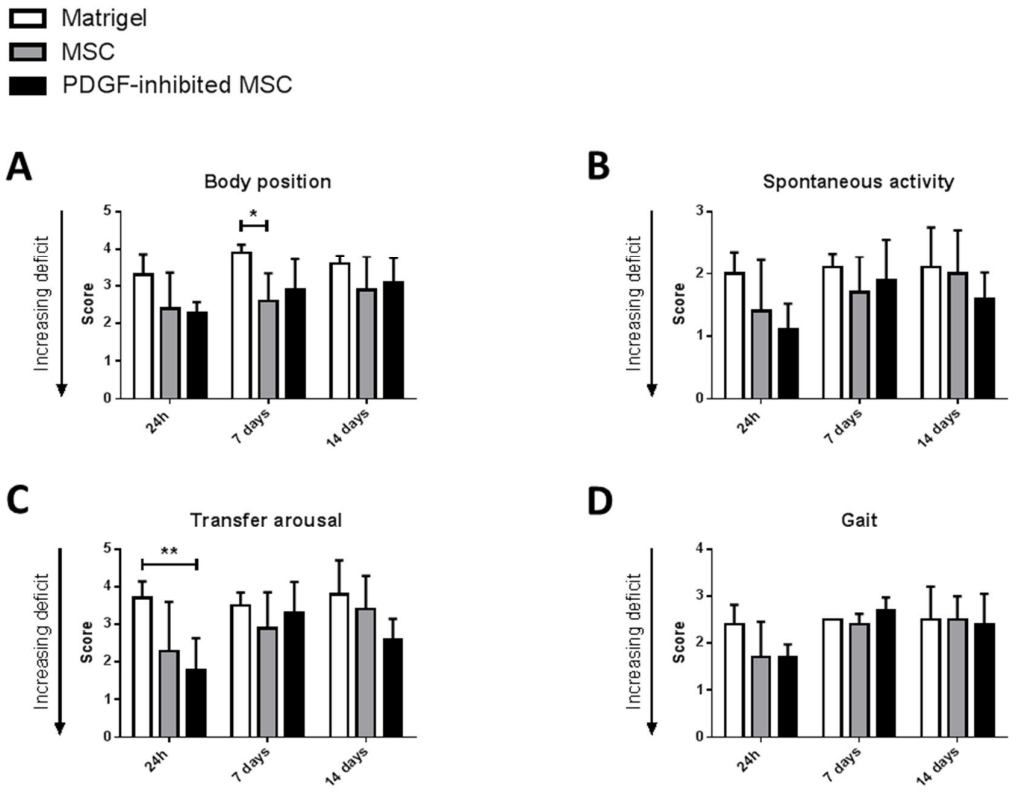

Figure 6.22: Behavioural characterisation of mice treated with matrigel, 10 MSC spheroids or 10 PDGF-inhibited MSC spheroids followed by 30min MCAo. In general, control mice scored better than MSC-treated mice in body position (A), spontaneous activity (B), transfer arousal (C) and gait (D). MSC-treated mice scored significantly worse than control mice in body position at 7 days, and mice treated with PDGF-inhibited MSCs scored significantly lower than control mice for transfer arousal at 24h. *P<0.05, **P<0.01. (Two-way ANOVA). Data presented as mean ±SD. N=5.

6.4.5.5 Open field test

Motor function was tested in mice by the open field test. There was no significant difference between treatment groups at any time-point, however all groups showed a trend for continuing to decline by 14 days (Figure 6.23). However, MSC-treated mice seemed to have less of a decline than the other two treatment groups, and actually had a trend for improvement at 7 days compared to their 24h performance. MSC-treated mice showed trends for better performance than mice treated with PDGF-inhibited spheroids in terms of distance travelled, average speed, total time active, number of line crossings and number of rears, and at some time-points also performed better than control mice.

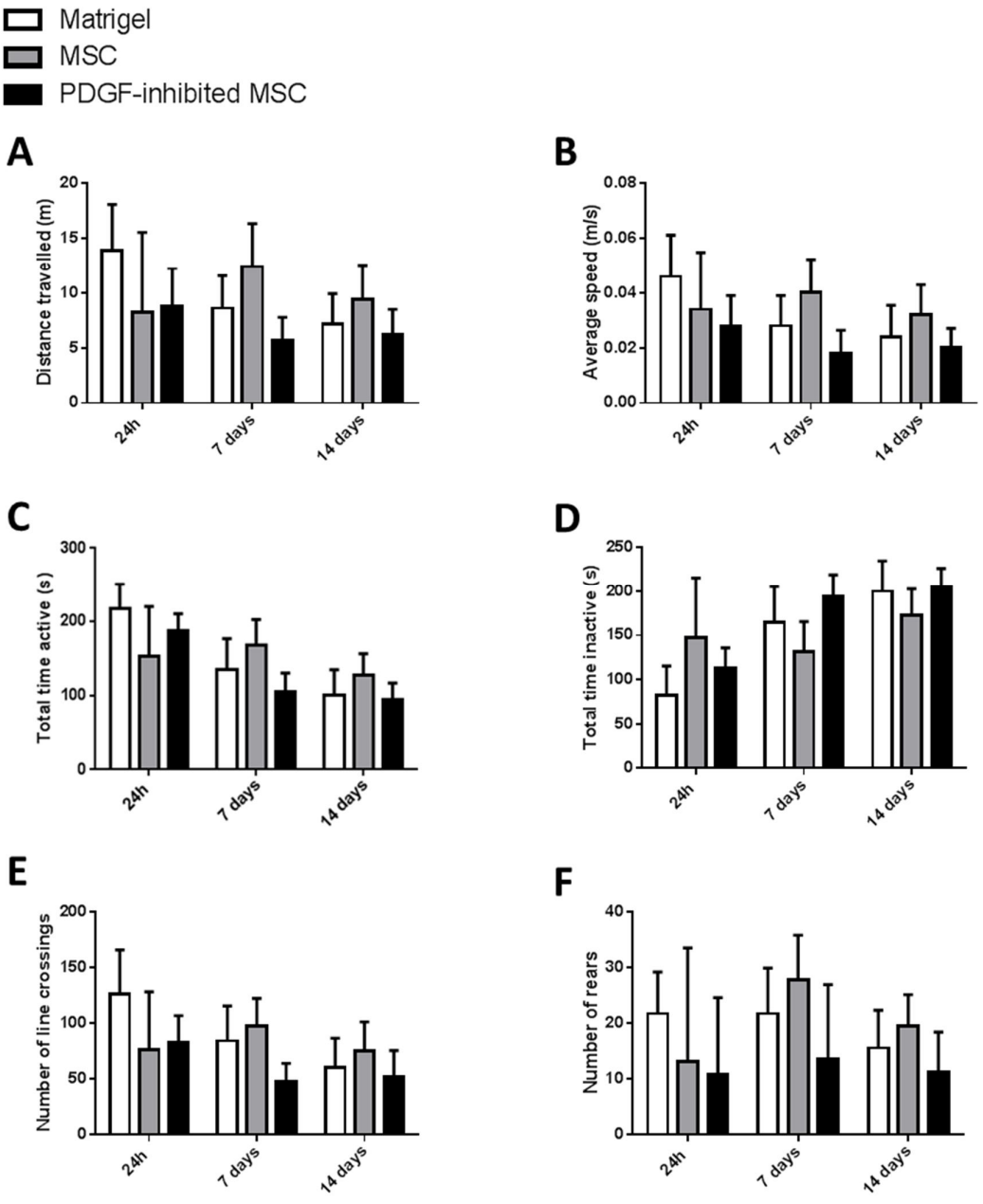

Figure 6.23: Open field test in mice treated with matrigel, 10 MSC spheroids or 10 PDGF-inhibited MSC spheroids followed by 30min MCAo. There was no significant difference between treatment groups in distance travelled (A), average speed (B), total time active (C), total time inactive (D), number of line crossings (E) or number of rears (F). In general, mice treated with PDGF-inhibited spheroids performed worse than the other two groups at all time-points. Control mice and mice treated with PDGF-inhibited spheroids declined over the two week period, whereas mice treated with MSCs improved at 7 days, and performed better than control mice at this time-point in all parameters tested. (Two-way ANOVA). Data presented as mean ±SD. N=5.

6.4.5.6 CYTOKINE PROFILE OF THE BLOOD

CBA analysis of plasma samples was performed to quantify levels of circulating cytokines. All groups showed an induction of KC immediately following reperfusion (Figure 6.24). At 24h, control mice appeared to have higher levels of KC than the two MSC-treated groups. However, at 3, 7 and 14 days, control and MSC-treated mice had comparable levels of circulating KC, whereas mice treated with PDGF-inhibited spheroids had much lower levels. G-CSF peaked in the blood at 3 days, and at this time-point MSC-treated mice had significantly more G-CSF than mice treated with PDGF-inhibited spheroids ($P<0.05$). The same pattern was true at 7 days, but by 14 days all groups had comparable levels, although they had not returned to baseline. IL-6 peaked in the blood between 24h and 3 days. Control mice appeared to have a trend for increased plasma IL-6 compared to the two MSC-treated groups.

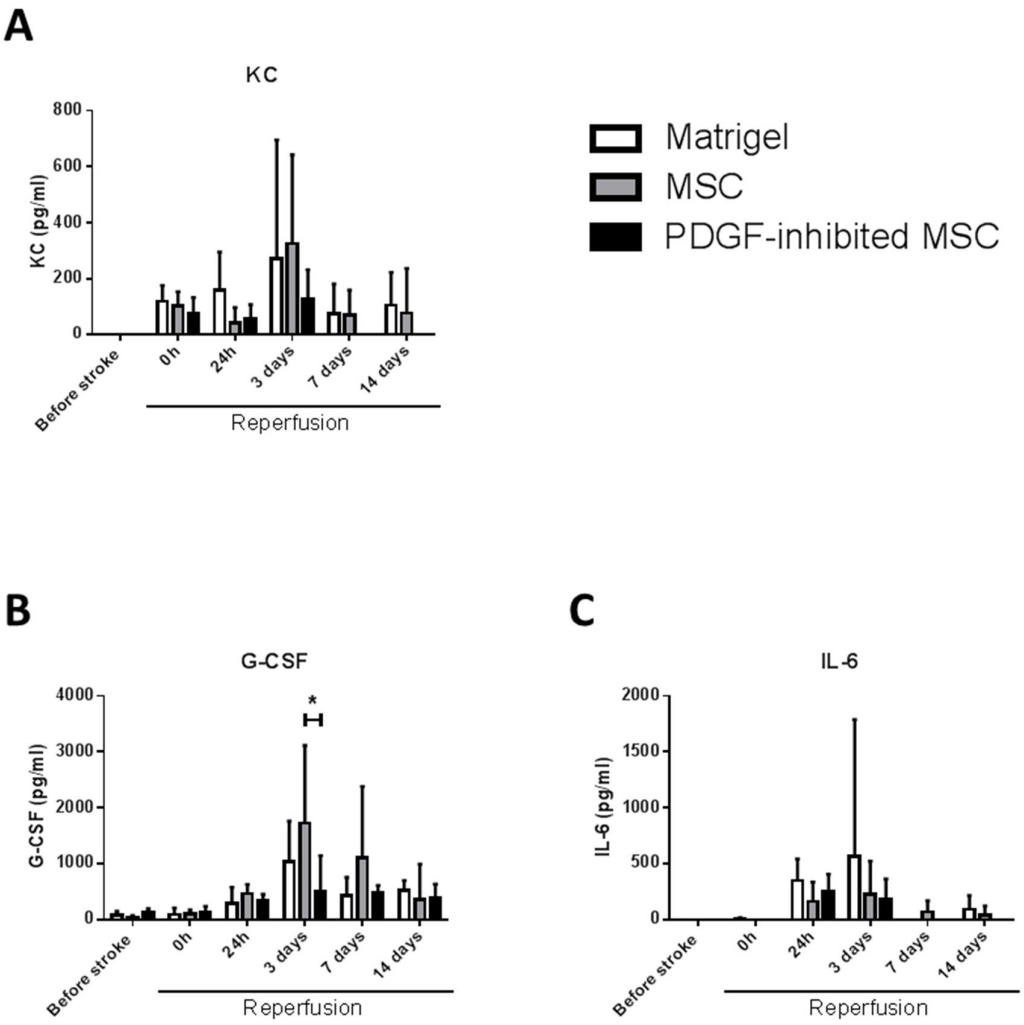

Figure 6.24: Cytokine expression in the blood of mice treated with matrigel, 10 MSC spheroids or 10 PDGF-inhibited MSC spheroids after 30min MCAo. There was no significant difference between treatment groups in plasma levels of KC (A). G-CSF (B) peaked in the blood after 3 days reperfusion, and MSC-treated mice had significantly more G-CSF than mice treated with PGDF-inhibited MSCs at this time-point. There was no significant difference in plasma concentrations of IL-6 (C). *P<0.05. (Two-way ANOVA). Data presented as mean ±SD. N=5.

6.5 DISCUSSION

This chapter of work has investigated the therapeutic potential of the paracrine properties of MSCs in experimental stroke. Due to a vast expansion of research into MSCs and inconsistencies in published data, a set of minimum criteria for characterisation of MSCs was published (Dominici et al., 2006). In this chapter, MSCs were characterised according to accepted standards in terms of morphology, plastic-adherence, cell surface marker expression and differentiation potential. There were no irregularities in the first three criteria tested. Immunohistological and morphological analysis of cultures induced during the differentiation assay identified clear differentiation down adipogenic, osteogenic and chondrogenic lineages. As an adjunct to the minimum suggested characterisation criteria, qPCR was also performed to analyse expression of further lineage-specific markers. All expression levels were as expected, however osteopontin (an osteoblast marker) was most highly expressed in cells treated with the manufacturer's control. There was a high degree of variability in this group, with a coefficient of variation of 58%, and it was not a statistically significant difference. Alkaline phosphatase is an early marker of osteogenic differentiation, and expression increases with osteoblast maturation, osteopontin is expressed throughout maturation of the matrix, whereas osteocalcin is expressed in the late phase of differentiation, once proliferation is complete and cells are committed to an osteogenic fate (Liu et al., 2003). The fact that osteocalcin staining was strong in differentiated cells but was absent in control cells, and that alkaline phosphatase was increased in differentiated cells suggests that cultures had differentiated to a mature osteogenic fate. It is likely that the result indicating osteopontin expression in control cells was due to an experimental error. Overall the characterisation of MSCs was successful and in line with published guidelines.

MSCs have shown therapeutic benefit in a range of disease models, and this has often been attributed to induction of the cells to express TSG-6 among other anti-inflammatory molecules (Danchuk et al., 2011; Kota et al., 2013; Lee et al., 2009b; Oh et al., 2012; Roddy et al., 2011; Wang et al., 2012). Previously published work has shown that MSCs cultured in 3D spheroids have higher expression of TSG-6 than cells grown in a 2D monolayer (Bartosh et al., 2010). This finding was replicated in this chapter, and additional work showed that IL-1-induced expression of TSG-6 is more

potent in 3D spheroids than in 2D cultures. The enhanced basal expression of TSG-6 is sufficient to promote the use of 3D cultures therapeutically. However, in addition, the increased expression potential of TSG-6 in response to IL-1 makes these 3D MSC cultures an exciting therapeutic potential for conditions in which there is a raised inflammatory profile and a marked presence of circulating cytokines, e.g. in stroke. The majority of stroke patients have some form of co-morbidity such as atherosclerosis, obesity or infection, and these diseases result in a systemic presence of IL-1 (Denes et al., 2011). In addition, it has been shown that peripheral IL-1 contributes to ischaemic brain damage (Denes et al., 2013; McColl et al., 2007). 3D spheroids would react to this systemic IL-1 and produce TSG-6, which has got proven therapeutic benefits. Furthermore, MSCs have also been shown to produce IL-1Ra (Ortiz et al., 2007), which has been shown experimentally and clinically to reduce ischaemic damage and improve outcome (Emsley et al., 2005; Mulcahy et al., 2003; Pradillo et al., 2012). In addition to MSCs responding to systemic cues, cultures could be primed before being used therapeutically, in order to alter their expression profile.

In this chapter, it was shown that stimulation of MSCs with IL-1 not only increases their expression of TSG-6, but it also induces expression of IL-6 and IL-8. IL-6 is a clinical biomarker of ischaemic stroke, with raised plasma concentrations being associated with poor outcome (Whiteley et al., 2009). It is unknown if IL-6 actively contributes mechanistically to development of a worse ischaemic insult, or whether it is a passive biomarker with limited pathological effect. However IL-6 has been shown to increase the probability of a thrombotic event, and it induces production of CRP which has been shown experimentally to exacerbate stroke (Gill et al., 2004; Kerr et al., 2001). Taking this into account, it is likely that MSC-derived IL-6 could be detrimental to stroke pathogenesis. Having said that, IL-6 can also induce expression of IL-1Ra by macrophages (Tilg et al., 1994), and it is becoming increasingly recognised that IL-6 has a duel function in stroke: pro-inflammatory in the acute phase and beneficial in the longer term (Suzuki et al., 2009). If MSCs were to be delivered therapeutically in the acute phase, it might be beneficial to inhibit their expression of IL-6 to reduce any pro-inflammatory impact. Increased IL-8 expression was also shown in MSCs in response to IL-1. There is relatively little information regarding the impact of IL-8 on stroke outcome, however plasma IL-8 has been seen to increase following stroke, particularly

in older patients, suggesting a possible role in the poorer outcome seen in more elderly stroke victims (Ormstad et al., 2011). The increased expression of IL-8 could be a potential reason for the trend seen for increased lesion volume with MSC treatment. IL-8 is a neutrophil chemoattractant, and although not directly homologous, it shares functional characteristics with murine KC and MIP-2 (Hol et al., 2010). If human IL-8 were able to initiate chemokine gradients and facilitate leukocyte migration, it could have contributed to the exacerbation of stroke outcomes. A full microarray and proteomic investigation of the expression profile of MSCs in response to inflammatory stimuli would be beneficial, and interventions to fine-tune their output could increase their power as a therapeutic tool. Furthermore, the impact of ischaemic conditions on MSC output is important to consider: it has been show that growing cells in a serum-deprived environment increases their production of pro-survival and pro-angiogenic factors (Oskowitz et al., 2011). It would be useful to be able to optimise the output of MSCs, to enhance the production of anti-inflammatory mediators whilst inhibiting the expression of factors detrimental to stroke pathogenesis. This is outside the direct scope of this work, but would be an interesting future avenue to explore. The conclusion reached from this section was that 3D cultures of MSCs express higher levels of TSG-6 both basally and in response to inflammation, so were the logical choice to take forward into *in vivo* experiments.

The *in vivo* experiments in this chapter were designed to investigate the paracrine effects of MSCs. Central administration of MSCs has been shown to be beneficial in animal models of stroke (Chen et al., 2001a; Moisan et al., 2012), yet in other diseases MSCs have shown therapeutic efficacy without engraftment or migration to the site of injury (Cheng et al., 2013; Ionescu et al., 2012; Lee et al., 2011; Pierro et al., 2013; Waszak et al., 2012). Conditioned media from MSCs also showed therapeutic efficacy in many of these studies, highlighting that the paracrine actions of the MSC secretome have strong therapeutic potential. However, published works have utilised intravenous administration, and benefit from subcutaneous delivery of MSCs has not been reported in any stroke models. In this chapter, 10 3D MSC spheroids were injected subcutaneously, either in PBS or in matrigel. The spheroids are visible to the naked eye, however they were not detected by gross inspection of the injection site after 7 or 14 days. It has been shown that adipose-derived MSCs injected subcutaneously in

saline solution did not migrate from the injection site and survived for 2, 4 or 17 months *in vivo* (López-Iglesias et al., 2011). However, immunodeficient mice were used in this study, so it is possible that cells were cleared more rapidly in the C57BL/6 mice used in this chapter. In future work it might be useful to label MSCs to investigate their migration, however in these experiments the main interest was the paracrine action of cells so this was not a priority. Nonetheless, it would be useful to measure the plasma concentration of TSG-6 to ensure that the cells maintained the same expression profile *in vivo* as in culture, however the lack of a commercial ELISA kit made this difficult. As mentioned in chapter 5, it is possible that subcutaneous administration is not the best option for TSG-6, due to the high presence of glycosaminoglycans in the interstitial space with which TSG-6 can bind (Milner et al., 2006; Porter and Charman, 2000). However, it is possible that MSCs might break off from spheroids and migrate into the blood before releasing TSG-6, although the study by López-Inglesias et al. (2011) suggests that this is not the case. In addition, it has been shown that MSCs delivered intraperitoneally or subcutaneously do not migrate from the site of injection, but maintain their therapeutic benefit through paracrine actions (Ball et al., 2013; Cheng et al., 2013). This considered, it is unlikely that the cells migrated from the subcutaneous space.

As touched on above, there are discrepancies in the literature surrounding the necessity to immunosuppress mice used for experiments with human MSCs. The majority of studies referenced utilised some sort of immunosuppression, either by using genetically immunocompromised mice or with an immunosuppressive agent. However, a number of studies have shown beneficial effects of MSCs in immunocompetent mice and rats (Moisan et al., 2012; Rodriguez et al., 2005; Watanabe et al., 2013). Additionally, it was shown that subcutaneously-administered undifferentiated human MSCs can survive in immunocompetent mice for at least 8 weeks (Niemeyer et al., 2008). The potential for human MSCs to avoid rejection by a murine immune system might be a combination of the lack of expression of human leukocyte antigen-DR (HLA-DR/MHCII) by undifferentiated MSCs, along with their expression of anti-inflammatory mediators and production of a locally immunosuppressed environment (Niemeyer et al., 2008). In this chapter's pilot studies immunocompetent mice were chosen due to the focus of this thesis on the importance

of inflammation to stroke pathogenesis. The whole scope of this work was to investigate the anti-inflammatory properties of TSG-6, particularly in terms of neutrophil migration, on stroke outcome. Therefore a functional immune system is required in order to fully appreciate the inflammatory contribution to stroke. However, the results suggested that in some cases MSC-treated mice exhibited exacerbated BBB disruption, neutrophil infiltration and systemic cytokine profiles, suggesting an immune response to the cells by the host. This heightened systemic immune profile is likely to have contributed to the trend for increased lesion volume. To avoid using immunodeficient mice, one possible future avenue would be to encapsulate human MSCs to avoid rejection by the murine immune system (Knippenberg et al., 2012). A further possibility would be to use murine MSCs, however this raises questions about the translational relevance. Human MSCs are the potential therapy, therefore human MSCs should be tested. Furthermore not as much is known about the properties of murine MSCs, for example whether or not they produce TSG-6. It has been reported that MSCs obtained from different strains of mice have very different properties, which would further complicate their use (Peister et al., 2004). Furthermore, beneficial anti-microbial properties have been found in human MSCs, but were absent in murine MSCs (Meisel et al., 2011). This property might be particularly important for stroke research: many patients succumb to infection after stroke, due to being immunosuppressed (Emsley and Hopkins, 2008). The fact that MSCs also contribute to immunosuppression might cause concerns for stroke therapy, as it may render patients even more susceptible to infection. However the finding that human MSCs have anti-bacterial properties should increase their popularity as a potential therapeutic tool. To conclude this section, evidence suggests that differences between MSCs from different species make it important that human MSCs are used in pre-clinical experiments. Despite reports that human MSCs can be used in immunocompetent mice without rejection, the results in this chapter do suggest that the cells initiated some level of immune response. To avoid immunosuppressing mice, encapsulation of MSCs would be a good future option to explore.

In the first pilot study, MSCs led to no change in lesion volume or BBB disruption, although there was a significant increase in cortical neutrophils. Despite this, there were trends for functional improvements in the MSC-treated mice. This suggests that

neutrophils might not be a key contributor to functional outcome. MSC-treated mice in this study also had a trend for increased plasma monocytes and cytokines, backing up the suggestion made above that there was some level of rejection of the human cells by the immune system. However, the trends for improvements in behaviour suggested that there was some degree of a beneficial effect induced by the MSCs. However, this was not the case in the second study, in which MSC treatment resulted in trends for worsened BBB disruption, neutrophil infiltration, behaviour (although there were promising results in some behavioural tests) and plasma cytokine expression, suggesting a marked immune response in response to the human cells. The main difference between the two studies was the time of administration: in the first experiment MSCs were administered 30 min prior to occlusion onset, whereas in the second study they were given 10 min post-reperfusion. Although the first experiment had better outcomes, the time-point used in the second study is more translationally relevant, so perhaps the results from this should be taken more seriously. The occlusion time was also different: the first study used a 45min occlusion which resulted in a more severe stroke than the 30min occlusion used in the second experiment. There was also a difference in the vehicle used: PBS in the first study and matrigel in the second. There is likely to be some level of immune response to the matrigel, however the MSC-treated groups still generally did worse than the group treated with matrigel alone. Matrigel is likely to have kept the MSCs more localised to the site of injection for a longer period than when PBS was used as the vehicle. It might be that having a more concentrated presence of human MSCs led to a greater immune response by the host, resulting in exacerbated outcome after stroke. Having said that, a more concentrated transplant of MSCs would also mean a greater production of anti-inflammatory mediators by the cells, creating a locally immunosuppressed zone which should have made it harder for the murine immune system to react. Using PBS as a vehicle potentially made it easier for the MSCs to disperse and release beneficial mediators. Perhaps this carrier resulted in a more dilute distribution of cells, which did not induce such a strong rejection response. Despite the worse outcomes seen in the second study (using matrigel) compared to the first study (using PBS), the plasma cytokine response was actually more marked in the first experiment. Additionally, in the second study treatment with PDGF-inhibited MSCs resulted in a less marked response in plasma KC and G-CSF than treatment with normal MSCs, suggesting a

potential difference in recognition by the host immune system. However, in the open field test mice treated with PDGF-inhibited cells appeared to do worse than mice treated with normal MSCs. It is known that the PDGF receptor inhibitor increases multipotency, changes cell shape and regulates expression of Oct4 and Nanog by MSCs (Ball et al., 2012). It would be useful to further investigate the output of cells treated with this inhibitor, in order to elucidate their role as moderators of inflammation.

Like in the previous chapter, the performance of mice in all treatment groups in the open field test was still declining at the final time-point. An investigation into the long-term functional outcome after treatment with MSCs would benefit from extended recovery periods, along with a more sophisticated array of behavioural tests. The studies conducted in this chapter were pilot investigations, but this data can help to direct future work in terms of time of administration, optimisation of the MSC secretome, immunosuppression of mice or encapsulation of MSCs and choice of sensitive behavioural outcomes. Although much of data in this chapter suggested a detrimental effect of MSCs in stroke, it is likely that this was largely due to a rejection of the human cells by the host. The large body of literature promoting the effects of MSCs, in particular via paracrine actions, suggests that these cells are still potentially a very valuable tool for the treatment of diseases such as stroke.

6.6 SUMMARY

In this chapter, human MSCs were characterised for their cell surface marker expression profile and multipotency according to published standards. It was shown that 3D MSC spheroids have a higher expression of TSG-6 than 2D cultures, and that expression of TSG-6 can be increased by stimulation of cells by IL-1. However IL-1 treatment also resulted in up-regulation of IL-6 and IL-8, suggesting that it would be useful to manipulate the secretome of MSCs before they are used therapeutically. Two pilot *in vivo* studies were conducted, testing the effect of human 3D MSC spheroids in a mouse model of ischaemic stroke. Overall there was evidence of an immune response to the cells, in some cases resulting in worse outcome. MSCs are still an excellent candidate for anti-inflammatory therapy in stroke, however administration in mouse models needs to be optimised in future work in order to fully elucidate any effect.

CHAPTER 7:

GENERAL DISCUSSION

7.1 SUMMARY OF FINDINGS

The work in this thesis was carried out with the aim of exploring the role of peripheral inflammation in ischaemic stroke, and investigating the effects of immunomodulatory therapies to protect against inflammation-induced brain damage. Inflammation is a key mediator of the pathogenesis of stroke, with both central and systemic inflammatory responses contributing to brain damage and subsequent outcome. Leukocytes, in particular neutrophils, are mobilised from the bone marrow after stroke, and migrate to the brain where they exacerbate the ischaemic damage. TSG-6, either as a recombinant protein or as a secreted protein from MSCs, has been shown to inhibit neutrophil migration *in vivo*. Therefore, the aims of this thesis were:

1. To investigate the effect of Link_TSG6 on IL-1-induced brain damage and inflammation.

2. To explore the temporal and spatial expression pattern of TSG-6 in the brain after experimental ischaemic stroke.

3. To examine the effects of Link_TSG6 on chronic outcome after experimental stroke.

4. To investigate the expression of TSG-6 by MSCs cultured in different conditions.

5. To explore the potential of systemic TSG-6-expressing MSC transplants as immunomodulatory therapies for ischaemic stroke.

A dose-response study identified a dose of systemic IL-1 that significantly exacerbated lesion volume. This was previously shown to be dependent on neutrophils, so Link_TSG6 was used to protect against IL-1-induced brain damage and inflammation. Treatment with Link_TSG6 reduced neutrophils in the striatum, but not in the cortex, yet there were positive effects on BBB disruption and haemorrhagic transformation, though these did not quite reach significance. Overall therefore Link_TSG6 seemed to exert a positive effect on brain inflammation after stroke, with a trend for a reduction in lesion volume.

The second aim was to investigate the expression of TSG-6 in the brain after stroke, and this revealed an expression pattern associated with the glial scar, peaking at 5 days post-MCAo. This suggested a role for TSG-6 in the post-acute reparative phase of stroke, hence subsequent experiments were extended out to 7 or 14 days recovery.

In the investigation into post-acute recovery there were some trends for improvement with Link_TSG6 treatment after 7 days reperfusion, however the results were variable and significant changes were not observed.

The fourth aim was to explore MSCs as immunomodulatory mediators, and to analyse and exploit their expression of TSG-6. It was shown that MSCs grown in 3D spheroids express higher levels of TSG-6 than cells grown in 2D monolayers, and treatment of cultures with IL-1 was shown to increase expression further, with 3D cultures being more responsive.

The final aim tested the potential of 3D MSC spheroids as a treatment for ischaemic stroke. Systemically-transplanted human MSC spheroids were tested in MCAo with 7 and 14 days reperfusion. Although some trends were observed, there were no robust effects and the results suggested that the human MSCs were rejected by the murine immune system.

Overall the studies in this thesis suggested that TSG-6 or MSCs might have some therapeutic value in stroke, however treatments and experiments need to be further optimised to fully elucidate their potential.

7.2 ANTI-NEUTROPHIL THERAPY: HITTING THE RIGHT TARGET?

TSG-6 was chosen to study due to its anti-inflammatory properties, primarily its ability to inhibit neutrophil migration. Clinically, neutrophil recruitment into the ischaemic area is correlated with the extent of the damage and is associated with poor outcome (Akopov et al., 1996; Buck et al., 2008; Price et al., 2004). Furthermore, many pre-clinical studies have shown protection with blockade of CAMs involved in neutrophil migration (Chopp et al., 1994; Ishikawa et al., 2004; Kitagawa et al., 1998; Soriano et al., 1999; Zhang et al., 2003; Zhang et al., 1995). However, there is some evidence that neutrophil infiltration does not affect stroke, and there have been a number of studies in which blockade of neutrophils had no effect on lesion volume or behavioural outcomes (Hayward et al., 1996; Takeshima et al., 1992). Furthermore, a clinical trial of a neutrophil inhibitory factor was stopped early due to futility (Grieve and Krams, 2005). In addition to neutrophils, other leukocytes such as T cells have been shown to contribute to ischaemic brain damage, so it is possible that selectively blocking one type of immune cell is insufficient for protection. Having said that, the prevalence of post-stroke immunosuppression and infection means that broadly inhibiting the immune system is likely to result in increased infection and mortality so might not be a viable therapeutic option. Neutrophils have been shown to be particularly important for the development of ischaemic damage in the presence of systemic inflammation (McColl et al., 2007). Indeed, in this thesis the most promising effects of TSG-6 were seen in the experiments involving administration of systemic IL-1. However, despite neutrophil infiltration being blocked to some degree, there was no significant effect on lesion volume, suggesting that neutrophils might be able to exert their damaging effects from the cerebrovasculature without crossing into the brain parenchyma. Having said that, Link_TSG6 still seemed to exert some protective effects without fully inhibiting neutrophils. The IL-1 experiment was the more relevant study in a translational context, due to most stroke patients presenting with inflammatory co-morbidities such as atherosclerosis and diabetes. However, this experiment only investigated an acute 24h time-point, whereas the post-acute Link_TSG6 intervention study explored recovery over 7 days. Neutrophils are the first immune cell to migrate to the brain after stroke, so it is likely that acute time-points are more likely to reveal changes in parameters affected by infiltration (Jin et al., 2010). However, functional

recovery is a more clinically relevant outcome than histological parameters, so long-term experiments are key in elucidating a clear idea about how a treatment affects recovery. Future experiments would benefit from exploring cohorts of animals at different time-points, to verify whether any inhibition of neutrophil migration took place, and to explore whether or not it had any effects on functional outcomes. The exploration into IL-1-induced brain damage and inflammation would benefit from an extended recovery period and behavioural outcomes, to fully assess the effect of TSG-6, and neutrophils, on functional recovery.

Overall, although there is abundant published data suggesting a detrimental role for neutrophils in stroke, the work in this thesis has not provided robust evidence to support this. Even when neutrophil migration was successfully blocked to some degree with Link_TSG6 there was no clear improvement on lesion volume or behavioural outcomes, although some BBB protection was evident. However, the variation in lesion volume made it difficult to see a robust effect, so it is difficult to firmly conclude whether or not neutrophils are important for the development of cerebral ischaemia. Link_TSG6 treatment always resulted in a trend for protection, so it's possible that the true effect was masked by the variability. Optimisation of the model would be necessary to fully elucidate the effect of TSG-6 on lesion volume. Another possible conclusion is that neutrophils might not need to transmigrate into the brain parenchyma in order to exert their detrimental effects. Blocking release of neutrophils from the bone marrow rather than blocking migration into the brain might be a more viable therapeutic option, however this won't stop other leukocyte subsets contributing to the development of ischaemic damage. Furthermore this release occurs too early after stroke to be a therapeutically viable target.

Another consideration when talking about inhibiting leukocytes is the recent discovery of an immunosuppressive subset of neutrophils. It has been shown that during acute inflammation, humans mobilise a particular phenotype of neutrophils ($CD11c^{bright}/CD62L^{dim}/CD11b^{bright}/CD16^{bright}$) that are able to inhibit T cell proliferation (Pillay et al., 2012). Blocking T cell proliferation could be beneficial in the acute phase of stroke, as T cells have been shown to contribute to stroke pathogenesis (Liesz et al., 2011; Yilmaz et al., 2006a). However, as mentioned above, stroke-linked

immunosuppression and infection causes increased mortality, so dampening of the adaptive immune system might not be beneficial in the treatment of stroke. It could be that differential targeting of neutrophil subsets at different time-points after stroke might have more therapeutic potential than a broad blockade of all neutrophils.

Overall, the exact contribution of neutrophils in stroke is still unclear, and more work is necessary to fully clarify whether they are indeed the key detrimental mediators of cell death, particularly in the presence of clinically relevant increased systemic inflammation.

7.3 OPTIMISING ROUTES OF ADMINISTRATION

As discussed previously, it appeared that the routes of administration used in these experiments were not always optimal. Intraperitoneal administration of IL-1 was discontinued due to variability of responses, suggesting that in some cases the drug had penetrated the bladder resulting in rapid excretion. Many studies have shown beneficial effects of TSG-6 after intravenous administration, and this route was attempted in chapter 5. However, restraining mice for intravenous injection so soon after recovery from surgery led to distress and greater mortality, beyond that stated in the project licence. Therefore subcutaneous administration was subsequently used. Future work should explore cannulation of a vessel to allow repeated dosing without causing excessive distress. Subcutaneous injection was a valid route to explore, but the results suggested that Link_TSG6 did not exert much beneficial effect from this type of delivery, possibly due to the presence of glycosaminoglycans in the interstitial space (Porter and Charman, 2000). On the other hand, in the MSC experiments it was purely paracrine actions which were being explored, so subcutaneous delivery was a good starting point for these studies, as migration of cells was not necessarily desired. Furthermore, these experiments were investigating the effects of 3D MSC spheroids, which are too large to administer intravenously. However, future work could explore the effect of MSCs cultured in 3D spheroids and dissociated immediately prior to injection. Overall, the work in this thesis has suggested that intraperitoneal or intravenous delivery of TSG-6 might exert more therapeutic benefit than subcutaneous administration. A distinct weakness of the work in this thesis stems from the lack of available reagents for measuring plasma concentrations of TSG-6. It would be extremely useful to be able to measure the amount of the protein in the blood, in order to get an idea of bioavailability. However, the fact that Link_TSG6 always exerted some effect on neutrophil migration confirms that it was active to some degree *in vivo*. One other route to consider is administration directly into the brain: central administration of MSCs has shown benefit in pre-clinical models of stroke (Chen et al., 2001a; Moisan et al., 2012). However equally, other studies have shown benefits of MSCs without migration or engraftment. Intracranial administration however could be useful for initial “proof of concept” experiments. Overall, intravenous administration is likely to be the best compromise between allowing accessibility and an acceptable

bioavailability of the drug, and future work investigating TSG-6 or MSCs in stroke should explore this option.

7.4 TSG-6 AS A THERAPY FOR STROKE

The work in this thesis has provided mixed results with regard to how suitable TSG-6 is as a therapy for stroke, and further work needs to be done to clarify whether TSG-6 can provide therapeutic benefit. It would be useful to expand on the systemic IL-1 work, and focus on co-morbid disease models to fully test TSG-6 in a system in which there is a raised inflammatory profile, like seen in most stroke patients. One problem with investigations into TSG-6 is that the mechanism of action is unclear. Known actions in other models include inhibition of neutrophil migration (the focus of this work), suppression of TNF-α production by macrophages and ECM remodelling – all of which might be beneficial in stroke (Choi et al., 2011; Getting et al., 2002; Szántó et al., 2004). It is possible that TSG-6 might have brain-specific actions – perhaps having a suppressive action on microglia similar to its effect on peripheral macrophages. However, the *in vitro* experiments conducted in chapter 3 did not suggest any modulatory effect on glia or neurones. The results from the IL-1 experiment suggest that Link_TSG6 exerted a protective effect on the BBB, probably due to its inhibitory effects on plasmin and its promotion of stability in the ECM. This in turn might have a knock-on inhibitory effect on neutrophil migration. The diverse immunomodulatory actions of TSG-6 mean that it remains an attractive therapeutic possibility for stroke, however experiments need to be optimised to fully investigate its potential. The inflammatory phase of stroke is a strong candidate for protective drugs to target, due to its proven harmful effects and its time of onset and longevity meaning that intervention is likely to be possible in a realistic time-frame. Indeed, in traumatic brain injury TSG-6 led to protection in a range of histological and behavioural outcomes, even when administered 6h after the insult (Watanabe et al., 2013). Another useful investigation would be to assess the outcome of wild-type and TSG-6 knockout mice after MCAo, with the hypothesis that mice lacking TSG-6 would show poorer recovery. TSG-6 has shown potential in such a wide range of peripheral inflammatory diseases as well as in traumatic brain injury that one would expect at least some benefit in stroke.

The expression data in chapter 4 also points to a role for TSG-6 in stroke. The association with the glial scar suggested a role in the reparative phase of stroke, but it is possible that delivering exogenous TSG-6 before it is expressed endogenously could "kick-start" the reparative phase and help to reduce damaging inflammation. It would be useful to block this expression of TSG-6 to try and elucidate the role of expression within the scar. Potential roles could include ECM remodelling, promotion of angiogenesis, inhibition of neutrophil migration and dampening of pro-inflammatory cytokines. Blocking TSG-6 expression and assessing these outcomes would help to deduce the role that TSG-6 plays in ischaemic stroke.

However, one important consideration when investigating TSG-6 as a stroke therapy is its dampening effect on plasmin. The only drug currently available for the treatment of ischaemic stroke is tPA, which works by generating plasmin (a serine protease) from its precursor, plasminogen, resulting in the degradation of fibrin clots (Vivien et al., 2011). Any potential new therapies need to be able to work in combination with tPA, as this treatment cannot be withheld from eligible stroke patients. However the majority of patients are not eligible to receive tPA, so it is possible that trials could be conducted in its absence. TSG-6 dampens the protease activity of plasmin through interactions with IαI and heparin – so it's possible that co-administration of the two drugs could inhibit the activity of tPA. It might be possible to selectively inhibit this mechanism of TSG-6, however it is likely that this property is behind the observed protective effects on the BBB. Future work should carefully consider any interactions between the two drugs, to decipher whether or not TSG-6 is a suitable candidate for stroke therapy when tPA is given.

7.5 MSCs AS A THERAPY FOR STROKE

MSCs have been the subject of vast amounts of research in recent years, and numerous groups have shown their therapeutic potential for ischaemic stroke (Chen et al., 2001a; Chen et al., 2001b; Honma et al., 2006; Li et al., 2002; Moisan et al., 2012). More and more research has emerged suggesting that MSCs don't need to engraft or even migrate to the site of injury to be beneficial, and that it's largely via paracrine actions that they exert their therapeutic effects (Cheng et al., 2013; Ionescu et al., 2012; Lee et al., 2011; Pierro et al., 2013; Waszak et al., 2012). One of the key

paracrine mediators of the MSC secretome has been revealed as TSG-6, and so MSCs are currently under investigation in a wide range of conditions as a potential immunomodulatory therapy. In this thesis it was shown that MSCs cultured in 3D spheroids produce more TSG-6 than cells cultured in a 2D monolayer (previously shown by (Bartosh et al., 2010)), and that TSG-6 expression can be increased further by stimulation with IL-1. This highlights the potential to modulate the secretome of MSCs, either by manipulation of culture conditions, or by harnessing the inflammatory stimuli likely to be circulating after stroke. Further work would need to assess whether circulating inflammatory stimuli are sufficient to up-regulate expression of TSG-6, or whether MSCs need to be primed in culture before administration. In this work, human MSCs were used without any immunosuppressive agents. Although there are examples in the literature of "immunoprivileged" human MSCs being used successfully in immunocompetent mice and rats (Moisan et al., 2012; Rodriguez et al., 2005; Watanabe et al., 2013), the results from this work suggested a level of rejection by the murine immune system. Despite this, the vast amount of promising literature suggests that if rejection could be overcome, either by immunosuppressive drugs or by encapsulation of the cells, MSCs represent an extremely promising therapy for the treatment of stroke. The huge amount of failures in stroke research in recent years suggests that ischaemia is simply too complex to target with one agent. There are so many mechanisms contributing to neurotoxicity simultaneously that a multi-target therapy is likely to have greater efficacy at treating stroke. MSCs are essentially factories of secreted factors that can be manipulated to alter their output, meaning that chemokines, cytokines, growth factors, angiogenic factors, neurotrophic factors, ECM molecules and many more can all be produced. MSCs have the potential to target inflammation (the main role studied here), but also have a proven pro-regenerative capacity through their secretion of growth and neurotrophic factors (Paul and Anisimov, 2013). Furthermore, to complement the paracrine actions, there is the possibility that MSCs could be manipulated to be able to differentiate into functioning neurones, although this has not yet been fully achieved (Liu et al., 2012b). The vast number of successful pre-clinical trials testing MSCs in stroke have reported a range of beneficial effects, including reduced apoptosis, induction of neurogenesis, neurite outgrowth and axonal sprouting, increased synaptogenesis, reduced microglial activation and reduced glial scar formation (reviewed in (Paul and Anisimov, 2013)).

Figure 7.1 depicts the varied properties of MSCs that could be beneficial in the treatment of stroke.

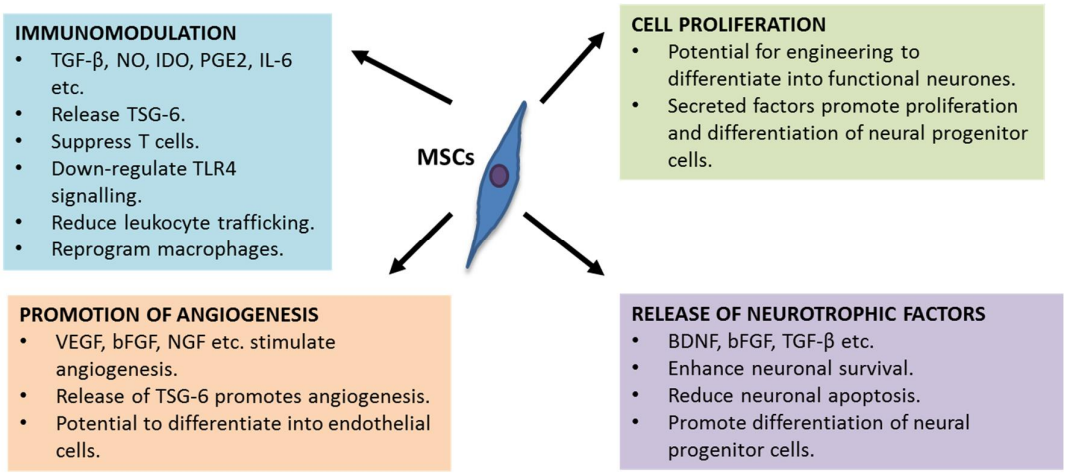

Figure 7.1: Potential mechanisms of MSC benefit in the treatment of ischaemic stroke. MSCs have a varied secretome which could exert a range of effects beneficial to the treatment of stroke. Secreted factors can dampen inflammation, promote angiogenesis and encourage proliferation of neural progenitor cells.

Although in this thesis subcutaneous transplantation was used to assess the paracrine actions of MSCs, intravenous administration could be investigated to try and achieve a greater bioavailability of secreted factors, including TSG-6. Equally, central administration could be tested to reduce the impact of neuroinflammation, or the two routes could be used in tandem to suppress central and peripheral inflammation together. The paracrine potential of MSCs has been highlighted by the therapeutic efficacy of conditioned media, so this is a further avenue that could be explored.

In conclusion, the vast array of neurotrophic and immunosuppressive properties of MSCs make them an extremely attractive therapeutic option for the treatment of stroke. A multi-targeted approach is likely to be more beneficial than focusing on a single mechanism, especially in a disease as complex and multifactorial as stroke. The 3D spheroid culture system appears to have benefits over the traditional monolayer culture system, and optimisation of the secretome and of delivery in mice could reveal real therapeutic potential for the treatment of ischaemia.

7.6 LIMITATIONS AND CLINICAL RELEVANCE

The MCAo model, and *in vivo* systems in general, allow investigations to be carried out in the context of a whole organism, taking into account interactions between different organs, tissues and systems. No disease model is perfect, however MCAo is widely accepted as a relatively good model of ischaemic stroke. Occluding the MCA results in a loss of oxygen and glucose supply to an area of the brain, much like what happens during human stroke. Withdrawing the filament allows reperfusion, which happens clinically either spontaneously or after infusion of tPA. However, this model doesn't involve an actual blood clot, and the need for surgery and anaesthesia will impact on the outcomes after occlusion. Due to the failure of the stroke research community to translate pre-clinical findings into successful therapeutic candidates, the Stroke Therapy Academic Industry Roundtable (STAIR) outlined criteria to try and improve pre-clinical studies to increase the chance of successful drug candidates being put forward (Fisher et al., 2009). One of the main mismatches between experimental stroke research and the type of patient seen in the clinic is the presence of co-morbidities. Stroke patients are typically elderly, and tend to have an array of co-morbid conditions such as hypertension, atherosclerosis, diabetes and obesity. In contrast, pre-clinical studies are normally carried out in a homogenous population of young, healthy, predominantly male rodents. This thesis has been concerned with the impact that peripheral inflammation has on stroke outcome. The experiments in chapter 3 used IL-1 as a model of a raised inflammatory profile, however all other studies used naïve healthy mice. It would be beneficial to conduct future experiments using co-morbid animals, particularly as TSG-6 was used with the aim of limiting the impact of peripheral inflammation.

A further consideration relating to clinical relevance is the time of drug delivery. In these experiments drugs were delivered either before stroke onset, or within 30min of reperfusion. One of the main issues with tPA is that it can only be given safely within 4.5h of a stroke occurring, meaning that only a small proportion (~10-20%) of patients are eligible to receive it. Therefore new drugs need to have a large therapeutic window, and be effective even with delayed administration. However, early administration is acceptable for early proof-of-concept studies. Had promising effects on lesion volume and behaviour been seen with early delivery of TSG-6 or MSCs,

further experiments could have explored the effect of delayed administration. However these initial experiments need to be optimised before this is tested. In human stroke, the lesion evolves over time, however the evolution is probably faster in rodent brains, meaning that delayed administration might be less likely to show efficacy. A further concern of the STAIR criteria was assessment of long-term outcomes. Early work in this thesis only looked at acute 24h outcomes, whereas the later chapters observed mice over 7-14 days post-stroke. To get a true idea of functional recovery, mice need to be observed for months after MCAo, with a more sophisticated array of behavioural tests to assess all aspects of functional recovery. In stroke patients it is not only the size of the lesion that is important, rather whether or not they can function without a carer.

Overall the experiments in this thesis were well-designed as initial pilot investigations, but are insufficient for full clarification of the effects of TSG-6 or MSCs in stroke. Further inclusion of inflammatory co-morbidities, optimisation of routes of administration, reduction of variability and longer-term assessments of functional outcomes would all be beneficial in future investigations into these potential therapies.

7.7 Future Work

7.7.1 Clarification of the effect of TSG-6 in experimental stroke

Intravenous TSG-6 should be tested in animals with inflammatory co-morbidities such as atherosclerosis, hypertension and obesity. Long-term functional and behavioural outcomes should be monitored, however it would be useful to investigate additional early time-points to assess the effect on neutrophil infiltration into the brain at its peak. Initial work in this thesis has suggested a potential beneficial role of TSG-6, however optimisation of delivery and outcome measurement would help to elucidate whether or not it is a viable treatment option. Optimisation of the model would also be required to reduce variability. Intravenous TSG-6 showed strong therapeutic efficacy in a model of traumatic brain injury, so it is likely that a similar effect would be observed in stroke (Watanabe et al., 2013). A study should also be conducted assessing the effect of TSG-6 and tPA in combination, to assess whether or not the anti-plasmin activity of TSG-6 impacts on the fibrinolytic action of tPA. This study would need to be conducted using a thromboembolic model of stroke, rather than MCAo.

In addition to treating mice with TSG-6, it would be useful to block endogenous TSG-6, either with knockout mice or through the use of a neutralising antibody, and see the effect on stroke outcome. Identification of TSG-6 within the glial scar suggested a protective function of the protein, so it would be interesting to observe the consequences of this expression being blocked. It would be useful to assess any differences in behaviour and functional recovery, lesion volume, BBB disruption, central and peripheral inflammation, angiogenesis and the formation of the glial scar. Any differences between groups would help to strengthen the case that TSG-6 might be a useful therapy for the treatment of ischaemic stroke.

7.7.2 Investigation into the MSC secretome

Vast amounts of research point to the therapeutic potential of the MSC secretome. The full composition of the secretome is still unknown, and it would be beneficial to screen the output of MSCs. Microarray profiling could be a good option for this. Once the basal expression profile is known, culture conditions could be manipulated to alter the expression of certain factors, in order to create a secretome optimal for targeting conditions in stroke. Many groups have already shown the benefit of MSCs manipulated to up-regulate expression of certain growth factors in stroke (Liu et al., 2006; Onda et al., 2008; Tao et al., 2012; Toyama et al., 2009). In this thesis it was shown that although treatment of MSCs with IL-1 resulted in increased expression of TSG-6, it also up-regulated IL-6 and IL-8 which might be detrimental to stroke pathogenesis. siRNA or specific inhibitors could be used to fine-tune the output of MSCs and create a "designer" secretome. Manipulated MSCs should be tested in co-morbid animals in long-term experiments with a range of behavioural and histological outcomes.

7.7.3 Further investigations into the effect of MSCs in stroke

Pilot work conducted in this thesis suggested that human MSCs were rejected by the murine immune system leading to a systemic inflammatory response. One option to get around this, without using immunosuppressive drugs (which might affect stroke outcome), is to encapsulate the MSC transplants (Knippenberg et al., 2012). It would be useful to further investigate the potential of subcutaneous spheroid transplants as paracrine therapeutic mediators – experiments should investigate the long-term effects of encapsulated MSCs in co-morbid animals after stroke, investigating behavioural, immunological and histological outcomes. Results should be compared to mice receiving the encapsulation material alone. Additional work could explore the impact of delayed administration, and could compare the effect of MSCs compared to TSG-6 protein. Subcutaneous transplants could also be compared to MSCs delivered intravenously, to identify any differential effects on stroke outcome. MSCs for intravenous delivery would need to be grown in 3D spheroids before dissociation, however encapsulation would not be viable for this route of administration. In this case, immunosuppressive drugs would need to be utilised, however this is not ideal for investigations into systemic inflammation.

A further consideration for future MSC experiments would be to label cells so that they can be identified post-mortem. Although paracrine actions were the main interest in this work, it would still be useful to track any migration and excretion of MSCs, to learn about their stability and longevity. Published work has shown that subcutaneously-administered MSCs do not migrate from the site of injection, so it would be useful to clarify whether or not this is the case in stroke, and if the paracrine activity of MSCs is optimal from the subcutaneous space (López-Iglesias et al., 2011).

7.8 CONCLUSIONS

In conclusion, the work in this thesis has suggested that modulation of the peripheral immune response remains a viable target for the treatment of ischaemic stroke. The most promising data came from testing Link_TSG6 in an IL-1-induced model of systemic inflammation – arguably the most translationally relevant experiment performed in this thesis. Link_TSG6 appeared to have positive effects on neutrophil migration, BBB disruption and haemorrhagic transformation. This work also raised the possibility that neutrophils can exert some of their detrimental effects without crossing from the blood into the brain parenchyma. Trends observed in the post-acute experiment also suggested a protective action of TSG-6, and optimisation of experimental conditions should help to further elucidate any therapeutic potential that this protein holds.

Investigations into the expression profile of TSG-6 revealed an association with astrocytes in the glial scar, peaking at 5 days after stroke. This suggests that TSG-6 plays a role in the reparative phase of stroke, and that it might be involved in matrix remodelling and in the control of angiogenesis. Intervention experiments would be key in further clarifying the purpose of TSG-6 expression in the brain.

MSCs are a highly attractive therapeutic option for the treatment of stroke, due to their many properties encompassing immunomodulation and promotion of neuro- and angiogenesis. This thesis concluded that culturing MSCs in 3D spheroids can alter their immunomodulatory properties and enhance their expression of TSG-6, however no firm conclusions could be drawn from *in vivo* experiments due to rejection of the human MSCs by the murine immune system. Despite this, the growing evidence in the literature suggests that MSCs remain a potential revolutionary therapy for the modulation of the peripheral immune response and the treatment of ischaemic stroke.

In conclusion, TSG-6, either as a single protein or as part of the MSC secretome, might still be a viable candidate for the treatment of ischaemic stroke. Inhibition of neutrophils might not be sufficient for protection in stroke, however a broader immunomodulatory action is likely to exert some therapeutic benefit. MSCs, through their secretion of TSG-6 and other immunomodulatory factors, are likely to be a good candidate for the treatment of ischaemic stroke.

REFERENCES

Abbott, N.J. (2002). Astrocyte-endothelial interactions and blood-brain barrier permeability. J Anat *200*, 629-638.

Abbott, N.J., Patabendige, A.A., Dolman, D.E., Yusof, S.R., and Begley, D.J. (2010). Structure and function of the blood-brain barrier. Neurobiol Dis *37*, 13-25.

Abumiya, T., Fitridge, R., Mazur, C., Copeland, B.R., Koziol, J.A., Tschopp, J.F., Pierschbacher, M.D., and del Zoppo, G.J. (2000). Integrin alpha(IIb)beta(3) inhibitor preserves microvascular patency in experimental acute focal cerebral ischemia. Stroke *31*, 1402-1409; discussion 1409-1410.

Afan, A.M., Broome, C.S., Nicholls, S.E., Whetton, A.D., and Miyan, J.A. (1997). Bone marrow innervation regulates cellular retention in the murine haemopoietic system. Br J Haematol *98*, 569-577.

Akopov, S.E., Simonian, N.A., and Grigorian, G.S. (1996). Dynamics of polymorphonuclear leukocyte accumulation in acute cerebral infarction and their correlation with brain tissue damage. Stroke *27*, 1739-1743.

Al'Qteishat, A., Gaffney, J., Krupinski, J., Rubio, F., West, D., Kumar, S., Kumar, P., Mitsios, N., and Slevin, M. (2006). Changes in hyaluronan production and metabolism following ischaemic stroke in man. Brain *129*, 2158-2176.

Allan, S., Tyrrell, P., and Rothwell, N. (2005). Interleukin-1 and neuronal injury. Nat Rev Immunol *5*, 629-640.

Allen, C., and Bayraktutan, U. (2009). Oxidative stress and its role in the pathogenesis of ischaemic stroke. Int J Stroke *4*, 461-470.

Allen, C., Thornton, P., Denes, A., McColl, B.W., Pierozynski, A., Monestier, M., Pinteaux, E., Rothwell, N.J., and Allan, S.M. (2012). Neutrophil cerebrovascular transmigration triggers rapid neurotoxicity through release of proteases associated with decondensed DNA. J Immunol *189*, 381-392.

An, J.H., Park, H., Song, J.A., Ki, K.H., Yang, J.Y., Choi, H.J., Cho, S.W., Kim, S.W., Kim, S.Y., Yoo, J.J., *et al.* (2013). Transplantation of human umbilical cord blood-derived mesenchymal stem cells or their conditioned medium prevents bone loss in ovariectomized nude mice. Tissue Eng Part A *19*, 685-696.

Arakelyan, A., Petrkova, J., Hermanova, Z., Boyajyan, A., Lukl, J., and Petrek, M. (2005). Serum levels of the MCP-1 chemokine in patients with ischemic stroke and myocardial infarction. Mediators Inflamm *2005*, 175-179.

Astrup, J., Siesjö, B., and Symon, L. (1981). Thresholds in cerebral ischemia - the ischemic penumbra. Stroke *12*, 723-725.

Balami, J.S., Chen, R.L., Grunwald, I.Q., and Buchan, A.M. (2011). Neurological complications of acute ischaemic stroke. Lancet Neurol *10*, 357-371.

Ball, S., Worthington, J., Canfield, A., Merry, C., and Kielty, C. (2013). **Fibronectin depletion** and PDGF receptor inhibition induce MSC shape change and multipotency in 3D spheroid culture. . Stem Cells *In press*.

Ball, S.G., Shuttleworth, A., and Kielty, C.M. (2012). Inhibition of platelet-derived growth factor receptor signaling regulates Oct4 and Nanog expression, cell shape, and mesenchymal stem cell potency. Stem Cells *30*, 548-560.

Barbarroja, N., López-Pedrera, R., Mayas, M.D., García-Fuentes, E., Garrido-Sánchez, L., Macías-González, M., El Bekay, R., Vidal-Puig, A., and Tinahones, F.J. (2010). The obese healthy paradox: is inflammation the answer? Biochem J *430*, 141-149.
Bartosh, T.J., Ylöstalo, J.H., Mohammadipoor, A., Bazhanov, N., Coble, K., Claypool, K., Lee, R.H., Choi, H., and Prockop, D.J. (2010). Aggregation of human mesenchymal stromal cells (MSCs) into 3D spheroids enhances their antiinflammatory properties. Proc Natl Acad Sci U S A *107*, 13724-13729.
Baumann, H., and Gauldie, J. (1994). The acute phase response. Immunol Today *15*, 74-80.
Bederson, J.B., Pitts, L.H., Tsuji, M., Nishimura, M.C., Davis, R.L., and Bartkowski, H. (1986). Rat middle cerebral artery occlusion: evaluation of the model and development of a neurologic examination. Stroke *17*, 472-476.
Beray-Berthat, V., Croci, N., Plotkine, M., and Margaill, I. (2003). Polymorphonuclear neutrophils contribute to infarction and oxidative stress in the cortex but not in the striatum after ischemia-reperfusion in rats. Brain Res *987*, 32-38.
Bicknese, A.R., Sheppard, A.M., O'Leary, D.D., and Pearlman, A.L. (1994). Thalamocortical axons extend along a chondroitin sulfate proteoglycan-enriched pathway coincident with the neocortical subplate and distinct from the efferent path. J Neurosci *14*, 3500-3510.
Bodhankar, S., Chen, Y., Vandenbark, A.A., Murphy, S.J., and Offner, H. (2013). IL-10-producing B-cells limit CNS inflammation and infarct volume in experimental stroke. Metab Brain Dis *28*, 375-386.
Borghetti, P., Saleri, R., Mocchegiani, E., Corradi, A., and Martelli, P. (2009). Infection, immunity and the neuroendocrine response. Vet Immunol Immunopathol *130*, 141-162.
Borlongan, C.V., Lind, J.G., Dillon-Carter, O., Yu, G., Hadman, M., Cheng, C., Carroll, J., and Hess, D.C. (2004). Bone marrow grafts restore cerebral blood flow and blood brain barrier in stroke rats. Brain Res *1010*, 108-116.
Borregaard, N. (2010). Neutrophils, from marrow to microbes. Immunity *33*, 657-670.
Bradbury, E.J., Moon, L.D., Popat, R.J., King, V.R., Bennett, G.S., Patel, P.N., Fawcett, J.W., and McMahon, S.B. (2002). Chondroitinase ABC promotes functional recovery after spinal cord injury. Nature *416*, 636-640.
Brait, V.H., Arumugam, T.V., Drummond, G.R., and Sobey, C.G. (2012). Importance of T lymphocytes in brain injury, immunodeficiency, and recovery after cerebral ischemia. J Cereb Blood Flow Metab *32*, 598-611.
Brait, V.H., Jackman, K.A., Walduck, A.K., Selemidis, S., Diep, H., Mast, A.E., Guida, E., Broughton, B.R., Drummond, G.R., and Sobey, C.G. (2010). Mechanisms contributing to cerebral infarct size after stroke: gender, reperfusion, T lymphocytes, and Nox2-derived superoxide. J Cereb Blood Flow Metab *30*, 1306-1317.
Broughton, B., Reutens, D., and Sobey, C. (2009). Apoptotic mechanisms after cerebral ischemia. Stroke *40*, e331-339.
Brouns, R., and De Deyn, P. (2009). The complexity of neurobiological processes in acute ischemic stroke. Clin Neurol Neurosurg *111*, 483-495.
Buck, B.H., Liebeskind, D.S., Saver, J.L., Bang, O.Y., Yun, S.W., Starkman, S., Ali, L.K., Kim, D., Villablanca, J.P., Salamon, N.*, et al.* (2008). Early neutrophilia is associated with volume of ischemic tissue in acute stroke. Stroke *39*, 355-360.
Bárdos, T., Kamath, R.V., Mikecz, K., and Glant, T.T. (2001). Anti-inflammatory and chondroprotective effect of TSG-6 (tumor necrosis factor-alpha-stimulated gene-6) in murine models of experimental arthritis. Am J Pathol *159*, 1711-1721.

Calbo, E., Alsina, M., Rodríguez-Carballeira, M., Lite, J., and Garau, J. (2010). The impact of time on the systemic inflammatory response in pneumococcal pneumonia. Eur Respir J *35*, 614-618.
Cao, T.V., La, M., Getting, S.J., Day, A.J., and Perretti, M. (2004). Inhibitory effects of TSG-6 Link module on leukocyte-endothelial cell interactions in vitro and in vivo. Microcirculation *11*, 615-624.
Carman, C.V., Sage, P.T., Sciuto, T.E., de la Fuente, M.A., Geha, R.S., Ochs, H.D., Dvorak, H.F., Dvorak, A.M., and Springer, T.A. (2007). Transcellular diapedesis is initiated by invasive podosomes. Immunity *26*, 784-797.
Carrette, O., Nemade, R.V., Day, A.J., Brickner, A., and Larsen, W.J. (2001). TSG-6 is concentrated in the extracellular matrix of mouse cumulus oocyte complexes through hyaluronan and inter-alpha-inhibitor binding. Biol Reprod *65*, 301-308.
Carruth, L., Demczuk, S., and Mizel, S. (1991). Involvement of a calpain-like protease in the processing of the murine interleukin 1 alpha precursor. J Biol Chem *266*, 12162-12167.
Cesari, M., Penninx, B.W., Newman, A.B., Kritchevsky, S.B., Nicklas, B.J., Sutton-Tyrrell, K., Rubin, S.M., Ding, J., Simonsick, E.M., Harris, T.B.*, et al.* (2003). Inflammatory markers and onset of cardiovascular events: results from the Health ABC study. Circulation *108*, 2317-2322.
Chamberlain, J., Yamagami, T., Colletti, E., Theise, N.D., Desai, J., Frias, A., Pixley, J., Zanjani, E.D., Porada, C.D., and Almeida-Porada, G. (2007). Efficient generation of human hepatocytes by the intrahepatic delivery of clonal human mesenchymal stem cells in fetal sheep. Hepatology *46*, 1935-1945.
Chamorro, Á., Meisel, A., Planas, A.M., Urra, X., van de Beek, D., and Veltkamp, R. (2012). The immunology of acute stroke. Nat Rev Neurol *8*, 401-410.
Chaplin, D. (2010). Overview of the immune response. J Allergy Clin Immunol *125*, S3-23.
Chapman, K., Dale, V., Dénes, A., Bennett, G., Rothwell, N., Allan, S., and McColl, B. (2009). A rapid and transient peripheral inflammatory response precedes brain inflammation after experimental stroke. J Cereb Blood Flow Metab *29*, 1764-1768.
Chen, J., Li, Y., Katakowski, M., Chen, X., Wang, L., Lu, D., Lu, M., Gautam, S.C., and Chopp, M. (2003). Intravenous bone marrow stromal cell therapy reduces apoptosis and promotes endogenous cell proliferation after stroke in female rat. J Neurosci Res *73*, 778-786.
Chen, J., Li, Y., Wang, L., Lu, M., Zhang, X., and Chopp, M. (2001a). Therapeutic benefit of intracerebral transplantation of bone marrow stromal cells after cerebral ischemia in rats. J Neurol Sci *189*, 49-57.
Chen, J., Li, Y., Wang, L., Zhang, Z., Lu, D., Lu, M., and Chopp, M. (2001b). Therapeutic benefit of intravenous administration of bone marrow stromal cells after cerebral ischemia in rats. Stroke *32*, 1005-1011.
Chen, Y., Ito, A., Takai, K., and Saito, N. (2008). Blocking pterygopalatine arterial blood flow decreases infarct volume variability in a mouse model of intraluminal suture middle cerebral artery occlusion. J Neurosci Methods *174*, 18-24.
Chen, Y., and Swanson, R. (2003). Astrocytes and brain injury. J Cereb Blood Flow Metab *23*, 137-149.
Cheng, K., Rai, P., Plagov, A., Lan, X., Kumar, D., Salhan, D., Rehman, S., Malhotra, A., Bhargava, K., Palestro, C.J.*, et al.* (2013). Transplantation of bone marrow-derived MSCs improves cisplatinum-induced renal injury through paracrine mechanisms. Exp Mol Pathol *94*, 466-473.

Chiba, T., and Umegaki, K. (2013). Pivotal roles of monocytes/macrophages in stroke. Mediators Inflamm *2013*, 759103.
Cho, Y.J., Song, H.S., Bhang, S., Lee, S., Kang, B.G., Lee, J.C., An, J., Cha, C.I., Nam, D.H., Kim, B.S*., et al.* (2012). Therapeutic effects of human adipose stem cell-conditioned medium on stroke. J Neurosci Res *90*, 1794-1802.
Choi, H., Lee, R.H., Bazhanov, N., Oh, J.Y., and Prockop, D.J. (2011). Anti-inflammatory protein TSG-6 secreted by activated MSCs attenuates zymosan-induced mouse peritonitis by decreasing TLR2/NF-{kappa}B signaling in resident macrophages. Blood *118*, 330-338.
Chopp, M., Zhang, R.L., Chen, H., Li, Y., Jiang, N., and Rusche, J.R. (1994). Postischemic administration of an anti-Mac-1 antibody reduces ischemic cell damage after transient middle cerebral artery occlusion in rats. Stroke *25*, 869-875; discussion 875-866.
Copin, J.C., Ledig, M., and Tholey, G. (1992). Free radical scavenging systems of rat astroglial cells in primary culture: effects of anoxia and drug treatment. Neurochem Res *17*, 677-682.
Cray, C., Zaias, J., and Altman, N. (2009). Acute phase response in animals: a review. Comp Med *59*, 517-526.
Danchuk, S., Ylostalo, J.H., Hossain, F., Sorge, R., Ramsey, A., Bonvillain, R.W., Lasky, J.A., Bunnell, B.A., Welsh, D.A., Prockop, D.J*., et al.* (2011). Human multipotent stromal cells attenuate lipopolysaccharide-induced acute lung injury in mice via secretion of tumor necrosis factor-alpha-induced protein 6. Stem Cell Res Ther *2*, 27.
Day, A.J., Aplin, R.T., and Willis, A.C. (1996). Overexpression, purification, and refolding of link module from human TSG-6 in Escherichia coli: effect of temperature, media, and mutagenesis on lysine misincorporation at arginine AGA codons. Protein Expr Purif *8*, 1-16.
del Zoppo, G.J. (2008). Virchow's triad: the vascular basis of cerebral injury. Rev Neurol Dis *5 Suppl 1*, S12-21.
del Zoppo, G.J., Frankowski, H., Gu, Y.H., Osada, T., Kanazawa, M., Milner, R., Wang, X., Hosomi, N., Mabuchi, T., and Koziol, J.A. (2012). Microglial cell activation is a source of metalloproteinase generation during hemorrhagic transformation. J Cereb Blood Flow Metab *32*, 919-932.
del Zoppo, G.J., Schmid-Schönbein, G.W., Mori, E., Copeland, B.R., and Chang, C.M. (1991). Polymorphonuclear leukocytes occlude capillaries following middle cerebral artery occlusion and reperfusion in baboons. Stroke *22*, 1276-1283.
Denes, A., McColl, B.W., Leow-Dyke, S.F., Chapman, K.Z., Humphreys, N.E., Grencis, R.K., Allan, S.M., and Rothwell, N.J. (2010). Experimental stroke-induced changes in the bone marrow reveal complex regulation of leukocyte responses. J Cereb Blood Flow Metab *31*, 1036-50.
Denes, A., Pinteaux, E., Rothwell, N.J., and Allan, S.M. (2011). Interleukin-1 and stroke: biomarker, harbinger of damage, and therapeutic target. Cerebrovasc Dis *32*, 517-527.
Denes, A., Vidyasagar, R., Feng, J., Narvainen, J., McColl, B.W., Kauppinen, R.A., and Allan, S.M. (2007). Proliferating resident microglia after focal cerebral ischaemia in mice. J Cereb Blood Flow Metab *27*, 1941-1953.
Denes, A., Wilkinson, F., Bigger, B., Chu, M., Rothwell, N.J., and Allan, S.M. (2013). Central and haematopoietic interleukin-1 both contribute to ischaemic brain injury in mice. Dis Model Mech *6*, 1043-1048.
Dénes, A., Boldogkoi, Z., Uhereczky, G., Hornyák, A., Rusvai, M., Palkovits, M., and Kovács, K.J. (2005). Central autonomic control of the bone marrow: multisynaptic tract tracing by recombinant pseudorabies virus. Neuroscience *134*, 947-963.

Dénes, A., Ferenczi, S., and Kovács, K.J. (2011). Systemic inflammatory challenges compromise survival after experimental stroke via augmenting brain inflammation, blood- brain barrier damage and brain oedema independently of infarct size. J Neuroinflammation *8*, 164.
Derouesné, C., Cambon, H., Yelnik, A., Duyckaerts, C., and Hauw, J.J. (1993). Infarcts in the middle cerebral artery territory. Pathological study of the mechanisms of death. Acta Neurol Scand *87*, 361-366.
Detante, O., Moisan, A., Dimastromatteo, J., Richard, M.J., Riou, L., Grillon, E., Barbier, E., Desruet, M.D., De Fraipont, F., Segebarth, C.*, et al.* (2009). Intravenous administration of 99mTc-HMPAO-labeled human mesenchymal stem cells after stroke: in vivo imaging and biodistribution. Cell Transplant *18*, 1369-1379.
Dhungana, H., Malm, T., Denes, A., Valonen, P., Wojciechowski, S., Magga, J., Savchenko, E., Humphreys, N., Grencis, R., Rothwell, N.*, et al.* (2013). Aging aggravates ischemic stroke-induced brain damage in mice with chronic peripheral infection. Aging Cell *12*, 842-50.
Dominici, M., Le Blanc, K., Mueller, I., Slaper-Cortenbach, I., Marini, F., Krause, D., Deans, R., Keating, A., Prockop, D., and Horwitz, E. (2006). Minimal criteria for defining multipotent mesenchymal stromal cells. The International Society for Cellular Therapy position statement. Cytotherapy *8*, 315-317.
Du, Z., Wei, C., Cheng, K., Han, B., Yan, J., Zhang, M., Peng, C., and Liu, Y. (2013). Mesenchymal stem cell-conditioned medium reduces liver injury and enhances regeneration in reduced-size rat liver transplantation. J Surg Res *183*, 907-915.
Eash, K.J., Greenbaum, A.M., Gopalan, P.K., and Link, D.C. (2010). CXCR2 and CXCR4 antagonistically regulate neutrophil trafficking from murine bone marrow. J Clin Invest *120*, 2423-2431.
Easton, A.S. (2013). Neutrophils and stroke - Can neutrophils mitigate disease in the central nervous system? Int Immunopharmacol *13*, 256-7.
Eckert, M.A., Vu, Q., Xie, K., Yu, J., Liao, W., Cramer, S.C., and Zhao, W. (2013). Evidence for high translational potential of mesenchymal stromal cell therapy to improve recovery from ischemic stroke. J Cereb Blood Flow Metab *33*, 1322-34.
Emsley, H.C., and Hopkins, S.J. (2008). Acute ischaemic stroke and infection: recent and emerging concepts. Lancet Neurol *7*, 341-353.
Emsley, H.C., Smith, C.J., Gavin, C.M., Georgiou, R.F., Vail, A., Barberan, E.M., Hallenbeck, J.M., del Zoppo, G.J., Rothwell, N.J., Tyrrell, P.J.*, et al.* (2003). An early and sustained peripheral inflammatory response in acute ischaemic stroke: relationships with infection and atherosclerosis. J Neuroimmunol *139*, 93-101.
Emsley, H.C., Smith, C.J., Georgiou, R.F., Vail, A., Hopkins, S.J., Rothwell, N.J., Tyrrell, P.J., and Investigators, A.S. (2005). A randomised phase II study of interleukin-1 receptor antagonist in acute stroke patients. J Neurol Neurosurg Psychiatry *76*, 1366-1372.
English, K. (2013). Mechanisms of mesenchymal stromal cell immunomodulation. Immunol Cell Biol *91*, 19-26.
English, K., Barry, F.P., Field-Corbett, C.P., and Mahon, B.P. (2007). IFN-gamma and TNF-alpha differentially regulate immunomodulation by murine mesenchymal stem cells. Immunol Lett *110*, 91-100.
English, K., Barry, F.P., and Mahon, B.P. (2008). Murine mesenchymal stem cells suppress dendritic cell migration, maturation and antigen presentation. Immunol Lett *115*, 50-58.

Fawcett, J.W., and Asher, R.A. (1999). The glial scar and central nervous system repair. Brain Res Bull *49*, 377-391.
Fessler, M.B., Malcolm, K.C., Duncan, M.W., and Worthen, G.S. (2002). Lipopolysaccharide stimulation of the human neutrophil: an analysis of changes in gene transcription and protein expression by oligonucleotide microarrays and proteomics. Chest *121*, 75S-76S.
Finlayson, O., Kapral, M., Hall, R., Asllani, E., Selchen, D., Saposnik, G., Network, C.S., and Group, S.O.R.C.S.W. (2011). Risk factors, inpatient care, and outcomes of pneumonia after ischemic stroke. Neurology *77*, 1338-1345.
Fisher, M., Feuerstein, G., Howells, D.W., Hurn, P.D., Kent, T.A., Savitz, S.I., Lo, E.H., and Group, S. (2009). Update of the stroke therapy academic industry roundtable preclinical recommendations. Stroke *40*, 2244-2250.
Fisher-Shoval, Y., Barhum, Y., Sadan, O., Yust-Katz, S., Ben-Zur, T., Lev, N., Benkler, C., Hod, M., Melamed, E., and Offen, D. (2012). Transplantation of placenta-derived mesenchymal stem cells in the EAE mouse model of MS. J Mol Neurosci *48*, 176-184.
François, M., Romieu-Mourez, R., Li, M., and Galipeau, J. (2012). Human MSC suppression correlates with cytokine induction of indoleamine 2,3-dioxygenase and bystander M2 macrophage differentiation. Mol Ther *20*, 187-195.
Frostegård, J., Ulfgren, A.K., Nyberg, P., Hedin, U., Swedenborg, J., Andersson, U., and Hansson, G.K. (1999). Cytokine expression in advanced human atherosclerotic plaques: dominance of pro-inflammatory (Th1) and macrophage-stimulating cytokines. Atherosclerosis *145*, 33-43.
Furze, R., and Rankin, S. (2008). Neutrophil mobilization and clearance in the bone marrow. Immunology *125*, 281-288.
Fülöp, C., Kamath, R.V., Li, Y., Otto, J.M., Salustri, A., Olsen, B.R., Glant, T.T., and Hascall, V.C. (1997). Coding sequence, exon-intron structure and chromosomal localization of murine TNF-stimulated gene 6 that is specifically expressed by expanding cumulus cell-oocyte complexes. Gene *202*, 95-102.
Fülöp, C., Szántó, S., Mukhopadhyay, D., Bárdos, T., Kamath, R.V., Rugg, M.S., Day, A.J., Salustri, A., Hascall, V.C., Glant, T.T*., et al.* (2003). Impaired cumulus mucification and female sterility in tumor necrosis factor-induced protein-6 deficient mice. Development *130*, 2253-2261.
Galea, J., Armstrong, J., Gadsdon, P., Holden, H., Francis, S.E., and Holt, C.M. (1996). Interleukin-1 beta in coronary arteries of patients with ischemic heart disease. Arterioscler Thromb Vasc Biol *16*, 1000-1006.
Ge, W., Jiang, J., Arp, J., Liu, W., Garcia, B., and Wang, H. (2010). Regulatory T-cell generation and kidney allograft tolerance induced by mesenchymal stem cells associated with indoleamine 2,3-dioxygenase expression. Transplantation *90*, 1312-1320.
Getting, S.J., Mahoney, D.J., Cao, T., Rugg, M.S., Fries, E., Milner, C.M., Perretti, M., and Day, A.J. (2002). The link module from human TSG-6 inhibits neutrophil migration in a hyaluronan- and inter-alpha -inhibitor-independent manner. J Biol Chem *277*, 51068-51076.
Gill, R., Kemp, J.A., Sabin, C., and Pepys, M.B. (2004). Human C-reactive protein increases cerebral infarct size after middle cerebral artery occlusion in adult rats. J Cereb Blood Flow Metab *24*, 1214-1218.
Giunti, D., Parodi, B., Usai, C., Vergani, L., Casazza, S., Bruzzone, S., Mancardi, G., and Uccelli, A. (2012). Mesenchymal stem cells shape microglia effector functions through the release of CX3CL1. Stem Cells *30*, 2044-2053.

Glant, T.T., Kamath, R.V., Bárdos, T., Gál, I., Szántó, S., Murad, Y.M., Sandy, J.D., Mort, J.S., Roughley, P.J., and Mikecz, K. (2002). Cartilage-specific constitutive expression of TSG-6 protein (product of tumor necrosis factor alpha-stimulated gene 6) provides a chondroprotective, but not antiinflammatory, effect in antigen-induced arthritis. Arthritis Rheum *46*, 2207-2218.
Grieve, A.P., and Krams, M. (2005). ASTIN: a Bayesian adaptive dose-response trial in acute stroke. Clin Trials *2*, 340-351; discussion 352-348, 364-378.
Griffin, M.D., Elliman, S.J., Cahill, E., English, K., Ceredig, R., and Ritter, T. (2013). Adult Mesenchymal Stromal Cell Therapy for Inflammatory Diseases: How Well are We Joining the Dots? Stem Cells *31,* 2033-41.
Grossman, A.W., and Broderick, J.P. (2013). Advances and challenges in treatment and prevention of ischemic stroke. Ann Neurol *74*, 363-72.
Gry, M., Rimini, R., Strömberg, S., Asplund, A., Pontén, F., Uhlén, M., and Nilsson, P. (2009). Correlations between RNA and protein expression profiles in 23 human cell lines. BMC Genomics *10*, 365.
Gubern, C., Hurtado, O., Rodríguez, R., Morales, J.R., Romera, V.G., Moro, M.A., Lizasoain, I., Serena, J., and Mallolas, J. (2009). Validation of housekeeping genes for quantitative real-time PCR in in-vivo and in-vitro models of cerebral ischaemia. BMC Mol Biol *10*, 57.
Guo, Y., Xiao, P., Lei, S., Deng, F., Xiao, G.G., Liu, Y., Chen, X., Li, L., Wu, S., Chen, Y.*, et al.* (2008). How is mRNA expression predictive for protein expression? A correlation study on human circulating monocytes. Acta Biochim Biophys Sin (Shanghai) *40*, 426-436.
Gutiérrez-Fernández, M., Rodríguez-Frutos, B., Ramos-Cejudo, J., Teresa Vallejo-Cremades, M., Fuentes, B., Cerdán, S., and Díez-Tejedor, E. (2013). Effects of intravenous administration of allogenic bone marrow- and adipose tissue-derived mesenchymal stem cells on functional recovery and brain repair markers in experimental ischemic stroke. Stem Cell Res Ther *4*, 11.
Hacke, W., Kaste, M., Bluhmki, E., Brozman, M., Dávalos, A., Guidetti, D., Larrue, V., Lees, K.R., Medeghri, Z., Machnig, T.*, et al.* (2008). Thrombolysis with alteplase 3 to 4.5 hours after acute ischemic stroke. N Engl J Med *359*, 1317-1329.
Hanisch, U.K. (2002). Microglia as a source and target of cytokines. Glia *40*, 140-155.
Hanisch, U.K., and Kettenmann, H. (2007). Microglia: active sensor and versatile effector cells in the normal and pathologic brain. Nat Neurosci *10*, 1387-1394.
Hankey, G.J. (2006). Potential new risk factors for ischemic stroke: what is their potential? Stroke *37*, 2181-2188.
Hayward, N.J., Elliott, P.J., Sawyer, S.D., Bronson, R.T., and Bartus, R.T. (1996). Lack of evidence for neutrophil participation during infarct formation following focal cerebral ischemia in the rat. Exp Neurol *139*, 188-202.
Hofstetter, C.P., Schwarz, E.J., Hess, D., Widenfalk, J., El Manira, A., Prockop, D.J., and Olson, L. (2002). Marrow stromal cells form guiding strands in the injured spinal cord and promote recovery. Proc Natl Acad Sci U S A *99*, 2199-2204.
Hol, J., Wilhelmsen, L., and Haraldsen, G. (2010). The murine IL-8 homologues KC, MIP-2, and LIX are found in endothelial cytoplasmic granules but not in Weibel-Palade bodies. J Leukoc Biol *87*, 501-508.
Honma, T., Honmou, O., Iihoshi, S., Harada, K., Houkin, K., Hamada, H., and Kocsis, J.D. (2006). Intravenous infusion of immortalized human mesenchymal stem cells protects against injury in a cerebral ischemia model in adult rat. Exp Neurol *199*, 56-66.

Horie, N., Pereira, M.P., Niizuma, K., Sun, G., Keren-Gill, H., Encarnacion, A., Shamloo, M., Hamilton, S.A., Jiang, K., Huhn, S*., et al.* (2011). Transplanted stem cell-secreted vascular endothelial growth factor effects poststroke recovery, inflammation, and vascular repair. Stem Cells *29*, 274-285.
Howells, D., Porritt, M., Rewell, S., O'Collins, V., Sena, E., van der Worp, H., Traystman, R., and Macleod, M. (2010). Different strokes for different folks: the rich diversity of animal models of focal cerebral ischemia. J Cereb Blood Flow Metab *30*, 1412-1431.
Hu, Q., Ma, Q., Zhan, Y., He, Z., Tang, J., Zhou, C., and Zhang, J. (2011). Isoflurane enhanced hemorrhagic transformation by impairing antioxidant enzymes in hyperglycemic rats with middle cerebral artery occlusion. Stroke *42*, 1750-1756.
Hunter, A.J., Hatcher, J., Virley, D., Nelson, P., Irving, E., Hadingham, S.J., and Parsons, A.A. (2000). Functional assessments in mice and rats after focal stroke. Neuropharmacology *39*, 806-816.
Hurn, P.D., Subramanian, S., Parker, S.M., Afentoulis, M.E., Kaler, L.J., Vandenbark, A.A., and Offner, H. (2007). T- and B-cell-deficient mice with experimental stroke have reduced lesion size and inflammation. J Cereb Blood Flow Metab *27*, 1798-1805.
Hynds, D.L., and Snow, D.M. (1999). Neurite outgrowth inhibition by chondroitin sulfate proteoglycan: stalling/stopping exceeds turning in human neuroblastoma growth cones. Exp Neurol *160*, 244-255.
Håberg, A., Qu, H., Saether, O., Unsgård, G., Haraldseth, O., and Sonnewald, U. (2001). Differences in neurotransmitter synthesis and intermediary metabolism between glutamatergic and GABAergic neurons during 4 hours of middle cerebral artery occlusion in the rat: the role of astrocytes in neuronal survival. J Cereb Blood Flow Metab *21*, 1451-1463.
Iadecola, C., and Anrather, J. (2011). The immunology of stroke: from mechanisms to translation. Nat Med *17*, 796-808.
Iihoshi, S., Honmou, O., Houkin, K., Hashi, K., and Kocsis, J.D. (2004). A therapeutic window for intravenous administration of autologous bone marrow after cerebral ischemia in adult rats. Brain Res *1007*, 1-9.
Ionescu, L., Byrne, R.N., van Haaften, T., Vadivel, A., Alphonse, R.S., Rey-Parra, G.J., Weissmann, G., Hall, A., Eaton, F., and Thébaud, B. (2012). Stem cell conditioned medium improves acute lung injury in mice: in vivo evidence for stem cell paracrine action. Am J Physiol Lung Cell Mol Physiol *303*, L967-977.
Ishikawa, M., Stokes, K.Y., Zhang, J.H., Nanda, A., and Granger, D.N. (2004). Cerebral microvascular responses to hypercholesterolemia: roles of NADPH oxidase and P-selectin. Circ Res *94*, 239-244.
Janzer, R.C., and Raff, M.C. (1987). Astrocytes induce blood-brain barrier properties in endothelial cells. Nature *325*, 253-257.
Jin, R., Yang, G., and Li, G. (2010). Inflammatory mechanisms in ischemic stroke: role of inflammatory cells. J Leukoc Biol *87*, 779-789.
Johansen-Berg, H. (2003). Motor physiology: a brain of two halves. Curr Biol *13*, R802-804.
Jurynec, M.J., Riley, C.P., Gupta, D.K., Nguyen, T.D., McKeon, R.J., and Buck, C.R. (2003). TIGR is upregulated in the chronic glial scar in response to central nervous system injury and inhibits neurite outgrowth. Mol Cell Neurosci *23*, 69-80.
Kahle, K., Simard, J., Staley, K., Nahed, B., Jones, P., and Sun, D. (2009). Molecular mechanisms of ischemic cerebral edema: role of electroneutral ion transport. Physiology (Bethesda) *24*, 257-265.

Kaptoge, S., Di Angelantonio, E., Lowe, G., Pepys, M.B., Thompson, S.G., Collins, R., Danesh, J., and Collaboration, E.R.F. (2010). C-reactive protein concentration and risk of coronary heart disease, stroke, and mortality: an individual participant meta-analysis. Lancet *375*, 132-140.
Kavanagh, H., and Mahon, B.P. (2011). Allogeneic mesenchymal stem cells prevent allergic airway inflammation by inducing murine regulatory T cells. Allergy *66*, 523-531.
Kennedy, A., and DeLeo, F. (2009). Neutrophil apoptosis and the resolution of infection. Immunol Res *43*, 25-61.
Kerr, R., Stirling, D., and Ludlam, C.A. (2001). Interleukin 6 and haemostasis. Br J Haematol *115*, 3-12.
Kitagawa, K., Matsumoto, M., Mabuchi, T., Yagita, Y., Ohtsuki, T., Hori, M., and Yanagihara, T. (1998). Deficiency of intercellular adhesion molecule 1 attenuates microcirculatory disturbance and infarction size in focal cerebral ischemia. J Cereb Blood Flow Metab *18*, 1336-1345.
Kleinschnitz, C., Schwab, N., Kraft, P., Hagedorn, I., Dreykluft, A., Schwarz, T., Austinat, M., Nieswandt, B., Wiendl, H., and Stoll, G. (2010). Early detrimental T-cell effects in experimental cerebral ischemia are neither related to adaptive immunity nor thrombus formation. Blood *115*, 3835-3842.
Knippenberg, S., Thau, N., Dengler, R., Brinker, T., and Petri, S. (2012). Intracerebroventricular injection of encapsulated human mesenchymal cells producing glucagon-like peptide 1 prolongs survival in a mouse model of ALS. PLoS One *7*, e36857.
Kolaczkowska, E., and Kubes, P. (2013). Neutrophil recruitment and function in health and inflammation. Nat Rev Immunol *13*, 159-175.
Korherr, C., Hofmeister, R., Wesche, H., and Falk, W. (1997). A critical role for interleukin-1 receptor accessory protein in interleukin-1 signaling. Eur J Immunol *27*, 262-267.
Kota, D.J., Wiggins, L.L., Yoon, N., and Lee, R.H. (2013). TSG-6 produced by hMSCs delays the onset of autoimmune diabetes by suppressing Th1 development and enhancing tolerogenicity. Diabetes *62*, 2048-2058.
Kumar, A.D., Boehme, A.K., Siegler, J.E., Gillette, M., Albright, K.C., and Martin-Schild, S. (2012). Leukocytosis in Patients with Neurologic Deterioration after Acute Ischemic Stroke is Associated with Poor Outcomes. J Stroke Cerebrovasc Dis *22*, 111-7.
Kupcova Skalnikova, H. (2013). Proteomic techniques for characterisation of mesenchymal stem cell secretome. Biochimie *95*, 2196-211.
Kuznetsova, S.A., Day, A.J., Mahoney, D.J., Rugg, M.S., Mosher, D.F., and Roberts, D.D. (2005). The N-terminal module of thrombospondin-1 interacts with the link domain of TSG-6 and enhances its covalent association with the heavy chains of inter-alpha-trypsin inhibitor. J Biol Chem *280*, 30899-30908.
Lau, L.T., and Yu, A.C. (2001). Astrocytes produce and release interleukin-1, interleukin-6, tumor necrosis factor alpha and interferon-gamma following traumatic and metabolic injury. J Neurotrauma *18*, 351-359.
Lazennec, G., and Richmond, A. (2010). Chemokines and chemokine receptors: new insights into cancer-related inflammation. Trends Mol Med *16*, 133-144.
Le Cabec, V., Cowland, J.B., Calafat, J., and Borregaard, N. (1996). Targeting of proteins to granule subsets is determined by timing and not by sorting: The specific granule protein NGAL is localized to azurophil granules when expressed in HL-60 cells. Proc Natl Acad Sci U S A *93*, 6454-6457.

Le, Y., Zhou, Y., Iribarren, P., and Wang, J. (2004). Chemokines and chemokine receptors: their manifold roles in homeostasis and disease. Cell Mol Immunol *1*, 95-104.
Leali, D., Inforzato, A., Ronca, R., Bianchi, R., Belleri, M., Coltrini, D., Di Salle, E., Sironi, M., Norata, G.D., Bottazzi, B.*, et al.* (2012). Long pentraxin 3/tumor necrosis factor-stimulated gene-6 interaction: a biological rheostat for fibroblast growth factor 2-mediated angiogenesis. Arterioscler Thromb Vasc Biol *32*, 696-703.
Lee, H., Park, J.W., Kim, S.P., Lo, E.H., and Lee, S.R. (2009a). Doxycycline inhibits matrix metalloproteinase-9 and laminin degradation after transient global cerebral ischemia. Neurobiol Dis *34*, 189-198.
Lee, J.W., Fang, X., Krasnodembskaya, A., Howard, J.P., and Matthay, M.A. (2011). Concise review: Mesenchymal stem cells for acute lung injury: role of paracrine soluble factors. Stem Cells *29*, 913-919.
Lee, R.H., Pulin, A.A., Seo, M.J., Kota, D.J., Ylostalo, J., Larson, B.L., Semprun-Prieto, L., Delafontaine, P., and Prockop, D.J. (2009b). Intravenous hMSCs improve myocardial infarction in mice because cells embolized in lung are activated to secrete the anti-inflammatory protein TSG-6. Cell Stem Cell *5*, 54-63.
Lee, R.T., Yamamoto, C., Feng, Y., Potter-Perigo, S., Briggs, W.H., Landschulz, K.T., Turi, T.G., Thompson, J.F., Libby, P., and Wight, T.N. (2001). Mechanical strain induces specific changes in the synthesis and organization of proteoglycans by vascular smooth muscle cells. J Biol Chem *276*, 13847-13851.
Lee, T.H., Lee, G.W., Ziff, E.B., and Vilcek, J. (1990). Isolation and characterization of eight tumor necrosis factor-induced gene sequences from human fibroblasts. Mol Cell Biol *10*, 1982-1988.
Lee, T.H., Wisniewski, H.G., and Vilcek, J. (1992). A novel secretory tumor necrosis factor-inducible protein (TSG-6) is a member of the family of hyaluronate binding proteins, closely related to the adhesion receptor CD44. J Cell Biol *116*, 545-557.
Lesley, J., Gál, I., Mahoney, D.J., Cordell, M.R., Rugg, M.S., Hyman, R., Day, A.J., and Mikecz, K. (2004). TSG-6 modulates the interaction between hyaluronan and cell surface CD44. J Biol Chem *279*, 25745-25754.
Ley, K., Laudanna, C., Cybulsky, M.I., and Nourshargh, S. (2007). Getting to the site of inflammation: the leukocyte adhesion cascade updated. Nat Rev Immunol *7*, 678-689.
Li, J.J., Xing, S.H., Zhang, J., Hong, H., Li, Y.L., Dang, C., Zhang, Y.S., Li, C., Fan, Y.H., Yu, J.*, et al.* (2011). Decrease of tight junction integrity in the ipsilateral thalamus during the acute stage after focal infarction and ablation of the cerebral cortex in rats. Clin Exp Pharmacol Physiol *38*, 776-782.
Li, Y., Chen, J., Chen, X.G., Wang, L., Gautam, S.C., Xu, Y.X., Katakowski, M., Zhang, L.J., Lu, M., Janakiraman, N.*, et al.* (2002). Human marrow stromal cell therapy for stroke in rat: neurotrophins and functional recovery. Neurology *59*, 514-523.
Liesz, A., Zhou, W., Mracskó, É., Karcher, S., Bauer, H., Schwarting, S., Sun, L., Bruder, D., Stegemann, S., Cerwenka, A.*, et al.* (2011). Inhibition of lymphocyte trafficking shields the brain against deleterious neuroinflammation after stroke. Brain *134*, 704-720.
Lilly, C.M., Tateno, H., Oguma, T., Israel, E., and Sonna, L.A. (2005). Effects of allergen challenge on airway epithelial cell gene expression. Am J Respir Crit Care Med *171*, 579-586.
Lin, Q.M., Zhao, S., Zhou, L.L., Fang, X.S., Fu, Y., and Huang, Z.T. (2013). Mesenchymal stem cells transplantation suppresses inflammatory responses in global cerebral ischemia: contribution of TNF-α-induced protein 6. Acta Pharmacol Sin *34*, 784-792.

Lin, Y.C., Ko, T.L., Shih, Y.H., Lin, M.Y., Fu, T.W., Hsiao, H.S., Hsu, J.Y., and Fu, Y.S. (2011). Human umbilical mesenchymal stem cells promote recovery after ischemic stroke. Stroke *42*, 2045-2053.
Liu, F., Malaval, L., and Aubin, J.E. (2003). Global amplification polymerase chain reaction reveals novel transitional stages during osteoprogenitor differentiation. J Cell Sci *116*, 1787-1796.
Liu, H., Honmou, O., Harada, K., Nakamura, K., Houkin, K., Hamada, H., and Kocsis, J.D. (2006). Neuroprotection by PlGF gene-modified human mesenchymal stem cells after cerebral ischaemia. Brain *129*, 2734-2745.
Liu, H., Liu, S., Li, Y., Wang, X., Xue, W., Ge, G., and Luo, X. (2012a). The role of SDF-1-CXCR4/CXCR7 axis in the therapeutic effects of hypoxia-preconditioned mesenchymal stem cells for renal ischemia/reperfusion injury. PLoS One *7*, e34608.
Liu, J., Song, L., Jiang, C., Liu, Y., George, J., Ye, H., and Cui, Z. (2012b). Electrophysiological properties and synaptic function of mesenchymal stem cells during neurogenic differentiation - a mini-review. Int J Artif Organs *35*, 323-337.
Liu, Q., Luo, Z., He, S., Peng, X., Xiong, S., Wang, Y., Zhong, X., Zhou, X., Eisenberg, C.A., and Gao, B.Z. (2013). Conditioned serum-free medium from umbilical cord mesenchymal stem cells has anti-photoaging properties. Biotechnol Lett *35*, 1707-14.
Longa, E., Weinstein, P., Carlson, S., and Cummins, R. (1989). Reversible middle cerebral artery occlusion without craniectomy in rats. Stroke *20*, 84-91.
Luheshi, N., Rothwell, N., and Brough, D. (2009). Dual functionality of interleukin-1 family cytokines: implications for anti-interleukin-1 therapy. Br J Pharmacol *157*, 1318-1329.
Lyck, R., Ruderisch, N., Moll, A.G., Steiner, O., Cohen, C.D., Engelhardt, B., Makrides, V., and Verrey, F. (2009). Culture-induced changes in blood-brain barrier transcriptome: implications for amino-acid transporters in vivo. J Cereb Blood Flow Metab *29*, 1491-1502.
López-Iglesias, P., Blázquez-Martínez, A., Fernández-Delgado, J., Regadera, J., Nistal, M., and Miguel, M.P. (2011). Short and long term fate of human AMSC subcutaneously injected in mice. World J Stem Cells *3*, 53-62.
Madec, A.M., Mallone, R., Afonso, G., Abou Mrad, E., Mesnier, A., Eljaafari, A., and Thivolet, C. (2009). Mesenchymal stem cells protect NOD mice from diabetes by inducing regulatory T cells. Diabetologia *52*, 1391-1399.
Mahoney, D.J., Mikecz, K., Ali, T., Mabilleau, G., Benayahu, D., Plaas, A., Milner, C.M., Day, A.J., and Sabokbar, A. (2008). TSG-6 regulates bone remodeling through inhibition of osteoblastogenesis and osteoclast activation. J Biol Chem *283*, 25952-25962.
Mahoney, D.J., Mulloy, B., Forster, M.J., Blundell, C.D., Fries, E., Milner, C.M., and Day, A.J. (2005). Characterization of the interaction between tumor necrosis factor-stimulated gene-6 and heparin: implications for the inhibition of plasmin in extracellular matrix microenvironments. J Biol Chem *280*, 27044-27055.
Maier, R., Wisniewski, H.G., Vilcek, J., and Lotz, M. (1996). TSG-6 expression in human articular chondrocytes. Possible implications in joint inflammation and cartilage degradation. Arthritis Rheum *39*, 552-559.
Maina, V., Cotena, A., Doni, A., Nebuloni, M., Pasqualini, F., Milner, C.M., Day, A.J., Mantovani, A., and Garlanda, C. (2009). Coregulation in human leukocytes of the long pentraxin PTX3 and TSG-6. J Leukoc Biol *86*, 123-132.
Malcolm, K.C., Arndt, P.G., Manos, E.J., Jones, D.A., and Worthen, G.S. (2003). Microarray analysis of lipopolysaccharide-treated human neutrophils. Am J Physiol Lung Cell Mol Physiol *284*, L663-670.

Manuguerra-Gagné, R., Boulos, P.R., Ammar, A., Leblond, F.A., Krosl, G., Pichette, V., Lesk, M.R., and Roy, D.C. (2013). Transplantation of mesenchymal stem cells promotes tissue regeneration in a glaucoma model through laser-induced paracrine factor secretion and progenitor cell recruitment. Stem Cells *31*, 1136-1148.
Martin, C., Burdon, P.C., Bridger, G., Gutierrez-Ramos, J.C., Williams, T.J., and Rankin, S.M. (2003). Chemokines acting via CXCR2 and CXCR4 control the release of neutrophils from the bone marrow and their return following senescence. Immunity *19*, 583-593.
Martin, L., Al-Abdulla, N., Brambrink, A., Kirsch, J., Sieber, F., and Portera-Cailliau, C. (1998). Neurodegeneration in excitotoxicity, global cerebral ischemia, and target deprivation: A perspective on the contributions of apoptosis and necrosis. Brain Res Bull *46*, 281-309.
Martin, R., Lloyd, H., and Cowan, A. (1994). The early events of oxygen and glucose deprivation: setting the scene for neuronal death? Trends Neurosci *17*, 251-257.
Massena, S., Christoffersson, G., Hjertström, E., Zcharia, E., Vlodavsky, I., Ausmees, N., Rolny, C., Li, J.P., and Phillipson, M. (2010). A chemotactic gradient sequestered on endothelial heparan sulfate induces directional intraluminal crawling of neutrophils. Blood *116*, 1924-1931.
McColl, B. (2004). Pathophysiology of cerebral ischaemia: Effects of APOE genotype on outcome and endocytosis. Division of Clinical Neuroscience, Glasgow The University of Glasgow.
McColl, B., Allan, S., and Rothwell, N. (2009). Systemic infection, inflammation and acute ischemic stroke. Neuroscience *158*, 1049-1061.
McColl, B., Rothwell, N., and Allan, S. (2007). Systemic inflammatory stimulus potentiates the acute phase and CXC chemokine responses to experimental stroke and exacerbates brain damage via interleukin-1- and neutrophil-dependent mechanisms. J Neurosci *27*, 4403-4412.
McColl, B., Rothwell, N., and Allan, S. (2008). Systemic inflammation alters the kinetics of cerebrovascular tight junction disruption after experimental stroke in mice. J Neurosci *28*, 9451-9462.
McColl, B.W., Carswell, H.V., McCulloch, J., and Horsburgh, K. (2004). Extension of cerebral hypoperfusion and ischaemic pathology beyond MCA territory after intraluminal filament occlusion in C57Bl/6J mice. Brain Res *997*, 15-23.
Meairs, S., Wahlgren, N., Dirnagl, U., Lindvall, O., Rothwell, P., Baron, J.C., Hossmann, K., Engelhardt, B., Ferro, J., McCulloch, J.*, et al.* (2006). Stroke research priorities for the next decade--A representative view of the European scientific community. Cerebrovasc Dis *22*, 75-82.
Meisel, R., Brockers, S., Heseler, K., Degistirici, O., Bülle, H., Woite, C., Stuhlsatz, S., Schwippert, W., Jäger, M., Sorg, R.*, et al.* (2011). Human but not murine multipotent mesenchymal stromal cells exhibit broad-spectrum antimicrobial effector function mediated by indoleamine 2,3-dioxygenase. Leukemia *25*, 648-654.
Mellor, A.L., and Munn, D.H. (1999). Tryptophan catabolism and T-cell tolerance: immunosuppression by starvation? Immunol Today *20*, 469-473.
Mestas, J., and Hughes, C.C. (2004). Of mice and not men: differences between mouse and human immunology. J Immunol *172*, 2731-2738.
Milner, C.M., and Day, A.J. (2003). TSG-6: a multifunctional protein associated with inflammation. J Cell Sci *116*, 1863-1873.
Milner, C.M., Higman, V.A., and Day, A.J. (2006). TSG-6: a pluripotent inflammatory mediator? Biochem Soc Trans *34*, 446-450.

Mindrescu, C., Thorbecke, G.J., Klein, M.J., Vilcek, J., and Wisniewski, H.G. (2000). Amelioration of collagen-induced arthritis in DBA/1J mice by recombinant TSG-6, a tumor necrosis factor/interleukin-1-inducible protein. Arthritis Rheum *43*, 2668-2677.
Mirabelli-Badenier, M., Braunersreuther, V., Viviani, G.L., Dallegri, F., Quercioli, A., Veneselli, E., Mach, F., and Montecucco, F. (2011). CC and CXC chemokines are pivotal mediators of cerebral injury in ischaemic stroke. Thromb Haemost *105*, 409-420.
Moisan, A., Pannetier, N., Grillon, E., Richard, M.J., de Fraipont, F., Rémy, C., Barbier, E.L., and Detante, O. (2012). Intracerebral injection of human mesenchymal stem cells impacts cerebral microvasculature after experimental stroke: MRI study. NMR Biomed *25*, 1340-1348.
Monaghan, D., Bridges, R., and Cotman, C. (1989). The excitatory amino acid receptors: their classes, pharmacology, and distinct properties in the function of the central nervous system. Annu Rev Pharmacol Toxicol *29*, 365-402.
Mora-Lee, S., Sirerol-Piquer, M.S., Gutiérrez-Pérez, M., Gomez-Pinedo, U., Roobrouck, V.D., López, T., Casado-Nieto, M., Abizanda, G., Rabena, M.T., Verfaille, C.*, et al.* (2012). Therapeutic effects of hMAPC and hMSC transplantation after stroke in mice. PLoS One *7*, e43683.
Mori, E., del Zoppo, G.J., Chambers, J.D., Copeland, B.R., and Arfors, K.E. (1992). Inhibition of polymorphonuclear leukocyte adherence suppresses no-reflow after focal cerebral ischemia in baboons. Stroke *23*, 712-718.
Mulcahy, N.J., Ross, J., Rothwell, N.J., and Loddick, S.A. (2003). Delayed administration of interleukin-1 receptor antagonist protects against transient cerebral ischaemia in the rat. Br J Pharmacol *140*, 471-476.
Muldoon, L.L., Alvarez, J.I., Begley, D.J., Boado, R.J., Del Zoppo, G.J., Doolittle, N.D., Engelhardt, B., Hallenbeck, J.M., Lonser, R.R., Ohlfest, J.R.*, et al.* (2013). Immunologic privilege in the central nervous system and the blood-brain barrier. J Cereb Blood Flow Metab *33*, 13-21.
Murphy, G., Ward, R., Gavrilovic, J., and Atkinson, S. (1992). Physiological mechanisms for metalloproteinase activation. Matrix Suppl *1*, 224-230.
Nagyeri, G., Radacs, M., Ghassemi-Nejad, S., Tryniszewska, B., Olasz, K., Hutas, G., Gyorfy, Z., Hascall, V.C., Glant, T.T., and Mikecz, K. (2011). TSG-6 protein, a negative regulator of inflammatory arthritis, forms a ternary complex with murine mast cell tryptases and heparin. J Biol Chem *286*, 23559-23569.
Najar, M., Raicevic, G., Boufker, H.I., Fayyad Kazan, H., De Bruyn, C., Meuleman, N., Bron, D., Toungouz, M., and Lagneaux, L. (2010). Mesenchymal stromal cells use PGE2 to modulate activation and proliferation of lymphocyte subsets: Combined comparison of adipose tissue, Wharton's Jelly and bone marrow sources. Cell Immunol *264*, 171-179.
Nederkoorn, P.J., Westendorp, W.F., Hooijenga, I.J., de Haan, R.J., Dippel, D.W., Vermeij, F.H., Dijkgraaf, M.G., Prins, J.M., Spanjaard, L., and van de Beek, D. (2011). Preventive antibiotics in stroke study: rationale and protocol for a randomised trial. Int J Stroke *6*, 159-163.
Niemeyer, P., Vohrer, J., Schmal, H., Kasten, P., Fellenberg, J., Suedkamp, N.P., and Mehlhorn, A.T. (2008). Survival of human mesenchymal stromal cells from bone marrow and adipose tissue after xenogenic transplantation in immunocompetent mice. Cytotherapy *10*, 784-795.
Nimmerjahn, A., Kirchhoff, F., and Helmchen, F. (2005). Resting microglial cells are highly dynamic surveillants of brain parenchyma in vivo. Science *308*, 1314-1318.

Nourshargh, S., and Marelli-Berg, F.M. (2005). Transmigration through venular walls: a key regulator of leukocyte phenotype and function. Trends Immunol *26*, 157-165.
Németh, K., Leelahavanichkul, A., Yuen, P.S., Mayer, B., Parmelee, A., Doi, K., Robey, P.G., Leelahavanichkul, K., Koller, B.H., Brown, J.M.*, et al.* (2009). Bone marrow stromal cells attenuate sepsis via prostaglandin E(2)-dependent reprogramming of host macrophages to increase their interleukin-10 production. Nat Med *15*, 42-49.
O'Neill, L., and Dinarello, C. (2000). The IL-1 receptor/toll-like receptor superfamily: crucial receptors for inflammation and host defense. Immunol Today *21*, 206-209.
Offner, H., Subramanian, S., Parker, S., Afentoulis, M., Vandenbark, A., and Hurn, P. (2006). Experimental stroke induces massive, rapid activation of the peripheral immune system. J Cereb Blood Flow Metab *26*, 654-665.
Offner, H., Vandenbark, A.A., and Hurn, P.D. (2009). Effect of experimental stroke on peripheral immunity: CNS ischemia induces profound immunosuppression. Neuroscience *158*, 1098-1111.
Oh, J.Y., Lee, R.H., Yu, J.M., Ko, J.H., Lee, H.J., Ko, A.Y., Roddy, G.W., and Prockop, D.J. (2012). Intravenous mesenchymal stem cells prevented rejection of allogeneic corneal transplants by aborting the early inflammatory response. Mol Ther *20*, 2143-2152.
Oh, J.Y., Roddy, G.W., Choi, H., Lee, R.H., Ylöstalo, J.H., Rosa, R.H., and Prockop, D.J. (2010). Anti-inflammatory protein TSG-6 reduces inflammatory damage to the cornea following chemical and mechanical injury. Proc Natl Acad Sci U S A *107*, 16875-16880.
Ohtaki, H., Ylostalo, J.H., Foraker, J.E., Robinson, A.P., Reger, R.L., Shioda, S., and Prockop, D.J. (2008). Stem/progenitor cells from bone marrow decrease neuronal death in global ischemia by modulation of inflammatory/immune responses. Proc Natl Acad Sci U S A *105*, 14638-14643.
Onda, T., Honmou, O., Harada, K., Houkin, K., Hamada, H., and Kocsis, J.D. (2008). Therapeutic benefits by human mesenchymal stem cells (hMSCs) and Ang-1 gene-modified hMSCs after cerebral ischemia. J Cereb Blood Flow Metab *28*, 329-340.
Opitz, C.A., Litzenburger, U.M., Lutz, C., Lanz, T.V., Tritschler, I., Köppel, A., Tolosa, E., Hoberg, M., Anderl, J., Aicher, W.K.*, et al.* (2009). Toll-like receptor engagement enhances the immunosuppressive properties of human bone marrow-derived mesenchymal stem cells by inducing indoleamine-2,3-dioxygenase-1 via interferon-beta and protein kinase R. Stem Cells *27*, 909-919.
Ormstad, H., Aass, H.C., Lund-Sørensen, N., Amthor, K.F., and Sandvik, L. (2011). Serum levels of cytokines and C-reactive protein in acute ischemic stroke patients, and their relationship to stroke lateralization, type, and infarct volume. J Neurol *258*, 677-685.
Ortiz, L.A., Dutreil, M., Fattman, C., Pandey, A.C., Torres, G., Go, K., and Phinney, D.G. (2007). Interleukin 1 receptor antagonist mediates the antiinflammatory and antifibrotic effect of mesenchymal stem cells during lung injury. Proc Natl Acad Sci U S A *104*, 11002-11007.
Oskowitz, A., McFerrin, H., Gutschow, M., Carter, M.L., and Pochampally, R. (2011). Serum-deprived human multipotent mesenchymal stromal cells (MSCs) are highly angiogenic. Stem Cell Res *6*, 215-225.
Papayannopoulos, V., and Zychlinsky, A. (2009). NETs: a new strategy for using old weapons. Trends Immunol *30*, 513-521.
Park, P.W., Reizes, O., and Bernfield, M. (2000). Cell surface heparan sulfate proteoglycans: selective regulators of ligand-receptor encounters. J Biol Chem *275*, 29923-29926.
Paul, G., and Anisimov, S.V. (2013). The secretome of mesenchymal stem cells: Potential implications for neuroregeneration. Biochimie *95*, 2246-56.

Paxinos, G. (2004). The Mouse Brain in Stereotaxic Coordinates, Second edn (Texas, USA: Gulf Professional Publishing).
Peister, A., Mellad, J.A., Larson, B.L., Hall, B.M., Gibson, L.F., and Prockop, D.J. (2004). Adult stem cells from bone marrow (MSCs) isolated from different strains of inbred mice vary in surface epitopes, rates of proliferation, and differentiation potential. Blood *103*, 1662-1668.
Perry, V.H. (2004). The influence of systemic inflammation on inflammation in the brain: implications for chronic neurodegenerative disease. Brain Behav Immun *18*, 407-413.
Petri, B., Phillipson, M., and Kubes, P. (2008). The physiology of leukocyte recruitment: an in vivo perspective. J Immunol *180*, 6439-6446.
Petvises, S., and O'Neill, H.C. (2012). Hematopoiesis leading to a diversity of dendritic antigen-presenting cell types. Immunol Cell Biol *90*, 372-378.
Phillipson, M., Heit, B., Colarusso, P., Liu, L., Ballantyne, C.M., and Kubes, P. (2006). Intraluminal crawling of neutrophils to emigration sites: a molecularly distinct process from adhesion in the recruitment cascade. J Exp Med *203*, 2569-2575.
Pierro, M., Ionescu, L., Montemurro, T., Vadivel, A., Weissmann, G., Oudit, G., Emery, D., Bodiga, S., Eaton, F., Péault, B*., et al.* (2013). Short-term, long-term and paracrine effect of human umbilical cord-derived stem cells in lung injury prevention and repair in experimental bronchopulmonary dysplasia. Thorax *68*, 475-484.
Pillay, J., Kamp, V.M., van Hoffen, E., Visser, T., Tak, T., Lammers, J.W., Ulfman, L.H., Leenen, L.P., Pickkers, P., and Koenderman, L. (2012). A subset of neutrophils in human systemic inflammation inhibits T cell responses through Mac-1. J Clin Invest *122*, 327-336.
Pittenger, M.F., Mackay, A.M., Beck, S.C., Jaiswal, R.K., Douglas, R., Mosca, J.D., Moorman, M.A., Simonetti, D.W., Craig, S., and Marshak, D.R. (1999). Multilineage potential of adult human mesenchymal stem cells. Science *284*, 143-147.
Porter, C.J., and Charman, S.A. (2000). Lymphatic transport of proteins after subcutaneous administration. J Pharm Sci *89*, 297-310.
Pradillo, J.M., Denes, A., Greenhalgh, A.D., Boutin, H., Drake, C., McColl, B.W., Barton, E., Proctor, S.D., Russell, J.C., Rothwell, N.J*., et al.* (2012). Delayed administration of interleukin-1 receptor antagonist reduces ischemic brain damage and inflammation in comorbid rats. J Cereb Blood Flow Metab *32*, 1810-1819.
Price, C.J., Menon, D.K., Peters, A.M., Ballinger, J.R., Barber, R.W., Balan, K.K., Lynch, A., Xuereb, J.H., Fryer, T., Guadagno, J.V*., et al.* (2004). Cerebral neutrophil recruitment, histology, and outcome in acute ischemic stroke: an imaging-based study. Stroke *35*, 1659-1664.
Rehncrona, S. (1985). Brain acidosis. Ann Emerg Med *14*, 770-776.
Ren, G., Zhang, L., Zhao, X., Xu, G., Zhang, Y., Roberts, A.I., Zhao, R.C., and Shi, Y. (2008). Mesenchymal stem cell-mediated immunosuppression occurs via concerted action of chemokines and nitric oxide. Cell Stem Cell *2*, 141-150.
Roddy, G.W., Oh, J.Y., Lee, R.H., Bartosh, T.J., Ylostalo, J., Coble, K., Rosa, R.H., and Prockop, D.J. (2011). Action at a distance: systemically administered adult stem/progenitor cells (MSCs) reduce inflammatory damage to the cornea without engraftment and primarily by secretion of TNF-α stimulated gene/protein 6. Stem Cells *29*, 1572-1579.
Rodriguez, A.M., Pisani, D., Dechesne, C.A., Turc-Carel, C., Kurzenne, J.Y., Wdziekonski, B., Villageois, A., Bagnis, C., Breittmayer, J.P., Groux, H*., et al.* (2005). Transplantation

of a multipotent cell population from human adipose tissue induces dystrophin expression in the immunocompetent mdx mouse. J Exp Med *201*, 1397-1405.
Rosen, C.L., Dinapoli, V.A., Nagamine, T., and Crocco, T. (2005). Influence of age on stroke outcome following transient focal ischemia. J Neurosurg *103*, 687-694.
Rostène, W., Guyon, A., Kular, L., Godefroy, D., Barbieri, F., Bajetto, A., Banisadr, G., Callewaere, C., Conductier, G., Rovère, C.*, et al.* (2011). Chemokines and chemokine receptors: new actors in neuroendocrine regulations. Front Neuroendocrinol *32*, 10-24.
Rothstein, J.D., Patel, S., Regan, M.R., Haenggeli, C., Huang, Y.H., Bergles, D.E., Jin, L., Dykes Hoberg, M., Vidensky, S., Chung, D.S.*, et al.* (2005). Beta-lactam antibiotics offer neuroprotection by increasing glutamate transporter expression. Nature *433*, 73-77.
Sakai, H., Sheng, H., Yates, R.B., Ishida, K., Pearlstein, R.D., and Warner, D.S. (2007). Isoflurane provides long-term protection against focal cerebral ischemia in the rat. Anesthesiology *106*, 92-99; discussion 98-10.
Saksela, O., and Rifkin, D.B. (1988). Cell-associated plasminogen activation: regulation and physiological functions. Annu Rev Cell Biol *4*, 93-126.
Saqqur, M., Tsivgoulis, G., Molina, C.A., Demchuk, A.M., Siddiqui, M., Alvarez-Sabín, J., Uchino, K., Calleja, S., Alexandrov, A.V., and Investigators, C. (2008). Symptomatic intracerebral hemorrhage and recanalization after IV rt-PA: a multicenter study. Neurology *71*, 1304-1312.
Sasaki, M., Abe, R., Fujita, Y., Ando, S., Inokuma, D., and Shimizu, H. (2008). Mesenchymal stem cells are recruited into wounded skin and contribute to wound repair by transdifferentiation into multiple skin cell type. J Immunol *180*, 2581-2587.
Sasaki, M., Honmou, O., Radtke, C., and Kocsis, J.D. (2011). Development of a middle cerebral artery occlusion model in the nonhuman primate and a safety study of i.v. infusion of human mesenchymal stem cells. PLoS One *6*, e26577.
Schilling, M., Besselmann, M., Leonhard, C., Mueller, M., Ringelstein, E.B., and Kiefer, R. (2003). Microglial activation precedes and predominates over macrophage infiltration in transient focal cerebral ischemia: a study in green fluorescent protein transgenic bone marrow chimeric mice. Exp Neurol *183*, 25-33.
Schilling, M., Besselmann, M., Müller, M., Strecker, J.K., Ringelstein, E.B., and Kiefer, R. (2005). Predominant phagocytic activity of resident microglia over hematogenous macrophages following transient focal cerebral ischemia: an investigation using green fluorescent protein transgenic bone marrow chimeric mice. Exp Neurol *196*, 290-297.
Schroeter, M., Jander, S., Witte, O.W., and Stoll, G. (1994). Local immune responses in the rat cerebral cortex after middle cerebral artery occlusion. J Neuroimmunol *55*, 195-203.
Schwanhäusser, B., Busse, D., Li, N., Dittmar, G., Schuchhardt, J., Wolf, J., Chen, W., and Selbach, M. (2011). Global quantification of mammalian gene expression control. Nature *473*, 337-342.
Seder, R.A., and Ahmed, R. (2003). Similarities and differences in CD4+ and CD8+ effector and memory T cell generation. Nat Immunol *4*, 835-842.
Sharova, L.V., Sharov, A.A., Nedorezov, T., Piao, Y., Shaik, N., and Ko, M.S. (2009). Database for mRNA half-life of 19 977 genes obtained by DNA microarray analysis of pluripotent and differentiating mouse embryonic stem cells. DNA Res *16*, 45-58.
Shepherd, A.J., Downing, J.E., and Miyan, J.A. (2005). Without nerves, immunology remains incomplete -in vivo veritas. Immunology *116*, 145-163.
Shichita, T., Sugiyama, Y., Ooboshi, H., Sugimori, H., Nakagawa, R., Takada, I., Iwaki, T., Okada, Y., Iida, M., Cua, D.J.*, et al.* (2009). Pivotal role of cerebral interleukin-17-

producing gammadeltaT cells in the delayed phase of ischemic brain injury. Nat Med *15*, 946-950.
Shimogai, M., Ogawa, K., Tokinaga, Y., Yamazaki, A., and Hatano, Y. (2010). The cellular mechanisms underlying the inhibitory effects of isoflurane and sevoflurane on arginine vasopressin-induced vasoconstriction. J Anesth *24*, 893-900.
Shirozu, M., Nakano, T., Inazawa, J., Tashiro, K., Tada, H., Shinohara, T., and Honjo, T. (1995). Structure and chromosomal localization of the human stromal cell-derived factor 1 (SDF1) gene. Genomics *28*, 495-500.
Siegenthaler, J.A., Sohet, F., and Daneman, R. (2013). 'Sealing off the CNS': cellular and molecular regulation of blood-brain barriergenesis. Curr Opin Neurobiol *23*, 1057-64.
Silver, J., and Miller, J.H. (2004). Regeneration beyond the glial scar. Nat Rev Neurosci *5*, 146-156.
Smith, C.J., Emsley, H.C., Gavin, C.M., Georgiou, R.F., Vail, A., Barberan, E.M., del Zoppo, G.J., Hallenbeck, J.M., Rothwell, N.J., Hopkins, S.J*., et al.* (2004). Peak plasma interleukin-6 and other peripheral markers of inflammation in the first week of ischaemic stroke correlate with brain infarct volume, stroke severity and long-term outcome. BMC Neurol *4*, 2.
Smith, G.M., and Strunz, C. (2005). Growth factor and cytokine regulation of chondroitin sulfate proteoglycans by astrocytes. Glia *52*, 209-218.
Song, H., Stevens, C.F., and Gage, F.H. (2002). Astroglia induce neurogenesis from adult neural stem cells. Nature *417*, 39-44.
Soriano, S.G., Coxon, A., Wang, Y.F., Frosch, M.P., Lipton, S.A., Hickey, P.R., and Mayadas, T.N. (1999). Mice deficient in Mac-1 (CD11b/CD18) are less susceptible to cerebral ischemia/reperfusion injury. Stroke *30*, 134-139.
Spaggiari, G.M., Abdelrazik, H., Becchetti, F., and Moretta, L. (2009). MSCs inhibit monocyte-derived DC maturation and function by selectively interfering with the generation of immature DCs: central role of MSC-derived prostaglandin E2. Blood *113*, 6576-6583.
Spaggiari, G.M., Capobianco, A., Becchetti, S., Mingari, M.C., and Moretta, L. (2006). Mesenchymal stem cell-natural killer cell interactions: evidence that activated NK cells are capable of killing MSCs, whereas MSCs can inhibit IL-2-induced NK-cell proliferation. Blood *107*, 1484-1490.
Spaggiari, G.M., and Moretta, L. (2013). Cellular and molecular interactions of mesenchymal stem cells in innate immunity. Immunol Cell Biol *91*, 27-31.
Steiner, O., Coisne, C., Engelhardt, B., and Lyck, R. (2011). Comparison of immortalized bEnd5 and primary mouse brain microvascular endothelial cells as in vitro blood-brain barrier models for the study of T cell extravasation. J Cereb Blood Flow Metab *31*, 315-327.
Suzuki, S., Tanaka, K., and Suzuki, N. (2009). Ambivalent aspects of interleukin-6 in cerebral ischemia: inflammatory versus neurotrophic aspects. J Cereb Blood Flow Metab *29*, 464-479.
Szántó, S., Bárdos, T., Gál, I., Glant, T.T., and Mikecz, K. (2004). Enhanced neutrophil extravasation and rapid progression of proteoglycan-induced arthritis in TSG-6-knockout mice. Arthritis Rheum *50*, 3012-3022.
Takatsuru, Y., Eto, K., Kaneko, R., Masuda, H., Shimokawa, N., Koibuchi, N., and Nabekura, J. (2013). Critical role of the astrocyte for functional remodeling in contralateral hemisphere of somatosensory cortex after stroke. J Neurosci *33*, 4683-4692.

Takeshima, R., Kirsch, J.R., Koehler, R.C., Gomoll, A.W., and Traystman, R.J. (1992). Monoclonal leukocyte antibody does not decrease the injury of transient focal cerebral ischemia in cats. Stroke *23*, 247-252.
Tamura, A., Graham, D.I., McCulloch, J., and Teasdale, G.M. (1981). Focal cerebral ischaemia in the rat: 2. Regional cerebral blood flow determined by [14C]iodoantipyrine autoradiography following middle cerebral artery occlusion. J Cereb Blood Flow Metab *1*, 61-69.
Tan, K.T., McGrouther, D.A., Day, A.J., Milner, C.M., and Bayat, A. (2011). Characterization of hyaluronan and TSG-6 in skin scarring: differential distribution in keloid scars, normal scars and unscarred skin. J Eur Acad Dermatol Venereol *25*, 317-327.
Tao, J., Ji, F., Liu, B., Wang, F., Dong, F., and Zhu, Y. (2012). Improvement of deficits by transplantation of lentiviral vector-modified human amniotic mesenchymal cells after cerebral ischemia in rats. Brain Res *1448*, 1-10.
Tatara, R., Ozaki, K., Kikuchi, Y., Hatanaka, K., Oh, I., Meguro, A., Matsu, H., Sato, K., and Ozawa, K. (2011). Mesenchymal stromal cells inhibit Th17 but not regulatory T-cell differentiation. Cytotherapy *13*, 686-694.
Terao, S., Yilmaz, G., Stokes, K.Y., Ishikawa, M., Kawase, T., and Granger, D.N. (2008). Inflammatory and injury responses to ischemic stroke in obese mice. Stroke *39*, 943-950.
Thornberry, N., Bull, H., Calaycay, J., Chapman, K., Howard, A., Kostura, M., Miller, D., Molineaux, S., Weidner, J., and Aunins, J. (1992). A novel heterodimeric cysteine protease is required for interleukin-1 beta processing in monocytes. Nature *356*, 768-774.
Thornton, P., Pinteaux, E., Gibson, R., Allan, S., and Rothwell, N. (2006). Interleukin-1-induced neurotoxicity is mediated by glia and requires caspase activation and free radical release. J Neurochem *98*, 258-266.
Tilg, H., Dinarello, C., and Mier, J. (1997). IL-6 and APPs: anti-inflammatory and immunosuppressive mediators. Immunol Today *18*, 428-432.
Tilg, H., Trehu, E., Atkins, M.B., Dinarello, C.A., and Mier, J.W. (1994). Interleukin-6 (IL-6) as an anti-inflammatory cytokine: induction of circulating IL-1 receptor antagonist and soluble tumor necrosis factor receptor p55. Blood *83*, 113-118.
Toyama, K., Honmou, O., Harada, K., Suzuki, J., Houkin, K., Hamada, H., and Kocsis, J.D. (2009). Therapeutic benefits of angiogenetic gene-modified human mesenchymal stem cells after cerebral ischemia. Exp Neurol *216*, 47-55.
Tuo, J., Cao, X., Shen, D., Wang, Y., Zhang, J., Oh, J.Y., Prockop, D.J., and Chan, C.C. (2012). Anti-inflammatory recombinant TSG-6 stabilizes the progression of focal retinal degeneration in a murine model. J Neuroinflammation *9*, 59.
Uhlar, C.M., and Whitehead, A.S. (1999). Serum amyloid A, the major vertebrate acute-phase reactant. Eur J Biochem *265*, 501-523.
Urra, X., Cervera, A., Obach, V., Climent, N., Planas, A.M., and Chamorro, A. (2009). Monocytes are major players in the prognosis and risk of infection after acute stroke. Stroke *40*, 1262-1268.
van Eeden, S.F., and Terashima, T. (2000). Interleukin 8 (IL-8) and the release of leukocytes from the bone marrow. Leuk Lymphoma *37*, 259-271.
Vassalli, J.D., Sappino, A.P., and Belin, D. (1991). The plasminogen activator/plasmin system. J Clin Invest *88*, 1067-1072.

Vendrame, M., Gemma, C., de Mesquita, D., Collier, L., Bickford, P.C., Sanberg, C.D., Sanberg, P.R., Pennypacker, K.R., and Willing, A.E. (2005). Anti-inflammatory effects of human cord blood cells in a rat model of stroke. Stem Cells Dev *14*, 595-604.
Verma, R.P., and Hansch, C. (2007). Matrix metalloproteinases (MMPs): chemical-biological functions and (Q)SARs. Bioorg Med Chem *15*, 2223-2268.
Vivien, D., Gauberti, M., Montagne, A., Defer, G., and Touzé, E. (2011). Impact of tissue plasminogen activator on the neurovascular unit: from clinical data to experimental evidence. J Cereb Blood Flow Metab *31*, 2119-2134.
Vogel, C., and Marcotte, E.M. (2012). Insights into the regulation of protein abundance from proteomic and transcriptomic analyses. Nat Rev Genet *13*, 227-232.
Wakitani, S., Saito, T., and Caplan, A.I. (1995). Myogenic cells derived from rat bone marrow mesenchymal stem cells exposed to 5-azacytidine. Muscle Nerve *18*, 1417-1426.
Wang, N., Li, Q., Zhang, L., Lin, H., Hu, J., Li, D., Shi, S., Cui, S., Zhou, J., Ji, J.*, et al.* (2012). Mesenchymal stem cells attenuate peritoneal injury through secretion of TSG-6. PLoS One *7*, e43768.
Wang, Y., Xue, M., Xuan, Y.L., Hu, H.S., Cheng, W.J., Suo, F., Li, X.R., Yan, S.H., and Wang, L.X. (2013). Mesenchymal Stem Cell Therapy Improves Diabetic Cardiac Autonomic Neuropathy and Decreases the Inducibility of Ventricular Arrhythmias. Heart Lung Circ *13*, 1037-8.
Warner, D.S., McFarlane, C., Todd, M.M., Ludwig, P., and McAllister, A.M. (1993). Sevoflurane and halothane reduce focal ischemic brain damage in the rat. Possible influence on thermoregulation. Anesthesiology *79*, 985-992.
Waszak, P., Alphonse, R., Vadivel, A., Ionescu, L., Eaton, F., and Thébaud, B. (2012). Preconditioning enhances the paracrine effect of mesenchymal stem cells in preventing oxygen-induced neonatal lung injury in rats. Stem Cells Dev *21*, 2789-2797.
Watanabe, J., Shetty, A.K., Hattiangady, B., Kim, D.K., Foraker, J.E., Nishida, H., and Prockop, D.J. (2013). Administration of TSG-6 improves memory after traumatic brain injury in mice. Neurobiol Dis *59*, 86-99.
Waterman, R.S., Tomchuck, S.L., Henkle, S.L., and Betancourt, A.M. (2010). A new mesenchymal stem cell (MSC) paradigm: polarization into a pro-inflammatory MSC1 or an Immunosuppressive MSC2 phenotype. PLoS One *5*, e10088.
Wei, X., Yang, X., Han, Z.P., Qu, F.F., Shao, L., and Shi, Y.F. (2013). Mesenchymal stem cells: a new trend for cell therapy. Acta Pharmacol Sin *34*, 747-754.
Wengner, A., Pitchford, S., Furze, R., and Rankin, S. (2008). The coordinated action of G-CSF and ELR + CXC chemokines in neutrophil mobilization during acute inflammation. Blood *111*, 42-49.
Westendorp, W.F., Nederkoorn, P.J., Vermeij, J.D., Dijkgraaf, M.G., and van de Beek, D. (2011). Post-stroke infection: a systematic review and meta-analysis. BMC Neurol *11*, 110.
Westendorp, W.F., Vermeij, J.D., Vermeij, F., Den Hertog, H.M., Dippel, D.W., van de Beek, D., and Nederkoorn, P.J. (2012). Antibiotic therapy for preventing infections in patients with acute stroke. Cochrane Database Syst Rev *1*, CD008530.
Whiteley, W., Chong, W.L., Sengupta, A., and Sandercock, P. (2009). Blood markers for the prognosis of ischemic stroke: a systematic review. Stroke *40*, e380-389.
Wilkins, A., Kemp, K., Ginty, M., Hares, K., Mallam, E., and Scolding, N. (2009). Human bone marrow-derived mesenchymal stem cells secrete brain-derived neurotrophic factor which promotes neuronal survival in vitro. Stem Cell Res *3*, 63-70.

Willis, C.L., Nolan, C.C., Reith, S.N., Lister, T., Prior, M.J., Guerin, C.J., Mavroudis, G., and Ray, D.E. (2004). Focal astrocyte loss is followed by microvascular damage, with subsequent repair of the blood-brain barrier in the apparent absence of direct astrocytic contact. Glia *45*, 325-337.
Winters, L., Winters, T., Gorup, D., Mitrečić, D., Curlin, M., Križ, J., and Gajović, S. (2013). Expression analysis of genes involved in TLR2-related signaling pathway: Inflammation and apoptosis after ischemic brain injury. Neuroscience *238*, 87-96.
Wisniewski, H.G., Hua, J.C., Poppers, D.M., Naime, D., Vilcek, J., and Cronstein, B.N. (1996). TNF/IL-1-inducible protein TSG-6 potentiates plasmin inhibition by inter-alpha-inhibitor and exerts a strong anti-inflammatory effect in vivo. J Immunol *156*, 1609-1615.
Wisniewski, H.G., Maier, R., Lotz, M., Lee, S., Klampfer, L., Lee, T.H., and Vilcek, J. (1993). TSG-6: a TNF-, IL-1-, and LPS-inducible secreted glycoprotein associated with arthritis. J Immunol *151*, 6593-6601.
Wolburg, H., and Lippoldt, A. (2002). Tight junctions of the blood-brain barrier: development, composition and regulation. Vascul Pharmacol *38*, 323-337.
Wood, P. (2006). Understanding Immunology, Second edn (Harlow: Pearson Education Limited).
Woodbury, D., Schwarz, E.J., Prockop, D.J., and Black, I.B. (2000). Adult rat and human bone marrow stromal cells differentiate into neurons. J Neurosci Res *61*, 364-370.
Xagorari, A., Siotou, E., Yiangou, M., Tsolaki, E., Bougiouklis, D., Sakkas, L., Fassas, A., and Anagnostopoulos, A. (2013). Protective effect of mesenchymal stem cell-conditioned medium on hepatic cell apoptosis after acute liver injury. Int J Clin Exp Pathol *6*, 831-840.
Ye, L., Mora, R., Akhayani, N., Haudenschild, C.C., and Liau, G. (1997). Growth factor and cytokine-regulated hyaluronan-binding protein TSG-6 is localized to the injury-induced rat neointima and confers enhanced growth in vascular smooth muscle cells. Circ Res *81*, 289-296.
Yen, H.C., Xu, Q., Chou, D.M., Zhao, Z., and Elledge, S.J. (2008). Global protein stability profiling in mammalian cells. Science *322*, 918-923.
Yenari, M.A., Kauppinen, T.M., and Swanson, R.A. (2010). Microglial activation in stroke: therapeutic targets. Neurotherapeutics *7*, 378-391.
Yilmaz, G., Arumugam, T.V., Stokes, K.Y., and Granger, D.N. (2006a). Role of T lymphocytes and interferon-gamma in ischemic stroke. Circulation *113*, 2105-2112.
Yilmaz, G., Arumugam, T.V., Stokes, K.Y., and Granger, D.N. (2006b). Role of T lymphocytes and interferon-gamma in ischemic stroke. Circulation *113*, 2105-2112.
Ylöstalo, J.H., Bartosh, T.J., Coble, K., and Prockop, D.J. (2012). Human mesenchymal stem/stromal cells cultured as spheroids are self-activated to produce prostaglandin E2 that directs stimulated macrophages into an anti-inflammatory phenotype. Stem Cells *30*, 2283-2296.
Yoshioka, S., Ochsner, S., Russell, D.L., Ujioka, T., Fujii, S., Richards, J.S., and Espey, L.L. (2000). Expression of tumor necrosis factor-stimulated gene-6 in the rat ovary in response to an ovulatory dose of gonadotropin. Endocrinology *141*, 4114-4119.
Zaremba, J., Skrobanski, P., and Losy, J. (2001). Tumour necrosis factor-alpha is increased in the cerebrospinal fluid and serum of ischaemic stroke patients and correlates with the volume of evolving brain infarct. Biomed Pharmacother *55*, 258-263.

Zeller, J.A., Lenz, A., Eschenfelder, C.C., Zunker, P., and Deuschl, G. (2005). Platelet-leukocyte interaction and platelet activation in acute stroke with and without preceding infection. Arterioscler Thromb Vasc Biol *25*, 1519-1523.
Zhang, L., Zhang, Z.G., Zhang, R.L., Lu, M., Krams, M., and Chopp, M. (2003). Effects of a selective CD11b/CD18 antagonist and recombinant human tissue plasminogen activator treatment alone and in combination in a rat embolic model of stroke. Stroke *34*, 1790-1795.
Zhang, Q., Shi, S., Liu, Y., Uyanne, J., Shi, Y., and Le, A.D. (2009). Mesenchymal stem cells derived from human gingiva are capable of immunomodulatory functions and ameliorate inflammation-related tissue destruction in experimental colitis. J Immunol *183*, 7787-7798.
Zhang, R.L., Chopp, M., Chen, H., and Garcia, J.H. (1994). Temporal profile of ischemic tissue damage, neutrophil response, and vascular plugging following permanent and transient (2H) middle cerebral artery occlusion in the rat. J Neurol Sci *125*, 3-10.
Zhang, R.L., Chopp, M., Jiang, N., Tang, W.X., Prostak, J., Manning, A.M., and Anderson, D.C. (1995). Anti-intercellular adhesion molecule-1 antibody reduces ischemic cell damage after transient but not permanent middle cerebral artery occlusion in the Wistar rat. Stroke *26*, 1438-1442; discussion 1443.
Zhao, L.R., Duan, W.M., Reyes, M., Keene, C.D., Verfaillie, C.M., and Low, W.C. (2002). Human bone marrow stem cells exhibit neural phenotypes and ameliorate neurological deficits after grafting into the ischemic brain of rats. Exp Neurol *174*, 11-20.
Zlotnik, A., and Yoshie, O. (2000). Chemokines: a new classification system and their role in immunity. Immunity *12*, 121-127.